Synthesis and Characterization of Novel inhibitors and Delivery systems for targeting HIV-1 entry.

DOCTOR OF PHILOSOPHY

By

Jagadeesh Senapathi



Department of Biotechnology and Bioinformatics School of Life Sciences University of Hyderabad Hyderabad-46, Telangana, India.

Synthesis and Characterization of Novel inhibitors and Delivery systems for targeting HIV-1 entry.

A thesis submitted to University of Hyderabad for the award of Ph.D. Degree in Biotechnology and Bioinformatics

By

Jagadeesh Senapathi



Department of Biotechnology and Bioinformatics School of Life Sciences University of Hyderabad Hyderabad-46, Telangana, India.

Enrollment No: 11LTPH12



UNIVERSITY OF HYDERABAD

(A central university established in 1974 by an act of Parliament) Department of Biotechnology and Bioinformatics School of Life Sciences University of Hyderabad, Hyderabad 500046, India.

CERTIFICATE

This is to certify that thesis entitled "Synthesis and Characterization of Novel inhibitors and Delivery systems for targeting HIV-1 entry" is a record of bonafide work done by Mr. Jagadeesh Senapathi, a research scholar for Ph.D. program in Department of Biotechnology and Bioinformatics, University of Hyderabad under my guidance and supervision. The thesis has not been submitted previously in part or full to this or any other university or institution for the award of any degree or diploma. I recommend his thesis for submission towards the partial fulfillment of Doctor of Philosophy degree in Biotechnology and Bioinformatics.

Snedlell

Prof. Anan Supervisor Biomeonnatics Debr of Biomethnology & E newity of Hydorabad, Ryderabad

Department of Biotechnology and **Bioinformatics**

अध्यक्ष / Head जैव प्रौद्योगिकी एवं जैव सूचना विज्ञान विभाग Department of Biotechnology & Bioinformatics

हैदराबाद विश्वविद्यालय University of Hyderabad हैदराबाद / Hyderabad - 500 046. School of Life Science DEAN

School of Life Sciences University of Hyderabad Hyderabad - 500 046.



CERTIFICATE

This is to certify that parts of the thesis "Synthesis and Characterization of Novel inhibitors and Delivery systems for targeting HIV-1 entry" submitted by Mr. Jagadeesh Senapathi, bearing registration number 11LTPH12 in partial fulfilment of the requirement for award of Doctor of philosophy has been

A) Published in following publications:

Jagadeesh Senapathi, Akhila Bommakanti, Suresh Mallepalli, Satyajit Mukhopadhyay, Anand K.Kondapi.
 Sulfonate modified Lactoferrin Nanoparticles as drug carriers with dual activity against HIV-1. Colloids and Surfaces B: Biointerfaces (under review).

B) Presented in following conferences:

- "A surface modified drug loaded nanoparticle as dual targeting anti-HIV agents" International Conference on Advances in Biological Systems and Material Science in Nano World (ABSMSNW-2017), Varanasi, India. (Jagadeesh Senapathi, Anand K.Kondapi, 19th-23rd Feb 2017).
- "Bidirectional targeting of nanoparticles to target recognition and receptor interaction" NANOBIOTECK 2017 organized by Indian Society of Nanomedicine., Trivandrum, India. (Jagadeesh Senapathi, Komal Dolasia, Sangita Mukhopadhyay Anand K.Kondapi, 6th -8th Dec 2017).
- "Design, synthesis and development of V3 loop targeted HIV-1 entry inhibitors" International
 conference on Biology and Therapeutics of HIV& Associated Infections -Jan 2019 at University of
 Hyderabad, Hyderabad. (Jagadeesh Senapathi, Akhila Bommakanti, Anand K.Kondapi, 19th-21st Jan 2019).

Further, the student has passed the following courses towards fulfilment of coursework requirement for Ph.D.

S. No	Course Code	Course Name	Credits	Pass//Fail
1	BT801	Seminar	1	PASS
2	BT802	Research Ethics & Management	2	PASS
3	BT803	Biostatistics	2	PASS
4	BT804	Analytical Techniques	3	PASS
5	BT805	Lab Work	4	PASS

Supervisor & Biol

Dept. of Bioscianos.
School of Life Sciences.
University of Hyderabad, Hyderabad
A.P.-560046, herbs.

Head

Department of Brotechilelogy and

जैव प्रौद्**ष्ठिलिक्षितिक्षालेखां इ**चना विज्ञान विभाग Department of Biotechnology & Bioinformatics

हैदराबाद विश्वविद्यालय University of Hydorob Dean

School of Life Science

DEAN

School of Life Sciences University of Hyderabad Hyderabad - 500 046.

141414 / Hyderabad - 500 046.



UNIVERSITY OF HYDERABAD

(A central university established in 1974 by an act of Parliament)
Department of Biotechnology and Bioinformatics School of Life Sciences
University of Hyderabad, Hyderabad 500046, India

Declaration

I, Jagadeesh Senapathi, hereby declare that the work presented in this thesis, entitled "Synthesis and Characterization of Novel inhibitors and Delivery systems for targeting HIV-1 entry" has been carried out by me under the supervision of Prof. Anand K. Kondapi, Department of Biotechnology and Bioinformatics. To the best of my knowledge this work has not been submitted for the award of any degree or diploma at any other university or institution. I hereby agree that my thesis can be deposited in Shodganga/INFLIBNET. A report on plagiarism statistics from the University Librarian is enclosed.

Place: Hyderabad Date: 11/11/2020

Jagadeesh Senapathi 11LTPH12

<u>ACKNOWLEDGEMENTS</u>

My Ph.D. journey has been allowed me to identify my strength, weakness, interest, and passion, and if not for this opportunity, I wouldn't have been exposed to new avenues and learnings, which I now consider my strengths. Many people have been instrumental in my journey, and I take this opportunity to thank them all.

I will always remain indebted to my supervisor Prof. Anand Kumar Kondapi, who has been instrumental in gently introducing me to the world of research and offering constant encouragement, freedom, and support in designing and implementing this thesis. His insights and knowledge provided a direction to the work helping in the completion.

I would like to express my sincere thanks to present Dean School of Life Sciences, Prof. S. Dayananda, and former Dean Prof. K.V.A Ramaiah, Prof. Reddanna, Prof. Aparna Dutta Gupta, Prof. R.P. Sharma, Prof. A. S. Raghavendra for permitting me to use necessary facilities to carry out my work.

I would also like to express my sincere regards to the present Head, Department of Biotechnology and Bioinformatics, Prof. K.P.M.S.V Padmasree, and former Head of the Department Prof. J.S.S Prakash, Prof. Anand. K Kondapi, Dr. Niyaz Ahmed. I offer my sincere gratitude to my doctoral committee members Dr.Prakash Prabhu and Dr. Vaibhav Vindal, for their valuable suggestions and guidance throughout my Ph.D. I sincerely thank all the faculty members of the School of Life sciences.

I thank CSIR & UGC for providing me fellowship during my Ph.D. and the funding bodies ICMR, DBT, and DST of Govt. of India for providing funds to our lab during my work.

I thank my present & previous lab mates Dr. Prabhakar, Dr. Bhaskar, Dr. Upendhar, Dr. Sarada, Dr. Sathish, Dr. Kishore, Dr. Anil, Dr. Farhan, Dr. Prashant, Dr. Pankaz, Dr. Lakshmi, Dr. Sonali, Dr. Kurumurthy, Dr. Harikiran, Kiran, Chuku, Satyajit, Neha, Pritikana, Vidya, Godan, Veena for being an enthusiastic and lively group, always ready to help during my work.

I thank all non-teaching staff of the department, school, and administration of UOH for their help. I thank Sreenivas, Bhanu, and Chandra for their dedicated work in the lab. I would like to express heartfelt thanks to my friends and my Ph.D. batchmates and seniors for their helping nature.

I thank CNF (Campus Network Facility), Google, and Sci Finder for being my companion.

My special thanks to Dr.Akhila, Suresh, Dr.Chandu.B(ACRHEM), Srinivas.V(Chemistry), Dr. Srinivas A (IIT-H) for their support, company and help in my work. Their presence has been a blessing and is beyond the scope of this section of acknowledgment.

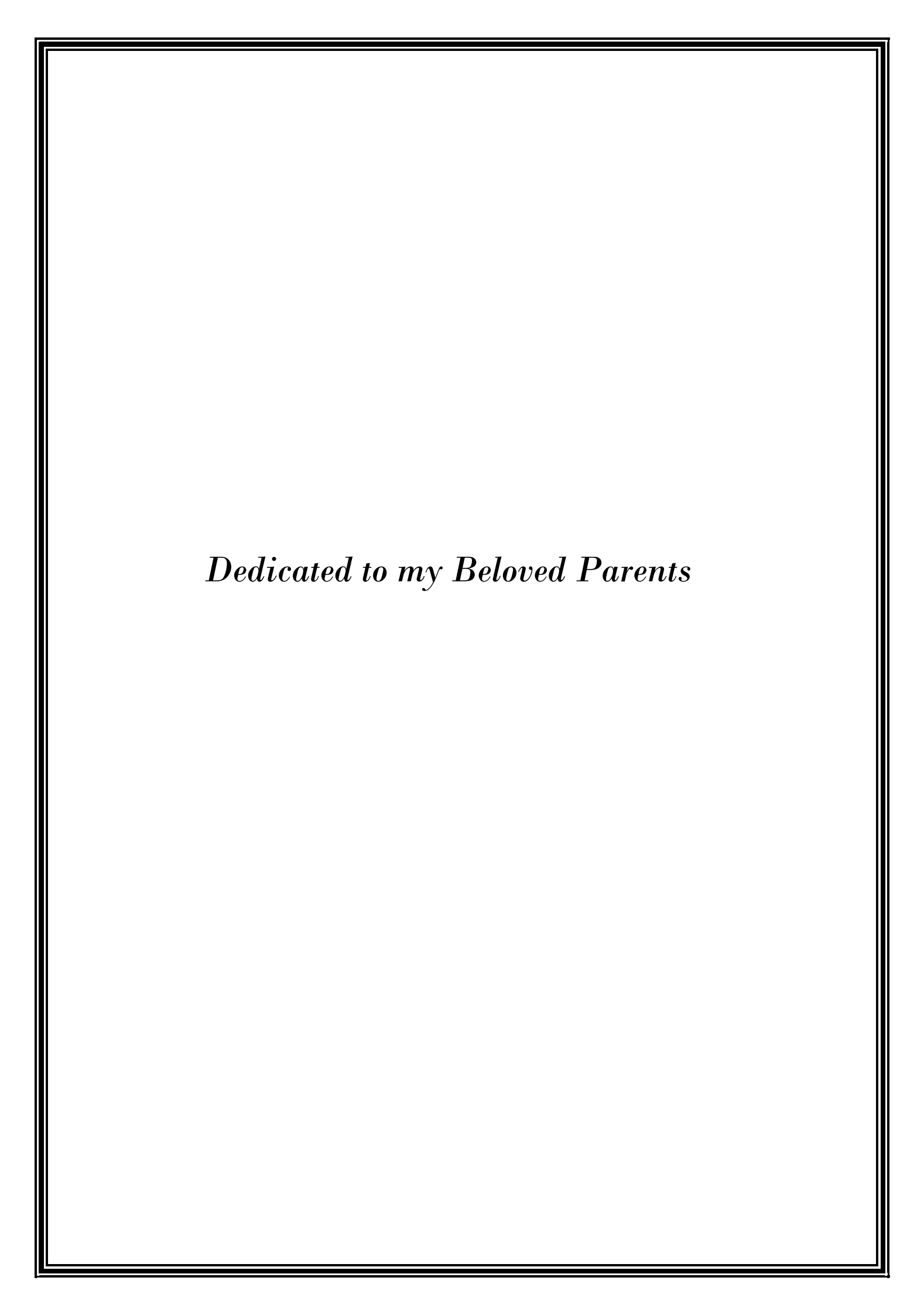
I would like to thank my childhood friends Venu, Varahamurthy, Santhu, Arjun, Ganesh, Nagaraju, Ganesh k, Krishnamurthy.

I will forever be indebted to my gurus' Chemistry lecturer A. Krishna Kumar and Prof. A Satyanarayana for their constant guidance and support.

Thanks to My wife and My daughter, for their understanding and encouragement in hectic workdays.

I would finally like to mention my wonderful parents and grandparents for giving me everything. Their encouragement and support have been the guiding torch in my life, for which I will always be indebted. I thank my lovely sisters, brother, and other family members, for their understanding and encouragement. Thank my extended family, Aunts, Uncles, and Cousins who have lived this journey through me, encouraging me throughout.

-Jagadeesh Senapathi



Abbreviations:

3TC: Lamivudine

AIDS: Acquired Immunodeficiency Syndrome

APC: Antigen-presenting cell

ART: Antiretroviral therapy

cDNA: Complementary DNA

DAPI: 4',6-diamidino-2-phenylindole

DCM: Dichloromethane

DHPM: Dihydropyrimidine

DMF: Dimethyl formamide

DMSO: Dimethyl sulfoxide

Doxo: Doxorubicin hydrochloride

EDTA: Ethylenediaminetetraacetic acid

EE: Encapsulation efficiency

ELISA: Enzyme-Linked Immunosorbent Assay

Epap-1: Early pregnancy-associated protein

ER: Endoplasmic reticulum

FESEM: Field Emission Scanning Electron Microscopy

FTIR: Fourier transform infrared

HAART: Highly Active Antiretroviral Therapy

HIV: Human Immunodeficiency Virus

HPLC: High Performance Liquid Chromatography

IFNs: Interferons

IN: Integrase enzyme

LC: Loading capacity

Lf: Lactoferrin

Lf-MES NPs: Lactoferrin-MES Nanoparticles

MES: Sodium 2-mercaptoethane sulfonate

MTT: 3-(4,5-dimethylthiozol-2-yl)-2,5-diphenyltetrazolium bromide

NMR: Nuclear Magnetic Resonance

NP: Nano particles

NRTIs: Nucleoside / Nucleotide Reverse Transcriptase inhibitors

NSI: Non-syncytia inducing

PLA: Poly (D, L-lactide)

PLGA: Poly (lactic-co-glycolic acid)

RNAi: RNA interference

RT: Reverse transcriptase

RTV: Ritonavir

SERS: Surface Enhanced Raman Spectroscopy

T20: Enfuvirtide

TEA: Triethylamine

TEM: Transmission Electron Microscopy

THPM:1,2,3,4 -Tetrahydropyrimidine

TLC: Thin layer chromatography

TMS: Tetramethyl silane

ZDV: Zidovudine

CONTENTS

Chapter 1: Introduction

1.1	Genera	l Introduction	1
1.2	HIV-1 Infection, transmission, and immune response		
1.3	HIV-1 Proteome		
1.4	HIV-1 life cycle and therapy		
1.5	HIV-1 inhibitors Reaction mechanism and Resistance		
1.6	HIV entry inhibitors development and challenges		
1.7	HIV nano-drug delivery and Importance		
1.8	Early pregnancy-associated protein (Epap-1) and its action		
1.9	Broadly neutralising antibody 447-52D against gp120		
1.10	Lactoferrin as nanocarrier		
1.11	Small	molecule drug discovery and Chemical structural evaluation of	
	hydroj	pyrimidine and s-triazane derivatives as inhibitors	21
1.12	Rational of the study		
1.13	Objectives of the work		
Chap	ter 2:	Materials and Methods	
2.1	Mater	als	24
	2.1.1	Reagents	24
	2.1.2	Cell lines	24
	2.1.3	Instruments & Tools	25
2.2	Metho	ds	25
	2.2.1	Design and Docking of molecules to target gp120	25
	2.2.2	Chemical synthesis of 2-(3-phenyl-1H-pyrazole-5-yl) pyridine	26
	2.2.3	General procedure for preparation of Ethyl -6-methyl-4-	
		Phenyl-2-thiox-1,2,3,4-tetrahydropyrimidine-5-carboxylate,	
		and Ethyl 6- methyl-2-oxo-4-phenyl-1,2,3,4	
		tetrahydropyrimidine-5 carboxylate derivative	27

	2.2.4	Synthesis of 2-(2-(5-bromo-2-hydroxybenzylidene)	
		hydrazinyl)-2-oxo-N-(p-tolyl) acetamide	28
	2.2.5	Synthesis of 2-(4-aminophenyl)-2,3-dihydroquinazolin-4(1H)- one	29
	2.2.6	General procedure for 2,4,6-trichloro -1,3,5 -triazene	
		substituted derivatives	29
	2.2.7	Preparation and Physical Characterization of nanoparticles	32
	2.2.8	Characterization of Size and shape of nanoparticles by	
		FE- SEM and TEM	33
	2.2.9	Size and charge distribution of nanoparticles in suspension	33
	2.2.10	Agarose gel electrophoresis for charge-based nanoparticle	
		migration study	33
	2.2.11	pH- dependant drug released study	34
	2.2.12	Drug Loading Capacity (LC) and Drug Encapsulation	
		Efficiency (EE)	34
	2.2.13	Analysis of MES conjugated Lf nanoparticles by solid state	
		NMR	35
	2.2.14	Characterization of functional groups on protein nanoparticles	35
	2.2.15	Cellular localization of fluorescent dug (Curcumin) loaded	
		NPs by Confocal study and localized drug (AZT) quantified	
		by HPLC	35
	2.2.16	Competitive binding of Lf-MES NPs to gp160 (gp120+gp41)	36
	2.2.17	Cell Cytotoxicity by MTT assay	37
	2.2.18	Inhibition of Cell Fusion	37
	2.2.19	HIV-1 Antiviral activity quantified by p24-ELISA Assay	38
Chapt	er 3:	Objective I	
K .		Synthesis and characterization of novel HIV-1 entry	
		inhibitors based on Epap-1 derived peptides targeting	
		envelope gp120.	
3.1	Introd	uction	40
		Design of small molecules by using Epap-1 and gp120 binding	-
		C - 7 - 6 F - 7 6 F 7 -	

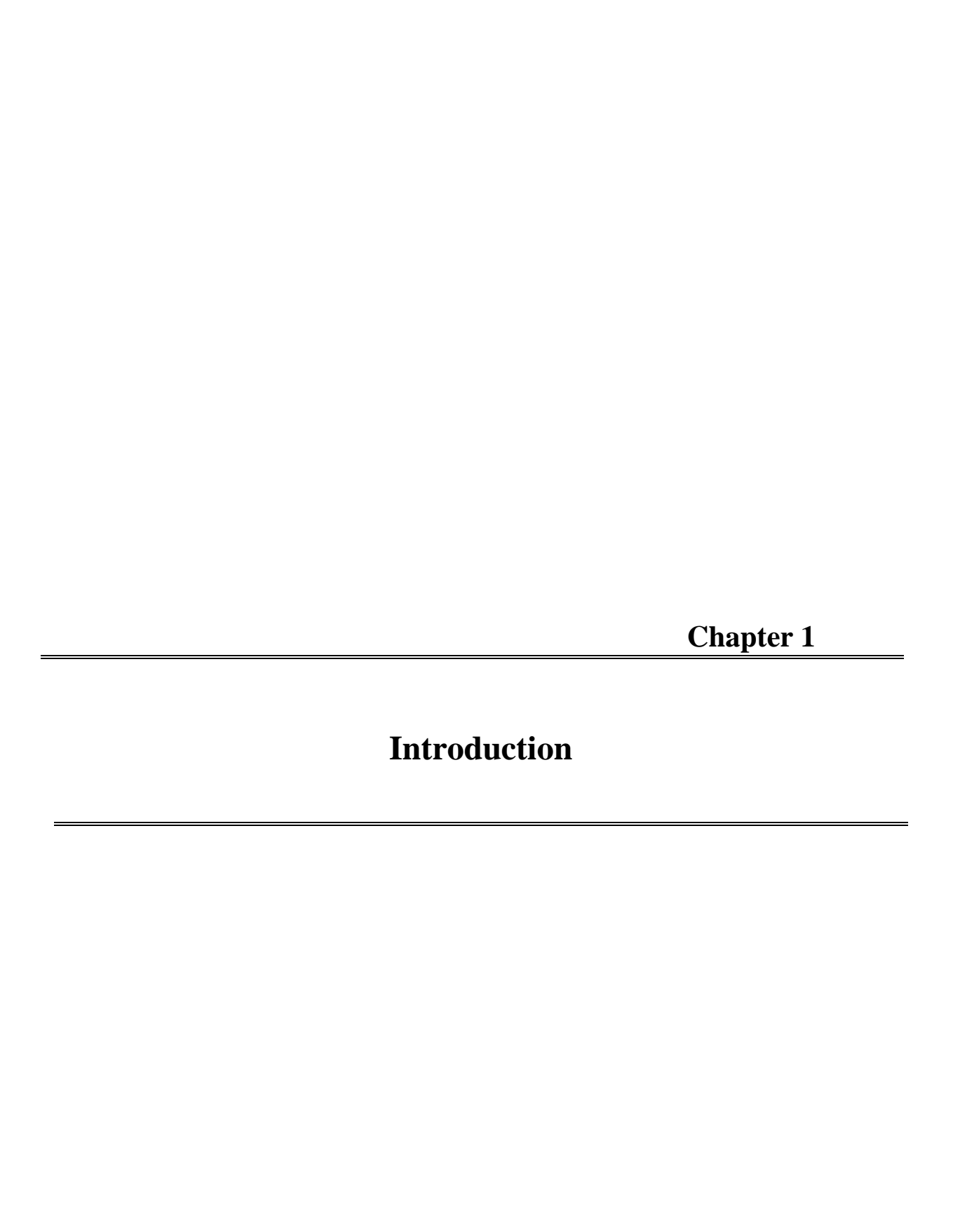
		sites	41
	3.1.2	Selection of small molecules for development as an entry	
		inhibitor	43
3.2	Ration	nale of the Objective I	44
3.3	Result	ts and discussion	44
	3.3.1	Design and development of pyrazole and DHPM derivatives	44
	3.3.2	Virtual screening of 1,2,3,4-Tetrahydropyrimidine (1,2,3,4-	
		THPM)-oxo and thioxo derivatives to a specific target to	
		"phe43 cavity"	46
	3.3.3	Synthesis and physical characterization of pyrazole derivatives	47
	3.3.4	Synthesis and physical characterization of THPM derivatives	48
	3.3.5	Cell cytotoxicity (MTT Assay) of molecules	50
	3.3.6	Anti-HIV-1 activity (p24 Assay) of molecules	52
Summo	ary of c	bjective I	53
Chapt	er 4:	Objective II	
Chapt	er 4:	Objective II HIV-1 envelope protein V3 loop and neutralizing antibody	
Chapt	er 4:	·	
Chapt	er 4:	HIV-1 envelope protein V3 loop and neutralizing antibody	
	er 4:	HIV-1 envelope protein V3 loop and neutralizing antibody 447-52D interactions based derived molecules development, synthesis, and characterization.	55
4.1	Introdu	HIV-1 envelope protein V3 loop and neutralizing antibody 447-52D interactions based derived molecules development, synthesis, and characterization.	55
4.1	Introdu	HIV-1 envelope protein V3 loop and neutralizing antibody 447-52D interactions based derived molecules development, synthesis, and characterization.	55 57
4.1	Introdu 4.1.1	HIV-1 envelope protein V3 loop and neutralizing antibody 447-52D interactions based derived molecules development, synthesis, and characterization. action Design of small molecules through gp120 and 447-52D epitopes	
4.1	Introdu 4.1.1 Ration	HIV-1 envelope protein V3 loop and neutralizing antibody 447-52D interactions based derived molecules development, synthesis, and characterization. action Design of small molecules through gp120 and 447-52D epitopes Interactions	57
4.1	Introdu 4.1.1 Ration Result	HIV-1 envelope protein V3 loop and neutralizing antibody 447-52D interactions based derived molecules development, synthesis, and characterization. action Design of small molecules through gp120 and 447-52D epitopes Interactions all of the Objective II	57 58
4.1	Introdu 4.1.1 Ration Result	HIV-1 envelope protein V3 loop and neutralizing antibody 447-52D interactions based derived molecules development, synthesis, and characterization. action Design of small molecules through gp120 and 447-52D epitopes Interactions all of the Objective II s and discussion	57 58 58
4.1	Introdu 4.1.1 Ration Results 4.3.1	HIV-1 envelope protein V3 loop and neutralizing antibody 447-52D interactions based derived molecules development, synthesis, and characterization. action Design of small molecules through gp120 and 447-52D epitopes Interactions all of the Objective II s and discussion Design and docking of new molecules to target the V3 loop	57 58 58 58
4.1	Introdu 4.1.1 Ration Results 4.3.1 4.3.2	HIV-1 envelope protein V3 loop and neutralizing antibody 447-52D interactions based derived molecules development, synthesis, and characterization. Inction Design of small molecules through gp120 and 447-52D epitopes Interactions and of the Objective II and discussion Design and docking of new molecules to target the V3 loop General discussion of Synthesized molecules	57 58 58 58 58
4.1	Introdu 4.1.1 Ration Result 4.3.1 4.3.2 4.3.3	HIV-1 envelope protein V3 loop and neutralizing antibody 447-52D interactions based derived molecules development, synthesis, and characterization. action Design of small molecules through gp120 and 447-52D epitopes Interactions all of the Objective II s and discussion Design and docking of new molecules to target the V3 loop General discussion of Synthesized molecules physical and spectral characterization of synthesized molecules	57 58 58 58 60 62

Chapter 5: Objective III

Sulfonate modified lactoferrin nanoparticles as drug carriers with dual activity against HIV-1.

5.1	Introduction		77
5.2	Ratio	ional of the Objective III	
5.3	Resul	Results & Discussion	
	5.3.1	Preparation and Physical Characterization of nanoparticles	79
	5.3.2	Analysis of MES conjugated Lf nanoparticles by solid state NMR	81
	5.3.3	Characterization of Functional groups on protein nanoparticles	83
	5.3.4	Cellular localization of fluorescent dug (curcumin) loaded NPs	
		by Confocal study and localization of drug (AZT) quantified	
		by HPLC	83
	5.3.5	Competitive interaction of MES nanoparticles with HL2/3 cell	
		surface gp160	85
	5.3.6	Cell Cytotoxicity Assay	87
	5.3.7	Inhibition of Cell Fusion	87
	5.3.8	Anti-viral activity of nanoparticles	88
Sumn	nary of o	objective III	89
Chap	oter 6: (Overall Summary & Conclusion of the Thesis	92
Refe	rences		96
Appe	endix		

- i) Copies of ¹H NMR, HRMS and IR spectra for representative compounds
- ii) Copyright permissions for figures reuse
- iii) Publication



1.1 General Introduction:

Globally 38.0 million people living with HIV and 6,90,000 people succumbed from HIV-related causes at the end of 2019 [1]. The people living with HIV (PLHIV) in India 21.40 lakh, while 69.11 thousand AIDS-related causalities nationally [2]. Human Immunodeficiency Virus (HIV) targets the human immune system and weakens the body's defense mechanism to fight disease. The infected individual's immune cells are destroyed and impaired by the virus. The body gradually becomes immunodeficient and finally develops into a life-threatening condition called Acquired Immunodeficiency Syndrome (AIDS) [3]. AIDS, a stage that occurs within 10 years after HIV infection, increases susceptibility to a wide range of chronic and life-threatening diseases leading finally to death [4]. The virus completely hijacks the human cell to integrate its genetic material to produce new virions [5]. The replication process of HIV is different than traditional viruses of the retrovirus family. The higher transcription error rate of the HIV reverse transcriptase enzyme creates huge heterogenicity in HIV virions [6]. Heterogenicity is the primary factor contributing to the difficulty of treating HIV. Different techniques and tests are used for diagnosing HIV and for guiding the treatment [7]. The cure for HIV is based on the infection mechanism and the lifecycle stage to be targeted [8].

In the highly active antiretroviral therapy (HAART), multiple antiretroviral drugs are used for the treatment of HIV/AIDS to decreases patient viral load, maintain the functioning of the immune system, and reduce circulating viremia to prevent transmission of the virus [9]. Antiretroviral drugs are used in multiple combinations to target different stages of the HIV life cycle. The WHO and other organizations support research to understand the complexity of HIV, the barrier it creates in the treatment intervention, and methods to overcome these barriers and prevent opportunistic infections that often lead to death [10].

1.2 HIV-1 Infection, transmission, and immune response:

CD4⁺ T cells and CD4⁺ cells of monocytes /macrophage lineages are the primary targets of HIV-1[11]. The CD4 receptor is primary for HIV-1 attachment to host cell membrane, and

Co-receptors, CCR5, CXCR4, and their subtypes support fusion and entry of the virion into the host cell [12]. The infected CD4⁺ T cells are destroyed during the infection, for instance, by activation pathways leading to cell death and cellular fusion through inducing syncytia. A group of healthy cells gathers around the single infected cell, forms multinucleated giant cells, and collectively lose their function and immune response [13]. Cell death occurs through membrane disruption and involves calcium channels and phospholipids formation [14]. HIV-1 strains exhibit selective infection to a cell type based on the receptors expressed on the surface, which refer to the tropics. Based on the feature of co-receptors usage, namely CxCR4-specific viruses referred to as T cell tropic, while CCR5 specific viruses referred to as Macrophage tropic viruses, some viruses exhibit dual tropics [15]. The infected macrophages that cannot form syncytia are called non-syncytia inducing (NSI) and are incapable of infecting T-cell lines [16]. Multiple routes of HIV viral transmission through mucosal surfaces and body fluids explains the diversity of the virus,

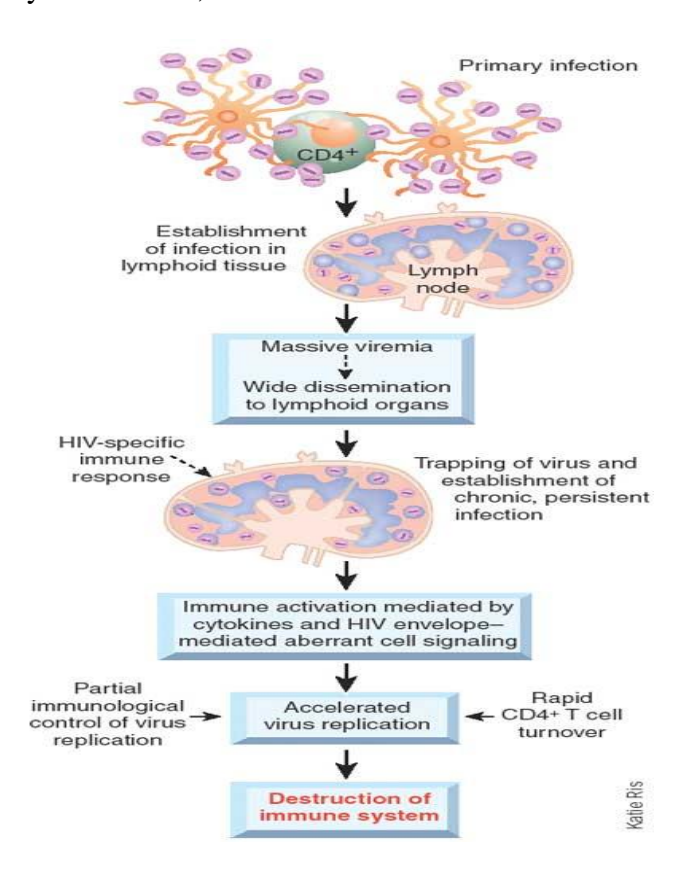


Fig. 1.1: HIV infection and immune response (Anthony S Fauci. Nature Medicine volume 9, pages839–843(2003)

the primary transmission routes are cervicovaginal, penile, rectal, oral, percutaneous, and intravenous [17]. The detection of the virus in plasma is challenging immediately after exposure transmission [18]. This period is called the eclipse phase, which generally lasts 7 to 21 days [19]. In the initial stages of infection, the nucleic acid amplification method is used for the quantitative determination of HIV, during which RNA reaches 1 to 5 copies per milliliter in plasma [20]. Quantitative assays do further detection of virus load in plasma through viral biomarkers and antibodies [21].

The infected virus enters the genital mucosal epithelium. It replicates and then passes through the intracellular epithelium and finally drains into lymphoreticular tissues to produce HIV-1 viremia in the acute phase [22]. This triggers a response from dendritic cells, macrophages, monocytes, activated T cells, and NK cells resulting in the production of cytokines, proinflammatory chemokines (IL-15, type I interferons (IFNs) and CXC-chemokine ligand 10 (CXCL10), TNF, IL-18, IL-22, and IFN γ) [23]. HIV suppressive agents like Beta chemokines MIP-1 α , MIP-1 β , and RANTES are released by CD8 T lymphocytes (**Fig. 1.1**) [24]. As the viremia concentration increases to reach a peak point, the adaptive immune system starts to produce non-neutralizing antibodies against virus envelope glycoprotein epitopes [25]. After a certain point, the virus's immune response declines due to a highly mutated virus that does not respond to the immune system [26]. The robust innate, adaptive immune system does not eliminate the virus entirely but continuously produces immune responsive markers against chronic HIV infection in some cells and tissue sites [27].

1.3 HIV-1 Proteome:

The viral proteins are divided into the following classes

Structural Proteins:

These are a group of proteins that form the virus particle and are essential for manipulating the viral genome to produce intact virions. The following proteins are coded by viral genome:

gag

Gag protein (Group Specific Antigen) is a precursor polyprotein that is eventually cleaved by viral proteases to give proteins that form a part of the virion particle [28]. The precursor is a myristoylated 55KDa protein p55 is processed to provide p17 matrix (MA), p24 Capsid (CA),

and p7 Nucleocapsid (NC) proteins [29]. Gag forms a part of a gag-pol polyprotein expressed due to a frameshift that occurs at the 3 end of gag (gag) [30].

pol

This gene encodes viral enzymes, protease, reverse transcriptase, and integrase. It is expressed as a 160KDa precursor Gag-pol polyprotein, packed into an assembling virion where it is processed to give the functional enzymes. (pol) [31].

env

This gene's product is the precursor for the trimeric spike subunits expressed on the virus particle (**Fig. 1.2**). The two subunits, gp160, and gp41, are glycosylated and linked covalently to form a heterodimeric spike exposed on the surface of the particle [32]. The gp160 subunit facilitates the binding to the CD4 receptor of the host cell, followed by engaging with seven membrane transmembrane co-receptor, eventually leading to the formation of fusion pore by gp41, which enable the transfer of viral capsid with its

contents to the host cell [33]. The gp120 also decides the co-receptor; thus, it is responsible for viral tropism (env).

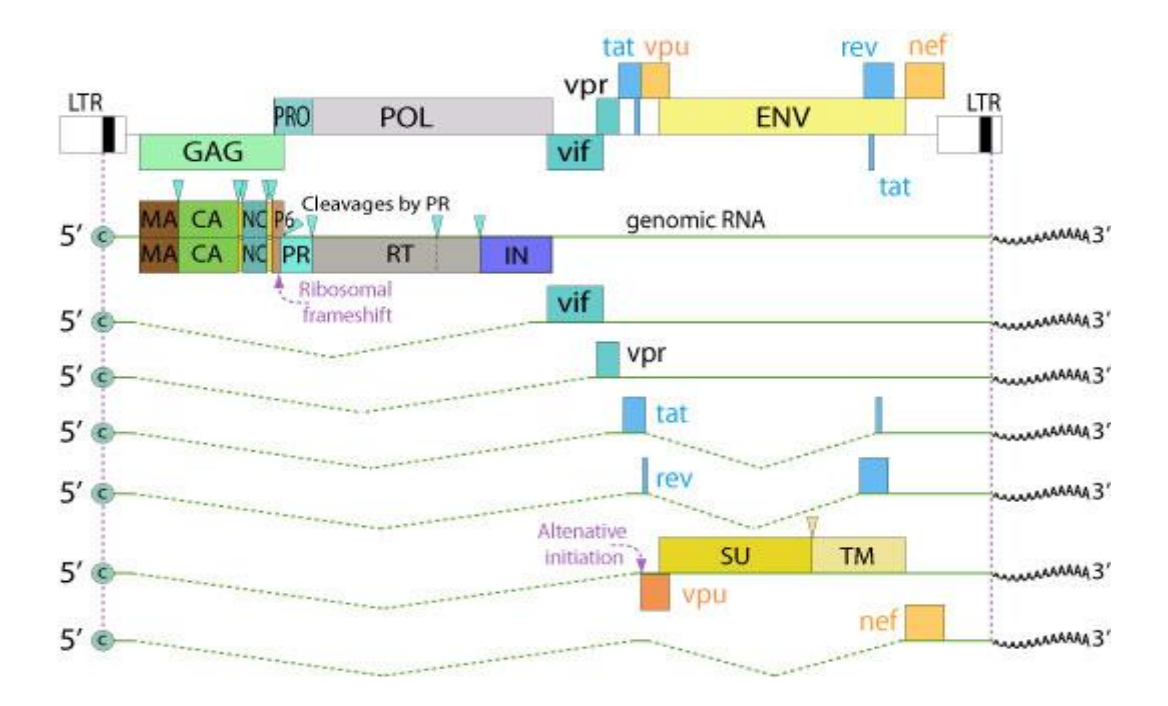


Fig. 1.2: RNA Splicing and HIV Proteome (ViralZone, SIB Swiss Institute of Bioinformatics)

Regulatory Proteins:

Tat

It is one of the two regulatory elements found to be localized in the nucleus during immunofluorescence experiments. [34]. It binds to the TAR (Trans Activation Response) domain present in the LTR region that acts as an RNA element rather than DNA and is responsible for activating transcription initiation and elongation from the promoter in the LTR region. It works like an antitermination factor by preventing the 5' polyadenylation signal from premature termination of transcription and polyadenylation [35]. It was observed that in the absence of Tat protein, despite the transcription initiation being efficient, the promoter engages with polymerases that disengage prematurely with the DNA template [36]. Tat is also a potential drug target, and many research efforts are focused on developing compounds that act on transactivation and thus inhibit HIV replication [37].

rev

This is the second important regulatory element that, in the nucleus, binds to the RRE element encoded into the viral mRNA [38]. It promotes export, stabilization, and utilization of viral mRNA containing the RRE element in the cytoplasm. Rev is highly conserved, and the localization of rev proteins alternates between the nucleus and cytoplasm [39].

Accessory Proteins

nef

One of the first proteins produced in host cells upon infection is a 27KDa myristoylated protein responsible for a myriad of functions. Mainly CD₄ and MHC class I down-regulation increased infectivity and modulated cells' activation states [40]. Several studies have suggested the role of attenuated or mutated Nef in delayed progression or non-progression of the disease in Long Term Non-Progressors [41]. It is a communicator between the virus and the host, attacking, and hijacking host cellular functions to promote viral growth [42].

vpu

Specific to HIV-1 and some forms of SIV, it is 16KDa transmembrane protein majorly responsible for the degradation of CD₄ in the endoplasmic reticulum and the releasing of virions from the plasma membrane [43].

vpr

14KDa protein is packed into the virion and localizes into the nucleus upon release into the host cell. It interacts with a gag precursor region to perform functions that include nuclear import of pre-integration complex, transactivation of cellular genes, and cellular differentiation [44].

vif

It is a 23KDa cytoplasmic protein present in soluble as well as membrane-bound forms. It affects the infectivity of virions but not the production of virus particles [45]. It has been shown that the virus produced in the absence of vif protein is defective, but it does not affect the cell-cell transmission of the virus [46].

1.4 HIV-1 life cycle and therapy:

Spherically shaped, HIV -1 consists of an outer lipid double layer envelope, which is embedded with three spikes of glycoproteins, gp120, and gp41 [47]. The matrix protein beneath the envelope surrounding the virus's core to form a cone-shaped capsid consists of p24 protein [48]. The capsid encloses two copies of RNA, and enzymes reverse transcriptase, integrase, protease, and other viral proteins [49]. The early step of virus entry is the interaction of gp120 with the CD4 receptor, followed by binding to co-receptors (CCR5 or CXCR4) [50]. The binding with receptors and co-receptors results in the modification in enveloping protein gp41 to form a sixhelix bundle that pulls the viral cell membrane close to the host cell, fuse, and transfers total virus content into the host cell cytosol by fusion [51].

Retrovirus, like HIV-1, uses reverse transcriptase to produce new proteins from RNA through complementary DNA (cDNA) [52]. RT synthesizes double-strand proviral DNA from the diploid viral RNA strand as a template. The double-stranded reoviral DNA in association with viral and host proteins forms pre-integration complexes, translated into the nucleus and integrates into host DNA with the integrase enzyme [53]. Once virus genetic material integrates into the cell, cell machinery is hijacked by the virus. The integrated DNA called The produced new virus copies maybe inactivate or active and replicate as a parent virus, evolving as a new virus. The higher error rate of RT makes a mutated virus, and the mutation rate varies within the components of provirus DNA participates in synthesizing complementary

The viral encoded genomic RNA and other enzymes come together within the viral core protein and then finally bud from the infected cell to produce a new virus [55]. RNA strands [54]. The RNA copies become messenger RNA and produce regular proteins necessary for budding the virus [56]. The gag and pol gene variability are less than the envelope gene, as it contains five hypervariable regions [57]. The diverse variability in virus components results in resistance for existing drugs, and mutated outer envelope protein is difficult to neutralize with antibodies (Fig. 1.3). The medical management of HIV/AIDS with affordable drugs is essential to reduce viral load in plasma at an undetectable level. After the detection of AIDS, researchers have been understanding the replication mechanism of HIV-1 and investing to use tools to design and synthesize specific targeted pharmacological agents. 25 Drugs are approved by the FDA, which are used as antiviral drugs in antiretroviral therapy (ART). These drugs are classified into different groups based on the mode of action [58].

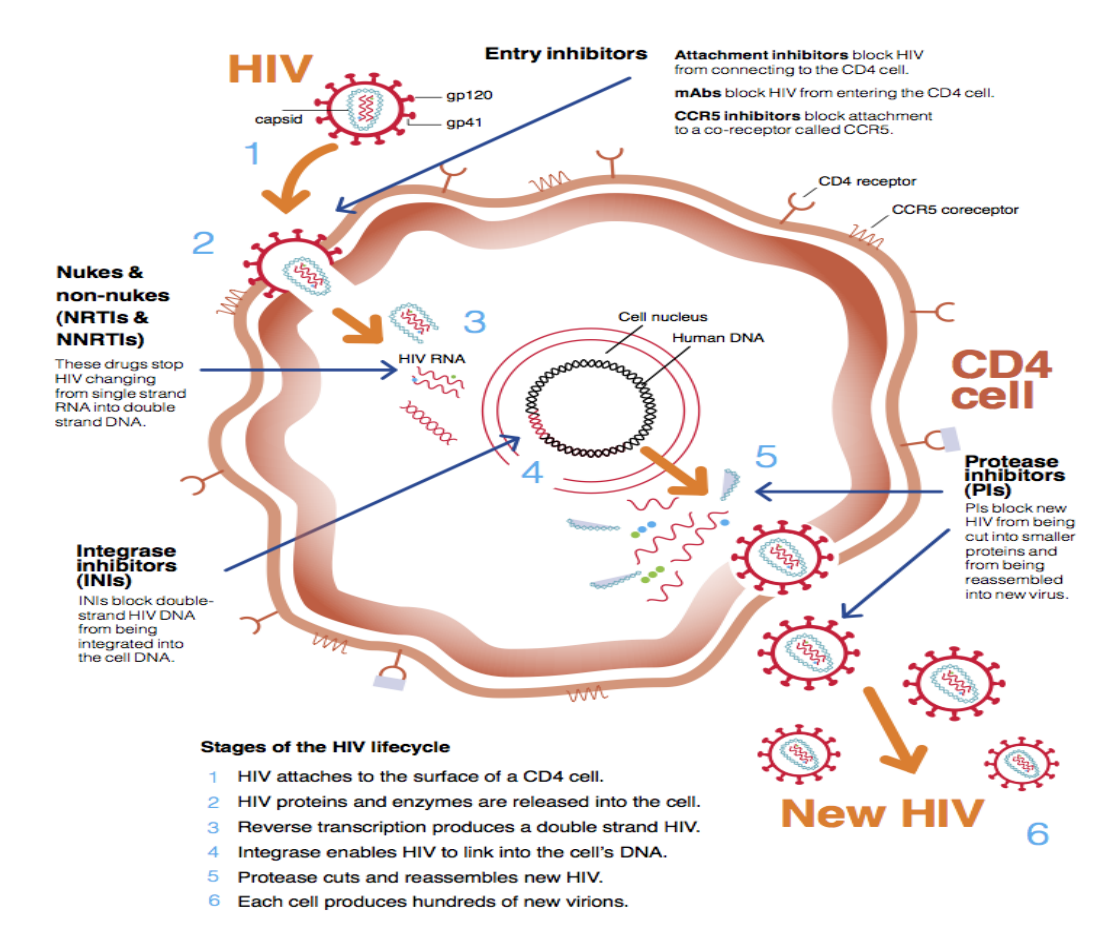


Fig. 1.3: HIV-Life cycle and inhibitors (https://i-base.info/guides/starting/hiv-life-cycle)

In 1986 first drug Zidovudine (ZDV) was introduced in ART, followed by other drugs in the next few years [59]. The initial use of monotherapy was encountered with resistance problems, resulting in dual and multiple drug combination therapies [60]. The primary goals for ART are

- Effective suppression of viral load.
- Repair and protect immunologic function.
- To control and decrease HIV-related morbidity and mortality.
- To enhance the quality of life of HIV-infected persons.
- To potentially curb Mother to Child Transmission (PMTCT).
- Post Exposure Prophylaxis (PEP).

WHO recommends the treatment guidelines based on clinical stage and CD4 count in peripheral blood [61]. At stage 1,2 of the disease, CD4 count is below 350 cells/ml, and in stage 3,4 of the disease, initiation of treatment is recommended irrespective of CD4 count [62]. Before initiation of ART treatment, a consideration for treatments of co-infections like tuberculosis, Hepatitis B, and C, etc. [63]. The opportunistic infections (OI) treatment is completed before initiation of ART; otherwise, it may be associated with a higher risk of AIDS-related deaths without significant virologic response [64]. The combination of antiretroviral therapy can be categorized into regimens, and the most approved regimen effectively decreases morbidity and mortality among the advanced HIV infection and AIDS [65]. The selection of regimen depends on the likelihood of adherence, affordability of drugs, cost of therapy, tolerability, and adverse effect profile, etc. NRTI drugs are used as a backbone in these therapies, and remaining drugs (PI, NNRTI, Integrase inhibitors) are combined in a dosage [66]. The recommended regimen is initiated after the failure of the previous line treatment. The assessment of treatment failure was explained in clinical, immunological, and virological terms [67].

Revised NACO ART Regimen [68]:

Regimen I	Zidovudine + Lamivudine + Nevirapine
Regimen I (a)	Tenofovir + Lamivudine + Nevirapine
Regimen II	Zidovudine + Lamivudine + Efavirenz
Regimen II (a)	Tenofovir + Lamivudine + Efavirenz
Regimen III	Zidovudine + Lamivudine + Atazanavir/ Ritonavir
Regimen III(a)	Zidovudine + Lamivudine + Lopinavir / Ritonavir
Regimen IV	Tenofovir + Lamivudine+ Atazanavir/ Ritonavir
Regimen IV (a)	Tenofovir + Lamivudine+ Lopinavir/Ritonavir
Regimen V	Stavudine+ Lamivudine+ Atazanavir/Ritonavir
Regimen V(a)	Stavudine+ Lamivudine+ Lopinavir/Ritonavir

1.5 HIV-1 inhibitors Reaction mechanism and resistance:

Nucleoside /Nucleotide Reverse Transcriptase inhibitors (NRTIs): In the HIV life cycle, reverse transcriptase plays a significant role in single-strand viral RNA translation to double-strand DNA [69]. Active drugs inhibit viral replication through chain termination. These inhibitors are competitive with natural dNTPs and are prodrugs converted by cellular kinases, which are phosphorylated to act as inhibitors. The growing viral chain is terminated by preventing the formation of 3'-5'phosphodiester bond in the presence of missing 3'-hydroxyl group moiety of the NRTIs [70]. Currently, there is eight FDA-approved NRTIs zidovudine (AZT, Retrovir), abacavir (ABC), lamivudine (3TC), zalcitabine (ddC), didanosine (ddI), emtricitabine (FTC), stavudine (d4T), and Tenofovir disoproxil fumarate (TDF)(Fig. 1. 4). The Resistance to RT is developed through the removal of NRTIs from the elongating chain resulting in transcription of dsDNA[71]. Resistance can also emerge by selective incorporation of native deoxyribonucleotide substrate over the inhibitor. However, some studies suggested that

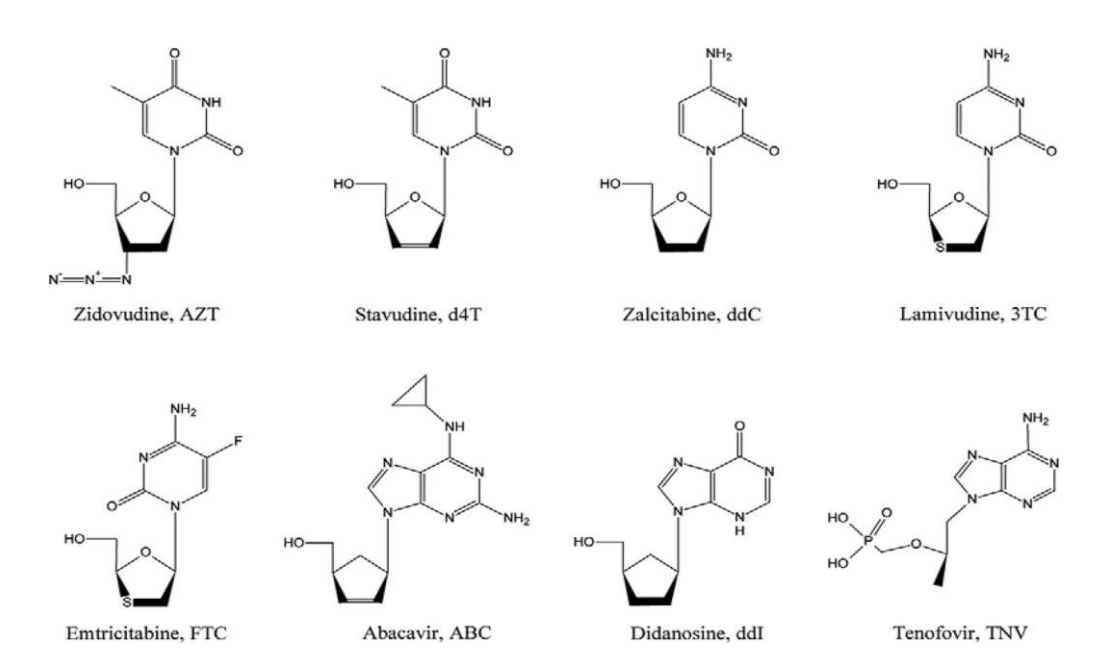


Fig. 1.4: NRTI reverse transcriptase inhibitors (Mem. Inst. Oswaldo Cruz. 2015, vol.110, n.7, pp.847-864).

Mutations specific for nucleoside/nucleotide (NAMs) or thymidine analogs are also reasons for the resistance [72].

NNRTI:

The NNRTIs mechanism is different from NRTIs and is used very extensively. The NNRTIs activity depends on how the molecules influence the RT enzyme active sites [73]. The observed crystal structure of HIV-1 RT consists of 66kDa(p66) and 51kDa(p51), two asymmetrical heterodimer subunits [74]. The p66 unit contained both polymerase and RNase H domains, whereas p51 has the polymerase active part [75]. The NNRTIs binding site is near the polymerase site and located far from the RNase H domain site [76]. Binding of NNRTIs to RT induces conformational changes in enzyme active site and reduces native substrate binding capacity for polymerization of the viral genome chain [77]. Unlike NRTIs, NNRTIs are structure-specific means those are not suitable for other viruses (HIV-2, SIV, etc.) [78]. The advantage of some NNRTI drugs is they have shown antiviral activity even after the integration of viral DNA, where they interfere in processing gag-pol polypeptide-mRNA slicing [79]. Approved drugs under this class include Delavirdine, Nevirapine, Efavirenz, Rilpivirine, Dapivirine, and Etravirine (Fig. 1.5) [80]. The resistance mechanism of the above drugs was explained in terms of allosteric site-specific mutations. Any single mutation in nucleotide can develop high resistance and affect RT's replicative fitness [81].

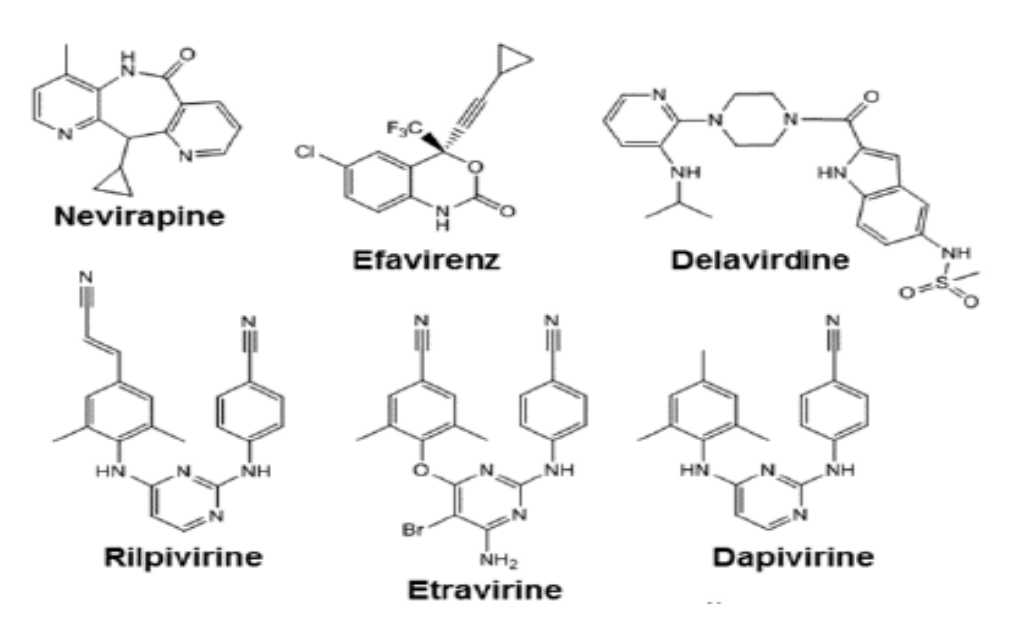


Fig. 1.5: NNRTI reverse transcriptase inhibitors (Viruses **2014**, 6, 2960-2973.)

Integrase inhibitors:

The role of the integrase enzyme (IN) in HIV infection is to integrate viral DNA obtained through reverse transcription into the host cell DNA. In catalyzes two reactions, 3'end processing involves exposed 3'hydroxyl group attached to CA dinucleotide. The second is the DNA strand transfer reaction, where the 3'hydroxyl group participates in the nucleophilic attack on phosphodiester bonds on opposing strands of chromosomal DNA [82]. The developed integrase target inhibitors mostly react on strand transfer reaction, where they specifically bind to integrase complex with DNA end strand [83]. The activity requires binding with two magnesium metal ion cofactors. Therefore, in the ART class, InSTIs essentially contain two pharmacophore sites, one for cofactor binding and other hydrophobic sites, specifically for binding to DNA. Approved Integrase inhibitors include Raltegravir (RA), dolutegravir, and Elvitegravir (EVG) [84]. A mutation mostly causes the Resistance of INIs in amino acids at magnesium cofactors binding active site and mutation in the integrase gene [85].

Fig. 1.6: Integrase Inhibitors (Future Sci OA. 2018 Sep 6;4(9): FSO338.)

Protease Inhibitors:

In HAART treatment, protease inhibitors are used as boosters in viral therapy combined with NRTIs and NNRTIs or integrase inhibitors [86]. The HIV-1 protease enzyme mediates the cleavage of viral gag and gag-pol polyprotein precursors during viral maturation. Pol polyprotein is cleaved from gag-pol polyprotein followed by further digestion into protease, reverse transcriptase, RNase H, and integrase [87]. The inhibitors that target protease cleavage active sites are highly effective with less resistance compared to NNRTIs [88]. However, PIs are associated with toxic side effects resulting from drug-drug interactions in regimen therapy and show adverse side effects in monotherapy [89]. The PIs currently approved include amprenavir (APV), indinavir (IDV), fosamprenavir (Lexiva), saquinavir (SQV), darunavir (TMC114), nelfinavir (NFV), lopinavir (LPV), atazanavir (ATZ), tipranavir (TPV), and ritonavir (RTV) [90].

The Resistance to PIs occurs mainly through the mutations at protease enzyme active site for gag-pol polyprotein cleavage and substrate /inhibitor binding site. The fully solved crystal

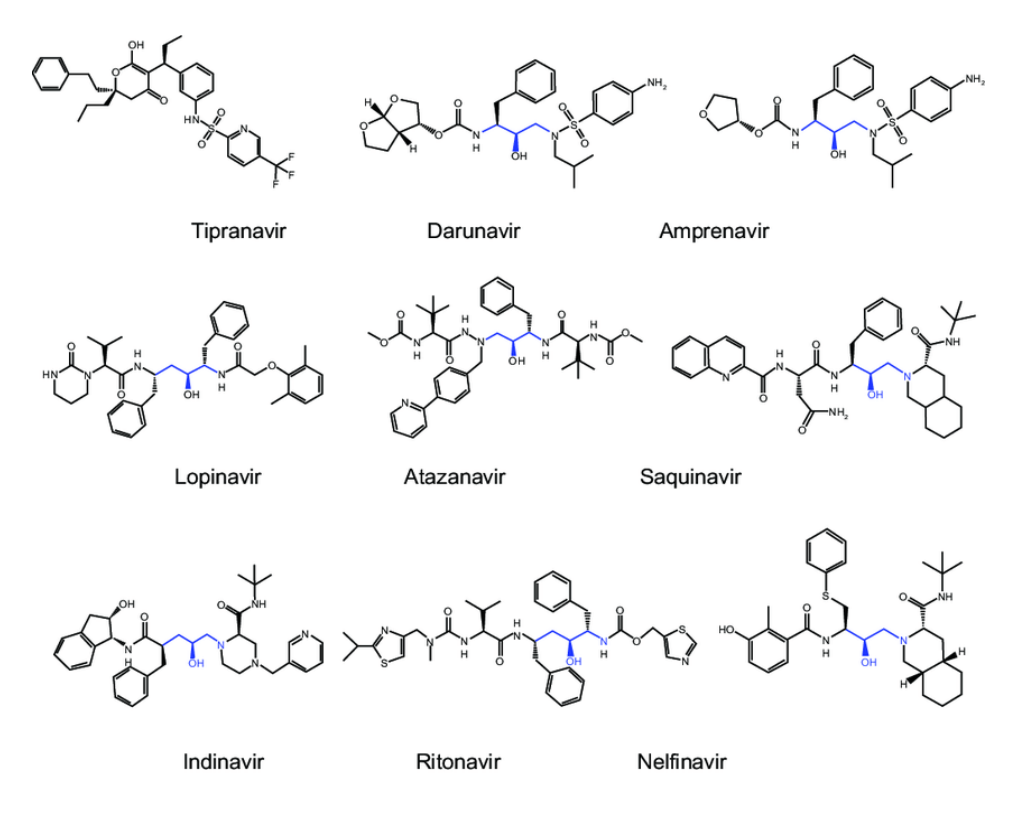


Fig. 1.7: Protease inhibitors (Lv Z, Chu Y, Wang Y. HIV AIDS (Auckl). 2015;7:95-104.).

structure of the protease enzyme facilitated the design and development of low resistance new inhibit

Capsid assembly inhibitors:

The capsid of the virus particle is made of building blocks of protein, arranged in a manner to form a cone structure [91]. The capsid contains the viral genome and essential proteins that play a vital role in the early and last viral replication and infection [92]. Hence, viral capsid disruption and inhibition of structural protein involved in capsid integrity are potential targets. Two inhibitors PF-3450071 and PF-3450074, have been developed that act on the capsid in the early HIV-1 replication stage [93].

HIV maturation inhibitors:

In HIV, maturation happens before the budding of the virus from the host cell. For viral growth, gag polyprotein precursor cleavage is necessary for positioning essential proteins for new virus development. Bevirimat (formerly PA-457) acts on gag processing, one of the active agents resulting in immature virions and a decline in plasma HIV -RNA level in patients [94].

Entry inhibitors:

The entry inhibitors act on the virus-cell entry process either on viral attachment to the host cell or on the fusion process after anchoring on the cell surface [95]. Protein-protein interactions and protein structural modification play a significant role during the entry process [96]. It is challenging to target highly mutated viral envelop protein; most of the drugs currently in a clinical study target host protein. The entry mechanism first involves envelope glycoprotein attachment to the CD4 receptor, followed by conformational modifications in viral envelope protein and further binding with co-receptors (CCR5 or CXCR4) [97]. The binding with the co-receptor ensures membrane fusion and viral core transfer into the host cell's cytosol. The exposed structure of envelope protein gp41 ectodomain participates in fusion. Active confirmation of gp41 forms a trimeric coil packed into a six-helix bundle [98]. Based on the inhibitor's target site, the entry inhibitors are subdivided into CD4 antagonists, co-receptor antagonists, and fusion inhibitors [99].

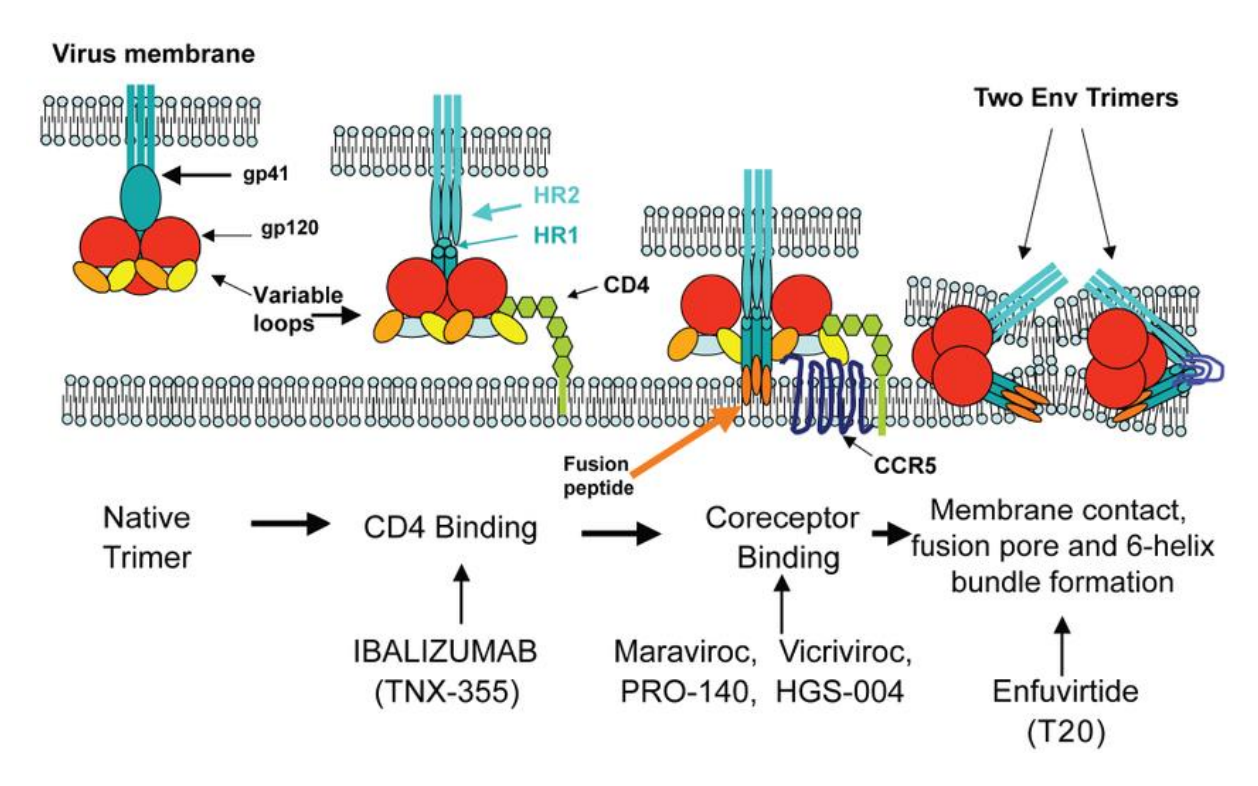


Fig. 1.8: HIV fusion, entry, and inhibitors (Latinovic O, Kuruppu J, Davis C, Le N, Heredia A.Clinical Medicine Therapeutics. January 2009.)

CD4 antagonist:

The antagonists block the attachment of gp120 -CD4 and the conformation suitable for coreceptor binding. Researchers developed a monoclonal antibody against the CD4 receptor, soluble CD4 (sCD4) against gp120, microbicide to control vaginal transmission, and some small molecules that disrupt gp120-CD4 binding [100]. However, all inhibitors failed in preclinical, clinical trials due to lack of physiological properties and resistance. Some developed CD4 antagonists include, BMS-378806 (CD4-gp120 Attachment inhibitor) PRO-542 (CD4-Ig fusion), TNX-355 (Ibalizumab, Anti-CD4 Mab) [101].

Co -receptor Antagonist:

The co-receptors are transmembrane G protein-coupled receptors that have been associated with multiple diseases such as cancer, rheumatoid arthritis, asthma, HIV, transplant rejection, etc. In HIV-1 essential co-receptors are CCR5, CXCR4 that play a significant role in viral entry through binding with CD4 induced conformation of gp120 variable loop (V3) [102]. Early after infection, most HIV-1 variants are CCR5 mediated, later converted to CXCR4; however, some viruses use both co-receptors. CCR5 is the essential co-receptor for virus infection, and hence

inhibition of conformational changes is necessary for inhibition of the virus [103]. Some of the antagonists have been developed, which are native/modified CCR5 substrates (CCL3 (MIP-1a), CCL5 (RANTES), CCL4 (MIP-1b), and RANTES analogs) and allosteric site binding small molecules. One of the small molecules maraviroc, approved by the FDA [104], binds at the hydrophobic pocket region in CCR5, creating conformational changes resulting in the blocking of v3 loop interaction ECL2 loop of CCR5. Some co-receptor antagonists under development currently include Aplaviroc (CCR5 antagonist), vicriviroc (CCR5 antagonist), TAK-652 (CCR5 antagonist), INCB009471 (CCR5 antagonist), AMD3100 (CXCR4 antagonist), and PSC-RANTES (Chemokine analog Microbicide) [105]. The host protein CCR5 targeted antagonist's resistance mechanism differs from other ARV drugs. The reasons can be explained in 1) virus tropism switching, 2) virus effectively using inhibitor bound receptors also for entry, 3) Faster rate of entry 4) high availability of co-receptors [106].

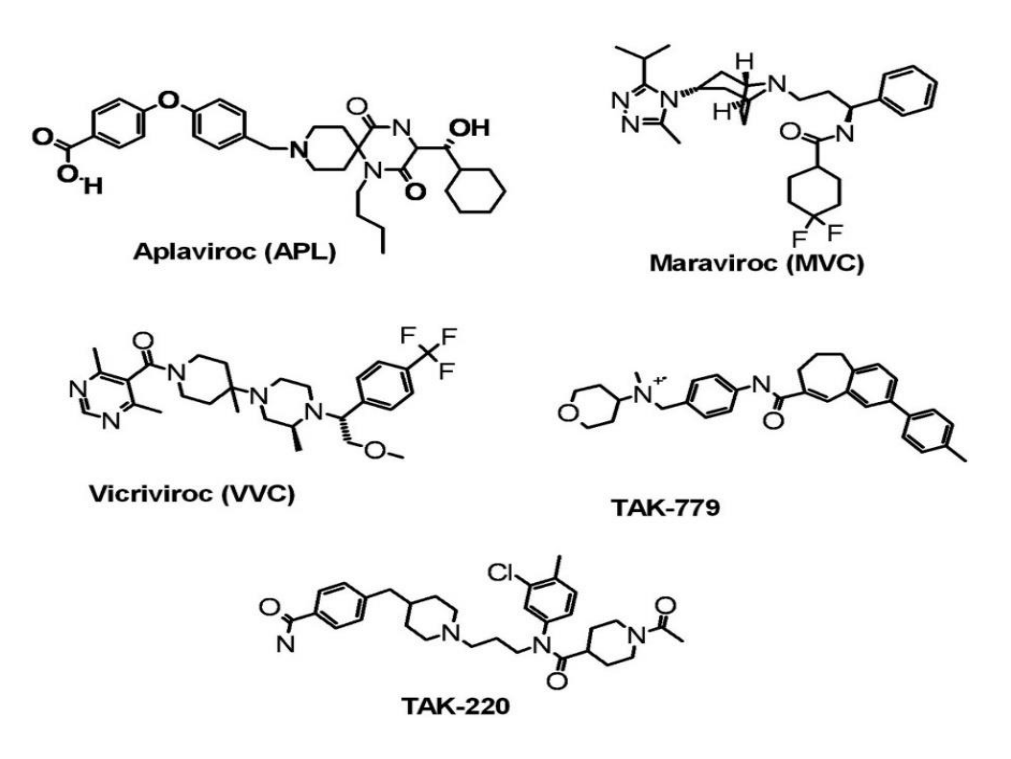


Fig. 1.9: CCR5 Antagonists (Rama Kondru et al., Molecular Pharmacology March 1, 2008, 73 (3) 789-800).

Fusion inhibitors:

The fusion process is an intermediate step between virus pre-entry and posts entry. The six-helix bundle formation is initiated at gp41 N -terminus, and two adjacent heptad repeats (HRs) reorient to form a thermostable helix bundle. After constructing the bundle, viral and cell membranes parallelly come together, followed by a hydrophobic fusion peptide region inserted into the cell membrane to form a pore for viral core transfer [107]. Disruption of the bundle formation by mimicry of one of the domains helps inhibit virus fusion. In the rational design of peptides, the alpha helix homolog, a 36 -amino acid peptide Enfuvirtide

(T20, Fuzeon) that binds with the HR2 region of gp41, was approved by the FDA in 2003 as a fusion inhibitor [108]. The problem with fusion inhibitors is the low oral bioavailability of the peptide molecules. Even though a substantial amount of research to successfully develop this class's compounds is being done, only the T-20 Fusion inhibitor is currently approved for patient use, the T-1249 Fusion inhibitor was discontinued, and the C- 34 Fusion inhibitor is under preclinical trials [109].

The resistance of enfuvirtide was shown to be by the virus was mutated in the heptad repeat region of gp41 and intrinsic susceptibility to mutations outside the enfuvirtide binding site [110]. The less availability of enfuvirtide drugs during co-receptor engagement and helix bundle formation is also a reason for resistance.

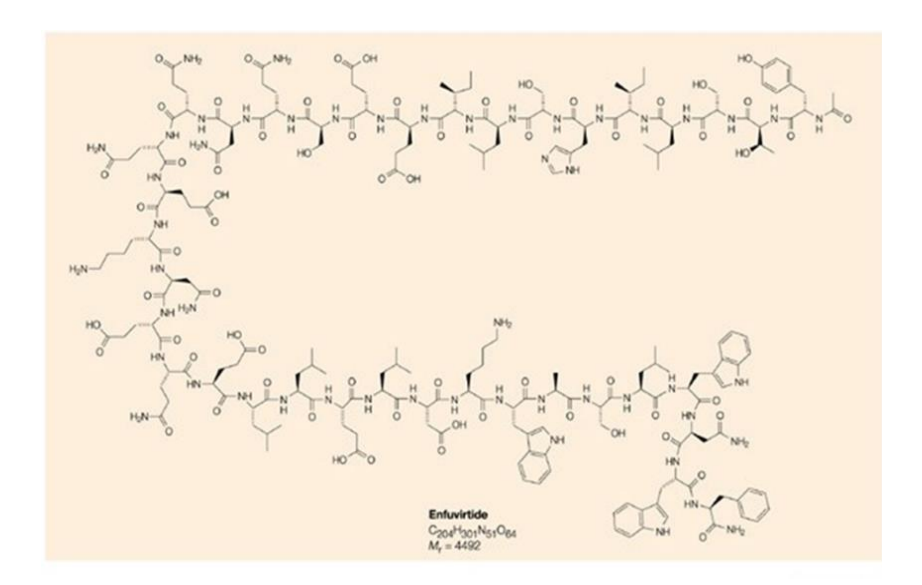


Fig. 1.10: Structure of T-20 (Enfuvirtide) (Nat Rev Drug Discov **3,** 215–225 (2004)).

1.6 HIV entry inhibitors development and challenges:

The envelope protein is a glycoprotein and is a precursor of viral gp160 and is synthesized at the endoplasmic reticulum (ER) followed by glycosylation and maturation gp120/gp41 trimeric complex at the trans-Golgi complex [111]. Subsequently, combined with HIV-1, Gag proteins embeds into the transmembrane of new infectious virus particles. In the early and late stages of the viral life cycle, envelop proteins are a prominent target for both the human immune system and other synthetic molecules (recombinant antibodies, peptides, and small molecules) to prevent and eliminate the viral infection [112]. In the process, the new direction of studies that include targeting latent virus reservoir activation and interferon-induced antiviral proteins, which are the target in enveloping protein maturation and assembly process, have been extensively taken up [113]. For example, cellular protease (furin, furin-like protease, and serine proteases) are involved in gp160 proteolytic cleavages, which are good targets for disrepute envelop function. The virus entry mechanism follows several structural strategies that facilitate drug design and development. The advantage of viral protein targeted entry inhibitors is that they need not cross the host cell membrane and attack free viral particles before attaching to the host receptors [114]. Entry inhibitors have been discovered in different strategies, which are 1) structure-based rational drug design, 2) phage display technique exposing with a library of peptides, 3) monoclonal antibodies towards conserved regions on gp120 4) small molecules screening by in-vitro assay [115]. The major hurdles for immunological and small molecule therapeutic intervention of virus infection are high mutations in gp120 regions and masking of the conserved region by carbohydrate groups (glycan shield) [116]. Structural biology and mutagenesis studies have given essential insights for drug design and development to block viral entry [117]. There are numerous therapies in the developing clinical stage for the US FDA, thus promising the arrival of multiple new entry inhibitors, either virus or cellular protein target.

1.7 HIV nano-drug delivery and Importance:

The durable mutagenesis nature and latency of HIV have been challenging to control and cure. It continues to be the center of research efforts as the complete cure and prevention remain elusive. Only ART treatment-based control of viral load over a lifetime. A drug has been taken

regularly during the HAART treatment, but it has some problems like toxicity, tolerability, and less adherence to patients [118]. Less commitment to treatments

is common among patients because of drug-drug interactions, less water-soluble drugs, multiple pharmacological reactions, target resistance, and nontargeted interactions [119]. To improve treatment adherence, revolutionary nanotechnology has been widely used in the present century. Different materials are used in nanoscale treatment to prepare formulations with specific properties that impact their delivery [120]. In clinical treatment, mostly biodegradable materials are considered to ensure biocompatibility with the human body [121]. The nanoscale drug delivery platform improves the half-life of drugs by control delivery and decreases side effects [122]. Additionally, structural modification on the particles' surface with functional groups facilitates the targeting receptor-specific delivery of drugs. The potential

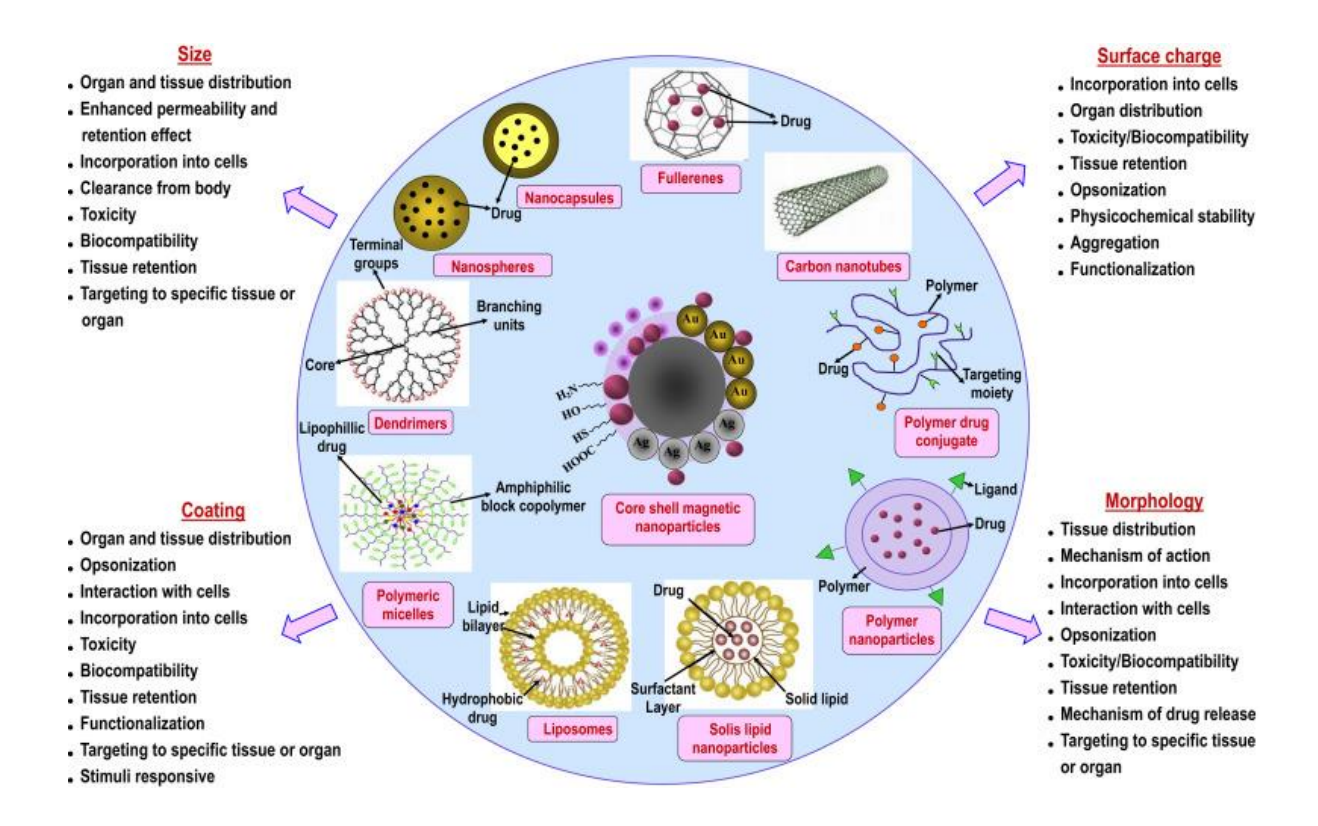


Fig. 1.11: Nanoparticles and Importance in drug delivery (VikasRana et al., Nanoscience and Nanotechnology in Drug Delivery Micro and Nano Technologies 2019, Pages 93-131).

nanotechnology also provides versatile preventive options for HIV in antiretroviral therapy, immunotherapy, vaccinology, gene therapy, and microbicides. [123].

Nano antiretroviral therapy: In nanoparticle-based antiretroviral treatment, the polymeric material is used for drug loading and delivery. Some of the materials Nano-drug delivery system could enhance the distribution of hydrophobic, hydrophilic, and macromolecules within the tissue and intercellular site with its small size [124]. Antiviral drugs can be loaded into nanomaterial to target CD4⁺ T cells and macrophages, major viral reservoirs. For example, polyethylene-polypropylene glycol (poloxamer 338) and PEGylated tocopherol succinate ester (TPGS 1000) was loaded with rilpivirine to improve the half-life of free drugs [125]. Another study demonstrated stavudine encapsulated other liposome surfaces modified with mannose and galactose used for receptor-mediated internalization at macrophages [126].

Nano gene therapy: Efforts to identify new and alternate antiviral therapy lead to gene therapy identification. This method involves a gene transported into cells to interfere with viral replication. Nucleic acid compounds like DNA, aptamers, and siRNA are used for gene therapy [127]. Nano delivery method is used in non-viral vector gene delivery and RNA interference (RNAi) in which target gene slicing and destruction of the mRNA of interest gene is done by the siRNA molecule [128]. In the case of HIV/AIDS, RNAi can target either cellular or viral proteins that are involved in infections. Non-viral siRNA delivery with polymers, liposomes, and peptide conjugated antibody was previously reported for effective delivery at macrophages and T-cells [129].

Nano immunotherapy: Another approach to preventing HIV infection to the host cell is immunotherapy. The immune system responds and releases active molecules against HIV to prevent virus infection and replication. But the human immune system is unable to adapt to the virus's escaping strategies [130]. Hence it becomes exceedingly difficult to eradicate the virus from the body. Immunomodulators are a class of molecules used to modulate and activate the immune system against HIV. CD8⁺T cells and B -cells play a major role in immune response to produce cytotoxic agents and neutralizing antibody, respectively. The immune system's susceptibility depends on the availability of antigen agent at antigen-presenting cells (APCs). The delivery of antigen agents at target cells is exceedingly difficult; hence nano delivery platform can enhance the modulator's availability through receptor-mediated delivery on target cells. Poly (lactic-co-glycolic acid) (PLGA), poly(D, L-lactide)

(PLA), and polyethyleneimine mannose (PEIm), etc. are used as delivery materials to deliver immunogenic agents in the vaccination process against HIV/AIDS [131].

Nano microbicides: Vaccination against HIV is complicated, and hence alternative methods for preventing viral transmission are studied. Majorly, viral transmission happens through sexual transmission, and prevention of this rote of infection and control of viral spread is of Utmost Importance [132]. Condoms are the current method to prevent transmission via this route. However, in the case of women, protecting methods have not been readily available. Microbicides are protecting agents used for preventing sexual transmission of HIV and other STDs. They are usually in the form of gels most applied internally in the vagina. Most of the ART drugs are formulated as microbicides and used in the sexual therapeutic intervention [133]. However, most microbicides are failures at clinical trials due to virus mutation and low availability of drugs in the mucosal layer of the vagina. This necessitates a new approach for improving the microbicidal activity of the drugs [134]. Nano formulation and inter vaginal nano delivery mechanism, which increases the availability of drugs, both external and internal tissues, are being explored to overcome the current challenges [135]. The formulation processes of these nanosystems use some unique materials like L-lysine dendrimer, poly (propylene imine and PLGA, etc. due to their properties that contribute to the requirement for this mode of delivery [136].

Nano drug delivery is a promising delivery approach for improving patient compliance with better target delivery and a superior safety profile [137]. The drug delivery route and dosage of active molecules vary with nano delivery system design. The essential properties of nanosystems, such as particle size, shape, surface charge, and specific functional groups, can modify bioavailability and targeting [138]. Small and specific functional groups can penetrate the cellular surface and promote intracellular drug delivery in a target-specific manner without extracellular degradation [139]. In HIV/AIDS treatment, the nano delivery system mostly favors elimination or prevention pathways such as vaccination, microbicides formulation, and receptor mediate inhibition.

1.8 Early pregnancy-associated protein (Epap-1) and its action:

The protein Epap-1 isolated from first-trimester pregnant women is 90 KDa protein. It has been reported to possess antiviral activity through broad interactions with conserved and variable regions on envelope protein (gp120 + gp41). The interactions are highly conserved in varied

strains of the virus leading to inhibition of viral entry [140]. However, in its clinical use, some challenges are raised related to the production, stability, and delivery of the protein. Hence, there is a need to develop new small peptidomimetics that work as the active protein.

1.9 Broadly neutralizing antibody 447-52D against gp120.

The immunological neutralization of highly variable HIV-1 like a virus through antibodies has been difficult due to predominate mutations in spike proteins along with glycosylation shielding. However, some conserved and variable regions on envelop proteins come out from the shieling and exposed outside during the entry mechanism. Those regions are immunogenic and induce antibodies in variant strains of the virus. For example, anti-V3 broadly neutralizes antibodies like 447-52D and 2219, interacting with other immunodominant regions on gp120 [141]. The interaction regions of the V3 loop and antibody guide in exploring small molecule for sight specific interactions on viral protein.

1.10 Lactoferrin as nanocarrier:

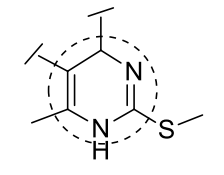
Lactoferrin (Lf) is a transferrin family 80KDa glycoprotein, abundantly available in mammal milk, secretory fluids, and white blood cells[142]. The protein has shown antiviral, antibacterial, and antifungal activity [143]. The biocompatible and multi-active protein was established as a nanocarrier for active drug delivery [144]. The preparation and site-specific delivery are essential for nano delivery, which could be possible by merely preparing and modifying functional groups on surface particles. In Lf, preparation and receptor-based delivery were possible by oil in the water sonication method and transferrin receptors on human cells, respectively [145]. However, Lf-NPs have been reported as drug carriers for HIV-1 ART drugs with optimal results[146]. To improve the efficiency and target specificity of the Lf - NPs, the surface was modified in some groups to target viral protein, which is acting as a dual-purpose carrier.

1.11 Small molecule drug discovery and Chemical structural evaluation of hydropyrimidine and s-triazane derivatives as inhibitors:

"Fragment-based drug discovery" [147] is a method in which protein-peptide and protein - interacting antibody fragments are considered for small molecule mimetics design. The antibody or specific peptide interactions provide knowledge about valid target site recognition,

consequently, reduce the biological and chemical rick of small molecules. The compounds invoke similar effects as antibodies on-site and modulate protein-protein interactions [148]. The mimicking chemosuperiors are considering as "hits" for lead molecule development with various modifications. In general, QSAR or pharmacophore models have been used to further develop molecules for better binding at target protein [149]. But here, the small molecules were designed for HIV-1 entry inhibition based on broadly neutralizing antibody(447-52D) and active peptide (Epap-1) fragment interactions for retardation of virus entry. The selected molecules participated in hydrophobic, hydrophilic, and hydrogen bonds at the targeted site. The structural consideration of drug-like molecules with pharmacological stability, conformational changes, and reduced metabolism[150]. For example, Tetrahydropyrimidine (THPM) derivatives used as HIV-1 fusion inhibitors [151], and dihydropyrimidine (DHPM) derivatives were used as replication inhibitors[152]. Moreover, other biological activity inhibitors contain hydropyrimidine as a core structure. The activity and metabolic stability of the DHPM or THPM scaffold vary with functional changes in core structure (hydropyrimidine) with different bioisosteres, which facilitate optimization of targetspecific binding [153].

Another biologically optimal core structure is s-triazane or 1,3,5 -triazines involved in many biological activity molecules that include antimicrobials, anticancer, tumor growth inhibition activities, and estrogen receptor modulators drugs [154]. The 1,3,5 -triazine scaffolds were synthesized by nucleophilic substitution of less expensive cyanuric chloride with different functional groups. The sequential ring substitution was depending on temperature and reaction time [155]. The triazine ring's structural advantage was electrostatic interaction with other rings based on electrons' nature donating and withdrawing group substitutions.



Dihydropyramidine



Tetrahydropyramidine



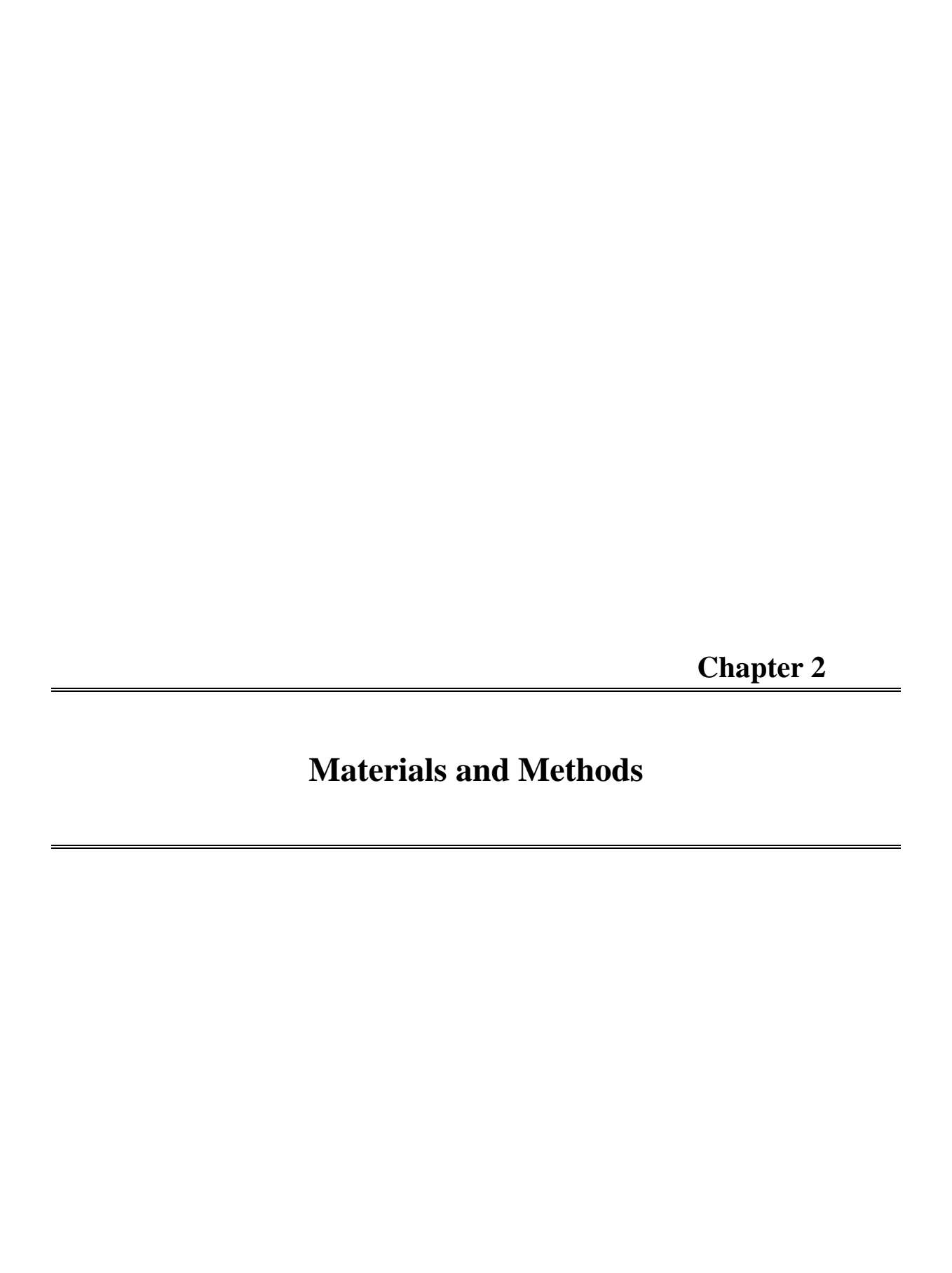
1,3,5- triazine

1.12 Rationale of the study:

Early HIV-1 inhibition is essential for viral load control, which is possible through entry inhibitors. But only two entry drugs have been used in antiretroviral therapy, with one targeted to host protein, another targeting viral protein. In the study, we design, develop, and synthesize small molecules to target viral protein. The Epap-1 and 447-52D antibody interacting with viral envelope protein gp120 and the interacting regions were used to design drug-like molecules. In the study, another part was entry inhibited surface-modified lactoferrin nanoparticles used as drug (AZT) carrier for post-entry inhibition. The dual nature nanoparticle preparation characterization and biological evaluation.

1.13 Objectives of the work

- **Objective I:** Synthesis and characterization of novel HIV-1 entry inhibitors based on Epap-1 derived peptide targeting envelope gp120.
- **Objective II:** HIV-1 envelope protein V3 loop and neutralizing antibody 447-52D interactions based on derived molecules development, synthesis, and characterization.
- **Objective III:** Sulfonate modified lactoferrin nanoparticles as drug carriers with dual activity against HIV-1.



2.1 Materials:

All reagents and solvents were of analytical grade and were used without further purification. High precision instruments were used for molecular characterization.

2.1.1 Reagents:

Bovine Lactoferrin was purchased from Symbiotics, USA. Purified pharmaceutical grade AZT. Doxorubicin hydrochloride (Doxo) purchased from TCI Co.,Ltd .MES (sodium 2mercaptoethane sulfonate) was purchased from (Sigma Aldrich, USA). Olive oil was procured from Leonardo. Curcumin (SRL Chemicals) - excitation/ emission 420 nm/470 nm. Uranyl Acetate (Spectrochem Pvt Ltd), Copper Grids (ICON Analytical), the lactoferrin receptor antibody (Interleukin 1 Invitrogen Cat No:PA577179), V3 loop antibody (NIH Reagents Programme, Cat No:2343), DNA ladder, MTT(Sigma Aldrich), P24 KIT (ABL INC), Coomassie Brilliant Blue R(sigma), DAPI (Thermo-Fisher scientific) -Excitation/Emission-358nm/461nm. Calcein AM (Cat No:C3100MP excitation/emission 488nm/570nm), Hoechst 33342(Invitrogen Cat No:H3570 excitation/emission 350nm/461 nm), Con A (sigma#c2010), Sepharose 4B (Cat No: 4B200). RPMI 1640 media((Gibco), DMEM/F-12(Gibco) media, MEM(Gibco), Foetal bovine serum (FBS, Gibco), Trypsin EDTA 0.5%, Penicillin Streptomycin antibiotic Sodium methoxide (SigmaAldrich), Acetophenone (Sigma Aldrich), Ethyl picolinate(Sigma Aldrich), Benzaldehydes(Sigma Aldrich), p-TsOH, glacial acetic acid (finar), 1,4- dibromo-3,4-butanone(sigma), K₂CO₃, dry DMF(finar), dry THF (finar), ethyl acetate(finar), tetramethyl silane (TMS), DMSO-d₆ (Sigma Aldrich), 2,4,6-trichloro -1,3,5 triazene (cynuric chloride, Sigma Aldrich). Isonizide(Sigma Aldrich) ,hydrazine(TCICo.,Ltd),ethyl2-chloro-2-oxoacetate(SigmaAldrich),Anthranilamide,ptoludine(SRL Chemicals), Acetone (finar), Culture grade DMSO (Sigma Aldrich)etc.

2.1.2 Cell lines:

Non-Hodgkin's T cell lymphoma, SupT1 cells, and Cervical epithelial HL2/3 cell lines (modified to contain stably integrated copies of the HIV-1 molecular clone HXB2/3gpt) obtained from NIH AIDS Reagent program.SK-N-SH cell lines (neuroblastoma) were obtained from ATCC. SKN-SH cell line derived from neuroblastoma, 3T3, a mouse fibroblast cell line acquired from NCCS, NIH were used to carry out the work.HIV-1 93IN101(Subtype C), HIV-1_{NL4-3} (Subtype C).

2.1.3 Instruments & Tools:

A Bruker AC NMR (400 MHz), HRMS, and FTIR, CO2 Incubator, Autodock Vina 4.0 (molecular docking), Graphpad Prism 6.0 (statistical analysis). Plate ELISA reader.Ultrasonicator (Model 300V/T of Bioloics Inc., USA), Transmission Electron Microscopy (TEM -Techni), FE-SEM-Carl ZEISS ultra-55, Germany, Nano sight (NS500), Zeta sizer (Malvern), Fluorescent Microscope (Carl-Zeiss), HPLC (Water), portable Raman spectrometer, B&W Tek, Nanodrop Lite (Thermo Scientific), Bruker Avance-500 MHz, MAS spectrometer, Bruker 4-mm H/X/Y MAS probe, Origin Pro software, topspin software, ImageJ Java 1.8.0_112.

2.2 Methods:

2.2.1 Design and Docking of molecules to target gp120:

The Epap-1 peptide interaction-based designed small molecules UHLMTA-E5 and UHLMTA-E8, E9 contains pyrazole and DHPM (dihydropyrimidine)as a significant scaffold, respectively. The slight modification in UHLMTA-E9 with a 2,3-diketobutane group and derived new derivatives UHLMTJ-E9.S(1-7). The development of major 1,2,3,4-THPM - thioxo,-oxo(UHLMTJ-254(a-g), UHLMTJ-255(a-g)) scaffold molecules towards target "phe43 cavity" binding were virtually explained through below molecular docking. The molecules were docked using Autodock Vina v4.0 [156]. For that, molecules were sketched using ChemSketch, and energy was minimized. The target gp120 molecule, 2B4C, was obtained from PDB and pre-processed before docking. Scanning for the binding region was set, and configuration files to run the docking were prepared. The grid box for the gp120 crystal structure, 2B4C, was set to 40*40*40 Å and was centered at X, Y, and Z coordinates of 99.723 -138.533, 136.561, respectively. The exhaustiveness of the run was set to 10. The default output was set as 10 conformations per molecule.

The molecules designed from 447-52D epitopes and gp120 interactions based are incredibly complicated to synthesize. In the molecules, most of them contained remarkably similar functional groups participating in gp120 interactions. Based on the previous literature [157], some of the molecules' parent chemical structures like s-triazane were shown to possess anti-

HIV-1 activity; hence, molecules with these structural frameworks were considered for new molecules design and development. The molecules were designed through the substitution of different functional groups on parent structure to facilitate better binding at the V3 loop. The virtual screening of molecules through docking was established as per the above docking procedure under coordinates. The grid box for the gp120 crystal structure, 2B4C, was set to 34x30x36 Å and was centered at X, Y, and Z coordinates of 52.777, 97.241, 59.716, respectively. The exhaustiveness of the run was set to 10. The default output was set as 10 conformations per molecule.

2.2.2 Chemical synthesis of 2-(3-phenyl-1H-pyrazole-5-yl) pyridine:

To take Acetophenone (19.8 mmol) and Sodium ethoxide (22.4 mmol) in dry THF solution (15ml) and a stirred suspension at room temperature (RT) followed by slow addition of ethyl picolinate (13.2 mmol) to the reaction, and the reaction was under reflux at RT for 20 hr. After completing the reaction, the suspension was neutralized with 2M HCl, and the compound was extracted with ethyl acetate. The resulting solid material was then dissolved in ethanol, and the further reaction was conducted with hydrazine hydrate under reflux at RT for 6h. The formed crude product was purified by sublimation at 85 °C, followed by recrystallization in a mixture of CH₂Cl₂ and hexane [158] (**Scheme 1**).

Scheme 1

2.2.3 General procedure for preparation of

Ethyl 6-methyl-4-phenyl-2-thioxo-1,2,3,4-tetrahydropyrimidine-5-carboxylate and Ethyl 6-methyl-2-oxo-4-phenyl-1,2,3,4-tetrahydro pyrimidine-5-carboxylate derivatives:

An aldehyde (1mmol) was taken in a 25ml round-bottom flask fitted with a reflux condenser, and added ketoester (1.2mmol), thiourea (1.5mmol), p-TsOH (25mg), EtOH (10ml). The mixture was heated to 78 °C under reflux for 0.5–4h, and the TLC was used for reaction progress monitoring. After completing the reaction, the solution cooled to room temperature and then filtered to get the crude product. The product purified by rinsing with toluene and water, then dried to obtain the desired products as a solid crystalline 2.2a-g [159].

The product of 2.2a-g (0.01 moles) and 1,4-dibromo-3,4-butanone (0.05 moles) was dissolved in 10 ml DMF and then basified with K_2CO_3 . The mixture heated at $100\,^{0}$ C overnight, and then the reaction was monitored by TLC. After completion, the response was cooled and washed with brain solution and extracted into ethyl acetate get the crude product that was purified by column chromatography and analyzed to get the product 2.4a-g despite 2.3a-g (**Scheme 2**).

Scheme 2

2.2.4 Synthesis of 2-(2-(5-bromo-2-hydroxybenzylidene) hydrazinyl)-2-oxo-N-(p-tolyl) acetamide:

p-toluidine (1eq) solution in dry dichloromethane (DCM) was added TE(triethylamine)(1.5eq), and then added to ethyl 2-chloro-2-oxoacetate(1.2eq) in DCM dropwise at 0 °C. The reaction was carried at 0 °C for 1 h and then at room temperature for 6 h. After completing the reaction, the reaction mixture was washed with 25% aqueous solution of K₂CO₃, followed by extraction with ethyl acetate and dried over Na₂SO₄. The solvent evaporated to get a solid white product with a 75% yield.

The white product of **2.5** (1eq) and the hydrazine hydrate (2eq) was reflexed overnight and then poured into crushed ice to get white precipitate finally crystallized from ethanol to obtain a white powder with 50% of yield.

A few drops of glacial acetic acid added to the ethanolic solution of product **2.6**(1eq), then 5-bromosalicylalhyde (1eq), was added, followed by a reaction mixture stirred for 4h at room temperature(RT), and then cooled on ice to precipitate the product. The yellowish-white precipitate was filtered off and then crystallized from hot ethanol to obtain **2.7**as a final product [160].

$$\begin{array}{c} & & & \\ & &$$

Scheme-3

2.2.5 Synthesis of 2-(4-aminophenyl)-2,3-dihydroquinazolin-4(1H)-one:

The anthranilamide (0.73 mmol) was dissolved in 2ml of acetonitrile, then mixed with 4-nitrobenzaldehyde (0.73 mmol) and cyanuric chloride (0.135 mmol, 10 mol %) at RT. The reaction mixture was reflexed at 70 °C for 0.5 hr, and after the reaction was completed, the access solvent was evaporated and washed with cooled water to get a yellow solid (2.8) with a 95 % yield [161]. The solid nitro, compound 2.8 (0.01mol), was dissolved in a mixture of ethanol (10 ml), water (0.05 ml), and added few drops of a con. HCl. The solution was gently stirred for 10 min at RT and then added iron metal powder (0.03 mol) and NH₄Cl (0.03mol). Finally, the total mixture was refluxed for 0.5 hr at 60 °C. TLC was used for monitoring the completion of the reaction. After completing the reaction, the reaction mixture was cooled at RT and then neutralized with the aq.solution of 10% NaHCO₃, poured into cooled water, and filtered to get the solid supernatant cake, which was washed with hot ethanol and chloroform in 1: 1 ratio. To obtain the final compound, evaporate the solvent, and got the pure amino compound (2.9) with a 40% yield; no further purification was required [162].

$$\begin{array}{c} O \\ NH_2 \\ NH_2 \\ \end{array} + \begin{array}{c} NO_2 \\ \hline \\ CH_3CN, \ 40^0C, 0.5 \ h \\ \end{array} \\ \begin{array}{c} O \\ NH \\ \hline \\ CH_3CN, \ 40^0C, 0.5 \ h \\ \end{array} \\ \begin{array}{c} O \\ NH \\ \hline \\ NH_2 \\ \end{array} \\ \begin{array}{c} COI.HCI, Fe, NH_4CI \\ \hline \\ Ih \\ NO_2 \\ \end{array} \\ \begin{array}{c} NH \\ NH_2 \\ \end{array} \\ \begin{array}{c} O \\ NH \\ NH_2 \\ \end{array} \\ \begin{array}{c} O \\ NH \\ NO_2 \\ \end{array} \\ \begin{array}{c} O \\ NH \\ NH_2 \\ \end{array} \\ \begin{array}{c} O \\ NH \\ NH_2 \\ \end{array} \\ \begin{array}{c} O \\ NH \\ NO_2 \\ \end{array} \\ \begin{array}{c} O \\ NH \\ NH_2 \\ \end{array} \\ \begin{array}{c} O \\ NH \\ NH_2 \\ \end{array} \\ \begin{array}{c} O \\ NH_2 \\ \end{array}$$

Scheme-4

2.2.6 General procedure for 2,4,6-trichloro -1,3,5 -triazene substituted derivatives:

Monochloride substitution of 2,4,6-trichloro -1,3,5 -triazene with Arylamines:

The mixture of 2,4,6-trichloro -1,3,5 -triazene (0.01mol) and arylamine (0.01 mol) was taken in acetone and stirring at 0-5 °C. After 1hr, 4% of NaOH solution was added dropwise with rapid stirring and then continue the reaction up to 2hr. After completing the reaction, the mixture was poured into crushed ice and then neutralized with 2M HCl under continuous

stirring to get solid. The solid compound was filtered, washed, and dried, and recrystallized in acetone [163].

In the case of sulfonic acid products, the ice water was acidified at pH 2.0 and filtered off to get sold product.

Dichloride substitution of 2,4,6-trichloro -1,3,5 -triazene with Arylamines:

The monochloride substituted triazene (0.01mole), and the arylamine (0.01mol) were dissolved in 1,4- dioxane at RT. During the reaction, the released HCl was neutralized with dropwise added 4% of NaOH (Alternatively, dry DMF as a solvent and K₂CO₃ as a neutralizing agent also used) and continue reaction up to 3hr and maintained reaction mixture at pH 7.5 to 8.0. After completing the reaction, the total blend was neutralized, washed with excess water, filtered to get the recrystallized product in acetone, and dry DMF [164].

In the case of sulfonic acid products, the ice water was acidified at pH 2.0 and filtered off to get sold product.

Trichloride substitution of 2,4,6-trichloro -1,3,5 -triazene with Arylamines:

Dichloro substituted triazene (0.01mole) and arylamine (0.02mol) in dry acetic acid under N_2 conditions were reflexed at 110 0 C for 1hr. After relaxation, the reaction mixture was cooled and into ice-cooled water, then was filtered to get a solid product. Finally, the compound was washed with hot water and hexane to get a required product, which was further crystallized with 1,4-dioxane [165].

Scheme-5

Scheme-6

Isonizide (2eq),

Dry AcetiC acid ,110
0
C,1hr

$$R = -\frac{1}{5} - NH_{2}$$

$$= -\frac{1}{5} - OH$$

$$= -\frac{1}{5} - OH$$

Scheme-7

Scheme-8

2.2.7 Preparation and Physical Characterization of nanoparticles:

For the preparation of drug-loaded Lf NPs, 10mg of the drug was dissolved in 100 µl of DMSO and added to 40mg/ml Lf in PBS (pH 7.4), followed by incubation on ice for a period of 60min. The incubated mixture is added slowly to 25ml of olive oil and sonicated at 4°C incubated on ice. The ultrasonicator horn was positioned at the oil-water interface, and the sonication was done at 20kHz with 60% efficiency over 15min, followed by incubation on ice for 4h. Finally, formed nanoparticles were separated by centrifugation at 6000rpm for 30 mins. The remaining oil was decanted; the remaining oil was removed from the pellet by washed with an excess of cold diethyl ether. Further, the pellet was dissolved in 1X PBS (pH 7.4) and stored at 4°C for later use [166]. Blank NPs were prepared using the method described, without incubation with the drug.

MES conjugated nanoparticles were prepared using 30mg of MES powder to the above mixture of drug and Lactoferrin and incubated for another 15min. Sonication and work-up to obtain the final nanoparticles were performed as described. The sonochemically prepared Lf-MES/Lf-MES-drug nanoparticles were dialyzed at 4°C overnight to remove an excess of MES. Formed particles were dissolved in 1X PBS (pH 7.4) and stored at 4°C for characterization and later experiments.

2.2.8 Characterization of Size and shape of nanoparticles by FE-SEM and TEM:

Evenly distributed nanoparticles ($10 \,\mu l$) were spotted onto the Copper grid (Carbon type B 200 mesh), followed by drying and staining with 2% (w/v) Uranyl acetate. The stained and dried particles were analyzed for size using Transmission Electron Microscopy. In the case of Field emission Scanning Electron Microscopy analysis, the sample was spotted on a sterile glass slide and allowed to dry. Dried slides were coated with gold and analyzed with FE-SEM as per imaging instructions.

2.2.9 Size and charge the distribution of nanoparticles in suspension:

The stability and incorporation of MES on Lf-NPs were explained by charge distribution on the particles. For sample preparation, a low concentration of nanoparticles was dissolved in Milli Q water and injected into the Nano sight and Zeta sizer, respectively, at 25^oC[167].

2.2.10 Agarose gel electrophoresis for charge-based nanoparticle migration study:

The native agarose gel (0.8%) was prepared in buffer A (25 mM Tris-Cl (pH 8.5) 19.2 mM glycine). 2-5 µg of each sample was mixed 1:1 (v/v) with 2x loading dye (20% glycerol, 0.2% bromophenol blue, 0.12 M Tris-Cl), an equal concentration of samples was loaded into the wells. DNA Ladder was loaded to mark the movement towards the anode. The gel was run at 50V constant Voltage at room temperature for 1 hr in Tris-Cl buffer pH 8.5. The gel was stained with Coomassie stain (0.12% Coomassie Brilliant Blue R 45% methanol 10% acetic acid) and destained with a destaining solution (45% methanol and 10% acetic acid[168]. The images of

the gel were captured in Gel Doc (ChemDoc Imaging system). Two images, one taken in UV range to visualize the DNA marker and the other taken to locate the protein (nanoparticles), were taken separately and merged.

2.2.11 pH- dependant drug released study:

Freshly prepared Lf-NPs containing 1mg of AZT (Lf-AZT NPs) were incubated with 1ml PBS at different pH (2.0-9.0) for 12hrs. Post-incubation, nanoparticles were treated with 200 µl of 30% AgNO₃ to precipitate the protein. The drug was further extracted into the organic phase by adding 1ml HPLC grade methanol. AZT was separated using a reversed-phase C-18 column. The mobile phase for AZT was acetonitrile: methanol (60:40 v/v) at wavelength 265 nm. The total mixture was centrifuged at 12000 rpm for 20 min, and the supernatant was filtered using a 0.4-micron syringe filter and quantified by HPLC [169]. The above method was followed for Lf-MES AZT NPs.

2.2.12 Drug Loading Capacity (LC) and Drug Encapsulation Efficiency (EE).

Nanoparticles were incubated in 1ml PBS (pH 5.0) at RT for 24 h on the rocker to release the drug into the aqueous phase. 200 µl of 30% AgNO₃ was added to the incubated NPs to precipitate protein. The drug was further extracted into the organic phase by adding 1ml HPLC grade methanol. The total mixture was centrifuged at 12000 rpm for 20 min and syringe filtered using a 0.4-micron filter and quantified by HPLC. LC and EE are then calculated by the below formula [169].

$$LC\% = (Mass\ of\ the\ drug\ in\ NP \div Mass\ of\ NP) \times 100$$

 $EE\% = (Amount\ of\ drug\ present\ in\ NP$
 $\div\ Initial\ amount\ of\ drug\ used\) \times 100$

1.4x10⁵ HL2/3 cells were seeded and allowed to adhere. Curcumin was used for tracking the drug due to its intrinsic fluorescence. Cells were incubated with 10µM of Curcumin containing Lf-NPs and Lf-MES NPs at time points 30min, 1hr, 2hr,4hr,8hr,12hr. The cells were washed with PBS (pH 7.4) to remove excess nanoparticles, followed by fixing and staining with DAPI.

The coverslips were washed, mounted on glass slides, and observed under Fluorescent Microscope. The fluorescence was quantified using ImageJ software.

2.2.13 Analysis of MES conjugated Lf nanoparticles by solid-state NMR:

Sample preparation: Preparation of Lf- MES NPs were prepared as per procedure given in section 4.3.1and then formed particles were lyophilized to get solid particles in powder form for Solid-state ²³Na NMR. The other chemicals MES and NaCl were used as controls in pure solid form.

MAS NMR: Solid-state 23 Na NMR spectrum was obtained under the Bruker Avance-500 MHz, MAS spectrometer, Bruker 4-mm H/X/Y MAS probe was used as sample spinning container with 0-15kHz range speed and operating at 132.336 MHz. All 23 Na chemical shifts were referenced to 0.1 M NaCl (aq), and the solid-state NaCl chemical shift was obtained at δ =7.2 ppm. The spectrums were plotted in the topspin software program.

2.2.14 Characterization of functional groups on protein nanoparticles:

The Lf NPs, Lf-MES NPs, and MES were dissolved in PBS (pH 7.4) and added to the gold nanoparticle (Au-NPs) coated glass slides. The nanoparticles could be adsorbed on the slide by over-drying under vacuum at room temperature. Dried samples were probed with 785nm excitation by Raman spectrometer. Finally, enhanced peaks were plotted by Origin Pro software.

2.2.15 Cellular localization of fluorescent dug (Curcumin) loaded NPs by Confocal study and localized drug (AZT) quantified by HPLC:

(i) Cellular localization of fluorescent dug (Curcumin) loaded NPs by Confocal study.

Cellular localization of NPs in the SK-N-SH cell line devoid of receptors of Lf-MES NPs was analyzed as a negative control. 1.4 x 10⁵ SKNSH cells were seeded and allowed to adhere. Cells were incubated with 10µM of Curcumin containing Lf-NPs and Lf-MES NPs at time points 30min, 1hr, 2hr,4hr,8hr,12hr. The cells were washed with PBS (pH 7.4) to remove

excess nanoparticles, followed by fixing and staining with DAPI. The coverslips were washed, mounted on glass slides, and observed under Fluorescent Microscope. The fluorescence was quantified using ImageJ software (ImageJ Java 1.8.0_112.).

(ii) Cellular localization of drug quantified by HPLC.

Cellular localization of fluorescent dug (Curcumin) loaded NPs was analyzed using the HIV-1 Env surface expressing cell line HL2/3, and SK-N-SH was used as a negative control. HPLC quantified the localized drug (AZT) on HL2/3 cells. The total experimental procedure is given below.

 1.4×10^5 HL2/3 cells were incubated with 150 μ M of AZT containing Lf-NPs and Lf-MES NPs at time points 30min, 1hr, 2hr,4hr,8hr,12hr. The cells were washed with PBS (pH 7.4) to remove excess nanoparticles. 200 μ l of 30% AgNO3 was added to the lysed cells to precipitate the protein. The drug was further extracted into the organic phase by adding 1ml HPLC grade methanol. The total mixture was centrifugated at 12000 rpm for 20 min and filtered through a 0.4-micron syringe filter, and quantified by HPLC.

2.2.16 Competitive binding of Lf-MES NPs to gp160 (gp120+gp41).

The affinity of surface-modified NPs to gp160 (gp120+gp41) was assessed using a competitive assay. The assay was carried out in the presence of soluble gp160 (1.8μg/μl), lactoferrin receptor antibody (ITLN-1) (1mg/ml), and a combination of both. 0.1x10⁶ HL2/3 cells were seeded and allowed to adhere to coverslips. The cells were treated with the Lf receptor antibody for one hour before incubation with Curcumin loaded NPs. In another experiment, the Curcumin loaded nanoparticles and sol.gp160 (1:1) were added to the cells. The cells were incubated at 37⁰ C in a 5% CO₂ incubator for up to 4hours. Finally, the supernatant was discarded to remove excess NPs, antibodies, or sol.gp160 (The soluble gp160 was purified from CHO cells, quantified using Nanodrop Lite). The cells were washed, fixed, stained with DAPI, and mounted. Fluorescent microscopy was used to visualize the mounted coverslips.

2.2.17 Cell Cytotoxicity by MTT assay:

Cytotoxicity in SUP-T1 cells was measured by quantifying 3-(4,5-dimethylthiozol-2-yl) color change -2,5-diphenyltetrazolium bromide (MTT, Sigma) in the presence of different concentrations of the synthesized compounds and nanoparticles. According to the procedure, the 96-well plate was the seed with SUP-T1 cells at a density of 0.2x10⁶ cells/well and incubated at 37°C in a 5% CO₂ incubator for 4 hours. The incubated cells were treated with different concentrations of the synthesized compounds and nanoparticles. After treatment, the cells were again incubated for 16 hours in the same incubation conditions. The cells were pelleted at 1200 rpm for 7 min and resuspended in complete medium. Now, 20µ1 of 5 mg/ml pre-dissolved MTT was added to each well and incubated for another 4h. After the incubation, the cells were pelleted at 1200 rpm for 10 minutes, discarded the media from wells, and formed MTT-formazan crystals were dissolved in DMSO by adding 100uL into each well. Finally, the plate was incubated in the dark for 5 mins, and the color change was recorded in an ELISA reader at 595 nm. The experiments were conducted in triplicate, and the average with standard deviation was plotted to represent the cell survival.

2.2.18 Inhibition of Cell Fusion.

HL2/3 labeling.

HL2/3 cells were incubated with 0.5 μ M of Calcein AM for 1 h at 37 °C. After incubation after incubation, the cells were washed by spinning 350xg. After washing, the pellet was incubated for 30 min at 37 °C. in fresh medium. The dye treated cells were incubated with Lf NPs and Lf-MES NPs for 1hr after loading the dye.

SupT1 labeling.

SupT1 cells were incubated with fluorescent dye Hoechst (20 μM) for 1 hr at 37 °C. After incubation, the cells were pellet out at 350xg, and the pellet was resuspended in fresh medium and incubated another 30 min.

Dye Redistribution Assay.

The fluorescent dye-labeled, Env protein-expressing cell line (HL2/3) and CD4+, CCR5+, CXCR4+ contained cell line (SupT1) were mixed co-cultured at a ratio of 1:1 and incubated at 37 °C for 2hrs. The fusion was monitored at 5μM concentration of the nanoparticles. The fusion in the presence of 50nM T20 was considered positive control and was regarded as a negative control in nanoparticles' absence. After incubation, the extent of fused cells was observed using a Leica Fluorescent microscope or Leica Confocal microscope.

2.2.19 HIV-1 Antiviral activity quantified by p24-ELISA Assay.

(i) HIV-1 Antiviral assay.

10⁶ SupT1 cells were suspended in RPMI 1640 supplemented with 0.1% FBS were seeded per well and followed by treatment with different concentrations of the synthesized compounds and nanoparticles. The compounds and NPs were added to the cells, followed by infection with 1ng/ml p24 equivalent of 93IN101 and NL43 virus strains of clade C and clade B were used to study the inhibition by the molecules. The cells were incubated for 4hrs at 37°C in a 5% CO₂ incubator. After incubation, the cells were pelleted at 1200 rpm for 7 mins, and the supernatant was discarded. The cells pellets were washed with fresh medium (RPMI 1640 supplemented with 10% FBS), resuspended in medium, and incubated for 96h. After the incubation was over, the cells were pellet down and collected supernatants for the p24 antigen estimation as per the below described protocol. p24 levels in the absence of compounds were considered 0% inhibition and were taken as a negative control, and in the presence of known drugs (T20 (Enfuvirtide) and sol.AZT) were considered positive control. Each experiment is conducted in triplicates; the data is presented as Mean±Standard Deviation.

(ii) p24-ELISA assay.

The HIV-1 core p24 antigen was collected from cells supernet and quantified by p24 Antigen ELISA Kit after 96hrs of incubation. The infection of the virus was quantified as on detected levels of viral antigen p24.

The p24 quantification was followed as per the manufacturer's guidelines. The collected supernatants were diluted to 10-fold with complete media and then added 100µl of the dilutions

to each well of the pre-coated ELISA plate. To each well, 25µl disruption buffer was added, and the plate was sealed. The plate was incubated for 1hr at 37°c. After incubation, each well's contents were aspirated, and the wells were washed with wash buffer 3x times. Followed, 100µl of the conjugate solution was added to each well, and again the plate was incubated for 1hr at 37°C. After 1hr incubation, the solution was aspirated, and the plate was washed for 3x times, and then 100µl of substrate solution was added to each well, and the pate was sealed. After incubation for 20min at room temperature, the reaction was stopped by adding 100µl of 1N HCl. Finally, the plate was inserted into the ELISA reader and measured each well's optical density at 450nm.

Chapter 3

Objective I

Synthesis and Characterization of novel HIV-1 entry inhibitors based on Epap-1 derived peptides targeting envelope gp120.

3.1 Introduction:

HIV-1 envelop protein gp120 is a highly mutated glycoprotein consisting of conserved (C1-C5) and variable regions (V1-V5) that participate in host cell interactions [170]. The sitespecific interactions are protein-protein interactions with host receptor CD4, co-receptors, CCR5, and CXCR4. The binding conformation of the virus varies with an amino acid sequence in the target regions. As per structural information of the gp120-CD4 binding complex, a hydrophobic cavity of gp120 is occupied by a phenyl ring located at residue 43 (phe43) for interaction with the CD4 receptor [171]. The CD4 further increased the interaction stability- Arg59 side chain that forms a double hydrogen bond with the gp120-Asp368 side chain. This interaction ensures the conformational changes in gp120 to open the third variable loop (V3) that mediates the contacts with CCR5 or CXCR4. The straindependent interactions with co-receptors (CCR5 or CCX4) depend on the amino acid composition of the V3 loop [172]. Some of the conserved residues in the V3 loop region are immunogenic and provides interactions with CCR5 -ECL2 loop [173]. Furthermore, Phe43 of gp120 is involved in HIV-1 sensitivity to Antibody-Dependent Cell-Mediated Cytotoxicity Responses (ADCC), suggesting further importance of this cavity in HIV-1 infection [174]. To avoid the complexity of targeting the variable viral protein, the host protein CCR5 is well-studied as a target to disrupt V3 loop interactions. The developed inhibitors either bind at the interaction interface or the allosteric site. FDA approved drug, maraviroc binds at the allosteric site of CCR5 and creates conformational changes unfavorable to V3 loop-ECL2 loop interaction [175]. However, the host protein targeted

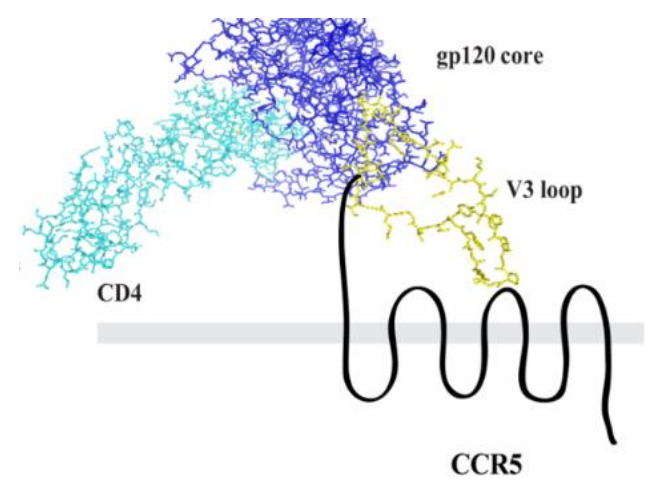


Fig. 3.1: Interaction of extended V3 loop with ECL2 loop of CCR5 upon binding with receptor CD4. (Viruses **2010**, 2(5), 1069-1105).

Inhibitors damage the original physiological functionality of receptors, ultimately leading to adverse events in the host. Present research mostly targets virus proteins either through the vaccination process or inhibitors to control early infections. In developing inhibitors against the entry process, natural ligands, and other proteins that interact with HIV-1 envelope regions are used as a guide to lead the small molecule design [176]. A protein isolated from women with pregnancy terminated in the first trimester has been reported to possess anti-HIV activity. A 90 kDa protein called the Early pregnancy-associated protein (Epap-1) displayed unaltered interaction with gp120 constant region -5 (C5), third variable region (V3), and interactions with V2, V4, C1, C2 regions. The antiviral activity of Epap-1 was observed in different strains of HIV -1 (HIV-1M-N, HIV-191US056, HIV-1VB7, HIVVB-66), and that could be explained by a ternary complex comprising of Epap-1, gp120-41, CD4, and CXCR4 [177]. This broad-spectrum activity is assumed to be because of the complex conformation being specific and highly conserved in all the strains, leading to viral entry [178]. However, Epap-1 delivery, stability, and production are complicated, necessitating the design of small molecular peptidomimetics, which provide interactions and activities like Epap-1. In this direction, the interaction interface of Epap-1 with gp120 was used to develop synthetic peptides, to mimic the binding and subsequent broad-spectrum activity of Epap-1 against strains of HIV-1[179]. Four peptides were developed and tested with peptides 2 and 3, showing better binding and activity (Fig. 3.2). Computational design, including molecular docking of the peptide 2 followed by the fragment-based structure of molecules (Fig. 3.3), led to identifying molecules with good activity against HIV-1. The derived scaffold was used for further design of compounds. This objective's rationale is synthesis, characterization, and biological evolution of the designed small molecular mimics and the derived molecules for potential antiviral activity against HIV-1.

3.1.1 Design of small molecules by using Epap-1 and gp120 binding sites:

In the small molecule designed to process, two peptides derived from the interacting region of Epap-1 with gp120 were selected. Peptides were modeled using PEPFOLD3.0 and, after iterative simulations, generate valid peptide interaction with more than ten aminoamides. Epap-1 peptides were docked with gp120 using the HEX 8.0.0 software suite. Based on peptide interaction with gp120, small-sized fragments containing aminoamides were

generated and docked into the gp120 to obtain best-hit fragments with improved docking scores. Based on the fragment interactions, synthesizability, and medical chemistry considerations, small molecules pharmacophore was designed simulating interaction conferred by the peptides to gp120. Designed molecules were docked to gp120 and were ranked based on the docking score using Autodock -Vina v1.2.MGL tools for docking and PyMol was used for visualization. [180].

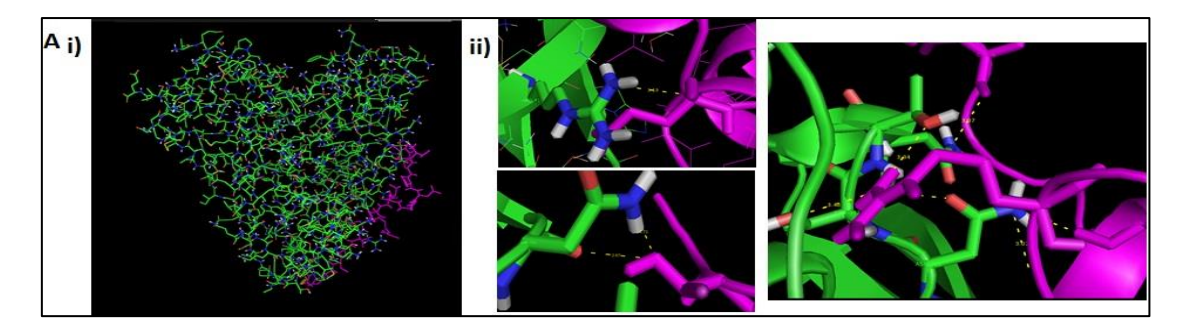


Fig. 3.2: A i) Docking of the peptide 2(magenta) with gp120(green) performed using HEX Docking suite. **ii)** Depicts the interactions between the peptide and the residues of V3 loop; The interacting residues of V3 loop are ASN386, SER387, THR388, ASN392 and ARG419. The interacting residues of peptide 2 include CYS4, VAL 23, ARG26.

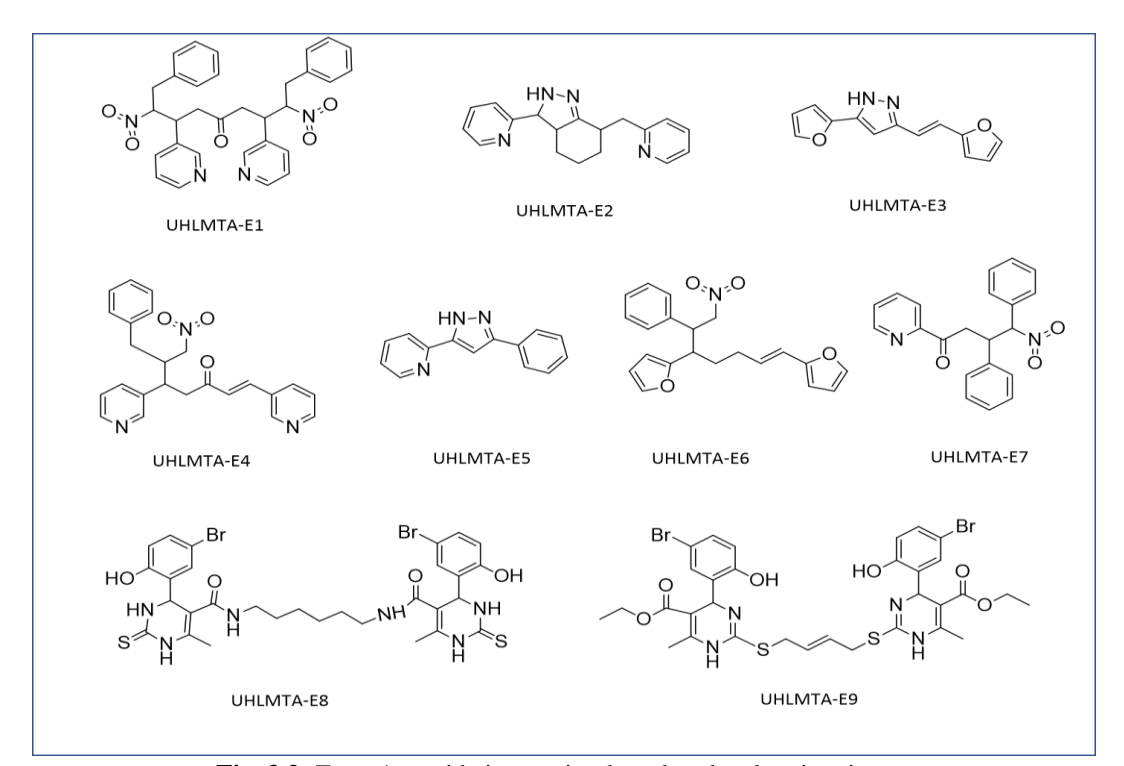


Fig. 3.3: Epap-1 peptide interaction-based molecule mimetics.

Molecule code	Binding	Interacting residues	Volume(Å)
	energy		
	(kcal/mol)		
UHLMTA-E1	-6.7	ASN362, SER447	706
UHLMTA-E2	-6.4	VAL255, ASN377	402
UHLMTA-E3	-5.8	VAL255, ASN377	301
UHLMTA-E4	-6.4	GLY379, SER447	440
UHLMTA-E5	-6.3	GLY379	512
UHLMTA-E6	-6.2	-	320
UHLMTA-E7	-5.8	-	461
UHLMTA-E8	-6.2	ARG252, GLY379,	820
UNLIVITA-LO		PHE210, ASN377	
LUU NATA FO	-6.7	ARG252, PHE210,	645
UHLMTA-E9		ASN377	

Table 3.1: Peptide mimetics interactions with gp120 and corresponding scores, interacting residues and volume of molecules.

3.1.2 Selection of small molecules for development as an entry inhibitor:

The biologically active small molecules involved in inhibition of the beginning of virus infection were considered entry inhibitors. Before selecting and developing entry inhibitors, we have a deep understanding of viruses' entry mechanisms and corresponding protein domain interactions. In HIV-1, the entry mechanism, and interacted proteins profile, the structural aspect of studies has been well established: spike protein interactions. The X-ray crystallography structural studies reveal that the cavity at phenylalanine 43 residue (phe43) on gp120, which participated in hydrophobic interaction with CD4 residues and another residue arginine 59 (arg59) of CD4 participate salt bridge-like hydrogen bond with carboxylic group of aspartic acid 368 (Asp368) on gp120 [181]. So that we need small molecules to interrupt the CD4-gp120 interactions. Among the above peptide-based derived molecules, UHLMTA-E5, UHLMTA-E8, and UHLMTA-E9 were contained -NH group may be useful for interaction with Asp368 residue. The pyrazole, dihydropyrimidine (DHPM)-thioxo ring moieties were pharmacologically significant and have been considered for entry inhibitor development [182 [183]. The marine extracted natural alkaloid compounds like batzelladine, crambescidins were found to possess potent antiviral activity [184]. Such an active isolated alkaloid contains dihydropyrimidine as a core unit that interacts with HIV-1gp120 in its CD4 interacting region [185]. Further evaluation of structural conformation of batzelladine analogs shown that hydrogens on the guanidine ring formed hydrogen bonds with the ASP368 carboxylic group, which is surrounding the Phe43 cavity [186]. The DHPM scaffold molecules further develop towards cavity and hydrophobic interactions; it will be considered affordable for entry inhibitors.

The interacting fragments of Epap-1 were considered for designing the pharmacophore of small molecules. The fragments contribute different kinds of interactions, such as hydrophobic, hydrophilic, Vander wall, and hydrogen bonds. In establishing a significant binding fragment with gp120, we must consider the fragment's volume and length were essential features. The high binding fragments' pharmacophoric future was used to design small molecules by bioinformatic tools to satisfy drug properties. The volume constraints and binding affinity of final designed molecules with gp120 were observed in protein-small molecules docking (Autodock -Vina v1.2 tool). The binding affinity and volume occupied by molecules expressed in (**Table 3.1**) and corresponding structures elucidated in (**Fig. 3.3**) [180].

3.2 Rationale of the Objective I:

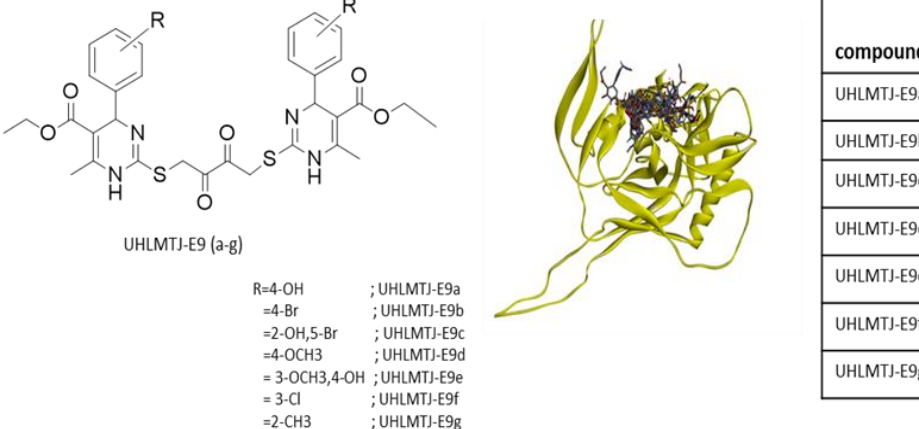
The HIV-1 envelop protein gp120 targeted molecules design and development is necessary to inhibit the virus entry in the early stage of infection. The rational molecule design has been possible considering protein-peptide or protein-protein interactions of anti-HIV-1 active small peptides with virus protein. In the study design, development, synthesis, and characterization of small molecules based on antiviral active peptide Epap-1 and gp120 interaction residues. To develop DHPM scaffold small molecules specifically towards the CD4 binding site (phe43 cavity) and then improve the interactions by substitutions with certain bioisosteres for better antiviral activity.

3.3 Results and Discussion:

3.3.1 Design and development of pyrazole and DHPM derivatives:

Based on the earlier studies [180], we have identified UHLMTA-E2, UHLMTA-E3, UHLMTA-E5 contain pyrazole UHLMTA-E8, UHLMTA-E9 contain DHPM as the

significant scaffolds. Our analysis showed the dimerization of two designed molecules (UHLMTA-E8, UHLMTA-E9), DHPM groups were separated by saturated and unsaturated carbon long chain. In the case of UHLMTA-E8, a saturated carbon chain bridge gives flexibility for interconvertible conformations of DHPM groups. Whereas in UHLMTA-E9, the unsaturated carbon chain provides separation to monomers to reduce the conformational The molecule's bridged chain was replaced with another chain containing flexibility. unsaturated oxygens to satisfy flexibility and length and enhance hydrogen bonds. Before proceeding to synthesis, molecules UHLMTJ-E9(a-g) were docked with gp120, and the docking score was found to be in the range of -5.0 to -7.0 kcal/mole (Fig. 3.4). All molecules docked in between the CD4 binding region ("phe43 cavity") and the V3 loop. But natural molecules of DHPM s shown antiviral activity against HIV-1 through pyrimidine -NH groups form hydrogen bonds with Asp368 residue of gp120 at CD4-gp120 interacting pocket (gp120-phe43 cavity). We have not observed any favorable interaction against CD4 binding at the phe43 cavity in the interaction studies' molecule. We should find the new molecules with an affinity towards the phe43 cavity blocking and forming a salt bridge with Asp368 for effective antiviral activity.



compound	Autodock binding Energy (Kcal/mol)
UHLMTJ-E9a	-5.2
UHLMTJ-E9b	-5.8
UHLMTJ-E9c	-7.0
UHLMTJ-E9d	-6.6
UHLMTJ-E9e	-6.5
UHLMTJ-E9f	-5.0
UHLMTJ-E9g	-5.5

Fig. 3.4: This depicts UHLMTJ-E9 a-g series molecules docking with gp120 and tabulated respective binding energies obtained by Auto dock vina.

3.3.2 Virtual screening of 1,2,3,4-Tetrahydropyrimidine (1,2,3,4-THPM)-oxo and thioxo derivatives to a specific target to "phe43 cavity":

The above long-chain separating DHPM dimer (UHLMTA-E8, E9) derivatives did not show any favorable interactions at the Phe43 cavity due to the rigid structure, but those binding close to the pocket. So, we need a small molecule with binding affinity to the phe43 cavity; towards this purpose, we have avoided the dimerization of DHPM, and monomer molecules showed docking to gp120 with the same docking coordinates. In the monomer molecules, the Pyrimidine ring contains a sulphur atom, which was replaced with an oxygen atom to derive another set of molecules with oxygen interacting environment. All molecules showed docking with gp120. Further, all THPM molecules were docking at phe43 pocket exhibited significant binding scores in the range of -4.5 kcal /mole to -6.5 kcal /mole.

However, oxo and thioxo derivatives have shown some deference in binding at the CD4 binding pocket vicinity, which was explained below (**Fig. 3.5**). The thioxo derivatives binding RMSD was more consistent than -oxo derivatives. This could explain sulfur atom contained molecules are favorable for site-specific binding than -oxo. In the structural aspect, an analysis of amino acid side chains around the molecules would further develop molecules with improved binding energy. All molecules designed were binding at CD4 binding pocket vicinity and form hydrophobic and hydrophilic interaction with side chains of GLY-473, ASP-474, TRP-427, ASN-425, ASP-368, MET-426 residues. In those molecules, the UHLMTJ-254a hydroxy group forms a hydrogen bond with the ASP-474

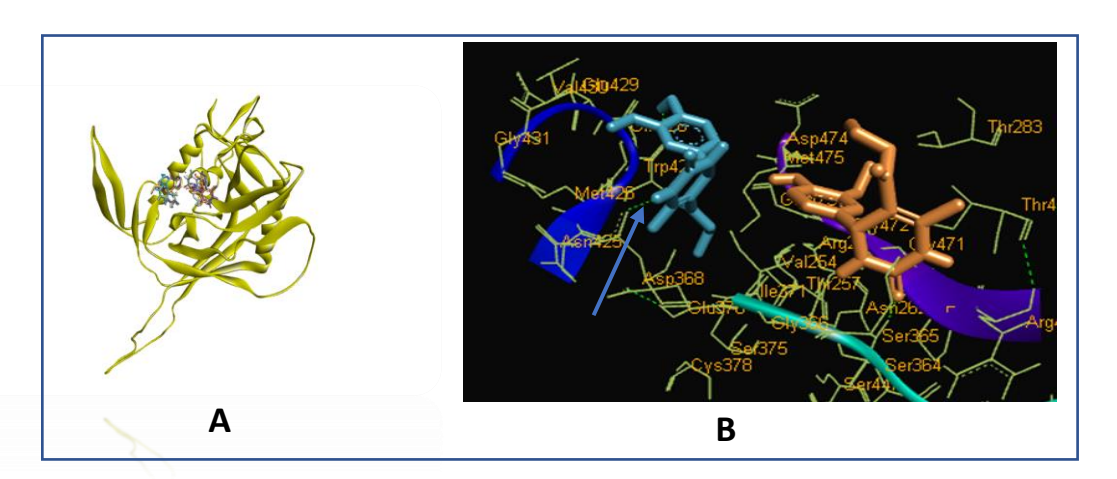


Fig. 3.5: Depicts THPM molecules' interactions with gp120 (A) Both -Oxo -Thioxo THPM molecules binding at the vicinity of the "phe43 cavity". (B) UHLMTJ-254e (blue) molecule binding at exact "phe43 cavity" and form a hydrogen bond with Asp368 (arrow mark), UHLMTJ-255e (orange) binding at Phe 43 cavity vicinity (not forming any hydrogen bond).

side chain and UHLMTJ-254e in a conformation to form a hydrogen bond with ASP-368 by

-NH group of Tetrahydropyrimidine ring. But that was not observed in -oxo derivatives(

UHLMTJ-255 a, e) that was depicted below (Fig. 3.5 B), which means atomic radii of the

sulfur atom in the ring may contributing toward the specific orientation of the molecule for

binding in the pocket along with hydrogen bond formation. All molecules contained a chiral

center at C4 carbon, which will facilitate ring orientation into the two different planes, and

molecules existed in one conformation for good binding at "phe43 pocket" on gp120.

3.3.3 Synthesis and physical characterization of pyrazole derivatives:

UHLMTA-E5 was synthesized following Scheme-1, given in the methodology section. As

per the procedure, ketone and keto ester condensation was carried out under reflux to form

the diketones, followed by the reaction of diketone in hydrazine hydride to form a five-

membered ring pyrazole as a final product by the cyclic reaction. The physical

characterization of molecules was explained below, and the corresponding spectra are

available in the **appendix**.

Compound name: 2-(3-phenyl-1H-pyrazol-5-yl) pyridine

Reaction entry: 2.1

Compound code: UHLMTA-E5

Yield: 90%

 $Mp({}^{0}C)$: 159-161 ${}^{0}C$

HN~N

¹H NMR (400 MHz,DMSO-d₆): δ 8.71(d,1H,Py-H), 7.90-7.77(d, 4H,Py-H,Ph-H), 7.47-

7.27(m,2H, ,Py-H,Ph-H), 7-26-7.25(d, 1H,Ph-H), 7.08(s,1H,Pz-H).

LC-MS: Calcd. For $C_{14}H_{11}N_3 : m/z \ 221$.Found: $222[M+1]^+$.

47

3.3.4 Synthesis and physical characterization of THPM derivatives:

The designed new molecules UHLMTJ-E9 (a-g) were synthesized following the **Scheme-2** as described in methods. The product of the first step (**2.2**) was prepared by a well-known "biginelli" three components reaction, and that was used as a reactant for the second step. In the second step, we have predicted the dimerization of two molecules with dibromo butanone in miner alkali condition to form the final compound. However, that reaction was not moved; on the other hand, to form a new compound with an oxygen atom in the sulfur atom of the first step product pyrimidine ring. We have synthesized **2.2a-g** and **2.4a-g** with varied substitutions, and the molecules melting point (Mp) and yield are given (**Table 3.2**). All THPM derivatives(UHLMTJ-254a-g, UHLMTJ-255a-g) possess similar structural patterns, while differences were in mass, and here, there are two molecules. Further, **2.2a,2.4a** molecules were characterized by NMR, HRMS, and FTIR. The spectral data are given below, and corresponding spectrums are presented in the **appendix**.

• Compound name: ethyl 4-(4-hydroxyphenyl)-6-methyl-2-thioxo-1,2,3,4-

tetrahydropyrimidine-5- carboxylate.

Compound code: UHLMTJ-254a

IR (neat): 3310, 3167, 3103, 2982, 2930, 2837, 2349, 2114, 1890, 1665, 1609, 1573, 1508, 1455, 1392, 1371, 1329, 1283, 1251, 1194, 1180, 1120, 1026, 954, 872, 835, 818 cm⁻¹.

¹H NMR (**400** MHz,DMSO-d₆): δ 10.50(s,1H,-NH),9.77(s,1H,-NH), 8.26-8.23(d,2H,Ph-H),7.51-7.48(d,2H,Ph-H), 5.32(s,1H,-NH-CH),4.04-3.99 (q,2H,- CH₂),2.32(s,3H,-CH₃), 1.12-1.09(t,3H, CH₂-CH₃).

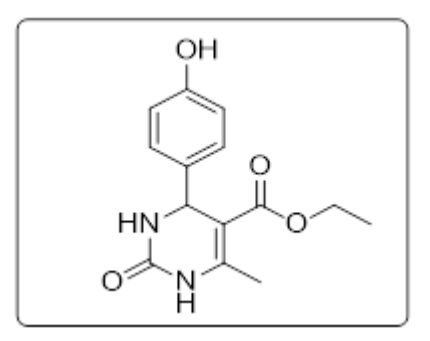
HRMS (**ESI**): Calcd. For $C_{14}H_{16}N_2SO_3$ [M⁺+H]: m/z 292.09. Found: 293.0963

• Compound name: ethyl 4-(4-hydroxyphenyl)-6-methyl-2-oxo-1,2,3,4-

tetrahydropyrimidine-5- carboxylate

Compound code: UHLMTJ-255a

IR(neat): 3347, 3272, 3140, 2926, 2853, 2349, 2165, 1879, 1716, 1650, 1555, 1473, 1412, 1371, 1324, 1265, 1204, 1184, 1103, 1092, 1025, 952, 893, 861, 816 cm⁻¹.



¹**H NMR (400 MHz,DMSO-d6):** δ 9.00(s,1H,-NH),7.60 (s,1H,-NH), 7.03-7.00 (d,2H,Ph-H),6.69-6.66(d,2H,Ph-H), 5.03(s,1H,-NH-CH),4.00-3.99(q,2H,- CH₂),2.22(s,3H,-CH₃), 1.11-1.06 (t,3H,-CH₂-CH₃).

HRMS (**ESI**): Calcd. for $C_{14}H_{16}N_2O_4$ [M⁺+H]: m/z 276.11. Found: 277.1189

S. No	R	Compound code	х	Reaction entry	Yield (%)	Mp (°C)
1	4-OH	UHLMTJ-254a	S	2.2a	82	223-225
2	4-Br	UHLMTJ-254b	S	2.2b	69	245-248
3	2-OH,5-Br	UHLMTJ-254c	S	2.2c	75	252-254
4	4-OCH3	UHLMTJ-254d	S	2.2d	85	205-207
5	3-OCH3,4- OH	UHLMTJ-254e	S	2.2e	82	230-234
6	3-Cl	UHLMTJ-254f	S	2.2f	65	195-197
7	2-CH3	UHLMTJ-254g	S	2.2g	68	175-178
8	4-OH	UHLMTJ-255a	0	2.4a	43	229-232
9	4-Br	UHLMTJ-255b	0	2.4b	35	232-235
10	2-OH,5-Br	UHLMTJ-255c	0	2.4c	52	265-267
11	4-OCH3	UHLMTJ-255d	0	2.4d	40	201-203
12	3-OCH3,4- OH	UHLMTJ-255e	0	2.4e	45	244-247
13	3-Cl	UHLMTJ-255f	0	2.4f	48	227-229
14	2-CH3	UHLMTJ-255g	0	2.4g	37	182-184

Mp= meting point, R= functional groups.

Table 3.2: Physical characterization of synthesized THPM derivatives.

3.3.5 Cell cytotoxicity (MTT Assay) of molecules:

Cytotoxicity of synthesized molecules was assessed by MTT assay (section 2.2.17) in SUP-T1 cells in the presence of increasing concentrations from 25 to 500 μ M of compounds, the dose-dependent analysis that the compound is shown in (Fig. 3.6) dose-dependent

cytotoxicity. Among the compounds, UHLMTA-E5 is comparatively toxic at 25 μ M, while all other compounds tested exhibited <20% toxicity at 25 μ M; these compounds are tested for antiviral activity below 25 μ M. The CC50 were computed and presented in (**Table 3.3**). The synthesized molecules contain both pyrazole and pyrimidine ring; these structures are reported to possess cytotoxicity. Hence the observed toxicity could be due to the presence of this substructure. Thus, the pyrazole ring containing UHLMTA-E5 exhibited higher more toxicity and CC50 at 37.7 μ M. Further, a comparison of cytotoxicity of compounds showed that the tetrahydopyrimidine (THPM) thioxo derivatives UHLMTJ-254 a-g exhibited higher toxicity than oxo derivatives UHLMTJ-255 a-g (**Fig. 3.6, Table 3.3**).

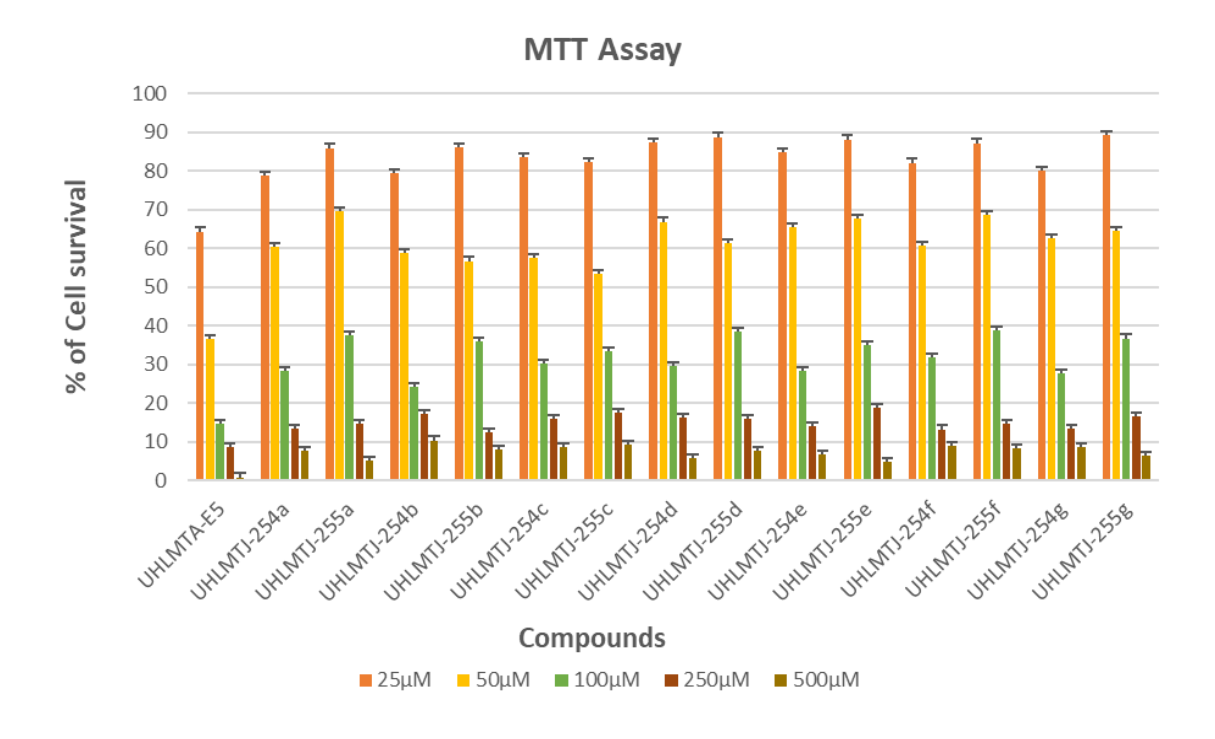


Fig. 3.6: Graphical representation of dose-dependent cytotoxicity of synthesized molecules in SUP T1 cells.

3.3.6 Anti-HIV-1 activity (p24 Assay) of molecules:

The molecules' activity in interfering HIV-1 replication was analyzed in Sup T1 cells as per the procedure given in **section 2.2.19**. Cells were challenged with HIV-1_{93IN101} in the presence of increasing concentrations of compounds in the range of 0.5 to 10 μ M; the IC50 values are computed and presented in Fig 16 and **Table 3.3**. The results showed that the tetrahydopyrimidine (THPM) thioxo derivatives (UHLMTJ-254 a-g) exhibits higher anti-HIV-1 activity than -oxo derivatives (UHLMTJ-255 a-g), and IC50 of compounds was at < 5 μ M. Among these, one of the molecules, UHLMTJ-254e, shown 50% inhibition at 2.2 μ M, while the molecule UHLMTA-E5 has shown IC50 at ~ 9 μ M. Further, the results suggest that sulfur-containing molecules have better activity than corresponding oxygen atom contained molecules, which is useful for developing gp120 targeted entry inhibitors.

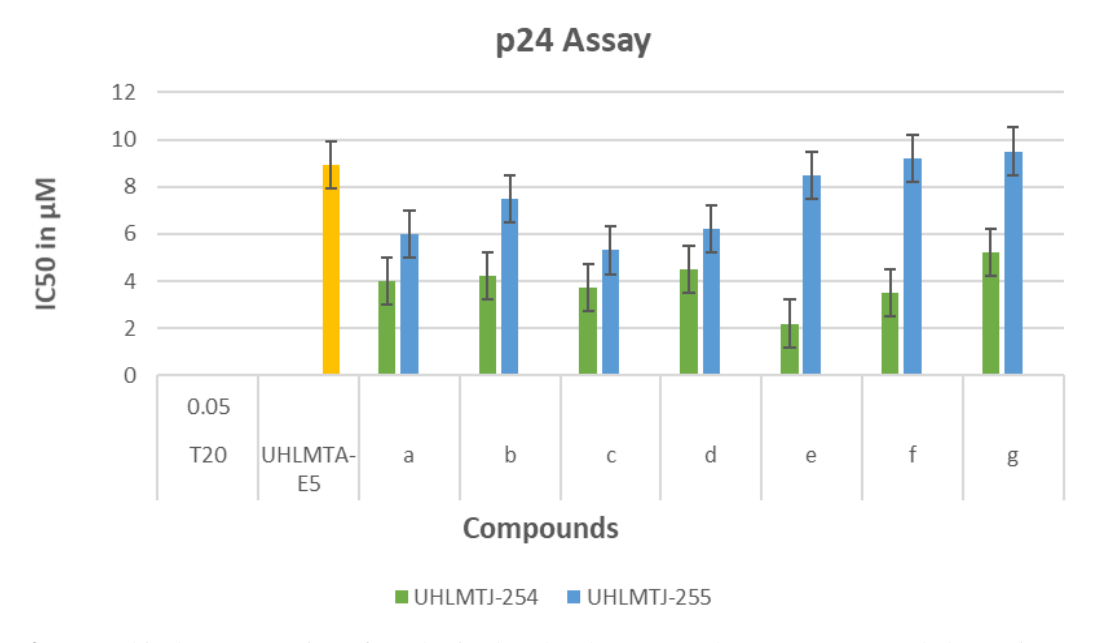


Fig. 3.7: Graphical representation of synthesized molecules' IC50 values on 93IN101 (clade C) virus. a) T20 considered as a control, UHLMTA-E5 (yellow bar), b) UHLMTJ- 254 a-g series molecules (green bars) and UHLMTJ-255 a-g series molecules (blue bars).

S. No	Compound code	CC50 (μM) (SupT1)	IC50±SD (μM) (93IN101,Clade C)
1	UHLMTA-E5	37.73	8.9±0.19
2	UHLMTJ-254a	88.91	4.0±0.14
3	UHLMTJ-254b	136.35	4.2±0.15
4	UHLMTJ-254c	83.41	3.7±0.15
5	UHLMTJ-254d	110.12	4.5±0.12
6	UHLMTJ-254e	100.90	2.2±0.19
7	UHLMTJ-254f	97.62	3.5±0.17
8	UHLMTJ-254g	124.36	5.2±0.18
9	UHLMTJ-255a	132.38	6.0±0.19
10	UHLMTJ-255b	112.93	7.5±0.13
11	UHLMTJ-255c	137.99	5.3±0.15
12	UHLMTJ-255d	103.43	6.2±0.12
13	UHLMTJ-255e	140.97	8.5±0.16
14	UHLMTJ-255f	95.86	9.2±0.18
15	UHLMTJ-255g	135.60	9.5±0.17

Table 3.3: The cell cytotoxicity (CC50) and antiviral activity (IC50±SD) of synthesized molecules represented in % inhibition concentration.

Summary of Objective I:

The development of HIV-1 entry inhibitors has been difficult due to random mutation, glycosylation, and low exposure of conserved regions of the virus's envelope protein. However, cell receptor-interacting regions on the virus are exposed during the virus's entry, which is a significant target for inhibitor design and development. Many molecules were attempted and even entered clinical trials, but most failed during different stages of development. The early stage of inhibition is essential to facilitate the control of infection

to new cells. The envelope interacting regions are generally blocked by small natural proteins (defensins, chemokines) and biological molecules, but the major problem with the availability of those molecules varies with gender and other infected bodies' physiological condition. One such molecule, Epap-1, is one of the natural proteins released at the time of the first trimester of pregnant women, which is involved in inhibiting viral entry through interaction with the V3 loop and the surroundings residues of the envelope [177]. Further characterization of Epap-1 and envelop interacting regions yielded peptide mimetics, which could interact with the envelope in the V3 area [180]. In this chapter, based on the conformation and interacting residues of Epap-1 peptide with envelope, small molecule mimics were designed with binding affinity to the V3 loop or CD4 binding region on gp120. Designed small molecule mimics were further evaluated for synthetics ease and stability. Here, three molecules, UHLMTA-E5, UHLMTA-E8, and UHLMTA-E9, are selected based on docking scores and moieties, which has involved the virus's interacting mechanism protein binding region. Since these molecules possess lower binding affinity, their structure is optimized further to obtain UHLMTJ-254, and 255, formed by removing rigidity in UHLMTA-E9 molecules, and the new derivatives were docked into gp120. These molecules showed significant binding at the "Phe43 cavity" vicinity and the structural similarity with the THPM derivative. Further, the deferences in oxygen and sulfur atom in the pyrimidine ring exhibited the differences in binding to the envelope. Among the molecules, the UHLMTJ-254e molecule forms a hydrogen bond with Asp368 residue on gp120, which is essential for CD4 binding at the time of viral entry. The designed molecules were synthesized and characterized. Activity results showed that THPM-thioxo (UHLMTJ-254 ag) molecules displayed more toxicity than THPM-oxo (UHLMTJ-255a-g) molecules and CC50 of molecules >80 µM except for UHLMTA-E5. The analysis of the antiviral activity of molecules on HIV-193IN101 (Subtype C)) showed significant anti-HIV activity. The results suggest that UHLMTJ-254 a-g molecules showed better activity than UHLMTJ-255a-g molecules and IC50 values were $<5 \mu M$ and $>5 \mu M$, respectively. One of the molecules, UHLMTJ-254e, has better activity in low concentration with IC₅₀ 2.2 μM. In the objective, we identify a molecular scaffold targeted to the CD4 binding region and useful for further developing entry inhibitors.

Chapter 4

Objective II

HIV-1 envelope protein V3 loop and neutralizing antibody 447-52D interactions based on derived molecules development, synthesis, and characterization.

4.1 Introduction

In the process of HIV-1 Entry, the outer surface spike protein (gp120) interacts with host cell protein by using its conserved (C1-C5) and variable (V1-V5) regions [170]. The molecular analysis of interactions revealed that this region was sufficiently exposed to the viral spike to generate neutralizing antibodies and facilitate the interaction with small molecule inhibitors. The glycosylation of envelope protein (gp120 and gp41) varies in different virus strains and may contribute to the generation of strain-specific antibodies in the serum of HIV-1 infected individuals [187]. Among these antibodies, most of them recognize the third hypervariable (V3) loop of gp120, especially T-cell line adapted strains of HIV-1[188]. The V3 loop contains 35 residues with an overall positive charge, which suggests that loop interactions are mostly control based on the negative charge tyrosine sulfate (-SO₃-) group region of CCR5 N-terminal [189]. V3 loop domain's structural aspect is further classified into three areas: a base, stem, and crown [190]. The base part contains the most conserved residues located at the core of gp120 with disulfide bridges followed by the highly flexible stem and crown that extends outside of gp120 core when the loop is conformationally open [191]. The conserved residues in the crown region are immunogenic and provide interactions with the CCR5-ECL2 loop [192]. High immunogenicity of the V3 loop facilitates the use of synthetic peptide mimics of the loop as an efficient antigen to produce antibodies in the immunization process [193]. X-ray crystallography studies disclosed that the crown part of the V3 loop adopted β- hairpin conformation in both V3 -containing gp120 core and complex antibody with V3 peptide [194]. This is assumed to be because of a conserved region in the center of the crown consisting of GPXR epitope (GPGR in subtype B and GPGQ in subtypes A, C, and D), which preserves the structural elements in the V3 loop irrespective of sequence variability in other portions of V3 loop [194]. Although most anti V3 -loop antibodies neutralize only a few strains, some of them neutralize diverse strains of the virus. The proper V3 loop native conformation can elicit anti-V3 broadly neutralizing antibodies like 447-52D and 2219, interacting with other immunodominant regions on gp120[195]. For example, the interaction studies of 447-52D show contact with both stem and tip of the V3 loop to neutralize the subtype B virus. From the crystal structure

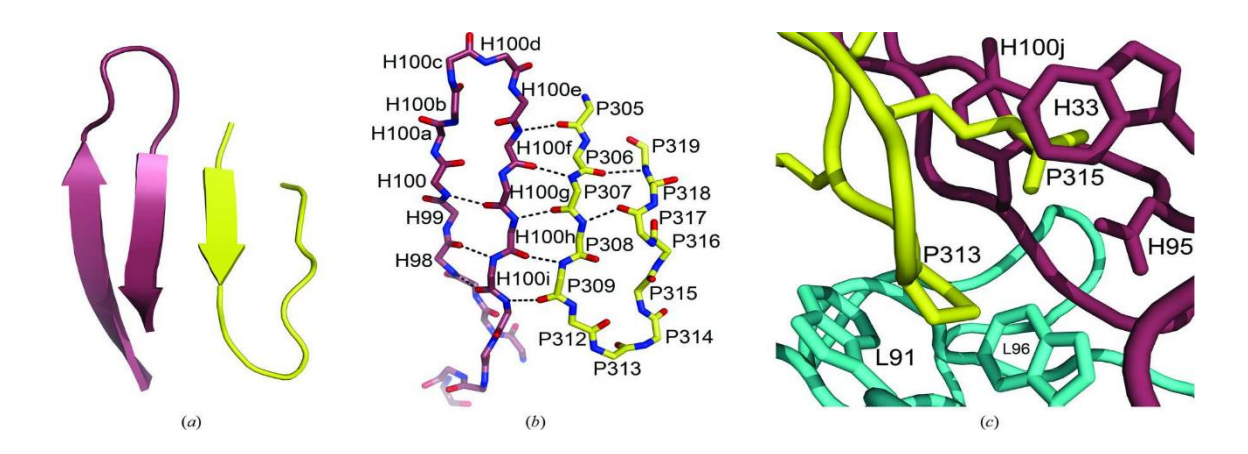


Fig. 4.1: Interactions between the v3 peptide and 447-52D. The violet ribbon represents the Fab CDR H3 of 447-52D, and the yellow ribbon represents the V3 peptide. (a) The three-strand β- sheet formed by 447-52D, and the V3 peptide was shown. (b) Black lines represent the hydrogen-bond interactions between the sheets. (c) Side-chain interactions, π -cation stacking between the peptide and the light chain (cyan), and heavy chain (violet).

(Acta Cryst (2008). D64, 792-802).

Analysis, 447-52D Ab CDRH3 C-terminal interacts with V3 crown N -terminal via mainchain interaction and side chains interaction with V3 tip residues [196]. Interaction stability was explained in different bindings:

- i. The anionic (AspH95 of the Ab) and cationic (V3 loop Arg315) formed the Salt bridge.
- ii. The antibody aromatic residues (TyrH100J and TrpH33 of the 447-52D heavy chain) formed π -cation stacking with cationic (Arg315 of V3 loop).
- iii. Van der Waals interaction between v3 loop residues (Pro313 of V3 loop TrpL91 and V3 loop -TrpL96).
- iv. Water-mediated hydrogen bond network at the antigen-binding site [197].

Moreover, antibodies can guide the exploration of small molecules that can modulate protein-protein interactions via significant site interactions. The designed molecules in this way have a similar therapeutic effect. This objective's rationale is to design molecular mimics of the interaction of 447-52D with gp120, synthesize, and characterization their interaction with gp120 and their anti-HIV-1 activity.

4.1.1 Design of small molecules through gp120 and 447-52D epitopes interactions:

For the development of peptide structure and interacting residues for small molecules design, we have used the crystal structure (PDB:1QIJ) of the 447-52D Fab in complex with a 16-mer V3 peptide at $2.5~\rm A^0$ resolution. The system reveals that the V3 loop peptide β - hairpin forms a three-stranded mixed β -sheet with CDR region H3 of antibody (heavy chain3) [198]. To search for peptidomimetics from the interaction interface using the pep: MMs: MIMIC tools associated with the MMsINC database, which provide and perform all options related to the generation of mimics. The founded peptidomimetics efficacy was assessed by molecular docking with V3 loop peptide. Pep; MMs: MIMIC is a web-oriented tool; when a three-dimensional peptide structure is given, it will prepare multi conformers automatically with a three-dimensional similarity search among 17 million conformers calculated from 3.9 million of commercially available chemicals collected in the MMsINC database [199]. The tool's input file is peptide structure, interacting residues, and the output file contains 200 structures with binding scores. Further docking was done by using GOLD version 3.2, and the input file is taken from the protein data bank, PDB ID is 2B4C, which is the structure of V3 in the context of an HIV-1 gp120 core, 200 structures and out file generated with docked conformations and scores considered 10 best score conformations.

Fig. 4.2 Top nine molecules selected from the virtual screening protocol for 447-52D mimics.

Among the above molecules, UHLMT-A2, UHLMT-A3, and UHLMT-A9 type molecules have a history as HIV-1 entry inhibitors [189], and s-triazine derivatives as

anti-HIV-1 RT inhibitors [154]. That primary scaffold was considering for new molecule development with different functional groups modifications for affective entry inhibition.

4.2 Rational of Objective II:

The immunogenic third variable loop (V3 loop) of gp120 plays a crucial role in virus entry through co-receptor interactions. The variable interactions have been neutralized with broadly neutralizing antibodies like 447-52D, etc. The availability of antibodies varies regularly among the patients, and exceedingly difficult to treat the patients with synthetic antibodies and small peptides. We need to design and develop small molecules to target at V3 loop conducted through 447-52D Antibody and V3 loop interactions. In the study, we focused on the V3 loop targeted drug-like molecules design; molecules were validated by binding analysis in silico followed, chemically synthesis, and inhibitory activity in-vitro.

4.3 Results and discussion:

4.3.1 Design and docking of new molecules to target the V3 loop:

As in Fig. 4.2 synthesized based on their features mimicking 447-52D and V3 loop interactions, the small molecules exhibited similar docking scores in docking with gp120 [180]. However, the selection of molecules and further development depends on both feasibilities of synthesis and the significant pharmacophore features of the parent structure. Some molecules, UHLMTA-A2 and UHLMTA-A9 type molecules, were used as HIV-1 inhibitors. Hence, their molecules were considered for further development; the components we considered were the type of interactions proposed to occur between the V3 loop and co-receptor CCR5 during the virus entry [189]. The V3 loop-CCR5 participates principally through ionic interactions involving the positively charged V3 region and negatively charged sulfate group of CCR5. So that, the phenyl sulfonate moiety mimicked tyrosine sulfate and was critical for the retained terminus of CCR5

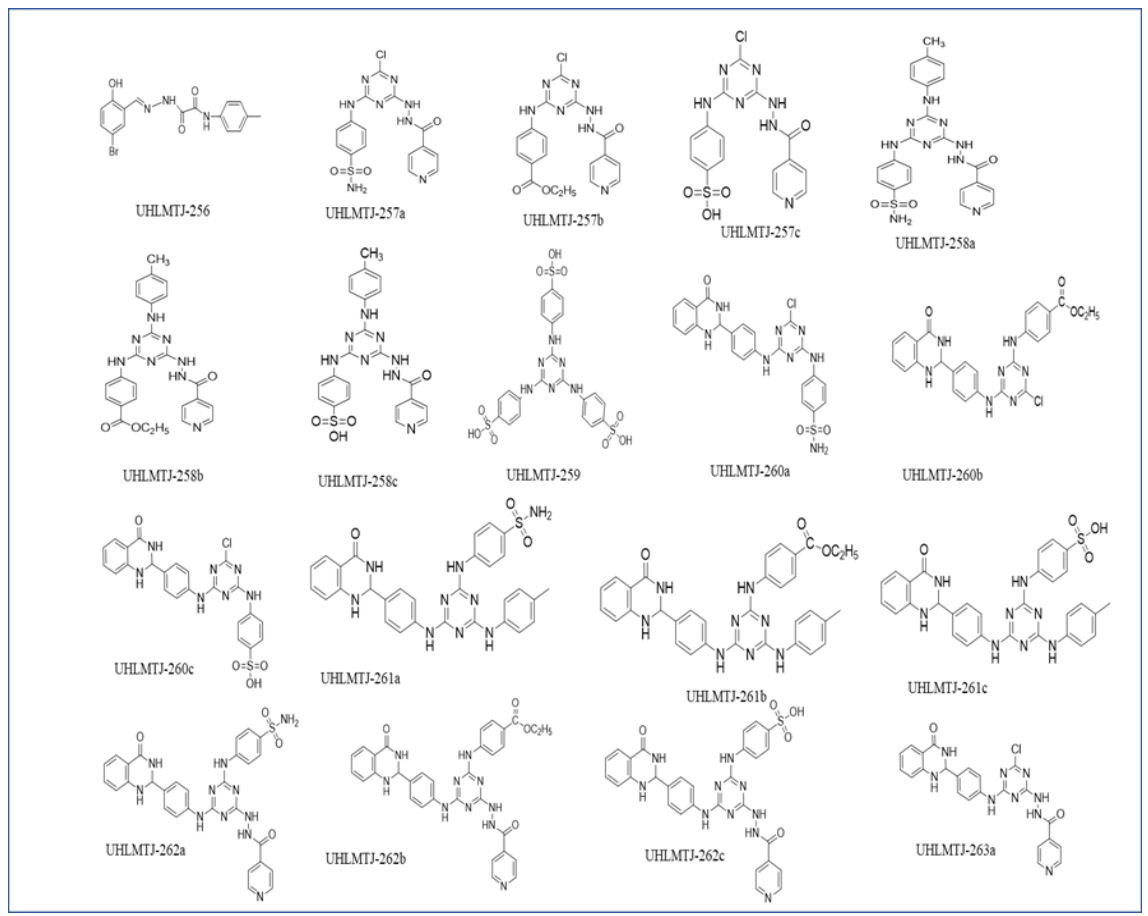


Fig. 4.3: Depicts all newly designed molecules and corresponding compound codes.

Interaction, which could form a feature analog design. However, the sulphonate group mediated interactions alone may not be sufficient to inhibit entry inhibition [200]. Although we need other moieties, whichever has strong interactions with flacked residues. So, we developing molecules containing electron abundant negative charge moieties for participation in hydrophilic, hydrophobic, and cation $-\pi$ stacking type interactions with V3 loop residues. The s-triazine skeleton of the UHLMT-A9 molecule is mainly substituted with different functional groups to design new derivatives with synthetic ease as blow **Fig. 4.3**. The analogs of UHLMT-A9 contains negative charge sulfonate groups, substituted benzene ring, dihydroquinazoline, Isonized, and other functional groups. The visual analysis of docked molecules with a V3 loop was suggested that designed molecules are binding at the base, stem, and crown regions with an excellent binding score (**Fig. 4.4, Table 4.1**) except the UHLMT-A2 molecule. The

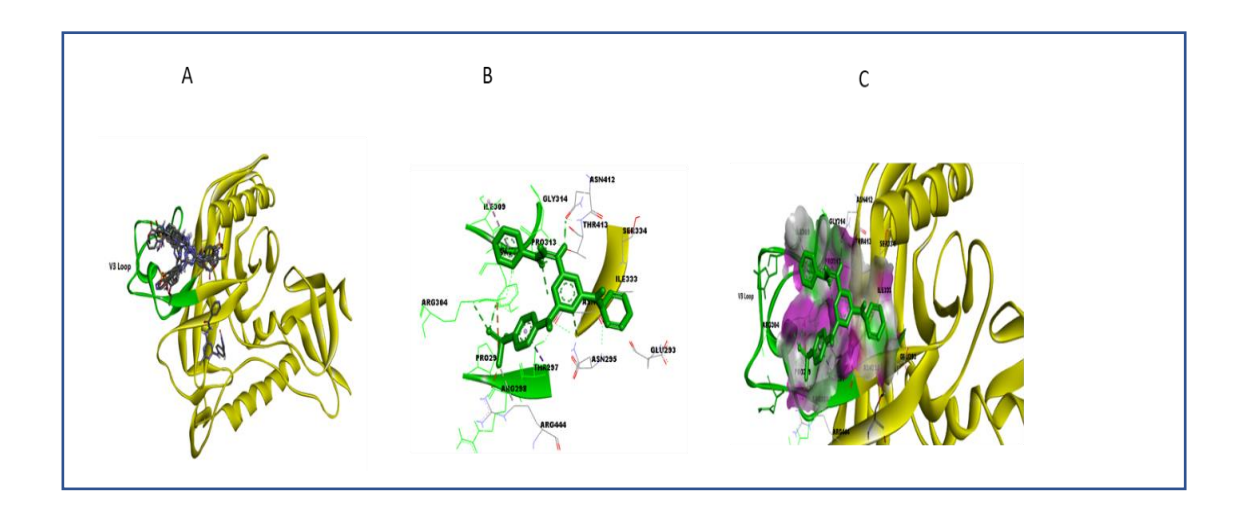


Fig. 4.4: A) Depicts the binding region of all molecules with gp120. The molecules can be seen bound in the interface of the folded V3 loop stem (green) and the base of the loop and surrounding residues (grey), B) Depicts the interface of the interaction of molecule UHLMTJ -258c with gp120, C) Depicts the surface and ribbon representation of molecule UHLMTJ -258c with gp120.

Comparison between molecules, trichloro substituted molecules are more significant binding, then dichloro substituted molecules with better binding energy.

Among them, aromatic and anionic properties contained moieties such as dihydro quinazoline, sulphonate, and sulphanilamide, isonizide substituted molecules have shown better binding energy above -8.0 kcal/mole. As per In-Silico dockings studies, moieties such as dihydroquinazoline ring (-NH-C=O), sulfonate(-SO₃⁻), safinamide(-SO₂NH₂), and ester groups(-COOC₂H₅) interact with side chains of the crown (HIS308, ILE309, GLY312, PRO313, TYR318), stem (THR 297PRO299, ARG304) regions to form hydrogen bonds. Along with those interactions, the isoniazid and s-triazine aromatic rings were also involved in cation - π stacking at the base part of the V3 loop (**Fig. 4.4**). In Silico analysis, these molecules were predicted to possess good antagonist activity that could be validated through in-vitro experiments.

4.3.2 General discussion of Synthesized molecules:

In the objective, synthesis was carried out mainly through substitutions and coupling reaction mechanisms in alkali conditions. That was observed in (Scheme 3,4,5,6,7,8

(Section 2.2.4,2.2.5,2.2.6) of chemical synthesis. The cyanuric chloride reaction with different aromatic amines to replace s-triazine chloride with amino groups to form mono, di, tri substituted - s-triazines (Section 2.2.5,2.2.6). The substituted groups' selection mainly depends on the area and type of interaction that could participate in the loop region. The s-triazine derivatives were fulfilled the required parameters with different amines and groups presenting on the benzene rings. In the developmental process, the necessary dihydroquinazoline intermediates were commercially unavailable; hence they were prepared according to the procedure given in Section 2.2.5 (Scheme 4). The substitution of the chlorine atom depends on the reaction conditions indicated therein. The substitution of single chloride on s-triazine with an amine group critically depended on temperature conditions. The whole reaction was controlled under low temperature <4°C) and the slow addition of alkali NaOH or K₂CO₃, which was used to neutralize released HCl during rection. After that, a second chloride replacement was carried out at room temperature in alkaline (NaOH) at pH 7.5 to 8.0. Finally, a third chloride replacement was carried out in an acetic acid solvent with an amino group of arylamines. This reaction requires a high temperature for the access equivalent of amine(-NH₂). In that, the access amine acting as a base to neutralize the reaction. All substituted compounds were further purified by washing, recrystallized, and characterized by NMR, IR, and HRMS. After the quenching of the reaction mixture in ice-cold water and the sulfonic acid group contained molecules extract from the water was exceedingly difficult. For that entire solution was acidified at pH 2.0 and to get the residue sold product. As per the experimental observation, the ordering of chloride atom substitution was essential. For that, we should follow the order as first electron-withdrawing groups contained amines and then bulky size amines, and finally, small, and electron-rich amines. The yield and melting points of molecules are depicted below and compare to other molecules. Sulfonic acid molecules yield significantly low. Before going to activity studies in vitro, all sulfonic acid groups were converted to sulfonate groups by dissolved in PBS buffer at pH 8.0. The hydrogen ion was replaced by sodium ion to form the sodium salt of sulfonic acid confirmed by molecules' solubility.

4.3.3 Physical and Spectral characterization of synthesized molecules:

• Compound name: 2-hydrazinyl-2-oxo-N-(p-tolyl)acetamide

Reaction entry: 2.6

Yield:80%

¹**H** NMR (DMSO-d₆): δ 10.69(s,1H,NH₂-N**H**-C=O),7.63-7.61(d,2H,Ph-**H**),7.16-7.13(d,2H, Ph- **H**),4.33-4.25 (d,2H,-N**H**₂),2.26 (s,3H,-C**H**₃).

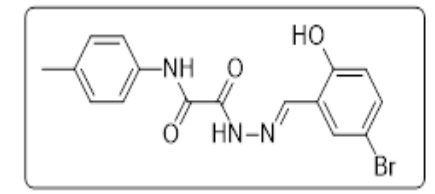
• **Compound name:** (E)-2-(2-(5-bromo-2-hydroxybenzylidene)hydrazinyl)-2-oxo-N-(p-tolyl)acetamide

Reaction entry: 2.7

Compound code: UHLMTJ-256

Yield:90 %

Mp (°C):262-265



IR (neat): 3283,3203,3044,2915, 2323,1914,1697,1658,1604,1593,1407,1350,1316 1272,1233,1188,1124,1096,1021,964,908,871,822 cm⁻¹.

¹**H NMR (DMSO-d₆):**δ12.64(s,1H,-N-N**H**-C=O),11.04(s,1H, -N**H**-C=O),10.75(s,1H, N=C**H**), 8.78(s,1H,Ph-**H**), 7.77-7.71(m,3H, Ph-**H**),7.46-7.42(d,1H,Ph-**H**), 7.18-6.91 (m,2H, Ph-**H**), 6.88(d, 1H,-O**H**),2.27(s,3H,- C**H**₃).

HRMS (**ESI**): Calcd. for $C_{16}H_{14}BrN_3O_3$ [M⁺+H]: m/z 375.02. Found: 376.0293

• Compound name: 2-(4-aminophenyl)-2,3-dihydroquinazolin-4(1H)-one

Reaction entry: 2.9

Yield:40%

IR (neat):

3287,1607,1557,1487,1408,1329,1176,1126, 1033,1007,832,800 cm⁻¹.

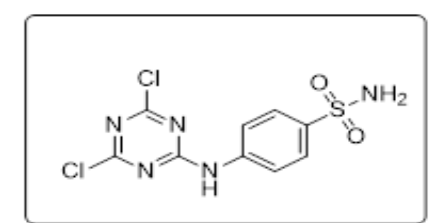
¹**H NMR (DMSO-d₆):**7.98(d, 1H, Ph-**H**), 7.61-7.58(d,2H, Ph-**H**), 7.22-7.12(d,1H,Ph-**H**), 6.88-6.83(d,1H,Ph-**H**), 6.74-6.63(m,4H, Ph-**H**), 6.55(s,2H,-N**H**₂), 5.71(s,1H,-NH-C**H**-NH), 5.58-5.54(d,1H,-N**H**).

• Compound name: 4-((4,6-dichloro-1,3,5-triazin-2-yl)amino)benzene sulphonamide.

Reaction entry: 2.10a

Yield: 92%

Mp(⁰C): Infusible



IR (neat): 3293, 3208, 1619, 1552, 1516, 1493, 1425, 1379, 1328, 1295, 1226, 1162,1022, 900, 875, 845, 831 cm⁻¹.

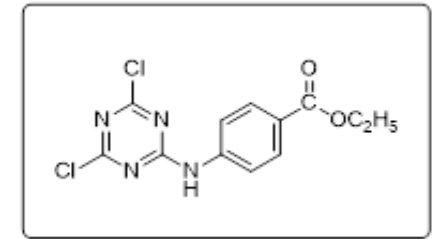
¹**H NMR (DMSO-d₆):** δ 11.37 (s,1H,-N**H**), 7.80-7.78 (d, 2H, Ph-**H**), 7.73-7.72 (d, 2H, Ph-**H**), 7.73 (s, 2H,-N**H**₂).

• Compound name: Ethyl 4-((4,6-dichloro-1,3,5-triazin-2-yl) amino) benzoate

Reaction entry: 2.10b

Yield:93%

 $Mp({}^{0}C):>300$



IR(neat): 3281,3201, 1687, 1607, 1541, 1504, 1431, 1387, 1337, 1318, 1282, 1253,1226, 1186, 1165, 1124, 1014, 960, 878,836, 814 cm⁻¹.

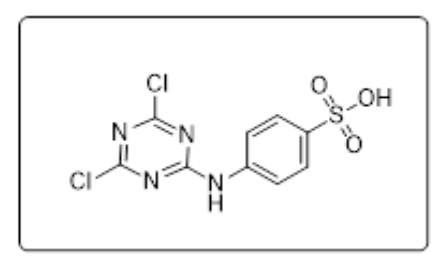
¹**H NMR (DMSO-d₆):** δ 10.88 (s,1H,-N**H**), 7.80-7.68 (m,4H, Ph-**H**),4.20 (q, 2H, -C**H**₂)1.22 (t, 3H,-C**H**₃).

• Compound name: 4-((4,6-dichloro-1,3,5-triazin-2-yl)amino)benzenesulfonic acid

Reaction entry: 2.10c

Yield: 73%

Mp(⁰C): Infusible



IR(neat): 3469, 3270, 1618, 1557, 1498, 1423, 1384, 1319, 1225, 1170, 1127, 1035, 1007, 962, 876, 846, 828 cm⁻¹

¹**H NMR (DMSO-d₆):** δ 11.16 (s,1H,-N**H**), 7.58-7.57 (d, 2H, Ph-**H**), 7.52-7.51 (d, 2H, Ph-**H**).

• **Compound name**:4-((4-chloro-6-(2-isonicotinoylhydrazinyl)-1,3,5-triazin-2

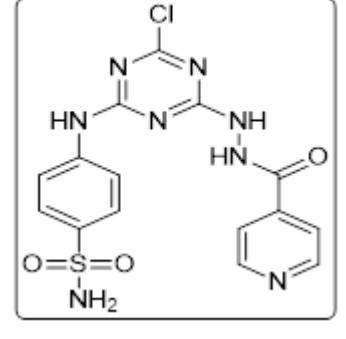
yl) amino) benzene sulfonamide

Reaction entry: 2.11a

Compound code: UHLMTJ-257a

Yield: 85%

Mp (⁰**C**): Infusible



IR (neat): 3206, 1555, 1514, 1408, 1327, 1189, 1154, 1100, 1034, 986, 903,833 cm⁻¹.

¹**H NMR (DMSO-d₆):** δ11.04(d,1H ,-N**H**-C=O), 10.65(s,1H,-N**H**-NH-C=O), 10.341(s, 1H, N**H)**, 8.80-8.76(m, 4H,-N**H**₂-S=O,Py-**H**),7.79-7.70 (m,4H, Ph-- **H**,Py-**H**) 7.26-7.19(d,2H, Ph-**H**).

HRMS (**ESI**): Calcd. for C₁₅H₁₃ClN₈O₃S [M⁺+H]: *m/z*. 420.05, Found: 421.0586

• **Compound name:** Ethyl4-((4-chloro-6-(2-isonicotinoylhydrazinyl)-1,3,5-triazin-2 yl)amino)benzoate.

Reaction entry: 2.11b

Compound code: UHLMTJ-257b

Yield: 83%

 $Mp(^{0}C):>300$

IR(neat): 3281, 1688, 1605, 1539, 1508, 1411, 1366, 1276, 1227, 1176, 1107, 1017,982, 901, 856 cm⁻¹.

¹**H NMR (DMSO-d₆):** δ 10.99 (d,1H,-N**H**-C=O), 10.63 (s,1H, -N**H**-NH -C=O),10.34 (1s, 1H, -N**H**), 8.80-8.75 (m, 2H,Py-**H**),7.88-7.41(m,6H,Py-**H**, Ph-**H**),4.26-4.16 (q, 2H, -C**H**₂),1.28-1.24 (t, 3H,-C**H**₃).

HRMS (**ESI**): Calcd. for $C_{18}H_{16}ClN_7O_3$ [M⁺+H]: m/z. 413.10, Found: 414.1079.

• **Compound name:** 4-((4-chloro-6-(2-isonicotinoylhydrazinyl)-1,3,5-triazin-2

yl)amino)benzenesulfonic acid

Reaction entry: 2.11c

Compound code: UHLMTJ-257c

Yield: 72%

 $Mp({}^{0}C):>300$

IR(neat): 3205, 1615, 1568, 1515, 1491, 1317, 1277, 1165,1030, 984, 908, 834cm⁻¹

¹**H NMR (DMSO-d₆):** δ 11.16 (s,1H,-N**H**-C=O),10.34-10.28 (d,1H,-N**H**-NH-C=O), 9.97(s,1H,-N**H**) ,8.96-8.91(d, 2H,Py-**H**) 8.06-8.03(d,2H,Py-**H**), 7.52-7.39 (m, 4H, Ph-H), 7.16 (s, 1H, ,-O**H**).

HRMS (**ESI**): Calcd. for $C_{15}H_{12}ClN_7O_4S$ [M⁺+H]: m/z. 421.04, Found: 422.0435.

• **Compound name:** 4-((4-(2-isonicotinoylhydrazinyl)-6-(p-tolylamino)-1,3,5-triazin-2

yl)amino)benzenesulfonamide

Reaction entry: 2.13a

Compound code: UHLMTJ-258a

Yield:80%

Mp(⁰C): Infusible

IR (neat):3263, 1561, 1487, 1405, 1321, 1154, 1034, 1007, 985, 905, 833cm⁻¹

¹**H NMR (DMSO-d₆):** δ 10.85(d,1H,-N**H**-C=O), 9.85 (br,1H,-N**H**-NH-C=O),9.59,9.26 (br,2H, -N**H**), 8.71(s,2H,-N**H**₂), 7.88-7.46(m,8H, Ph-**H**),7.19-7.07(br,4H,Py-**H**),2.23(s,3H,-C**H**₃).

HRMS (**ESI**): Calcd. for $C_{22}H_{21}N_9O_3S$ [M⁺+2]: m/z. 491.15, Found: 493.1405.

• Compound name: Ethyl 4-((4-(2-isonicotinoylhydrazinyl)-6-(p-tolylamino)-1,3,5-

triazin-2- yl)amino)benzoate.

Reaction entry: 2.13b

Compound code: UHLMTJ-258b

Yield :87%

 $Mp({}^{0}C):238-240$

IR (neat): 3267, 1571, 1486, 1407, 1364, 1273,1173, 1104, 1033, 1008, 805 cm⁻¹

¹**H NMR (δ in ppm):** δ10.89 (d, 1H, -N**H**-C=O), 9.57-9.21 (br,1H,-N**H**-NH-C=O,-N**H**), 8.79 (s,2H,-N**H**), 7.96-7.48(m,8H, Ph-**H**,Py-**H**),7.12-7.01(m,4H, Py- **H**, Ph-**H**), 4.23(q,2H, -C**H**₂ – CH₃), 2.23 (s,3H,-C**H**₃),1.25 (t,3H,-CH₂ – C**H**₃).

HRMS (ESI): Calcd. for $C_{25}H_{24}N_8O_3$ [M⁺+H]: m/z 484.20, Found: 485.2045

• **Compound name:** 4-((4-(2-isonicotinoylhydrazinyl)-6-(p-tolylamino)-1,3,5-triazin-2-yl)amino)benzenesulfonic acid

Reaction entry: 2.13c

Compound code: UHLMTJ-258c

Yield: 68%

 $Mp(^{0}C):>300$

¹**H** NMR (DMSO-d₆): δ 11.01(s,1H,-NH-N**H**-

C=O),9.49(s,1H,-N**H**-NH-C=O), 9.40(s,

1H,-N**H**),8.96(m,4H,-N**H**₂-S=O,Py-

H),8.09(m,4H,Py-**H**,Ph-**H**),7.67-7.48(m,3H,Ph **H**),7.09-7.07(m,2H, Ph-**H**),2.23(s,3H,-

 \mathbf{CH}_3).

HRMS (ESI): Calcd. for $C_{22}H_{20}N_8O_4S$ [M⁺+H]: m/z 492.15, Found: 493.1405

• **Compound name:** 4,4',4"-((1,3,5-triazine-2,4,6-triyl)tris(azanediyl))tribenzenesulfonic

acid

Reaction entry: 2.15

Compound code: UHLMTJ-259

Yield: 95%

 $Mp({}^{0}C):>300$

IR(KBr): 3414, 1622, 1580, 1558, 1488, 1407, 1328, 1171, 1121, 1068, 1032, 1004, 832cm⁻¹.

¹**H NMR (DMSO-d₆):** δ 9.70 (1s,3H,-N**H**), 7.67-7.51(m,12H, Ph-**H**).

HRMS (ESI): Calcd. for $C_{22}H_{20}N_6O_6S_2$ [M⁺+H]: m/z. 594.03, Found: 595.0382

• **Compound name:** 4-((4-chloro-6-((4-(4-oxo-1,2,3,4-tetrahydroquinazolin-2-yl)phenyl)amino)-1,3,5-triazin-2-yl)amino)benzenesulfonamide

Reaction entry: 2.12a

Compound code: UHLMTJ-260a

Yield:74%

Mp (°C): Infusible

IR(neat):3281,1560,1490, 1407, 1331,1237, 1155, 1129, 1035, 1007,988,900,832cm⁻¹.

¹**H NMR (δ in ppm):** δ 8.17(s,1H, -N**H**-C=O), 8.16 (d,2H,-N**H**₂-S=O), 7.79 (d,1H,-N**H**), 7.73-7.72 (m,2H, Ph-**H**), 7.70-7.68 (d,2H, Ph-**H**), 7.59-7.58 (d,2H,Ph-**H**),7.45(d,2H, Ph-**H**),7.27(s,2H,-N**H**),6.73-6.62(m,4H, Ph-**H**).5.71(s,1H,- NH- C**H**-NH).

• **Compound name:** Ethyl 4-((4-chloro-6-((4-(4-oxo-1,2,3,4-tetrahydroquinazolin-2-yl)phenyl)amino)-1,3,5-triazin-2-yl)amino)benzoate

Reaction entry: 2.12b

Compound code: UHLMTJ-260b

Yield:81%

Mp(⁰C):240-241

IR(neat): 3287, 1566, 1487, 1409, 1365, 1309, 1274, 1240, 1175, 1107, 1017cm⁻¹.

¹**H NMR (δ in ppm):** δ 8.26 (d,1H, Ph-**H**),7.86-7.43 (m,9H, Ph -**H**),6.72-6.62 (d,1H, Ph-**H**),5.70 (s,1H, ,-NH-C**H**-NH),4.24(q,2H,-C**H**₂), 1.27-1.25(t,3H,C**H**₃).

• **Compound name:** 4-((4-chloro-6-((4-(4-oxo-1,2,3,4-tetrahydroquinazolin-2-yl)phenyl)amino)-1,3,5-triazin-2-yl)amino)benzenesulfonic acid

Reaction entry: 2.12c

Compound code: UHLMTJ-260c

Yield: 68%

 $Mp({}^{0}C):>300$

IR (neat): 3270, 1556, 1489, 1405, 1322, 1162, 1121, 1031, 1006, 986, 832cm⁻¹

 1 H NMR (DMSO-d₆): δ 8.14-8.09 (m,2H, Ph-H),7.90-7.77(m,2H, Ph-H),7.58-

7.11(m,8H, Ph-**H**).

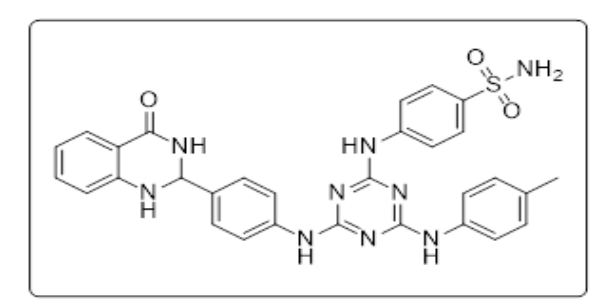
• **Compound name:** 4-((4-((4-(4-oxo-1,2,3,4-tetrahydroquinazolin-2-yl)phenyl)amino)-6- (p-tolylamino)-1,3,5-triazin-2-yl) amino) benzenesulfonamide.

Reaction entry: 2.14a

Compound code: UHLMTJ-261

Yield: 74%

 $Mp(^{0}C): >300$



IR(neat): 3272,2324,205,1914,1603,1566,1538,1486,1400,1320,1247,1151, 1095,987,833,802 cm⁻¹.

¹**H NMR (DMSO-d₆):** δ 9.83 (br,1H, -N**H**-C=O), 9.66 (s,1H, -N**H**),9.51(s,1H, -N**H**) 9.38 (s,1H, -N**H**),9.22 (s,1H,- N**H**),8.12 (d,2H,-N**H**₂-S=O, Ph-**H**), 7.97 (s,2H, Ph-**H**), 7.76-7.45(d,8H, Ph-**H**), 7.21-7.08 (d, 6H, Ph-**H**), 2.25 (s,3H,-C**H**₃).

• **Compound name:** ethyl 4-((4-((4-(4-oxo-1,2,3,4-tetrahydroquinazolin-2-yl)phenyl)amino)-6-(p-tolylamino)-1,3,5-triazin-2-yl)amino)benzoate

Reaction entry: 2.14b

Compound code: UHLMTJ-261b

Yield: 78%

, 7070

 $Mp(^{0}C)$: 258-260

IR(neat): 3272,2350,2285,2112,1981,1916,1681,1614,1567,1556,1514,1487, 1455,

1403,1214,1169,1120,1031,1006,870,836,803 cm⁻¹

¹**H NMR (DMSO-d6):** δ 9.84 (br,1H, -N**H**-C=O), 9.66 (br,1H, -N**H**),9.57(br,1H, -N**H**) 9.37 (s,1H, -N**H**),8.14-7.63(m,16H, Ph-**H**),7.45-6.81(m,2H, Ph-**H**),4.24-4.18(m,3H,NH-C**H**-NH,-C**H**₂),2.25(s,3H,-C**H**₃).1.27- 1.14(t,3H,- C**H**₃).

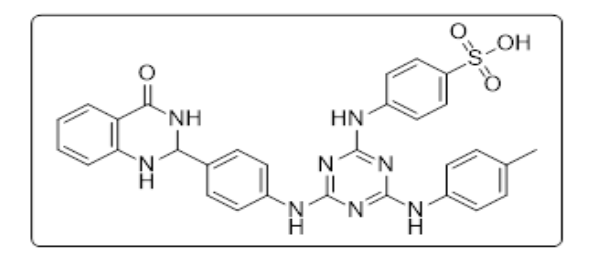
• **Compound name:** 4-((4-((4-(4-oxo-1,2,3,4-tetrahydroquinazolin-2- yl)phenyl)amino)-6-(p-tolylamino)-1,3,5-triazin-2- yl)amino)benzenesulfonic acid.

Reaction entry: 2.14c

Compound code: UHLMTJ-261c

Yield: 65%

Mp(⁰C): Infusible



IR (neat): 3291, 1557, 1486, 1405, 1324, 1164, 1121, 1031, 1005, 830 cm⁻¹.

¹H NMR (DMSO-d6): δ 9.72 (d, 1H,-NH=C=O), 9.48, 9.38(s,2H, -NH), 8.13-8.07(m,4H,Ph-H),7.85-7.49(m,12H,Ph-H),7.12-7.10(d,2H,-NH-CH-NH,-NH), 2.25(s,3H,- CH₃).

• **Compound name:** 4-((4-(2-isonicotinoylhydrazinyl)-6-((4-(4-oxo-1,2,3,4 tetrahydroquinazolin-2-yl)phenyl)amino)-1,3,5-triazin-2-yl)amino)benzene sulfonamide.

Reaction entry: 2.16a

Compound code: UHLMTJ-262a

Yield: 79%

Mp(⁰**C**): Infusible

IR(neat): 3287, 1556, 1486, 1407, 1327, 1228, 1155, 1035,1008, 832 cm⁻¹.

C=O),9.85,9.74(br,2H,-N**H**-C=O,-N**H**),8.74(s,2H,-N**H**₂-S=O)8.40-6.64(m,16H,Ph-**H,**Py-**H**).

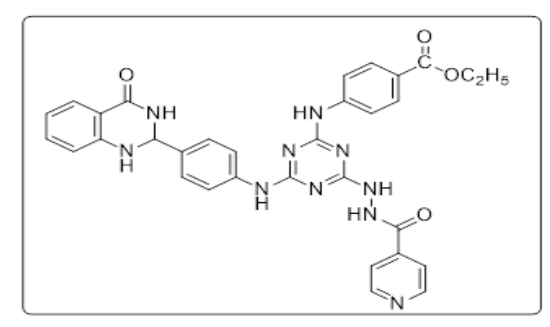
• Compound name: Ethyl 4-((4-(2-isonicotinoylhydrazinyl)-6-((4-(4-oxo-1,2,3,4tetrahydroquinazolin-2-yl)phenyl)amino)-1,3,5-triazin-2-yl)amino)benzoate

Reaction entry: 2.16b

Compound code: UHLMTJ-262b

Yield: 81%

 $Mp({}^{0}C)$: 260-262



¹H NMR (DMSO-d6): δ 10.84(br,1H, -NH-NH-C=O),9.84((br,2H,-NH-C=O,-NH), 8.73(s,2H,-NH),8.15-7.43(m,16H, Ph-H, Py-H),4.24-4.23(m,-NH-CH-NH,-CH₂), 1.26- $1.14(t,3H, -CH_3).$

• Compound name: 4-((4-(2-isonicotinoylhydrazinyl)-6-((4-(4-oxo-1,2,3, tetrahydroquinazolin-2-yl)phenyl)amino)-1,3,5-triazin-2-yl)amino)benzenesulfonic acid.

Reaction entry: 2.16c

Compound code: UHLMTJ-262c

Yield: 73%

Mp(⁰**C**): Infusible

HO,

IR (neat): 3291, 1556, 1488, 1407, 1325, 1171, 1123, 1032, 1006, 833 cm⁻¹.

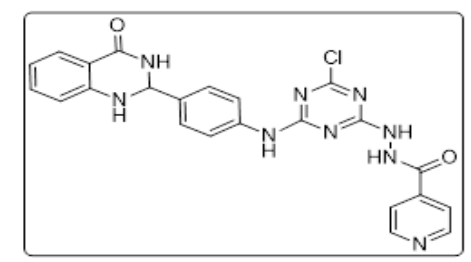
¹H NMR (DMSO-d6):δ 10.86(s,-NH-NH-C=O),8.90-8.86(d,2H,-NH),8.14-7.80(m,6H, Ph- **H**, Py-**H**), 7.72-7.47(m,10H, Ph-**H**, Py-**H**).

• **Compound name:** N'-(4-chloro-6-((4-(4-oxo-1,2,3,4-tetrahydroquinazolin-2-yl)phenyl)amino)-1,3,5-triazin-2-yl)isonicotinohydrazide.

Reaction entry: 2.18

Compound code: UHLMTJ-263a

Yield: 65%



IR(neat): 3205,1650, 1554, 1484, 1484, 1404, 1284,1177,1127,1035, 981,832,800 cm⁻¹.

¹**H NMR (DMSO-d6):**δ8.84-8.74(m,2H,-N**H**), 8.17-7.36(m,13H, Ph-**H**,Py-**H**,-N**H**),6.65 (br,1H,NH-C**H-**NH).

4.3.4 Cell Cytotoxicity (MTT Assay) of new molecules:

The cytotoxicity of the newly designed and synthesized drug-like molecules on human cell line SUP-T1 cells was conducted to increase concentrations 50, 100, 250, 500, and 750 μ M the cell viability was evaluated using MTT assay(section 2.2.17). The results of the analysis of 50% cell survival concentrations (CC₅₀) showed that the molecules containing sulfonic groups (UHLMTJ-257c, UHLMTJ-259, etc.) exhibited significant toxicity than the molecules devoid of the sulfonic group (UHLMTJ-257a,b). Along with dihydroquinazoline, isonized combination with sulfonic group molecules UHLMTJ-261c, UHLMTJ-265a were more toxic, and CC₅₀ was 176.02 μ M and 162.72 μ M, respectively. The remaining molecules were moderately toxic at concertation even > 300 μ M, depicted in Fig. 4.4 and Table 4.1. The cytotoxicity results are essential for conducting antiviral studies.

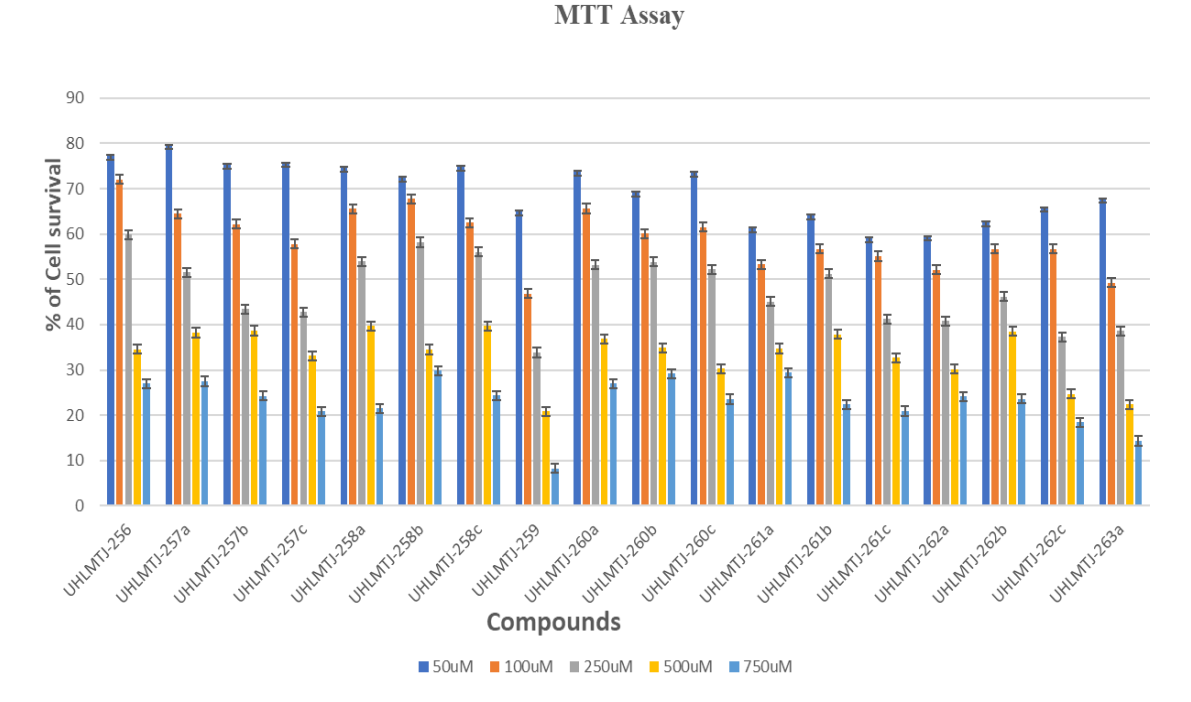


Fig. 4.4: Graphical representation of Cellular cytotoxicity of synthesized molecules at increasing concentrations in SUP T1 cells.

4.3.5 Anti-HIV-1 activity (p24 Assay) of new molecules:

The antiviral activity of molecules was analyzed against the replication of HIV-1 in SepT1 cells below their non-toxic concentrations according to the procedure given in section2.2.19. Acute infection conducted using 93IN101(clade C) and NL4-3 (clade B) virus in the Sup-T1 cell line in the presence of increasing concentrations (0.5 to 10 μM) of the compounds. The virus replicated was estimated in p24 using antigen-capture assay; the results are presented in Fig. 4.5, and IC₅₀ values are presented in Table 4.1. In comparing di and trichloro substituted compounds, trichloro substituted compounds showed better anti-HIV-1 activity than dichloro substitution of corresponding molecules. Among this dihydroquinazoline, isonized combination with sulfonic and sulphonamide contained molecules UHLMTJ-260c, UHLMTJ-261c, UHLMTJ-262a, UHLMTJ-262c, UHLMTJ-263a were highly active with IC₅₀ of 1.54 μM,0.94 μM. 0.76 μM,0.52 μM, respectively. The activity difference of molecules could be related to the interaction affinity with V3 loop residues. These molecules showed similar anti-HIV-1 activity

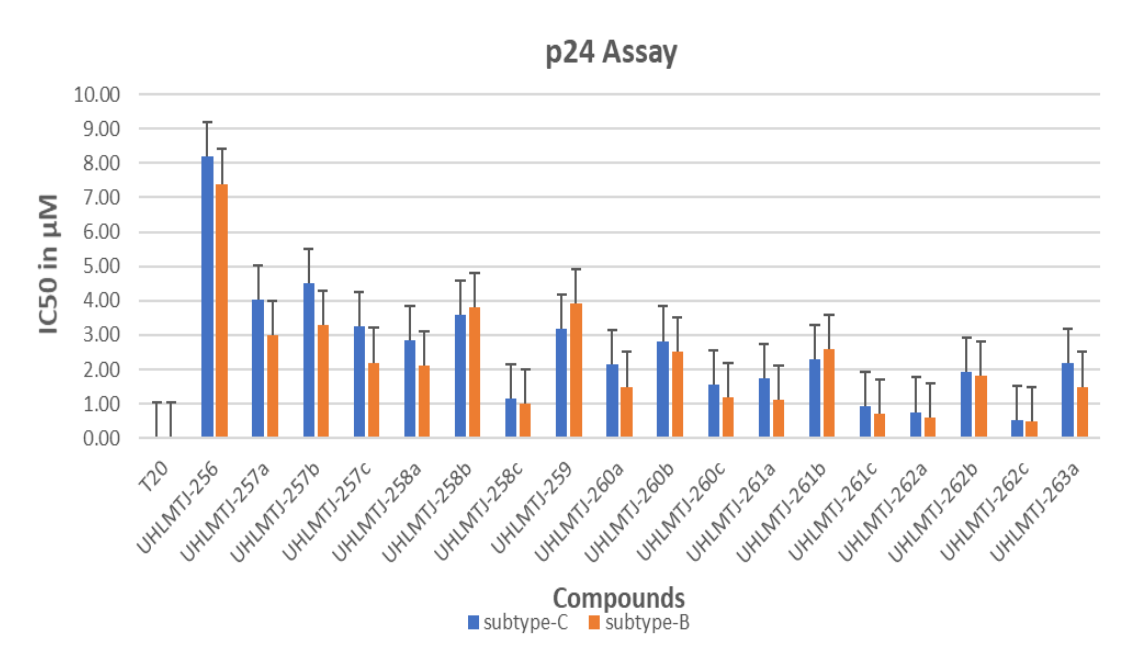


Fig. 4.5: Graphical representation of dose-dependent action of synthesized molecules against replication of HIV-1 subtype B (NL4-3) subtype C (93IN101). Each data point is an average of three independent experiments and presented as Mean±SD. T20 was used as a positive control.

Against clade C, clade B type of virus, while relatively better activity was exhibited against clade B.

S. No	Compound Code	Binding Energy (Kcal/mol)	CC50 (μΜ) (SupT1)	IC50±SD (μM) (93IN101, Clade C)	IC50±SD (μM) (NL4-3, Clade B)	TI (93IN101)	TI (NL4-3)
1	UHLMTJ- 256	-6.0	>300	8.20±0.13	7.4±0.11	>36.58	>40.54
2	UHLMTJ- 257a	-7.3	>300	4.03±0.15	3±0.14	>74.44	>100.0
3	UHLMTJ- 257b	-6.8	>300	4.50±0.18	3.3±0.15	>66.66	>90.90
4	UHLMTJ- 257c	-7.7	272.47	3.25±0.12	2.2±0.18	83.83	123.85
5	UHLMTJ- 258a	-8.0	>300	2.86±0.15	2.1±0.12	>104.89	>142.85
6	UHLMTJ- 258b	-7.2	>300	3.60±0.17	3.8±0.19	>83.33	>78.94
7	UHLMTJ- 258c	-8.7	>300	1.14±0.09	1.0±0.11	>263.15	>300.0
8	UHLMTJ- 259	-7.8	121.31	3.17±0.11	3.9±0.18	38.26	31.10
9	UHLMTJ- 260a	-8.7	>300	2.16±0.19	1.5±0.2	>138.88	>200.0
10	UHLMTJ- 260b	-8.3	>300	2.83±0.12	2.5±0.19	>106.00	>120.0
11	UHLMTJ- 260c	-8.8	>300	1.54±0.15	1.2±0.13	>194.80	>250.0
12	UHLMTJ- 261a	-9.5	209.28	1.74±0.12	1.1±0.15	120.27	190.25
13	UHLMTJ- 261b	-8.5	267.29	2.31±0.16	2.6±0.12	115.70	102.80
14	UHLMTJ- 261c	-9.4	176.02	0.94±0.08	0.7±0.04	187.25	251.45
15	UHLMTJ- 262a	-10.5	151.69	0.76±0.05	0.6±0.03	199.59	252.81
16	UHLMTJ- 262b	-9.0	244.22	1.93±0.12	1.8±0.1	126.53	135.67
17	UHLMTJ- 262c	-9.6	186.86	0.52±0.04	0.5±0.06	359.34	373.72
18	UHLMTJ- 263a	-8.6	162.72	2.20±0.23	1.5±0.12	73.96	108.48

Table 4.1: Binding energy (kcal/mol) in interaction with V3 loop, CC_{50} , IC50, and therapeutic index (TI) of newly synthesized compounds.

Summary of Objective II:

HIV-1 gp120 contains variable and constant regions; the 3rd variable loop (V3 loop) plays a vital role in interaction with co-receptor during viral entry. The V3 loop is composed of exposed and buried regions; the exposed regions have recognized the antibodies. In this study, we have used a V3 loop specific antibody, 447-52D, for identifying particular features associated with recognition and interaction with the V3 loop for developing small molecule mimics. Based on the structure 447-52D antibody and V3 loop interaction, peptides mimetics were designed by in silico methods. The designed mimetics were synthesized based on retained interactions and feasibility of the synthesis process. Here, we have selected two molecules, UHLMT-A2, and UHLMT-A9, as parent structures for further development. The UHLMT-A9 was functionally modified with a molecule containing an s-triazine scaffold. The functional modification was dependent on the V3 loop-CCR5 interaction mechanism and residues present in the interacting region. Most of the interactions were hydrophilic along with hydrophobic and π - π stacking. The interactions could be mimicked with negatively charged sulfonate, dihydroquinoline, isonazide, and other benzene substituted moieties on the s-triazine scaffold. The interaction studies disclosed that tri-substituted molecules interact effectively with better docking scores at the V3 loop range of -8.0 to -10.5 kcal/mol. The molecules were synthesized and characterized using NMR, HRMS, and IR. These molecules showed moderate toxicity >300 µM on SUP-T1 cells. However, a combination of sulfonate, isonized and dihydoquinozoline moieties contained molecules that showed high toxicity and $CC_{50} \sim 150 \,\mu\text{M}$. The antiviral activity results suggested that all molecules have IC₅₀ activity in $<5 \mu M$ except one molecule, UHLMTJ-256, with IC₅₀ $>7.0 \mu M$. The molecules showed similar activity against both subtype B and C viruses; further, sulfonate group-containing molecules have better antiviral activity than non-sulfonate group. In conclusion, sulfonate group-containing molecules will be promising lead molecules for developing molecules with IC₅₀ at nanomolar concentrations.

Chapter 5

Objective III

Sulfonate modified lactoferrin nanoparticles as drug carriers with dual activity against HIV-1.

5.1 Introduction:

HIV-1 can be treated with a range of 27 drugs that target various stages of the virus life cycle[58]. The existing drugs are categorized based on viral protein targets, such as entry inhibitors, fusion inhibitors, reverse transcriptase inhibitors, integrase, and protease inhibitors. However, all approved drugs have limitations due to high drug resistance and unfavorable properties like less half-life and adverse side effects[68]. This limitation necessitates developing novel drugs and treatment options to control infection and mitigate AIDS in infected individuals. Highly Active Antiretroviral Therapy (HAART) is a combination of antiviral drugs used for decreasing viral load in the patient body, which is highly effective than a single antiviral therapy[118]. HAART faces remarkable challenges due to lack of adherence to the treatment schedule, reduced availability of drug levels in the body, and unexpected heart, liver, kidney, and CNS toxicity [201][202]. Also, the present treatment is incapable of complete eradication of the latent virus. These factors warrant novel delivery mechanisms to improve therapeutic concentrations of drug with prolonged half-life and low toxicity.

The entry of HIV-1 into targeted cells is mediated by successive interaction of envelope protein, gp120 with primary receptor CD4 and co-receptors, CCR5, or CXCR4[171]. The variants of HIV-1 that utilize CCR5 for entry are known as R5 isolates, and the ones that use CXCR4 are X4 isolates. Some of the isolates, called R5X4, utilize both co-receptors. The CCR5 receptor is a seven-helix transmembrane protein with an N-terminal consisting of acidic amino acids and post-transitionally modified tyrosine sulphate residues. In the entry process, R5 isolates essentially use tyrosine sulphates and ECL-2 loop of CCR5[171][173]. The co-receptor usage depends on the sequence of the variable loop, V3 of the viral envelope gp120. The V3 loop, being highly immunogenic, plays an essential role in antibody recognition[193]. Previous studies of the gp120-CCR5 complex reported conserved epitopes and an overall positive charge on the V3 loop. This charge plays a vital role in electrostatic interaction with polyanion functional groups.

Further, studies demonstrating the anti-viral activity of small molecules substituted with sulfonates and phosphonates reported better inhibitory activity by the former. This difference in inhibition could be attributed to the V3 loop's affinity to the sulfates, as seen in the case of CCR5-Nt[189]. This established that polyanion sulfonated groups on the nanocarrier surface would have electrostatic interaction with the V3 loop of gp120.

In recent times, research in nanomedicine is focused on developing delivery options to treat HIV/AIDS. Nanomedicine is the nanoscale self-assembly of polymer materials by engineering technology for better therapeutic drug delivery. Polymer materials used in medical applications include lipids, organic, inorganic polymers, PEG, proteins, etc. [203]. Nanomedicine can facilitate the co-delivery of a combination of drugs in a therapeutic modality. It can also facilitate the delivery of poorly water-soluble drugs at the tissue or cell level and macromolecular drug delivery to intracellular actionable sites. Despite nanomedicine's advantage, many disadvantages like nonspecific delivery and toxicity of polymer materials have been observed in clinical applications. Today, only a few Nano-formulations are approved by the FDA [204]. Several parameters are considered for using Nano vehicles for drug delivery, such as biocompatibility of material, size, the surface charge of the particles, etc. More recently, pre functionalized biomaterials have been demonstrated as delivery vehicles for better cellular receptor interaction and uptake of loaded drugs [205]. In clinical translational research, surface modified nano-vehicles with specific functional group modifications have shown better biodistribution and interaction with a subset of cells in actionable tissue. The naturally available materials for the preparation of nanoparticles are mostly proteins, lipids, chatoyant, etc. Among this, proteins have been widely used as a matrix for nanoparticle preparation for better biocompatibility, higher biodegradability, and lower immunogenicity [206][207]. The availability of moieties on proteins for surface modification, with specific functional groups, provides an opportunity to develop nanoparticles for receptor-based internalization. Many proteins viz albumin, transferrin, gelatin, etc. are extensively used to prepare nano-drug carriers [208].

This study used Lactoferrin as a nanocarrier, known for its anti-viral, antibacterial, antifungal activity[143]. Lactoferrin (Lf) is a transferrin family 80KDa glycoprotein, abundantly available in mammal milk, secretory fluids, and white blood cells [142]. Previously, Lf-NPs have been reported as drug carriers for HIV-1 ART drugs with optimal results[146]. To improve the efficiency and target specificity of the Lf NPs, the surface was modified by sulfonate groups to target the V3 loop of gp120. We report the modified Lactoferrin-MES Nanoparticles' preparation, characterization, and biological activity (Lf-MES NPs).

5.2 Rational of Objective III:

Highly Active Antiretroviral Therapy (HAART) was a more effective treatment for AIDS patients. In the treatment process, a combination of drugs in different dosages was used continuously, which causes some side effects. To improve the drug availability at target continually with fewer side effects, we need new technology and delivery systems. Nanotechnology was used for drug delivery with different materials compatible with the human body and other properties. Mostly protein nanoparticles were used for drug delivery and modified surface with groups for target-specific. In the objective, we were using lactoferrin protein nanoparticles for antiretroviral drug delivery along with surface modified with small functional groups for viral envelope targeting. The drug carrier Lf-Nps loaded with AZT, and the surface modified with sulfonate groups acting against entry and post-entry of HIV-1. In the study, we were preparing the physical and biological characterization of surface modified AZT-loaded Lf-Nps.

5.3 Results & Discussion:

5.3.1 Preparation and Physical Characterization of nanoparticles:

The reported drug-loaded surface modified Lf-MES NPs were prepared by a sonochemical method (section 2.2.7) in MES's presence (Fig. 5.1). The nanoparticles were observed to be spherical, and the size measured by FE-SEM and TEM for Lf-AZT NPs was in the range of 90 nm to 120 nm Lf-MES-AZT NPs was in the range of 55nm to 79 nm (Fig. 5.2(i)A and B). In suspension, Lf-AZT NPs in Milli-Q showed size distribution below 102 nm, and Lf-MES-AZT NPs showed uniform size distribution of 72nm (Fig. 5.2 (ii)A and B). As explained by zeta potential, the electrostatic charge of formed NPs was observed to be -9.4mV and -20.4 mV for Lf NPs and Lf-MES NPs, respectively (Fig. 5.2(iii) A).

The native agarose gel electrophoresis technique was employed to study the particles' charge. The sign and charge are decided by their pI value and the running buffer((section 2.2.10)). This can be visualized by the difference in migration in the agarose gel. In the gel, sol. Lf, Lf-NPs, and Lf-MES NPs were loaded, and the DNA ladder was taken as a positive control. From (Fig. 5.2(iii) B) shows that the comparative migration of Lf-MES NPs increased towards anode at constant time and voltage. The results show that the negative charge on Lf-MES NPs is greater

than Lf-NPs. This charge difference may reflect the modification of Lf NPs by sulphonate groups.

The drug-releasing of loaded particles was explained in the presence of an acidic solvent (section 2.2.11). Lf NPs were seen to be sensitive in acidic conditions, as observed by estimated drug release at different pH. The delivery of AZT from nanoparticles varies with pH change from low to high with a maximum at pH 5.0 for both Lf NPs and Lf-MES NPs (Fig. 5.2(iv)). Drug loading capacity (LC) and encapsulation efficiency (EE) of nanoparticles are essential aspects that dictate effective therapeutic delivery at target. Based on the formula (section 2.2.12), the LC and EE of Lf-AZT NPs and Lf-MES-AZT NPs were calculated as 6.5%,63%, and 7.2%, 68%.

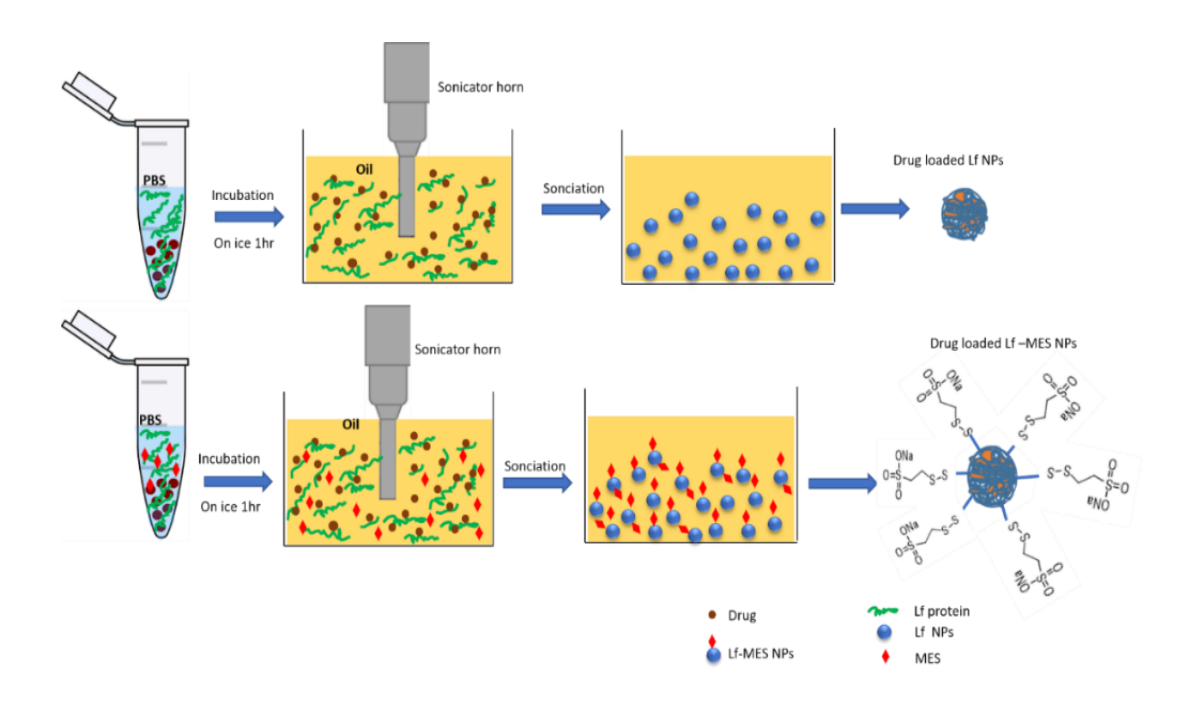


Fig. 5.1: Preparation of nanoparticles by sol-oil method A) Depicts the procedure followed for Drug loaded Lf NPs B) Depicts the procedure for drug-loaded MES conjugated Lf NPs.

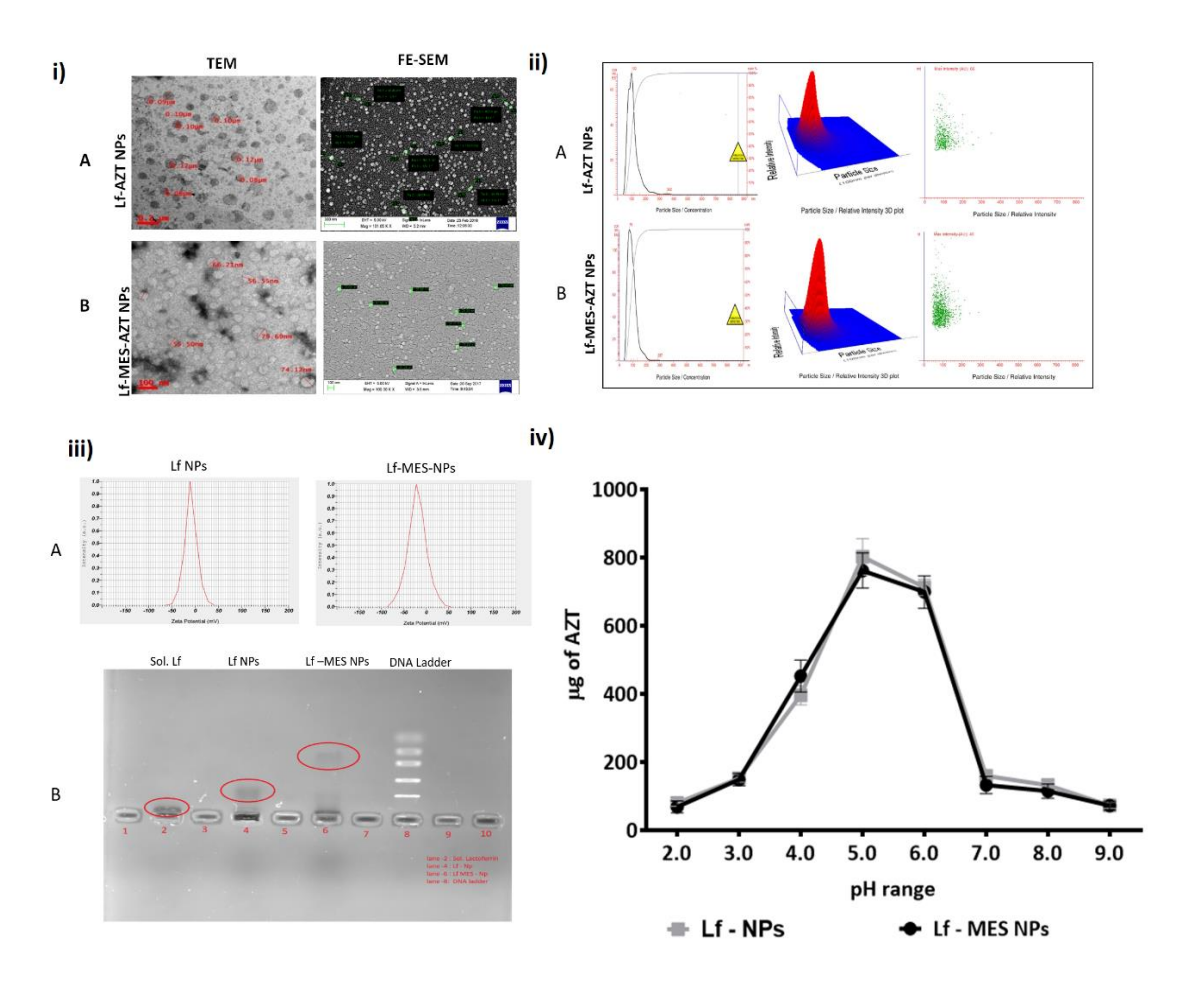


Fig. 5.2: (i) Characterization of size and shape of A) AZT loaded Lf-NPs B) and MES-Lf-NPs by TEM and FE-SEM. AZT loaded Lf NPs showed a size range of 90nm to 120nm and AZT loaded Lf-MES NPs were in the size range of 55nm to 79nm.ii) Characterization of size distribution of NPs in suspension. A) distribution of Lf-AZT NPs B) distribution of MES-Lf-AZT NPs by Nanosight. The distribution of particles in milliQ reported a mode of 102nm for Lf-AZT NPs and 76nm for MES-Lf-AZT NPs. (iii) A) Characterization of charge distribution of NPs in suspension by Zeta Sizer, Lf NPs showed a zeta potential of -9.4mV and Lf-MES NPs showed a potential of -20.4 mV. B) Merged image of Agarose gel loaded with soluble Lactoferrin, Lactoferrin NPs and MES conjugated Lactoferrin NPs. DNA Ladder was used as a control. Lf-MES NPs showed greater movement towards anode in comparison to sol.Lf and Lf NPs. iv) Graph plotted between pH and concentration of AZT to represent pH dependent drug release of Lf-AZT NPs and Lf-MES-AZT NPs. Maximum drug release was observed between pH 5.0-6.0. No Significant difference was observed between the Lf-AZT and Lf-MES-AZT

5.3.2 Analysis of MES conjugated Lf nanoparticles by solid-state NMR:

The functional characterization of surface modified NPs (Lf-MES NPs) was performed by solid-state NMR (section 2.2.13). The NMR active nucleus ¹H, ¹³C, ³³S, ¹⁵N, ¹⁷O, ²³Na of Lf-MES NPs mainly used to determine particles' functionality. The MES molecule conjugated on protein nanoparticle by a disulfide bond formed by reaction between sulfhydryl (thiol) groups of a cysteine residue of protein and MES during sonication. For the conformation

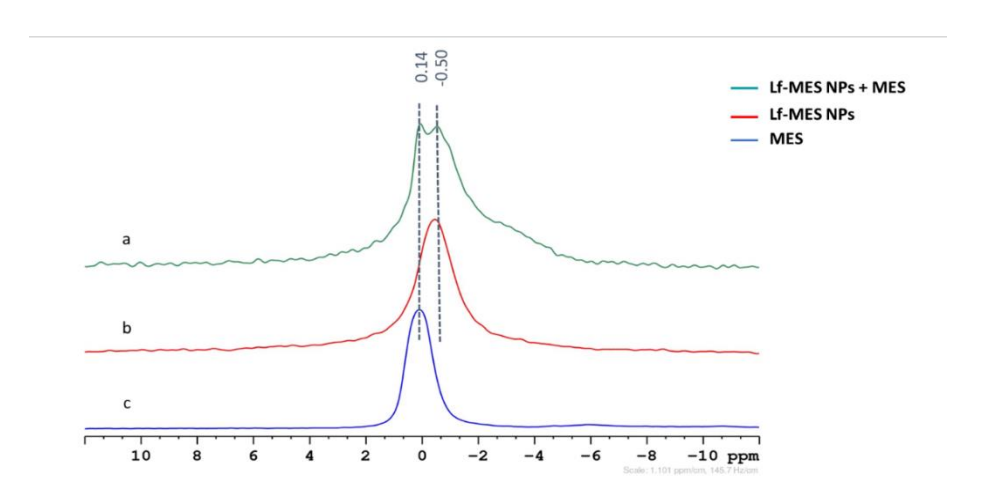


Fig. 5.3: Characterization of MES group on Lf – MES NPs by ²³Na nucleus with MAS NMR at 132.33 MHz. a) ²³Na nucleus spectra of Lf-MES NPs + MES physical mixture b) ²³Na nucleus spectra of Lf-MES NPs c) ²³Na nucleus spectra of MES molecules.

Of that bond generally, sulfur NMR was useful. Still, the sulfur NMR performance was tough due to low natural abundance (0.76%), a small gyromagnetic ratio (g= 2.055×10⁷ rad T ⁻¹ S⁻¹) of NMR active isotope of sulfur ³³S nucleus[209]. However, the analysis of other NMR -active nucleus (¹H, ¹³C, ¹⁵N, ¹⁷O) spectrum of Lf-MES NPs was complicated by the complexity of macromolecular spectral overlapping from a large number of unique signals [210]. Here, we performed solid-state NMR of the active quadrupole nucleus ²³Na of Lf-MES NPs for functional validation of Sodium -2 -mercaptoethanesulfonate (MES) on Lf-NPs. In the below spectral analysis, the difference in the chemical shift of ²³Na nucleus in MES and Lf-

MES NPs was observed in the range of 0.64 ppm. The negative chemical shift (δ = -0.50 ppm) of ²³Na nucleus in Lf-MES NPs represents the protein field's shielding effect on the nucleus due to the chemical bond. Otherwise, the physical mixture of MES and Lf-MES NPs generated two peaks corresponding to individual molecules with similar chemical shifts (**Fig. 5.3**). That means in a mixture compound protein filed not shown any shielding effect on ²³Na nucleus. The results suggest that the MES molecule binds with Lf-NPs through chemical bonds offered in a new chemical shift but not observed in the physical mixture. The detailed spectra of individual molecules are shown in the **appendix**.

5.3.3 Characterization of Functional groups on protein nanoparticles.

Lf-NPs, Lf-MES NPs, and MES were analyzed for changes in functional groups' vibrational mode at different wavelengths, and the experiment conducts as per the procedure **section 2.2.14**. In the study, significant differences were explained through the disulphide bonds and sulphonate groups on Lf-MES NPs. From the spectrum (**Fig. 5.4**), the CYS-CYS disulphide bonds conformation (g-g-t) was observed at 523 cm⁻¹, the CYS-MES disulphide bonds were observed at 589 cm⁻¹. $C_{\beta}H_2$ wagging mode was seen at 795 cm⁻¹; the band at 1064 cm⁻¹ corresponds to Sulfonate (SO₃⁻) in the MES spectrum. The same peak was shifted (8 cm⁻¹) to a lower wavenumber in the Lf-MES spectrum due to a difference in cation ionic pairs' interaction in solution. The peaks at 1584 cm⁻¹ and 1610 cm⁻¹ correspond to Phe, Tyr (C=O stretching vibration) groups. The vibrations of Lys NH₃⁺ was observed at 1121 cm⁻¹-1185 cm⁻¹.

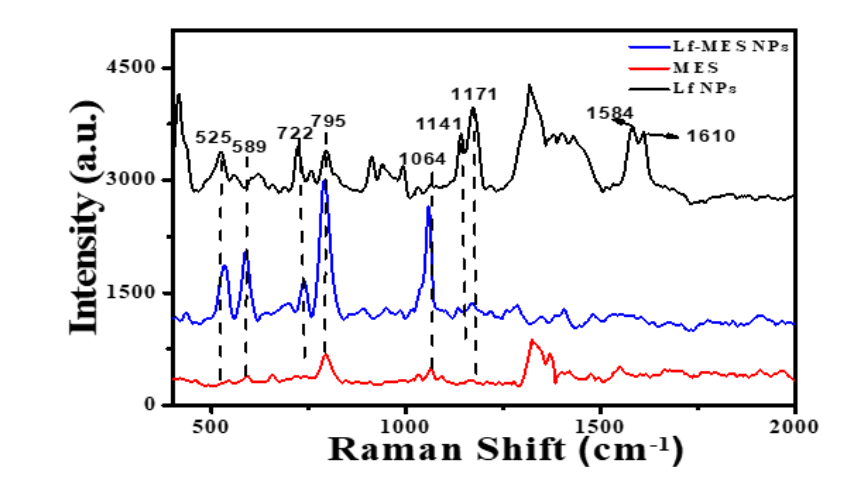


Fig. 5.4: Characterization of Functional groups on protein nanoparticles by SERS at 785nm excitation. The CYS-CYS disulphide bonds conformation (g-g-t) was observed at 523 cm⁻¹, the CYS-MES disulphide bonds were observed at 589 cm⁻¹. The band at 1064 cm⁻¹ corresponds to Sulfonate (SO_3^-) group. The Spectrum of Lf-NPs is in black , Lf-MES NPs is in blue and MES in red.

5.3.4 Cellular localization of fluorescent drug (Curcumin) loaded NPs by Confocal study and localization of drug (AZT) quantified by HPLC.

Curcumin-loaded Nanoparticles were used to visualize the nanoparticles' localization in HL2/3 cells at different time intervals from 30 min to 12 hrs. As seen in **Fig. 5.5(i)**, the localization of Curcumin (Green fluorescence) in Lf-Cur NPs treated cells (panel A) were observed starting from 1hr time point reaching to a maximum at 4hr followed by the decreased intensity in later

time points. In Lf-MES-CUR NPs (panel B), the localization started at a 30min time point and reached the maximum at 4hr. Despite a minor decrease in the fluorescence in later time points, the localization sustained up to 12hrs. The drug's availability was quantified by measuring Curcumin's fluorescence intensity and is depicted in the graph (Fig. 5.5(i)C). SKNSH cells were used as negative control. The results represented in Fig. 5.6 showed an increased localization in the SK-N-SH cells at 2hr and 4hr time points, 4hr being the highest. No significant difference was observed between cells treated with Lf-CUR NPs and Lf-MES-CUR NPs, unlike in HL2/3 cells, suggesting the role of gp120 in nanoparticle localization. The internally localized AZT in HL2/3 cells was further quantified at different time points by HPLC. From (Fig. 5.5(ii)), the availability of AZT was significantly high at all time points starting from 30mins in Lf-MES-AZT NPs, suggesting that Lf-MES-AZT NPs highly interact

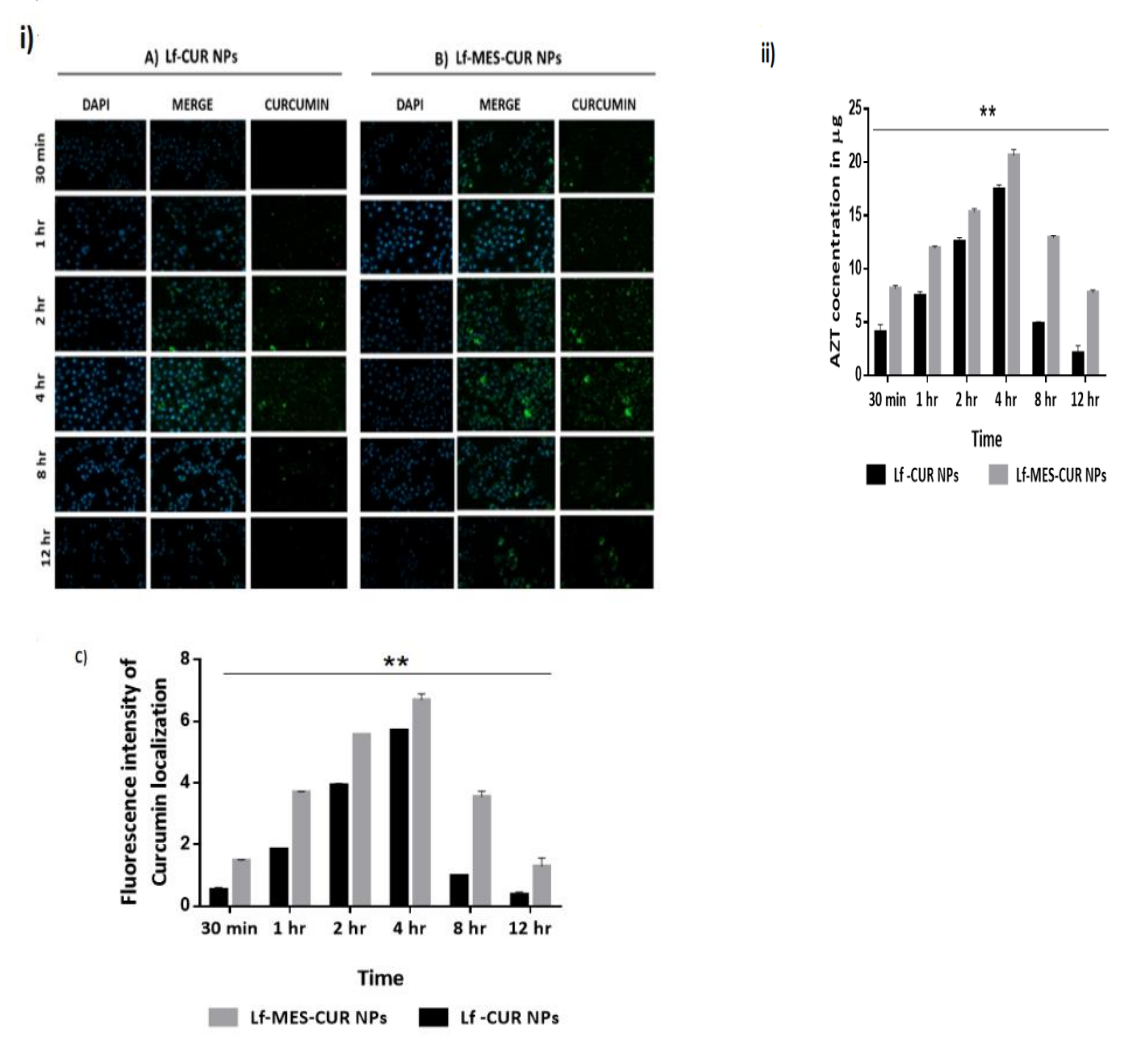


Fig. 5.5: (i) Cellular (HL2/3) localization of fluorescent drug, Curcumin loaded A) Lf NPs and B) Lf-MES NPs 0.5hr, 1hr, 2 hr, 4hr, 8hr, 12 hr time points. As visualized by the fluorescence (green), Lf-MES-CUR NPs, showed better localization of the drug than Lf-NPs at all time points. Lf-MES- CUR NPs showed effective localization and long-term delivery at 30 min and 12hr time points respectively. C) The fluorescent intensity was plotted as a graph using ImageJ software. (ii) The amount of AZT localized in the cell at different time points when delivered through Lf NPs and Lf-MES NPs was estimated through HPLC and plotted as a graph. The results reflected the localization assay with Cur NPs. Both Lf-AZT NPs and Lf-MES-AZT NPs showed maximum localization at 4hr time point but Lf-MES-AZT NPs sustained the localization until 12hr.

Objective III

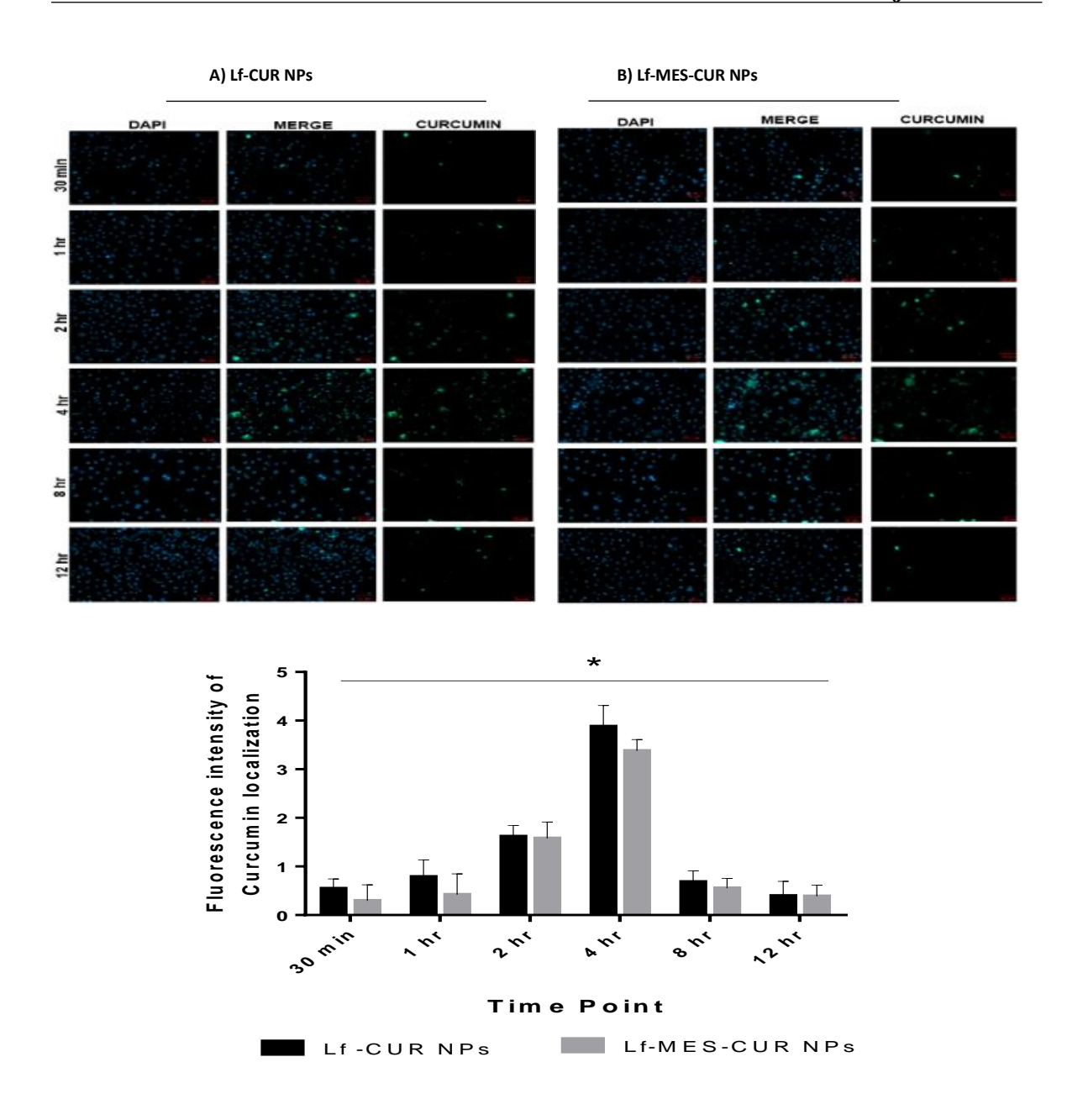
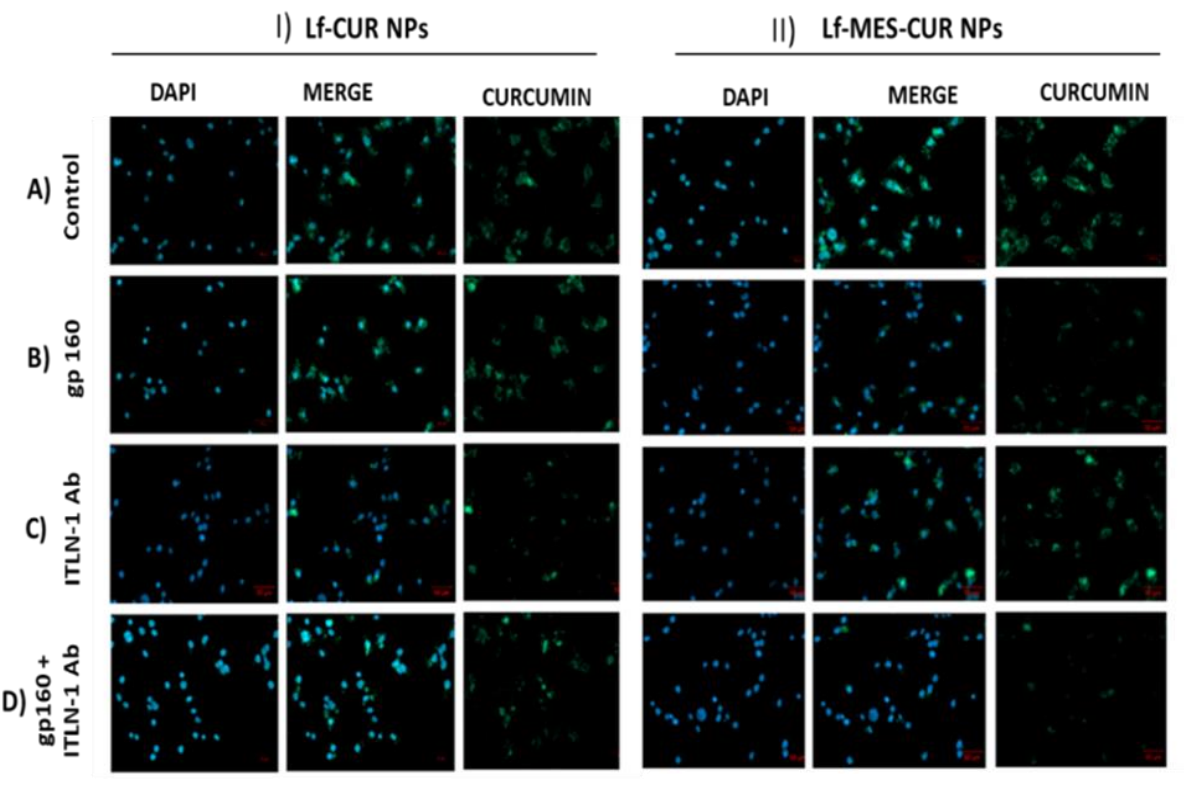


Fig. 5.6: Cellular (SKNSH) localization of fluorescent drug, Curcumin loaded A) Lf NPs and B) Lf-MES NPs 0.5hr, 1hr, 2 hr, 4hr, 8hr, 12 hr time points. As visualized by the fluorescence (green), Lf-CUR NPs, and Lf-MES- CUR NPs didn't show significant difference of the drug at all time points C) The fluorescent intensity was plotted as a graph.

5.3.5 Competitive interaction of MES nanoparticles with HL2/3 cell surface gp160:

The affinity of MES nanoparticles to bind with gp160 was determined by treating HL2/3 cells with NPs in the presence of lactoferrin receptor antibody (ITNL-1) and purified gp160 (**section 2.2.16**). Curcumin-loaded Lf and Lf-MES nanoparticles were used to visualize the difference

in localization. The results are depicted in (**Fig. 5.7**) with (panel I) comprising of Lf-CUR NPs and (panel II) comprising of Lf-MES-CUR NPs localization. In Lf-CUR NPs, a notable decrease in fluorescence intensity was observed in HL2/3 cells treated with ITLN-1, which blocks the interaction and receptor-mediated endocytosis of the NPs. No significant difference in fluorescence was observed in cells treated with ITLN-1+gp160, suggesting no involvement of gp160 in localization of Lf-CUR NPs. This was also confirmed in cells treated with sol.gp160 only, where no difference in fluorescence than control was observed. In Lf-MES-CUR NPs, a significant decrease in fluorescence intensity was observed in cells treated with sol.gp160 and a combination of sol.gp160+ ITLN-1 Ab. Sol.gp160 binds to free Lf-MES-CUR NPs, reducing its availability to HL2/3 cells, thus decreasing Curcumin's localization. Similar results were observed in the presence of ITLN-1 and gp160. However, treatment with ITLN-1 Ab alone showed an exceptionally low decrease in intensity. The results confirm the interaction of MES NPs with gp160. Treatment with NPs in the absence of sol gp160 and ITLN-1 was



taken as control.

Fig. 5.7. The figure depicts the localization of Lf-CUR NPs and Lf-MES-CUR NPs in the presence of agents B) sol gp160 to competitively bind Lf-MES-CUR NPs C) ITLN-1 Ab to bind to Lf receptors on HL2/3 cell surface D) ITLN1+gp160. A) The localization in the absence of agents was taken as control. The localization in Lf-MES-CUR NPs was majorly inhibited in the presence of gp160 and a combination of ITLN-1 Ab and gp160. The localization of Lf-CUR NPs was majorly inhibited in the presence of ITLN-1 Ab, and no difference was observed in the presence of other agents.

5.3.6 Cell Cytotoxicity Assay:

Cytotoxicity of the nanoformulations (Blank Lf, Lf-MES NPs, and Lf-AZT, Lf-MES-AZT) was assessed by MTT Assay (section 2.2.17). The cell survival in the presence of nanoparticles was compared with sol. AZT. MES was used as a control, and cell survival was measured at concentrations 25μ M, 50μ M, 75μ M, 100μ M, and 150μ M. The blank Lf, Lf-MES, and AZT loaded nanoparticles showed low toxicity at all concentrations. Toxicity induced by MES powder was also observed to be negligible. A significant difference in cell survival between the nano-formations and sol. AZT was observed at all concentrations with a 35% difference at 150μ M (p-value < 0.0001) (Fig. 5.8).

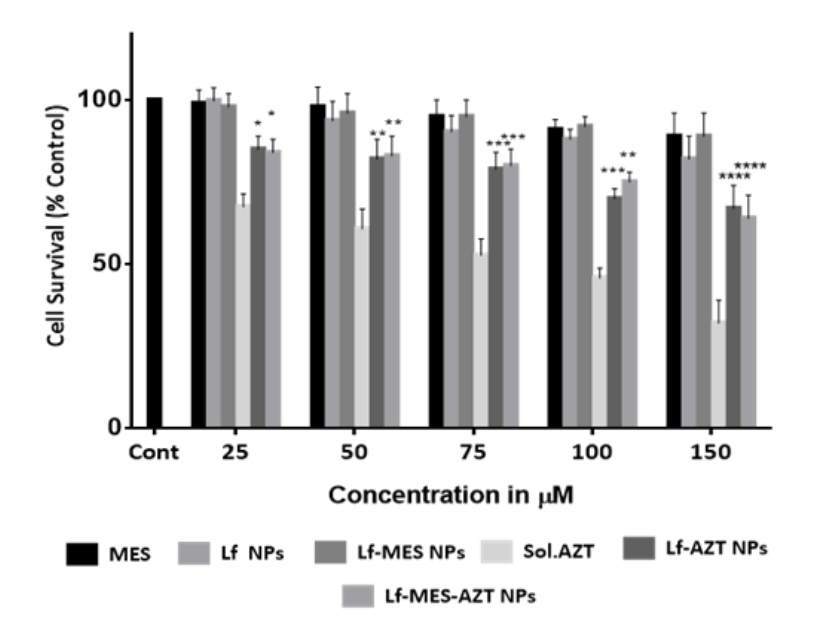


Fig. 5.8: Depicts the cell survival in terms of % control. The nano-formulations of AZT showed significantly lower toxicity than soluble AZT. The blank nanoparticles and MES showed negligible toxicity. Data is represented as Mean+SD of triplicate experiments and significance was calculated using Two-way Annova. * indicates a p-value ≤ 0.05 _** indicates value ≤ 0.01 , *** signifies value ≤ 0.001 and **** signifies value ≤ 0.0001 vs sol.AZT.

5.3.7 Inhibition of Cell Fusion:

The role of Lf-MES NPs in inhibiting the fusion of the virus to the host cell was monitored using the dye redistribution assay according to the protocol described in **section 2.2.18**. HL2/3 and T-Cell line, SupT-1 previously loaded with cell-permeable dyes, were allowed to contact and fuse in the presence of nanoparticles. The cellular mixing of the dyes was observed to

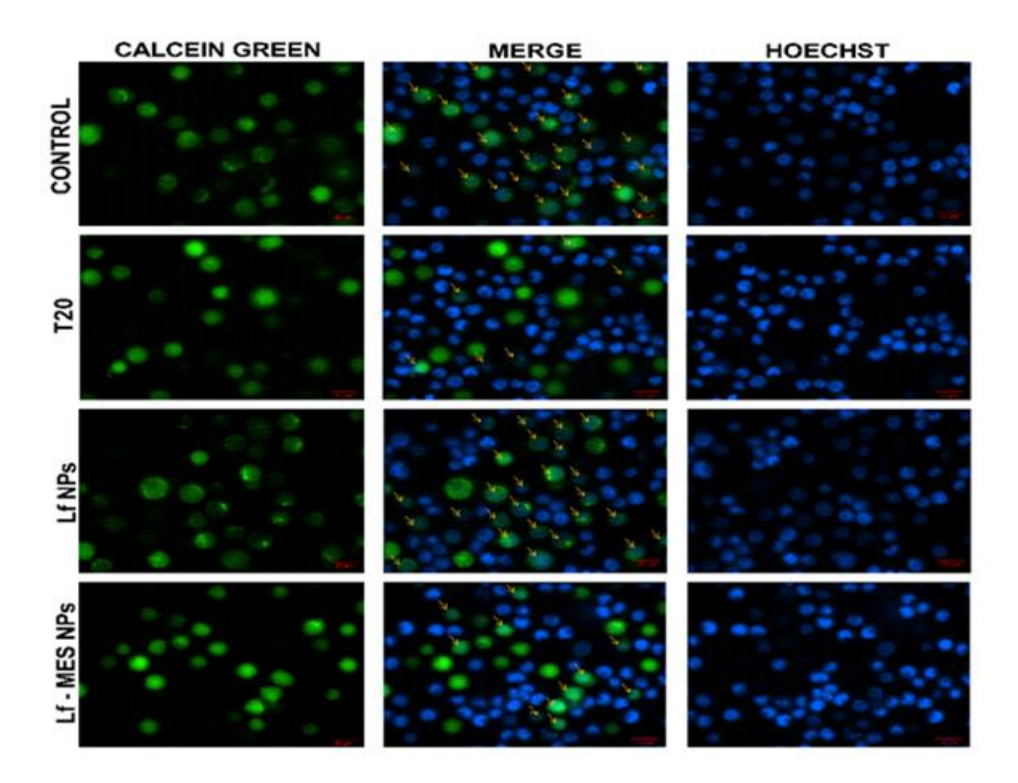


Fig. 5.9: Inhibition of Cell Fusion depicted by dye redistribution assay. The fusion was monitored in presence of Lf NPs and Lf-MES NPs and T20. Both, Lf NPs and Control experiment showed 80-100% fusion, with green and blue dye mixing in the fused cells. Lf-MES showed inhibition of fusion with only 50% of the cells showing dye mixing.

Confirm the fusion of the cells. The results obtained are represented in (**Fig. 5.9**). The fusion of the cells in control and Lf NPs treated cells shows an approximate 100% and 80% fusion, respectively, while in the positive Control (T-20 treated cells), the fusion was negligible. In Lf-MES NPs, the cells' fusion was seen to be inhibited, with only 50% of cells participating in the fusion. This suggests the activity of Lf-MES in the entry/ fusion of the virus.

5.3.8 Anti-viral activity of nanoparticles :

The inhibition of HIV-1 infection was analyzed by quantifying the viral p-24 antigen by ELISA Assay (**section 2.2.19**). The Lf-MES-AZT NPs (IC50:15.2nM) showed significantly greater inhibition (p-value ≤ 0.0001) than sol.AZT (IC50:46.7nM) and Lf-AZT (IC50:34.2nM). The percent inhibition of viral replication versus concentration was plotted in (**Fig. 5.10**). Blank Lf-

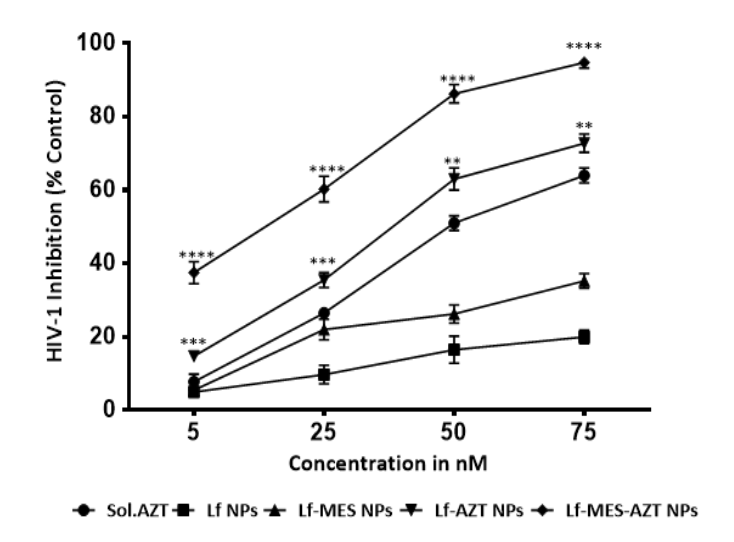


Fig. 5.10: Depicts the HIV-1 inhibition in terms of % control. The Lf-MES-AZT NPs showed significantly better activity in comparison to both Sol. AZT and Lf-AZT NPs. The blank Lf-MES NPs showed inhibition when compared to Blank Lf-NPs. Data is represented as Mean+SD of duplicate experiments and significance was calculated using Two-way Annova between Sol.AZT vs Lf-MES-AZT NPs and Lf-AZT NPs vs Lf-MES-AZT NPs. **** indicates p-value ≤ 0.0001 , *** indicates value ≤ 0.01 , *** signifies value ≤ 0.001 .

MES NPs showed marginally better inhibition of infection in comparison to Blank Lf NPs. This suggests the probable involvement of MES nanoparticles in controlling the disease.

Summary of objective III:

We present a surface modified protein nanoparticle that can control HIV-1infection by inhibiting the entry and successfully delivering the ART drugs to the infected cell. The advantage of using the protein polymers as drug carriers is the interaction of hydrophobic and hydrophilic side chains of amino acids with both water-soluble, insoluble molecules [211]. The preparation method presented is simple water in the oil sonochemical way without using toxic surfactants to stabilize particles [212]. The sol-oil process ensures the particles' spherical structure necessary for drug interactions, and the sonication step enables self-assembly to form nano-sized particles. The presence of 34 cysteines, two disulfide bonds, and freely available Cysteine groups allows Lf to create intra/intermolecular disulphide bonds within the protein or other external molecules [213][214]. The surface modification of the Lf NPs is initiated by

HO₂* free radicals generated by sonochemical irradiation activating either sulfhydryl group of CYS (cysteine) residue or MES [215][216].

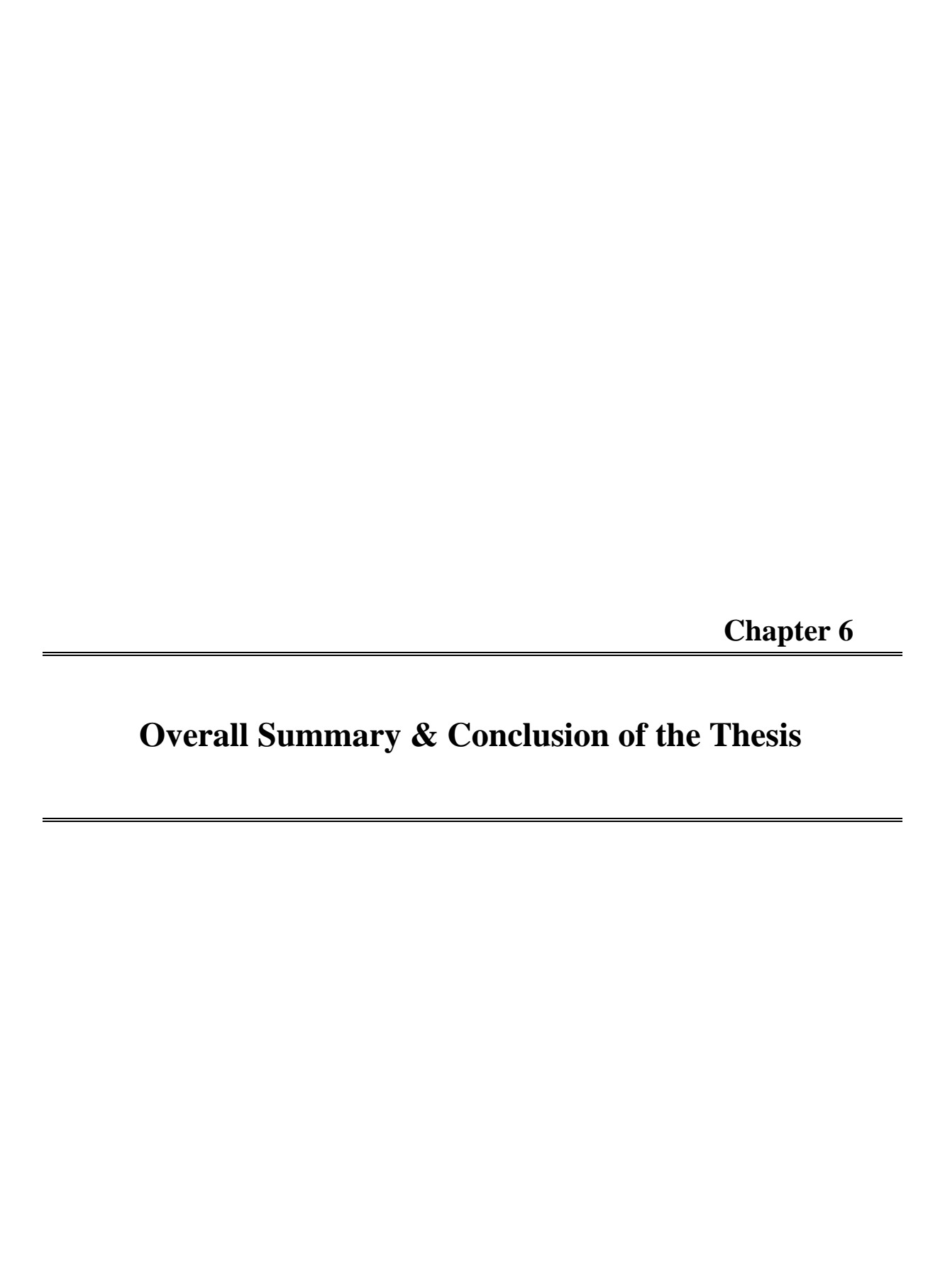
The formed nanoparticles showed acceptable morphological parameters such as size and shape, influencing the particles' biological response and interactions. The particles' spherical shape enables easy cellular entry, and the smaller size optimizes the enrichment of particles on the receptors [217]. The range observed for the Lf-MES-AZT NPs is optimal for cellular uptake of particles by the endosomal mechanism, thus making them an acceptable delivery vehicle. The zeta potential decides the stability arising from repulsion between the formed particles [218]. The magnitude of the zeta potential observed is permissible to consider the particles stable. The dominant-negative charge confirmed by particles' migration towards the anode in a native agarose gel plays a pivotal role in biological interactions[168]. In blood fluidic distribution, nanoparticles interact with several protein coronae based on the particles[219]. Negatively charged particles are abundantly available at the target site, unlike the positively charged particles, which tend to interact more with serum or other biological fluid proteins, decreasing its half-life in blood[220]. This makes the formed particles acceptable carriers. The observation from the native agarose gel electrophoresis confirmed the surface modification of Lf NPs with a sulfonate group.

The functional characterization to confirm newly formed nanoparticles' surface modification was performed through the surface-enhanced Raman spectroscopy (SERS). The SERS is a powerful analytical tool to study complex biomolecules and to observe dynamic structural changes in the biochemical fingerprint region. The Raman signals of the target sample are enhanced by the energy transfer mechanism when placed onto metal nanostructures (Au-NSs) [221]. The surface-enhanced resonance spectrum is analyzed to give structural modification of functional groups of samples at the Near-infrared (NIR) region[222]. In the case of the protein spectrum, significant conformational changes are observed in certain amino acids (Cys, Phe, Gly, Pro, Met) and their corresponding functional groups' vibrations like C=O,-COO $^{-}$,-NH₃+,-C-S,-C-H,-S-S- [223]. The other primary vibrational frequency of CYS-CYS disulphide bond conformation (g-g-t), CYS-MES disulphide bond, C $_{\beta}$ H $_{2}$ wagging mode, and the band corresponds to Sulfonate (SO₃- $^{-}$) of MES were observed in the spectrum[224][225]. The influence of cation ionic pair interaction in solution on functional group peak shifting, as shown in the spectrum [226][227]. Overall, the SERS spectrum of Lf-

MES NPs provided vital information of functional groups suggesting the addition of sulfonate groups on nanoparticles.

The enrichment of the active pharmaceutical ingredient of the Nanoformulation at the target site is ensured by its control release from the carrier polymer. The nanoparticle's drug release depends on the polymer's chemical nature and external stimuli, such as pH or temperature, which degrade the polymer to release the drug[228]. Like other Acidic sensitive nanoparticles that degrade at pH 4.5 -5.5[229], biodegradable Lf NPs, Lf-MES NPs also showed a maximum drug release at pH 5.0. The receptor-based localization and drug(Curcumin) release of NPs was evaluated by fluorescent studies[146]. The increase in fluorescence seen in Lf-MES-CUR NPs is contributed by the gp160 targeted enrichment of the MES NPs, facilitating their internalization availability. The fluorescence suggests early localization followed by sustained presence even at higher time points, making these viable nano-carriers for prolonged drug release. The results confirm that surface-modified NPs are more specific towards gp160 protein and slow-release during the action. The results were reconfirmed using AZT loaded NPs by using semi-preparative HPLC.

The reported particles demonstrated an acceptable toxicity profile, similar to other in-vitro and in-vivo studies conducted, that showed better safety with Lf-AZT NPs in comparison to sol AZT[146]. The viral inhibition observed in fusion assay and p24-ELISA assay suggests a dual activity via drug release and control in the viral particles' entry/fusion. Overall, the Lf-MES NPs obtained by surface modification with sulfonate groups conjugated by disulphide bonds were shown to be efficient against HIV-1. The specificity of Lf-MES NPs to virus envelope protein was confirmed through cellular localization studies, and binding affinity was confirmed by competitive assay. The surface modified nanoparticles can be loaded with ART single or multiple drugs for long term control release and for increased drug concentration at that target site.



The thesis's outcome can be divided into two parts. The first part of the thesis explored HIV-1 entry inhibitors' development based on the active peptide and broadly neutralizing antibody interacting mimetics explained in Objective I and II. The other part of the thesis was the protein nano delivery system for antiviral drug delivery and surface modified with functional groups acting as a target-specific and inhibiting HIV-1 entry. The dual nature nano-drug delivery system was briefly explored in Objective III.

Objective I:

- The protein Epap-1 was taken to design compounds to target HIV-1 entry by binding to the V3 loop of gp120.
- From designed molecules, pharmacologically stable pyrazole, dihydropyrimidine (DHPM) mother structure compounds were selected for development.
- The three molecules, UHLMTA-E5, UHLMTA-E8, and UHLMTA-E9, contain pyrazole, dihydropyrimidine (DHPM), respectively.
- Compare to pyrazole, DHPM scaffolded natural molecules have shown entry inhibition, so UHLMTA-E8 and UHLMTA-E9 selected for further development.
- The Insilco docking studies reveal that DHPM derivatives are binding in-between V3 loop and CD4 binding site (phe43 cavity) with binding score -5.0 to -7.0 kcal/mole.
- Trying to synthesize UHLMTA-E9 derivative molecules by 1,2,3,4-tetrhydropyrimidine (THPM)-thioxo molecules used as reactants, but the reaction was a failure to get a set of molecules are 1,2,3,4-THPM-oxo compounds.
- The 1,2,3, 4-THPM-thioxo (UHLMTJ-254a-g) and 1,2,3, 4-THPM-oxo (UHLMTJ-255a-g) molecules were docking with gp120 to get binding results at "phe43 cavity" and near phe43 cavity region respectively.
- The UHLMTJ-254e molecule binding at the pocket of CD4 binding and participated in hydrogen bonding with ASP-368 of gp120, crucial for gp120 -CD4 interactions.
- The synthesized series of molecules were structurally similar, but only two atoms (S, O) were exchanged, which was Confirmed by physical characterization with NMR, HRMS, and FTIR of two molecules UHLMTJ-254a, UHLMTJ-255a.
- Total synthesized 15 molecules UHLMTA-E5, UHLMTJ-254 a-g, and UHLMTJ-255a-g were further biologically characterized.
- The compounds cytotoxicity was testing (MTT assay)on SUP- T1 cells in different concentrations from 25 to 500 μ M, and HIV-1_{93IN101} Subtype C virus was used for the antiviral test (P24 assay) and used compound concentrations in the range of 0.5 to 10 μ M.

- UHLMTA-E5 (CC₅₀ = 37.7 μ M) is comparatively toxic at 25 μ M, while all other compounds tested exhibited <20% toxicity at 25 μ M.
- Cytotoxicity of compounds showed that Tetrahydopyrimidine (THPM) thioxo derivatives UHLMTJ-254 a-g exhibited higher toxicity than oxo derivatives UHLMTJ-255 a-g.
- The antiviral results showed that UHLMTJ-254 a-g exhibits higher anti-HIV-1 activity than UHLMTJ-255 a-g, and IC50 of compounds was at $< 5 \mu M$. Among these, one of the molecules, UHLMTJ-254e, shown 50% inhibition at 2.2 μM , while the molecule UHLMTA-E5 has shown IC₅₀ at $\sim 9 \mu M$.
- ➤ The overall conclusion of Objective I was 1,2,3,4- tetrahydopyrimidine (THPM)-thioxo derivatives were showed better activity with site-specific (phe43 cavity) binding and used for further development as entry inhibitors.

Objective II:

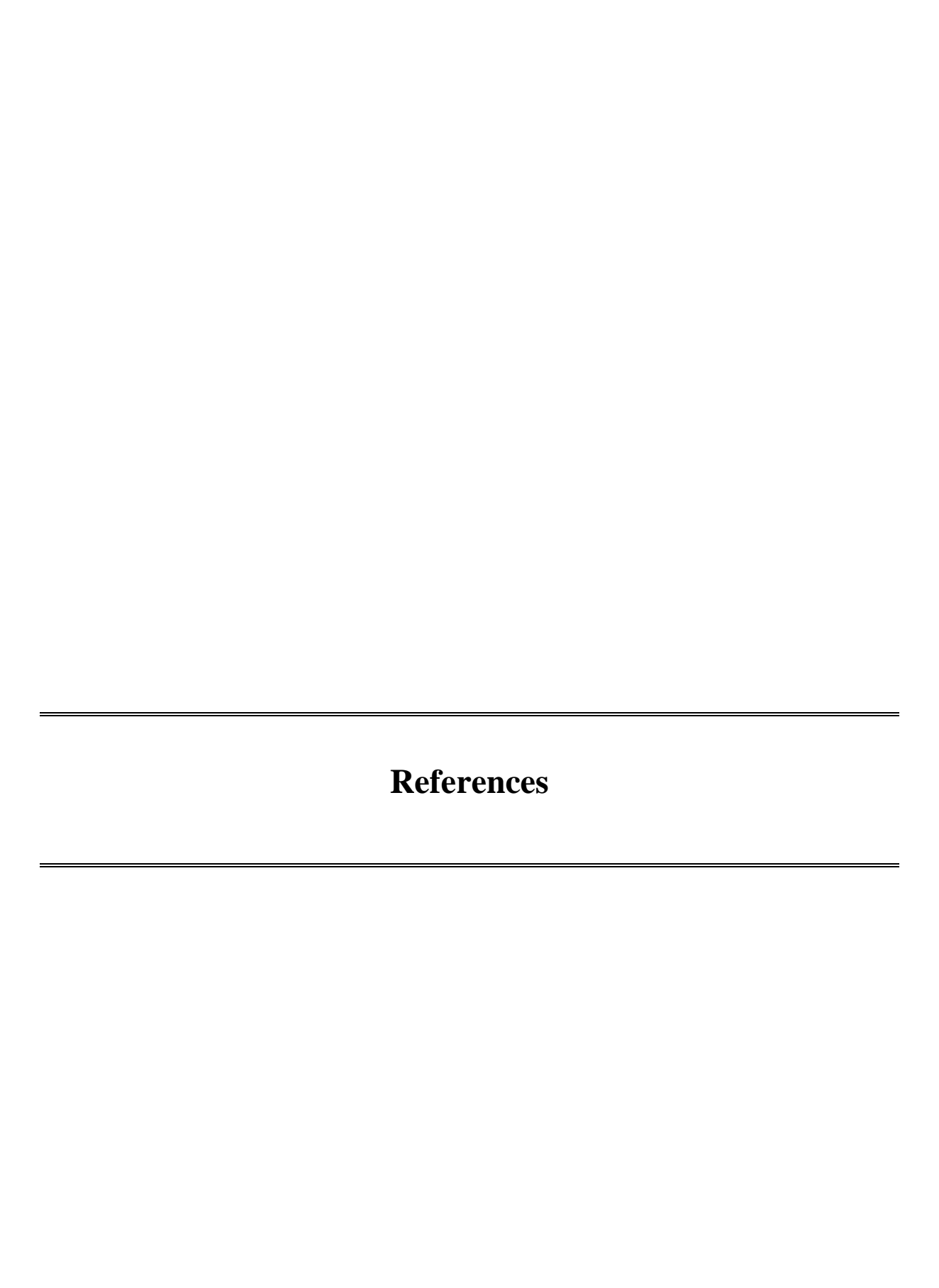
- The Broadly neutralizing antibody 447-52D was taken to design small-molecule mimics based on specific features associated with recognition and interaction with the V3 loop.
- The designed mimetics UHLMT-A2 and UHLMT-A9 were selected for synthesis based on retained interactions, the synthesis process's feasibility, and parent structures for further development.
- The s-triazine scaffold contained UHLMT-A9 molecules derivatives were prepared with different functional groups to interpret the V3 loop-CCR5 interactions.
- The interactions could be mimicked with negatively charged sulfonate, dihydroquinoline, isoniazid, and other benzene substituted moieties on the s-triazine scaffold.
- The interaction studies disclosed that most of the interactions were hydrophilic along with hydrophobic and π - π stacking.
- Tri-substituted molecules interact effectively with better docking scores at the V3 loop range of -8.0 to -10.5 kcal/mol than disubstituted molecules.
- The molecules were synthesized with better yields, and the cytotoxicity of molecules was conducted on SUP-T1 cells in increasing concentrations 50, 100, 250, 500, and 750 μ M, and the cell viability was evaluated using MTT assay.
- Sulfonic groups contained molecules UHLMTJ-257c,UHLMTJ-259 .etc showed significant toxicity then UHLMTJ-257a,b molecules .
- Most of the molecules showed moderate toxicity >300 μ M. However, a combination of sulfonate, isonized and dihydoquinozoline moieties contained molecules (UHLMTJ-261c, UHLMTJ-265a) showed high toxicity and CC50 ~150 μ M.

- Anti-viral activity of molecules conducted on 93IN101(clade C) and NL4-3 (clade B) virus in Sup-T1 cell line in the presence of increasing concentrations (0.5 to 10 μ M) of the compounds.
- UHLMTJ-260c, UHLMTJ-261c, UHLMTJ-262a, UHLMTJ-262c, UHLMTJ-263a were highly active with IC50 of 1.54 μM,0.94 μM. 0.76 μM,0.52 μM, respectively.
- The antiviral activity results suggested that all molecules have IC₅₀ activity in <5 μ M except one molecule, UHLMTJ-256, with IC₅₀ >7.0 μ M.
- ➤ Overall conclusion of Objective II was neutralizing antibody-based drug design and development to provide knowledge about valid target site recognition, consequently, reduce the biological and chemical rick of small molecules.
- ➤ The mimicking chemo superiors are considered as "hits" for lead molecule development with various modifications. In general, QSAR or pharmacophore models have been used to further develop molecules for better binding at target protein.

Objective III:

- Preparation of surface-modified Lactoferrin nanoparticles (NPs) with Sodium 2-mercaptoethanol sulfonate (MES) in oil in the water sonochemical method to form new particles Lf-MES NPs.
- The surface-modified Lf-MES NPs acted as a mimic of CCR5 sulfonate groups to target the V3 loop of gp120.
- Lf-MES NPs were loaded with AZT drugs and physically characterized.
- TEM and FE-SEM were used to measure the size of NPs, AZT loaded Lf NPs, and AZT loaded Lf-MES NPs showed a size range of 90nm to 120nm and 55nm to 79nm, respectively.
- Characterization of charge distribution of NPs in suspension by Zeta Sizer, Lf NPs showed a zeta potential of -9.4mV. Lf-MES NPs showed a potential of -20.4 mV, thus suggesting the presence of sulfonate groups on the surface, and a native agarose gel experiment confirmed that.
- pH-dependent drug release of Lf-AZT NPs and Lf-MES-AZT NPs. A maximum drug release was observed between pH 5.0-6.0 in both.
- Structural changes in Sol-Lactoferrin, Lactoferrin Np, and Drug Loaded Lactoferrin NPs were recorded by Surface-Enhanced Raman Spectra and ²³Na nucleus solid-state NMR.

- Enhanced localization of Lf-MES NPs was observed on HIV-1 gp160 envelope proteinexpressing HL2/3 cell line using curcumin-loaded Nanoparticles at different time intervals from 30 min to 12 hrs, and SKNSH cells were used as a negative control.
- Lf-MES NPs affinity to bind with gp160 was determined NPs in the presence of lactoferrin receptor antibody (ITNL-1) and purified gp160.
- MTT Assay assessed the nanoformulations' cytotoxicity (Blank Lf, Lf-MES NPs, and Lf-AZT, Lf-MES-AZT) results in negligible toxicity at 150 μM.
- Dye distribution assay was conducted with HL2/3 and SUP-T1, which is predicted the role of Lf-MES NPs in inhibiting the fusion of the virus to the host cell.
- Cell fusion results suggested that Lf-MES NPs, the fusion of the cells, was inhibited with only 50% of cells participating in the fusion, and T20 was used as the positive control.
- Antiviral activity of Lf-MES-AZT NPs (IC50:15.2nM) showed significantly greater inhibition when compared to sol.AZT (IC50:46.7nM) and Lf-AZT (IC50:34.2nM).
- ➤ The conclusion of Objective III was surface-modified biocompatible protein nanoparticle drug delivery was essential for safe drug delivery along with target-specific for chronic diseases.



- 1. HIV/AIDS. http://www.who.int/hiv/en/
- 2. http://naco.gov.in/hiv-facts-figures
- 3. A Boasso, G. M. Shearer, and C. Chougnet. Immune dysregulation in human immunodeficiency virus infection: know it, fix it, prevent it? J Intern Med. 2009 Jan; 265(1): 78–96.
- 4. Time from HIV-1 seroconversion to AIDS and death before widespread use of highly active antiretroviral therapy: a collaborative re-analysis. Collaborative Group on AIDS Incubation and HIV Survival including the CASCADE EU Concerted Action. Concerted Action on SeroConversion to AIDS and Death in Europe. Lancet. 2000; 355:1131–1137. [No authors listed]
- 5. Fredric S. Cohen. How Viruses Invade Cells. Biophys J. 2016 Mar 8; 110(5): 1028–1032.
- 6. i) Preston BD, Poiesz BJ, Loeb LA. 1988. Fidelity of HIV-1 reverse transcriptase. Science 242:1168–71. ii) Nowak M. 1990. HIV mutation rate. Nature 347:522.
- 7. Bonhoeffer S, Holmes EC, Nowak MA. 1995. Causes of HIV diversity. Nature 376:125
- 8. M. M. Prokofjeva, S. N. Kochetkov, and V. S. Prassolov. Therapy of HIV Infection: Current Approaches and Prospects. Acta Naturae. 2016 Oct-Dec; 8(4): 23–32.
- 9. i) Autran B, Carcelain G, Li TS, Blanc C, Mathez D, Tubiana R, Katlama C, Debre P, Leibowitch J. 1997. Positive effects of combined antiretroviral therapy on CD4b T cell homeostasis and function in advanced HIV disease. Science 277: 112 –116. ii) Komanduri KV, Viswanathan MN, Wieder ED, Schmidt DK, Bredt BM, Jacobson MA, McCune JM. 1998. Restoration of cytomegalovirus-specific CD4b T-lymphocyte responses after ganciclovir and highly active antiretroviral therapy in individuals infected with HIV-1. Nat Med 4: 953–956
- 10. Lederman MM, Connick E, Landay A, Kuritzkes DR, Spritzler J, St Clair M, Kotzin BL, Fox L, Chiozzi MH, Leonard JM, et al. 1998. Immunologic responses associated with weeks of combination antiretroviral therapy consisting of zidovudine, lamivudine, and ritonavir: Results of AIDS Clinical Trials Group Protocol 315. J Infect Dis 178: 70–79.
- 11. i) Dalgleish AG, Beverley PC, Clapham PR, Crawford DH, Greaves MF, Weiss RA. 1984. The CD4 (T4) antigen is an essential component of the receptor for the AIDS retrovirus. Nature 312: 763 –767. ii) Klatzmann D, Champagne E, Chamaret S, Gruest J, Guetard D, Hercend T, Gluckman JC, Montagnier L. 1984. T-lymphocyte T4 molecule behaves as the receptor for human retrovirus LAV. Nature 312: 767–768.

- 12. i) Alkhatib G, Combadiere C, Broder CC, Feng Y, Kennedy PE, Murphy PM, Berger EA. 1996. CC CKR5: A RANTES, MIP-1a, MIP-1b receptor as a fusion cofactor for macrophage-tropic HIV-1. Science 272: 1955–1958. ii) Deng H, Liu R, Ellmeier W, Choe S, Unutmaz D, Burkhart M, Di Marzio P, Marmon S, Sutton RE, Hill CM, et al. 1996. Identification of a major co-receptor for primary isolates of HIV-1. Nature (London) 381: 661–666.
- 13. i) Stine GJ. 2000. AIDS Update 2000: An Annual Overview of Acquired Immune Deficiency Syndrome. Englewood Cliffs, NJ: Prentice Hall. 486 pp. ii) Connor RI, Mohri H, Cao Y, Ho DD. 1993. Increased viral burden and cytopathicity correlate temporally with CD4+ T-lymphocyte decline and clinical progression in human immunodeficiency virus type 1-infected individuals. J. Virol. 67:1772–77.
- 14. i) Gupta S,Vayuvegula B. 1987. Human immunodeficiency virus-associated changes in signal transduction. J. Clin. Immunol. 7(6):486–89. ii) Lynn WS, Tweedale A, Cloyd MW. 1988. Human immunodeficiency virus (HIV-1) cytotoxicity: perturbation of the cell membrane and depression of phospholipid synthesis. Virology 163:43–51.
- 15. Doms RW, Moore JP. 1997. HIV-1 coreceptor use: a molecular window into viral tropism. In Human Retroviruses and AIDS. http://hivweb.lanl.gov/compendium.
- 16. i) Schuitemaker H, Koot M, Kootstra NA, Dercksen MW, Goede REY, et al. 1992. Biological phenotype of human immunodeficiency virus type 1 clones at different stages of infection: progression of disease is associated with a shift from monocytotropic to T-celltropic virus population. J. Virol. 66:1354–60. ii) 17th Global report 2010. Geneva: UNAIDS; 2010.
- i) http://www.unaids.org/globalreport/documents/ 20101123_GlobalReport_full_en.pdf.
 ii) Hladik F, Sakchalathorn P, Ballweber L, et al. Initial events in establishing vaginal entry and infection by human immunodeficiency virus type 1. Immunity. 2007; 26:257–270.
- Keele BF, Giorgi EE, Salazar-Gonza-lez JF, et al. Identification and characterization of transmitted and early founder virus envelopes in primary HIV-1 infection. Proc Natl Acad Sci U S A. 2008; 105:7552–7557.
- 19. Lee HY, Giorgi EE, Keele BF, et al. Modeling sequence evolution in acute HIV-1 infection. J Theor Biol. 2009; 261:341–360.

- 20. Palmer S, Wiegand AP, Maldarelli F, et al. New real-time reverse transcriptase-initiated PCR assay with single-copy sensitivity for human immunodeficiency virus type 1 RNA in plasma. J Clin Microbiol. 2003; 41:4531–4536.
- 21. Fiebig EW, Wright DJ, Rawal BD, et al. Dynamics of HIV viremia and antibody seroconversion in plasma donors: implications for diagnosis and staging of primary HIV infection. AIDS. 2003; 17:1871–1879.
- 22. Weiss HA, Dickson KE, Agot K, Han-kins CA. Male circumcision for HIV prevention: current research and programmatic issues. AIDS. 2010; 24(Suppl 4): S61–S69. [PubMed: 21042054].
- 23. Stacey AR, et al. Induction of a striking systemic cytokine cascade prior to peak viremia in acute human immunodeficiency virus type 1 infection, in contrast to more modest and delayed responses in acute hepatitis B and C virus infections. J. Virol. 2009; 83:3719–3733. doi: 10.1128/JVI.01844-08.
- 24. Cocchi F, DeVico AL Garzino-Demo A, Arya SK, Gallo RC, Lusso P. 1995. Identification of RANTES, MIP-1α, and MIP-1β as the major HIV-suppressive factors produced by CD8+ T cells. Science 270:1811–15.
- 25. Fiebig EW, Wright DJ, Rawal BD, et al. Dynamics of HIV viremia and antibody seroconversion in plasma donors: implications for diagnosis and staging of primary HIV infection. AIDS. 2003; 17:1871–1879.
- 26. Leslie AJ, Pfafferott KJ, Chetty P, et al. HIV evolution: CTL escape mutation and reversion after transmission. Nat Med. 2004; 10:282–289.
- 27. Liovat AS, et al. Acute plasma biomarkers of T cell activation set-point levels and of disease progression in HIV-1 infection. PLoS ONE. 2012;7:e46143.
- 28. Park J, Morrow CD. 1993. Mutations in the protease gene of human immunodeficiency virus type 1 affect release and stability of virus particles. Virology 194: 843 –850.
- 29. Tang, C., Ndassa, Y. & Summers, M. F. Structure of the N-terminal 283-residue fragment of the immature HIV-1 Gag polyprotein. Nat. Struct. Biol. 9, 537–543 (2002).

- 30. Doyon L, Payant C, Brakier-Gingras L, Lamarre D. 1998. Novel Gag-Pol frameshift site in human immunodeficiency virus type 1 variants resistant to protease inhibitors. J Virol 72: 6146–6150.
- 31. Gitti, R. K. et al. Structure of the amino-terminal core domain of the HIV-1 capsid protein. Science 273, 231–235 (1996).
- 32. Gelderblom HR. Assembly and morphology of HIV: potential effect of structure on viral function. AIDS. 1991;5:617–637.
- 33. i) Dimmock NJ, Primrose SB. 1987. Introduction to Modern Virology. Oxford: Blackwell Sci. 362 pp. ii)Stine GJ. 2000. AIDS Update 2000: An Annual Overview of Acquired Immune Deficiency Syndrome. Englewood Cliffs, NJ: Prentice Hall. 486 pp.
- 34. Nagahara H., Vocero-Akbani, A.M., Snyder, E.L., Ho, A., Latham, D.G., Lissy, N.A., Becker-Hapak, M., Ezhevsky, S.A. and Dowdy, S.F. (1998) Transduction of full-length TAT fusion proteins into mammalian cells: TAT-p27Kip1 induces cell migration. Nature Med., 4, 1449–1452
- 35. i) Levy JA. Virus-host interactions in HIV pathogenesis: directions for therapy. Adv Dent Res. 2011;23:13–18. ii) Todd Mayhood, Neerja Kaushik, Pradeep K. Pandey, Fatah Kashanchi, Longwen Deng, and Virendra N. Pandey Inhibition of Tat-Mediated Transactivation of HIV-1 LTR Transcription by Polyamide Nucleic Acid Targeted to TAR Hairpin Element. *Biochemistry* 2000, 39, 38, 11532–11539.
- 36. Zhou Q., Li T., Price D.H. RNA Polymerase II Elongation Control. Annu. Rev. Biochem. 2012;81:119–143.
- 37. Massari S, Sabatini S, Tabarrini O. Blocking HIV-1 replication by targeting the Tathijacked transcriptional machinery. Curr Pharm Des. 2013;19(10):1860–1879.
- 38. Pollard VW, Malim MH. The HIV-1 Rev protein. Annu Rev Microbiol. 1998;52:491–532.
- 39. Malim MH, Hauber J, Le SY, Maizel JV, Cullen BR. The HIV-1 rev trans-activator acts through a structured target sequence to activate nuclear export of unspliced viral mRNA. Nature. 1989;338:254–7.

- 40. Doria M. Role of the CD4 down-modulation activity of Nef in HIV-1 infectivity. Curr HIV Res. 2011;9:490–495.
- 41. Premkumar DR, Ma XZ, Maitra RK, Chakrabarti BK, Salkowitz J, Yen-Lieberman B, et al. The nef gene from a long-term HIV type 1 nonprogressor. AIDS Res Hum Retroviruses (1996) 12:337–4510.1089/aid.1996.12.337.
- 42. Landi A, Iannucci V, Nuffel AV, Meuwissen P, Verhasselt B. One protein to rule them all: modulation of cell surface receptors and molecules by HIV Nef. Curr HIV Res. 2011;9:496–504.
- 43. Terwilliger EF, Cohen EA, Lu YC, Sodroski JG, Haseltine WA. Functional role of human immunodeficiency virus type 1 vpu. Proc Natl Acad Sci U S A. 1989; 86:5163–5167.
- 44. Fujita M, Otsuka M, Nomaguchi M, Adachi A. Multifaceted activity of HIV Vpr/Vpx proteins: the current view of their virological functions. Rev Med Virol. 2010; 20:68–76.
- 45. Goila-Gaur R, Strebel K. HIV-1 Vif, APOBEC, and intrinsic immunity. Retrovirology. 2008; 5:51.
- 46. Walker RC, Jr, Khan MA, Kao S, Goila-Gaur R, Miyagi E, Strebel K. Identification of dominant negative human immunodeficiency virus type 1 Vif mutants that interfere with the functional inactivation of APOBEC3G by virus-encoded Vif. J Virol. 2010; 84:5201–5211.
- 47. Roux KH, Taylor KA. AIDS virus envelope spike structure. Curr Opin Struct Biol. 2007; 17(2): 244–252.
- 48. Rossitza K. Gitti, Brian M. Lee, Jill Walker, Michael F. Summers, Sanghee Yoo, Wesley I. Sundquist. Structure of the Amino-Terminal Core Domain of the HIV-1 Capsid Protein. Science 12 Jul 1996. Vol. 273, Issue 5272, pp. 231-235.
- 49. Wesley I. Sundquist and Hans-Georg Kräusslich .HIV-1 Assembly, Budding, and Maturation. Cold Spring Harb Perspect Med. 2012 Jul; 2(7): a006924.
- 50. Michael A. Lobritz, Annette N. Ratcliff and Eric J. Arts. HIV-1 Entry, Inhibitors, and Resistance. Viruses 2010, 2, 1069-1105.

- 51. Chan, D.C.; Fass, D.; Berger, J.M.; Kim, P.S. Core structure of gp41 from the HIV envelope glycoprotein. Cell 1997, 89, 263-273.
- 52. Dimmock NJ, Primrose SB. 1987. Introduction to Modern Virology. Oxford: Blackwell Sci. 362 pp.
- 53. Stine GJ. 2000. AIDS Update 2000: An Annual Overview of Acquired Immune Deficiency Syndrome. Englewood Cliffs, NJ: Prentice Hall. 486 pp.
- 54. Greene WC. 1993. AIDS and the immune system. Sci. Am. 269(3):98–105.
- 55. Nguyen, D. H. & Hildreth, J. E. Evidence for budding of human immunodeficiency virus type 1 selectively from glycolipid-enriched membrane lipid rafts. J. Virol. 74, 3264–3272 (2000).
- 56. Nowak M. 1990. HIV mutation rate. Nature 347:522.
- 57. Shaper EG, Mullins JI. 1993. Rates of amino acid change in the envelope protein correlate with pathogenicity of primate lentiviruses. J. Mol. Evol. 37:57–65.
- 58. E. De Clercq, Anti-HIV drugs: 25 compounds approved within 25 years after the discovery of HIV, International Journal of Antimicrobial Agents (2009); 33:307-320.
- 59. Furman PA, Fyfe JA, St Clair MH, Weinhold K, Rideout JL, Freeman GA, Lehrman SN, Bolognesi DP, Broder S, Mitsuya H. 1986. Phosphorylation of 30 -azido-30 -deoxythymidine and selective interaction of the 50 -triphosphate with human immunodeficiency virus reverse transcriptase. Proc Natl Acad Sci 83: 8333–8337.
- 60. Maenza J, Flexner C. Combination antiretroviral therapy for HIV infection. Am Fam Physician. 1998 Jun;57(11):2789-98. Erratum in: Am Fam Physician 1998 Oct 1;58(5):1084. PMID: 9636341.
- 61. i) Jennifer L. Weinberg and Carrie L. Kovarik, MD. The WHO Clinical Staging System for HIV/AIDS. Virtual Mentor. 2010;12(3):202-206.
 - ii) Jens D Lundgren, Abdel G Babiker, Fred Gordin, Sean Emery, Birgit Grund, Shweta Sharma, Anchalee Avihingsanon, David A Cooper, Gerd Fätkenheuer, Josep M Llibre, Jean-Michel Molina, Paula Munderi, Mauro Schechter, Robin Wood, Karin L Klingman, Simon Collins, H Clifford Lane, Andrew N Phillips, James D Neaton

- .Initiation of antiretroviral therapy in early asymptomatic HIV infection. N Engl J Med. 2015 Aug 27;373(9):795-807.
- 62. i) Sashi Sharma, National ART Guidelines 2009. National Centre for AIDS & STD Control (NCASC) Teku, Kathmandu. ii) World Health Organization (2013) Consolidated guidelines on the use of antiretroviral drugs for treating and preventing HIV infection: Recommendations for a public health approach. [Last accessed on 2013 Dec 9]. Available from: http://www.who.int/hiv/pub/guidelines/arv2013/.
- 63. Deepika Pandhi and Pallavi Ailawadi. Initiation of antiretroviral therapy. Indian J Sex Transm Dis AIDS. 2014 Jan-Jun; 35(1): 1–11.
- 64. Stephen D. Lawn,M. Estée Török, and Robin Wood .Optimum time to start antiretroviral therapy during HIV-associated opportunistic infections. Curr Opin Infect Dis. 2011 Feb; 24(1): 34–42.
- 65. Huldrych F. Günthard, MD, Michael S. Saag, MD, Constance A. Benson, MD, Carlos del Rio, MD, Joseph J. Eron, MD, Joel E. Gallant, MD, MPH, Jennifer F. Hoy, MBBS, FRACP, Michael J. Mugavero, MD, MHSc, Paul E. Sax, MD, Melanie A. Thompson, MD, Rajesh T. Gandhi, MD, Raphael J. Landovitz, MD, Davey M. Smith, MD, Donna M. Jacobsen, BS, and Paul A. Volberding, MD. Antiretroviral Drugs for Treatment and Prevention of HIV Infection in Adults. JAMA. 2016 Jul 12; 316(2): 191–210.
- 66. Panel on Antiretroviral Guidelines for Adults and Adolescents. Guidelines for the use of antiretroviral agents in HIV-1-infected adults and adolescents. Department of Health and Human Services; 2013. at
 - http://aidsinfo.nih.gov/contentfiles/lyguidelines/AdultandAdolescentGL.pdf.
- 67. HIV/AIDS Glossary.
 - https://aidsinfo.nih.gov/understanding-z hiv aids/glossary/873/treatment-failure.
- 68. NACO: ART guidelines for HIV-Infected Adults and Adolescents: May2013.
- 69. David Warnke, PharmD, Jason Barreto, PharmD, and Zelalem Temesgen, MD, AAHIVS. Antiretroviral Drugs. Journal of Clinical Pharmacology, 2007;47:1570-1579.

- 70. Fischl MA, Richman DD, Grieco MH, et al. The efficacy of azidothymidine (AZT) in the treatment of patients with AIDS and AIDS-related complex. A double-blind, placebocontrolled trial. The New England journal of medicine. 1987; 317:185–91.
- 71. Arion D, Kaushik N, McCormick S, Borkow G, Parniak MA. 1998. Phenotypic mechanism of HIV-1 resistance to 30 -azido-30 -deoxythymidine (AZT): Increased polymerization processivity and enhanced sensitivity to pyrophosphate of the mutant viral reverse transcriptase. Biochemistry 37: 15908–15917.
- 72. Boyer PL, Sarafianos SG, Arnold E, Hughes SH. 2001. Selective excision of AZTMP by drug-resistant human immunodeficiency virus reverse transcriptase. J Virol 75: 4832–4842.
- 73. de Bethune MP. Non-nucleoside reverse transcriptase inhibitors (NNRTIs), their discovery, development, and use in the treatment of HIV-1 infection: a review of the last 20 years (1989-2009). Antiviral Res. 2010; 85:75–90.
- 74. J Wang, S J Smerdon, J Jäger, L A Kohlstaedt, P A Rice, J M Friedman, and T A Steitz. Structural basis of asymmetry in the human immunodeficiency virus type 1 reverse transcriptase heterodimer. Proc Natl Acad Sci U S A. 1994 Jul 19; 91(15): 7242–7246.
- 75. Kohlstaedt LA, Wang J, Friedman JM, Rice PA, Steitz TA. 1992. Crystal structure at 3.5 A resolution of HIV-1 reverse transcriptase complexed with an inhibitor. Science 256: 1783–1790.
- 76. Spence RA, Kati WM, Anderson KS, Johnson KA. 1995. Mechanism of inhibition of HIV-1 reverse transcriptase by nonnucleoside inhibitors. Science 267: 988–993.
- 77. Sluis-Cremer N, Temiz NA, Bahar I. 2004. Conformational changes in HIV-1 reverse transcriptase induced by nonnucleoside reverse transcriptase inhibitor binding. Curr HIV Res 2: 323–332.
- 78. Witvrouw M, Pannecouque C, Van Laethem K, Desmyter J, De Clercq E, Vandamme AM. 1999. Activity of nonnucleoside reverse transcriptase inhibitors against HIV-2 and SIV. AIDS 13: 1477–1483.

- 79. Figueiredo A., Moore K.L., Mak J., Sluis-Cremer N., de Bethune M.P., Tachedjian G. Potent nonnucleoside reverse transcriptase inhibitors target HIV-1 Gag-Pol. PLoS Pathog. 2006;2: e119. doi: 10.1371/journal.ppat.0020119.
- 80. Kalyan Das and Eddy Arnold. HIV-1 Reverse Transcriptase and Antiviral Drug Resistance (Part 1 of 2). Curr Opin Virol. 2013 Apr; 3(2): 111–118.
- 81. Antinori A, Zaccarelli M, Cingolani A, Forbici F, Rizzo MG, Trotta MP, Di Giambenedetto S, Narciso P, Ammassari A, Girardi E, et al. 2002. Cross-resistance among nonnucleoside reverse transcriptase inhibitors limits recycling efavirenz after nevirapine failure. AIDS Res Hum Retroviruses 18: 835–838.
- 82. Espeseth AS, Felock P, Wolfe A, Witmer M, Grobler J, Anthony N, Egbertson M, Melamed JY, Young S, Hamill T, et al. 2000. HIV-1 integrase inhibitors that compete with the target DNA substrate define a unique strand transfer conformation for integrase. Proc Natl Acad Sci 97: 11244–11249.
- 83. McColl DJ, Chen X. 2010. Strand transfer inhibitors of HIV-1 integrase: Bringing IN a new era of antiretroviral therapy. Antiviral Res 85: 101 –118.
- 84. Hare S, Vos AM, Clayton RF, Thuring JW, Cummings MD, Cherepanov P. 2010. Molecular mechanisms of retroviral integrase inhibition and the evolution of viral resistance. Proc Natl Acad Sci 107: 20057–20062.
- 85. Marinello J, Marchand C, Mott B, Bain A, Thomas CJ, Pommier Y. 2008. Comparison of raltegravir and elvitegravir on HIV-1 integrase catalytic reactions and on a series of drug-resistant integrase mutants. Biochemistry 47: 9345–54.
- 86. Narasimha M. Midde, Benjamin J. Patters, a, PSS Rao, Theodore J. Cory, and Santosh Kumara. Investigational protease inhibitors as antiretroviral therapies. Expert Opin Investig Drugs. 2016 Oct; 25(10): 1189–1200.
- 87. Park J, Morrow CD. 1993. Mutations in the protease gene of human immunodeficiency virus type 1 affect release and stability of virus particles. Virology 194: 843 –850.

- 88. Kozal MJ, Shah N, Shen N, Yang R, Fucini R, Merigan TC, Richman DD, Morris D, Hubbel E, Chee M, et al. 1996. Extensive polymorphisms observed in HIV-1 clade B protease gene using high-density oligonucleotide arrays. Nature Med 2: 753–759.
- 89. José R Santos, Josep M Llibre, Daniel Berrio-Galan, Isabel Bravo, Cristina Miranda, Susana Pérez-Alvarez, Nuria Pérez-Alvarez, Roger Paredes, Bonaventura Clotet, José Moltó. Monotherapy with boosted PIs as an ART simplification strategy in clinical practice. J Antimicrob Chemother. 2015 Apr;70(4):1124-9.
- 90. Shafer RW, Dupnik K, Winters MA, Eshleman SH. 2000. A guide to HIV-1 reverse transcriptase and protease sequencing for drug resistance studies. In HIV sequence compendium 2000 (ed. Kuiken CL, et al.). Los Alamos National Laboratory, Los Alamos, NM.
- 91. Ganser-Pornillos BK, von Schwedler UK, Stray KM, Aiken C, Sundquist WI. Assembly properties of the human immunodeficiency virus type 1 CA protein. J Virol. 2004; 78:2545–2552.
- 92. Lemke, C. T. et al. Distinct effects of two HIV-1 capsid assembly inhibitor families that bind the same site within the N-terminal domain of the viral CA protein. J. Virol. 86, 6643–6655 (2012).
- 93. Wade S. Blair, Chris Pickford, Stephen L. Irving, David G. Brown, Marie Anderson, Richard Bazin, Joan Cao, Giuseppe Ciaramella, Jason Isaacson, Lynn Jackson, Rachael Hunt, Anne Kjerrstrom, James A. Nieman, Amy K. Patick, Manos Perros, Andrew D. Scott, Kevin Whitby, Hua Wu, and Scott L. Butler, HIV Capsid is a Tractable Target for Small Molecule Therapeutic Intervention. PLoS Pathog. 2010 Dec; 6(12): e1001220.
- 94. Uddhav Timilsina, Dibya Ghimire, Bivek Timalsina, Theodore J. Nitz, Carl T. Wild, Eric O. Freed & Ritu Gaur. Identification of potent maturation inhibitors against HIV-1 clade C. Scientific Reports volume 6, Article number: 27403 (2016).
- 95. Roux KH, Taylor KA. AIDS virus envelope spike structure. Curr Opin Struct Biol. 2007; 17(2): 244–252.

- 96. Lu M, Blacklow SC, Kim PS. A trimeric structural domain of the HIV-1 transmembrane glycoprotein. Nat Struct Biol. 1995; 2(12):1075–1082.
- 97. Speck RF, Wehrly K, Platt EJ, Atchison RE, Charo IF, Kabat D, Chesebro B, Goldsmith MA. Selective employment of chemokine receptors as human immunodeficiency virus type 1 coreceptors determined by individual amino acids within the envelope V3 loop. J Virol. 1997; 71(9):7136–7139.
- 98. Chen CH, Matthews TJ, McDanal CB, Bolognesi DP, Greenberg ML. A molecular clasp in the human immunodeficiency virus (HIV) type 1 TM protein determines the anti-HIV activity of gp41 derivatives: Implication for viral fusion. J Virol. 1995; 69(6):3771–3777.
- 99. Eric J. Arts1 and Daria J. Hazuda. HIV-1 Antiretroviral Drug Therapy. Cold Spring Harb Perspect Med 2012;2: a007161.
- 100. Guo Q, Ho HT, Dicker I, Fan L, Zhou N, Friborg J, Wang T, McAuliffe BV, Wang HG, Rose RE, Fang H, Scarnati HT, Langley DR, Meanwell NA, Abraham R, Colonno RJ, Lin PF. Biochemical and genetic characterizations of a novel human immunodeficiency virus type 1 inhibitor that blocks gp120-CD4 interactions. J Virol. 2003; 77(19):10528–10536.
- 101. Lin PF, Blair W, Wang T, Spicer T, Guo Q, Zhou N, Gong YF, Wang HG, Rose R, Yamanaka G, Robinson B, Li CB, Fridell R, Deminie C, Demers G, Yang Z, Zadjura L, Meanwell N, Colonno R. A small molecule HIV-1 inhibitor that targets the HIV-1 envelope and inhibits CD4 receptor binding. Proc Natl Acad Sci USA. 2003; 100(19):11013–11018.
- 102. Cormier EG, Dragic T. The crown and stem of the V3 loop play distinct roles in human immunodeficiency virus type 1 envelope glycoprotein interactions with the CCR5 coreceptor. J Virol. 2002; 76(17):8953–8957.
- 103. Briz V, Poveda E, Soriano V. HIV entry inhibitors: Mechanisms of action and resistance pathways. J Antimicrob Chemother. 2006; 57(4):619–627.

- 104. Cocchi F, DeVico AL, Garzino-Demo A, Arya SK, Gallo RC, Lusso P. Identification of RANTES, MIP-1 alpha, and MIP-1 beta as the major HIV-suppressive factors produced by CD8+ T cells. Science. 1995; 270(5243):1811–1815.
- 105. Keduo Qian, Susan L. Morris-Natschke, and Kuo-Hsiung Lee. HIV Entry Inhibitors and Their Potential in HIV Therapy. Med Res Rev. 2009 March; 29(2): 369–393.
- 106. Briz V, Poveda E, Soriano V. HIV entry inhibitors: Mechanisms of action and resistance pathways. J Antimicrob Chemother. 2006; 57(4):619–627.
- 107. Wilen CB, Tilton JC, Doms RW. 2011. HIV: Cell binding and entry. Cold Spring Harb Perspect Med doi: 10.1101/cshperspect. a006866.
- 108. Wild CT, Shugars DC, Greenwell TK, McDanal CB, Matthews TJ. Peptides corresponding to a predictive alpha-helical domain of human immunodeficiency virus type 1 gp41 are potent inhibitors of virus infection. Proc Natl Acad Sci U S A 1994; 91:9770–9774.
- 109. Lalezari JP, Bellos NC, Sathasivam K, Richmond GJ, Cohen CJ, Myers RA Jr, Henry DH, Raskino C, Melby T, Murchison H, Zhang Y, Spence R, Greenberg ML, Demasi RA, Miralles GD. T-1249 retains potent antiretroviral activity in patients who had experienced virological failure while on an enfuvirtide-containing treatment regimen. J Infect Dis. 2005; 191(7):1155–1163.
- 110. Poveda E, Rodes B, Lebel-Binay S, Faudon JL, Jimenez V, Soriano V. Dynamics of enfuvirtide resistance in HIV-infected patients during and after long-term enfuvirtide salvage therapy. J Clin Virol. 2005; 34(4):295–301.
- 111. Doms, R.W.; Lamb, R.A.; Rose, J.K.; Helenius, A. Folding and assembly of viral membrane proteins. Virology 1993, 193, 545-562.
- 112. Waheed A.A., Freed E.O. HIV Type 1 Gag as a Target for Antiviral Therapy. AIDS Res. Hum. Retroviruses. 2012; 28:54–75.
- 113. Saina Beitari, Yimeng Wang, Shan-Lu Liu and Chen Liang.HIV-1 Envelope Glycoprotein at the Interface of Host Restriction and Virus Evasion. Viruses 2019, 11, 311.

- 114. Zhou, T.; Dang, Y.; Zheng, Y.-H.; Sundquist, W.I. The Mitochondrial Translocator Protein, TSPO, Inhibits HIV-1 Envelope Glycoprotein Biosynthesis via the Endoplasmic Reticulum-Associated Protein Degradation Pathway. J. Virol. 2014, 88, 3474–3484.
- 115. Michael Caffrey.HIV envelope: challenges and opportunities for development of entry inhibitors. Volume 19, ISSUE 4, P191-197, April 01, 2011.
- 116. Stewart-Jones G. B., Soto C., Lemmin T., Chuang G. Y., Druz A., Kong R., Thomas P. V., Wagh K., Zhou T., Behrens A. J., Bylund T., Choi C. W., Davison J. R., Georgiev I. S., Joyce M. G., et al. (2016) Trimeric HIV-1-Env structures define glycan shields from clades A, B, and G. Cell 165, 813–826.
- 117. Agonist to an Antagonist. Joel R. Courter, Navid Madani, Joseph Sodroski, Arne Schön, Ernesto Freire, Peter D. Kwong, Wayne A. Hendrickson, Irwin M. Chaike, Judith M. LaLonde, and Amos B. Smith Structure-Based Design, Synthesis and Validation of CD4-Mimetic Small Molecule Inhibitors of HIV-1 Entry: Conversion of a Viral Entry. *Acc. Chem. Res.* 2014, 47, 4, 1228–1237.
- 118. Simona A. Iacob, Diana G. Iacob, and Gheorghita Jugulete. Improving the Adherence to Antiretroviral Therapy, a Difficult but Essential Task for a Successful HIV Treatment—Clinical Points of View and Practical Considerations. Front Pharmacol. 2017; 8: 831.
- 119. Rui Xue Zhang, Jason Li, Tian Zhang, Mohammad A Amini, Chunsheng He, Brian Lu, Taksim Ahmed, HoYin Lip, Andrew M Rauth & Xiao Yu Wu. Importance of integrating nanotechnology with pharmacology and physiology for innovative drug delivery and therapy an illustration with firsthand examples. Acta Pharmacologica Sinica volume 39, pages825–844(2018).
- 120.Supriya D Mahajan,Ravikumar Aalinkeel,Wing-Cheung Law,Jessica L Reynolds,Bindukumar Nair,Donald E Sykes,Ken-Tye Yong,Indrajit Roy,Paras N Prasad,Stanley A Schwartz. Anti-HIV-1 nanotherapeutics: promises and challenges for the future. International Journal of Nanomedicine 2012:7 5301–5314.
- 121. Ham AS, Cost MR, Sassi AB, et al. (2009). Targeted delivery of PSCRANTES for HIV-1 prevention using biodegradable nanoparticles. Pharm Res 26:502–11.

- 122. Wilhelm S, Tavares AJ, Dai Q, Ohta S, Audet J, Dvorak HF, *et al*. Analysis of nanoparticle delivery to tumours. *Nat Rev Mater* 2016; **1**: 1–12.
- 123. Tewodros Mamo, E Ashley Moseman, Nagesh Kolishetti, Carolina Salvador-Morales, Jinjun Shi, Daniel R Kuritzkes, Robert Langer, Ulrich von Andrian, and Omid C Farokhzad. Emergingnanotechnology approaches for HIV/AIDS treatment and prevention. Nanomedicine (Lond). 2010 February; 5(2): 269–285.
- 124. Mallipeddi R, Rohan LC. Progress in antiretroviral drug delivery using nanotechnology. Int J Nanomedicine. 2010; 5:533–547.
- 125.i) Amiji MM, Vyas TK, Shah LK. Role of nanotechnology in HIV/AIDS treatment:

 Potential to overcome the viral reservoir challenge. Discov Med 2006;6(34):157–162.
 - ii) Baert L, van't Klooster G, Dries W, et al. Development of a long-acting injectable formulation with nanoparticles of rilpivirine (tmc278) for HIV treatment. Eur J Pharm Biopharm 2009;72(3):502–508.
- 126. Garg M, Asthana A, Agashe HB, Agrawal GP, Jain NK. Stavudine-loaded mannosylated liposomes:In-vitro anti-HIV-i activity, tissue distribution and pharmacokinetics. J Pharm Pharmacol 2006;58(5):605–616.
- 127. Lundin KE, Simonson OE, Moreno PM, et al. Nanotechnology approaches for gene transfer. Genetica 2009;137(1):47–56.
- 128. Whitehead KA, Langer R, Anderson DG. Knocking down barriers: Advances in siRNA delivery. Nat Rev Drug Discov 2009;8(2):129–138.
- 129. Li M, Li H, Rossi JJ. RNAI in combination with a ribozyme and tar decoy for treatment of HIV infection in hematopoietic cell gene therapy. Ann NY Acad Sci 2006; 1082:172–179.
- 130. Neves JD, Amiji MM, Bahia BF, Sarmento B. Nanotechnology-based systems for the treatment and prevention of HIV/AIDS. *Adv Drug Deliv Rev.* 2010; 62:458–477.
- 131. i) McMichael AJ, Borrow P, Tomaras GD, Goonetilleke N, Haynes B. The immune response during acute HIV78-1 infection: Clues for vaccine development. Nat Rev Immunol. 2009. ii) Elamanchili P, Diwan M, Cao M, Samuel J. Characterization of poly

- (d,l-lactic-co-glycolic acid) based nanoparticulate system for enhanced delivery of antigens to dendritic cells. Vaccine 2004;22(19):2406–2412.
- 132. Grant RM, Hamer D, Hope T, et al. Whither or wither microbicides? Science 2008;321(5888):532–534.
- 133. Saidi H. Microbicides: An emerging science of HIV-1 prevention in women-15th conference on retroviruses and opportunistic infections, boston, USA, 3–6 February 2008. Rev Med Virol 2009;19(2):69–76.
- 134. Klasse PJ, Shattock R, Moore JP. Antiretroviral drug-based microbicides to prevent HIV-1 sexual transmission. Ann Rev Med 2008; 59:455–471.
- 135. das Neves J, Michiels J, Ariën KK, et al. Polymeric nanoparticles affect the intracellular delivery, antiretroviral activity, and cytotoxicity of the microbicide drug candidate dapivirine. *Pharm Res.* 2012;29(6): 1468–1484.
- 136. Pedziwiatr-Werbicka E, Ferenc M, Zaborski M, Gabara B, Klajnert B, Bryszewska M. Characterization of complexes formed by polypropylene imine dendrimers and anti-HIV oligonucleotides. *Colloids Surf B Biointerfaces*. 2011;83(2):360–366.
- 137. Zhang J, Li S, Li X. Polymeric nano-assemblies as emerging delivery carriers for therapeutic applications: A review of recent patents. *Recent Pat Nanotechnol*. 2009;3: 225–231.
- 138. Kuo YC, Yu HW. Polyethyleneimine/poly-(γ-glutamic acid)/poly (lactide-co-glycolide) nanoparticles for loading and releasing antiretroviral drug. *Colloids Surf B Biointerfaces*. 2011;88(1):158–164.
- 139. Fahmy TM, Demento SL, Caplan MJ, Mellman I, Saltzman WM. Design opportunities for actively targeted nanoparticle vaccines. Nanomed 2008;3(3):343–355.
- 140. Roda Rani KP, Pelluru D, Kondapi AK. A conserved molecular action of native and recombinant Epap-1 in inhibition of HIV-1 gp120 mediated viral entry. Arch Biochem Biophys. 2006 Dec 1; 456(1):79-92.

- 141. April Killikelly, Hui-Tang Zhang, Brett Spurrier, Constance Williams, Miroslaw K. Gorny, Susan Zolla-Pazner, and Xiang-Peng Kong. (2013) Thermodynamic Signatures of the Antigen Binding Site of mAb 447–52D Targeting the Third Variable Region of HIV-1 gp120. Biochemistry, 52, 6249–6257.
- 142. Baker, E. N.; Baker, H. M. Molecular Structure, Binding Properties and Dynamics of Lactoferrin. **2005**, *62*, 2531–2539.
- 143. Moore, S. A.; Anderson, B. F.; Groom, C. R.; Haridas, M.; Baker, E. N. Three Dimensional Structure of Diferric Bovine Ê Resolution Lactoferrin at 2 . 8 A. 1997, 222–236.
- 144. Gunaseelana, S.; Gunaseelana, K.; Deshmukha, M.; Zhanga, X.; Sinkoa, P. J. Surface Modifications of Nanocarriers for Effective Intracellular Delivery of Anti-HIV Drugs. Adv Drug Deliv Rev 2010, 62 (4–5), 518–531.
- 145. Divakar, A.; Krishna, S.; Mandraju, R. K.; Kishore, G.; Kondapi, A. K. An Efficient Targeted Drug Delivery through Apotransferrin Loaded Nanoparticles. 2009, *4* (10).
- 146. Kumar, P.; Lakshmi, Y.; Kondapi, A. Triple Drug Combination of Zidovudine, Efavirenz and Lamivudine Loaded Lactoferrin Nanoparticles: An Effective Nano First-Line Regimen for HIV Therapy. Pharm. Res. 2017, 34 (2), 257–268.
- 147. Murray, C. W. & Rees, D. C. The rise of fragment-based drug discovery. Nature Chem. 1, 187–192 (2009).
- 148. Alastair D. G. Lawson. Antibody-enabled small-molecule drug discovery.

 Nature Reviews, Drug Discovery Volume 11, July 2012,519.
- 149. Sabet R, Fassihi A, Hemmateenejad B, Saghaei L, Miri R, Gholami M (2012) Computeraided design of novel antibacterial 3-hydroxypyridine-4-ones: application of QSAR methods based on the MOLMAP approach. J Comput Aided Mol Des 26:349–361.
- 150. H. H. F. Refsgaard, B. F. Jensen, P. B. Brockhoff, S. B. Padkjaer, M. Guldbrandt, M. S. Chistensen, 'In silico Prediction of Membrane Permeability from Calculated MolecularParameters', J. Med. Chem. 2005, 48, 805 811.
- 151. S. Sepehri, S. Gharagani, L. Saghaie, M. R. Aghasadeghi, A.Fassihi, 'QSAR and Docking Studies of Some 1,2,3,4-Tetrahydropyrimidines: Evaluation of gp41 as Possible Target for Anti-HIV-1 Activity', Med. Chem. Res. 2015,24,1707 1724.
- 152. Junwon Kim , Taedong O , Changmin Park , Wonyoung S , Mina J , Youngmi Kim , Minjung S ,Doohyun Lee , Suyeon J , Yoonae K , Inhee Choi , Youngsam Park , Jaewan

- Yoon , Moon Kyeong Ju ,JiY Ahn, Junghwan Kim, Sung-Jun Han , Tae-Hee Kim, Jonathan Cechetto , Jiyoun Namc,Michel Liuzzi, Peter Sommer , Zaesung N , A novel 3,4-dihydropyrimidin-2(1H)-one: HIV-1 replication inhibitors with improved metabolic stability. Bioorg. Med. Chem. Lett. 22 (2012) 2522–2526.
- 153. Meanwell, N. A. Synopsis of Some Recent Tactical Application of Bioisosteres in Drug Design. J. Med. Chem. 2011, 54, 2529.
- 154. Birgit Viira, Anastasia Selyutina, Alfonso T. García-Sosa, Maarit Karonen, Jari Sinkkonen, Andres Merits, Uko Maran. Design, discovery, modelling, synthesis, and biological evaluation of novel and small, low toxicity s-triazine derivatives as HIV-1 non-nucleoside reverse transcriptase inhibitors. Bioorg. Med. Chem. 24 (2016) 2519–2529.
- 155. Afonso, C.A.M.; Lourenco, N.M.T.; Rosatella, A.D.A. Synthesis of 2,4,6-Tri-substituted-1,3,5-Triazines. Molecules 2006, 11, 81-102.
- 156. O. Trott, A. J. Olson, AutoDock Vina: improving the speed and accuracy of docking with a new scoring function, efficient optimization and multithreading, Journal of Computational Chemistry 31 (2010) 455-461.
- 157. Norikazu Sakakibara, Gianfranco Balboni, Cenzo Congiu, Valentina Onnis, Yosuke Demizu, Takashi Misawa, Masaaki Kurihara, Yoshihisa Kato, Tokumi Maruyama, Masaaki Toyama, Mika Okamoto, and Masanori Baba4. Design, synthesis, and anti-HIV-1 activity of 1-substituted 3-(3,5-dimethylbenzyl) triazine derivatives Antivir Chem Chemother. 2015 Apr; 24(2): 62–71.
- 158. Tsung-Yi Lin, Kuo-Chun Tang, Shen-Han Yang, Jiun-Yi Shen, Yi-Ming Cheng, Hsiao-An Pan, Yun Chi, and Pi-Tai Chou. The Empirical Correlation between Hydrogen Bonding Strength and Excited-State Intramolecular Proton Transfer in 2-Pyridyl Pyrazoles. J. Phys. Chem. A 2012, 116, 18, 4438–4444.
- 159. Tongshou Jin, Suling Zhang & Tongshuang Li (2002) P-Touluenesulfonic acid-catalyzed Efficient Synthesis of Dihydropyrimidines: Improved high yielding protocol for the Biginelli Reaction, Synthetic Communications, 32:12,1847-1851.
- 160. T.A. Yousefa, G.M. Abu El-Reashb, T.H. Rakhab, Usama El-Ayaanb First row transition metal complexes of (E)-2-(2-(2-hydroxybenzylidene) hydrazinyl)-2-oxo-N-phenylacetamide complexes. Spectrochimica Acta Part A 83 (2011) 271–278.

- 161. Moni Sharma, Kuldeep Chauhan, Rahul Shivahare, Preeti Vishwakarma, Manish K. Suthar, Abhisheak Sharma, Suman Gupta, Jitendra K. Saxena, Jawahar Lal, Preeti Chandra, Brijesh Kumar, and Prem M. S. Chauhan. Discovery of a New Class of Natural Product-Inspired Quinazolinone Hybrid as Potent Antileishmanial agents. J. Med. Chem. 2013, 56, 4374–4392.
- 162.Corey S. Keenan & S. Shaun Murphree (2017) Rapid and convenient conversion of nitroarenes to anilines under microwave conditions using nonprecious metals in mildly acidic medium, Synthetic Communications, 47:11, 1085-1089.
- 163. N.C. Desai, Atul H. Makwana, R.D. Senta Synthesis, characterization and antimicrobial activity of some new 4-(4-(2-isonicotinoylhydrazinyl)-6-((aryl)amino)-1,3,5-triazin-2-ylamino)-N-(pyrimidin-2-yl) benzenesulfonamides. Journal of Saudi Chemical Society (2017) 21, S25–S34.
- 164. Khadijah M. Al-Zaydi, Hosam H. Khalil, Ayman El-Faham and Sherine N. Khattab Synthesis, characterization, and evaluation of 1,3,5-triazine aminobenzoic acid derivatives for their antimicrobial activity. Al-Zaydi et al. Chemistry Central Journal (2017) 11:39.
- 165. Kirill A. Kolmakov. An Efficient, "Green" Approach to Aryl Amination of Cyanuric Chloride Using Acetic Acid as Solvent. J. Heterocyclic Chem., 45, 533 (2008).
- 166. A. Divakar, S. Krishna, R.K. Mandraju, G. Kishore, A.K. Kondapi, An Efficient Targeted Drug Delivery through Apotransferrin Loaded Nanoparticles, PLoS ONE 2009;4:10
- 167. A. Malloy. Count ,size and visualize nanoparticles, Materials Today. 2011;14:170–173.
- 168. R. Kim, Native Agarose Gel Electrophoresis of Multiprotein Complexes Protocol Native Agarose Gel Electrophoresis of Multiprotein Complexes, Cold Spring Harb Protoc. 2011.
- 169. P. Kumar, Y.S. Lakshmi, A.K. Kondapi, Triple drug combination of Zidovudine, Efavirenz and Lamivudine Loaded Lactoferrin Nanoparticles: An Effective Nano First-Line Regimen for HIV Therapy, Pharm. Res. 2017; 34: 257–268.
- 170. Elodie Crublet, Jean-Pierre Andrieu, Romain R. Vivès, and Hugues Lortat-Jacob. The HIV-1 Envelope Glycoprotein gp120 Features Four Heparan Sulfate Binding Domains,

- Including the Co-receptor Binding Site. J Biol Chem. 2008 May 30; 283(22): 15193–15200.
- 171. Berger, E. A.; Murphy, P. M.; Farber, J. M. CHEMOKINE RECEPTORS AS HIV-1 CORECEPTORS: Roles in Viral Entry, Tropism, and Disease. 1999, 657–700.
- 172. Kwong, P. D.; Wyatt, R.; Robinson, J.; Sweet, R. W.; Sodroski, J.; Hendrickson, W. A. Structure of an HIV gp120 envelope glycoprotein in complex with the CD4 receptor and a neutralizing human antibody. Nature 1998, 393, 648–659.
- 173. P. J. Klasse. A New Bundle of Prospects for Blocking HIV-1 Entry. Science 341, 1347 (2013).
- 174. Prévost J, Zoubchenok D, Richard J, Veillette M, Pacheco B, Coutu M, Brassard N, Parsons MS, Ruxrungtham K, Bunupuradah T, Tovanabutra S, Hwang K-K, Moody MA, Haynes BF, Bonsignori M, Sodroski J, Kaufmann DE, Shaw GM, Chenine AL, Finzi A. 2017. Influence of the envelope gp120 Phe 43 cavity on HIV-1 sensitivity to antibody dependent cell-mediated cytotoxicity responses. J Virol 91:e02452-16.
- 175. Qiuxiang Tan et al. Structure of the CCR5 Chemokine Receptor-HIV Entry Inhibitor Maraviroc Complex Science 341, 1387 (2013).
- 176. Seidah, N. G. & Prat, A. The biology and therapeutic targeting of the proprotein convertases. Nature Rev. Drug Discov. 11, 367–383 (2012).
- 177.A.K. Kondapi, M.A. Hafiz, T. Sivaram, Anti-HIV activity of a glycoprotein fromfirsttrimester placental tissue, Antivir. Res. 54 (2002) 47–57.[24]
- 178. K.P. Roda Rani, Dheeraj Pelluru, Anand K. Kondapi, A conserved molecular action of native and recombinant Epap-1 in inhibition of HIV-1 gp120 mediated viralentry, Arch. Biochem. Biophys. 456 (1) (2006) 79–92
- 179. C. Bhaskar, Palakolanu S. Reddy, K. Sarath Chandra, Sudeep Sabde, Debashis Mitra, Anand K. Kondapi .Identification of the potential regions of Epap-1 that interacts with V3loop of HIV-1 gp120C.,
- 180. Akhila B. Computational design, validation and delivery of HIV-1 entry and early replication inhibitors. july2019. University of Hyderabad (Ph.D. Thesis).

- 181. Francesca Curreli, Spreeha Choudhury,Ilya Pyatkin, Victor P. Zagorodnikov, Anna Khulianova Bulay, Andrea Altieri,Young Do Kwon,Peter D. Kwong, and Asim K. Debnath. Design, Synthesis, and Antiviral Activity of Entry Inhibitors That Target the CD4-Binding Site of HIV-1. J. Med. Chem. 2012, 55, 4764–4775.
- 182. Flavia Varano, Daniela Catarzi, Vittoria Colotta, Guido Filacchioni, Alessandro Galli, Chiara Costagli, and Vincenzo Carla. Synthesis and Biological Evaluation of a New Set of Pyrazolo[1,5-c] quinazoline-2-carboxylates as Novel Excitatory Amino Acid Antagonists. J. Med. Chem. 2002, 45, 1035-1044.
- 183. Shipra Baluja, Ravi Gajera, Sumitra Chanda. Antibacterial studies of dihydropyrimidinones and pyrimidinethiones. J Bacteriol Mycol Open Access. 2017;5(6):414–418.
- 184.Chang, Noel F. Whittaker, and Carole A. Bewley. Crambescidin 826 and Dehydrocrambine A: New Polycyclic Guanidine Alkaloids from the Marine Sponge Monanchora sp. that Inhibit HIV-1 Fusion. J. Nat. Prod. 2003, 66, 11, 1490–1494.
- 185. Ashok D. Patil, N. Vasant Kumar, Wilhelmus C. Kokke, Mark F. Bean, Alan J. Freyer, Charles De Brosse, Shing Mai, Alemseged Truneh, D. John Faulkner, Brad Carte, Ann L. Breen, Robert P. Hertzberg, Randall K. Johnson, John W. Westley, and Barbara C. M. Potts. Novel Alkaloids from the Sponge Batzella sp.: Inhibitors of HIVgp 120-Human CD4 Binding. J. Org. Chem. 1995, 60, 1182-1188.
- 186.Carole A. Bewley, Satyajit Ray, Frederick Cohen, Shawn K. Collins, and Larry E. Overman. Inhibition of HIV-1 Envelope-Mediated Fusion by Synthetic Batzelladine Analogues. J. Nat. Prod. 2004, 67, 1319-1324.
- 187. Dennis R Burton, and John R Mascola. Antibody responses to envelope glycoproteins in HIV-1 infection. Nat Immunol. 2015 Jun; 16(6): 571–576.
- 188. RL Stanfield, E Cabezas, AC Satterthwait, EA Stura, AT Profy and A Wilson. Dual conformations for the HIV-1 gp120 V3 loop in complexes with different neutralizing Fabs. Structure February 1999, 7:131–142.
- 189. Einat Schnur, Naama Kessler, Yuri Zherdev, Eran Noah, Tali Scherf, Fa-Xiang Ding, Svetlana Rabinovich, Boris Arshava, Victoria Kurbatska, Ainars Leonciks, Alexander Tsimanis, Osnat Rosen, Fred Naider, and Jacob Anglister. NMR mapping of RANTES

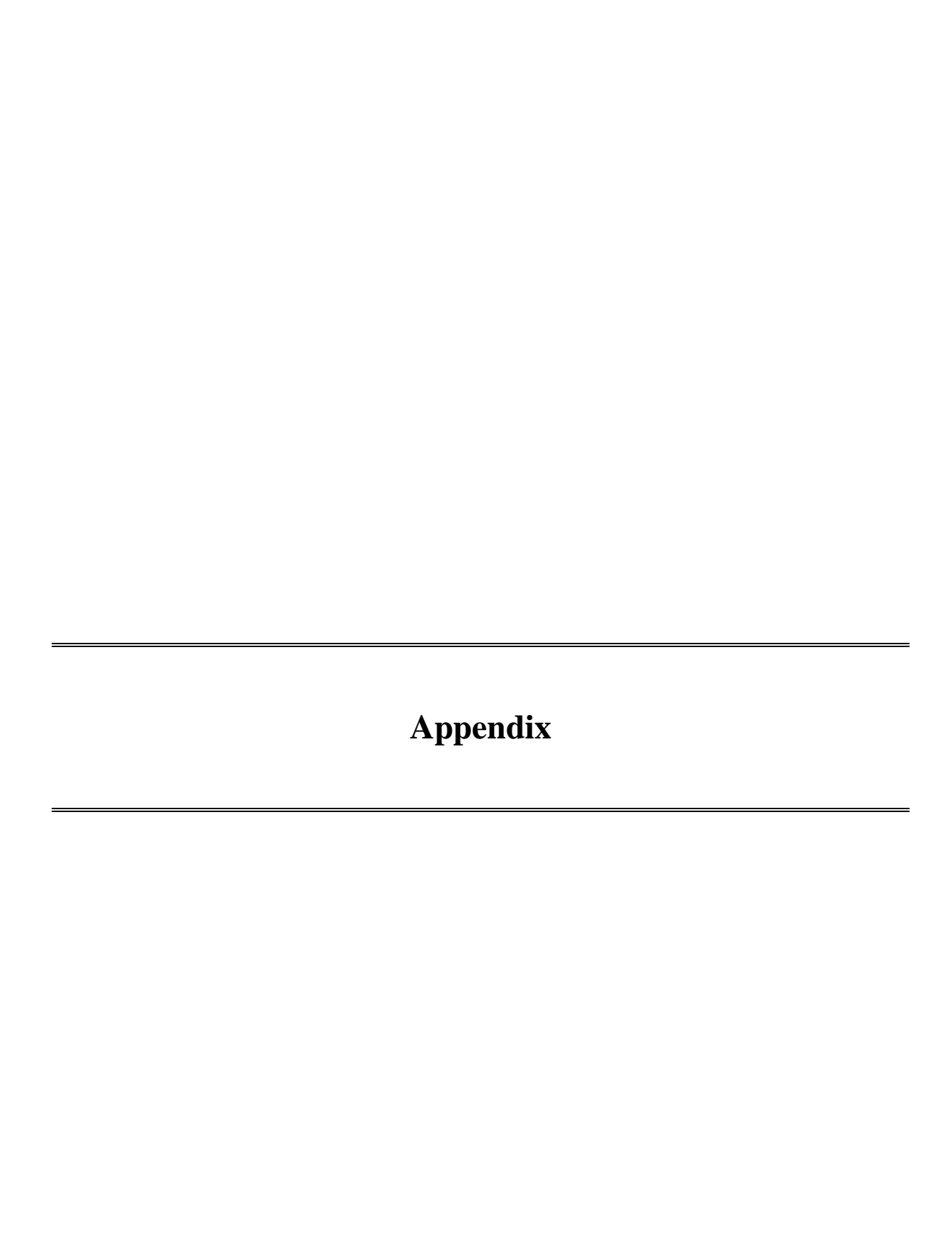
- surfaces interacting with CCR5 using linked extracellular domains. FEBS J. 2013 May; 280(9): 2068–2084.
- 190. Huang CC, Tang M, Zhang MY, Majeed S, Montabana E, Stanfield RL, Dimitrov DS, Korber B, Sodroski J, Wilson IA, Wyatt R, Kwong PD. Structure of a V3-containing HIV-1 gp120 core.Science. 2005 Nov 11; 310(5750):1025-8.
- 191. Stanfield R, Cabezas E, Satterthwait A, Stura E, Profy A, Wilson I. Dual conformations for the HIV-1 gp120 V3 loop in complexes with different neutralizing fabs. Structure. 1999 Feb 15; 7(2):131-42.
- 192. Tamamis P & Floudas CA (2014). Molecular recognition of CCR5 by an HIV-1 gp120 V3 loop. PLoS One 9, e95767.
- 193. Rini JM, Stanfield RL, Stura EA, Salinas PA, Profy AT, Wilson IA. Crystal structure of a human immunodeficiency virus type 1 neutralizing antibody, 50.1, in complex with its V3 loop peptide antigen. Proc Natl Acad Sci U S A. 1993 Jul 1; 90(13):6325-9.
- 194. i) April Killikelly, Hui-Tang Zhang, Brett Spurrier, Constance Williams, Miroslaw K. Gorny, Susan Zolla-Pazner, and Xiang-Peng Kong. Thermodynamic Signatures of the Antigen Binding Site of mAb 447–52D Targeting the Third Variable Region of HIV-1 gp120. Biochemistry 2013, 52, 6249–6257. ii) Acharya P, Dogo-Isonagie C, Lalonde JM, Lam SN,Leslie GJ, Louder MK, Frye LL, Debnath AK,Greenwood JR, Luongo TS et al. (2011) Structurebased identification and neutralization mechanism of tyrosine sulfate mimetics that inhibit HIV-1 entry. ACS Chem Biol 6, 1069–1077.
- 195. Jiang, X., Burke, V., Totrov, M., Williams, C., Cardozo, T., Gorny, M. K., Zolla-Pazner, S., and Kong, X.-P. (2010) Conserved structural elements in the V3 crown of HIV-1 gp120. Nat. Struct. Mol. Biol. 17,955–961.
- 196. Stanfield, R. L., Gorny, M. K., Williams, C., Zolla-Pazner, S., and Wilson, I. A. (2004) Structural Rationale for the Broad Neutralization of HIV-1 by Human Monoclonal Antibody 447–52D. Structure 12,193–204.
- 197.Amandeep K. Dhillon,a Robyn L. Stanfield,b,c Miroslaw K. Gorny,d Constance Williams,d Susan Zolla-Paznerd and Ian A. Wilsonb, Structure determination of an

- anti-HIV-1 Fab 447-52D-peptide complex from an epitaxially twinned data set. Acta Cryst. (2008). D64, 792–802.
- 198.Weik, M., Ravelli, R.B., Kryger, G., McSweeney, S., Raves, M.L., Harel, M., Gros, P., Silman, I., Kroon, J., Sussman, J.L.Specific chemical and structural damage to proteins produced by synchrotron radiation.(2000) Proc Natl Acad Sci U S A 97: 623-628.
- 199. Floris, M., Masciocchi, J., Fanton, M., & Moro, S. (2011). Swimming into peptidomimetic chemical space using pep- MMsMIMIC. Nucleic Acids Research, 39, W261–W269.
- 200. Cormier, E. G., Persuh, M., Thompson, D. A., Lin, S.W., Sakmar, T. P., Olson, W. C., and Dragic, T. (2000) Specific interaction of CCR5 amino-terminal domain peptides containing sulfotyrosines with HIV-1 envelope glycoprotein gp120. Proc. Natl. Acad. Sci. U.S.A. 97, 5762–5767.
- 201. P.R. Harrigan, R.S. Hogg, W.W.Y. Dong, B. Yip, B. Wynhoven, J. Woodward, C.J. Brumme, Z.L. Brumme, T. Mo, C.S. Alexander, J.S.G. Montaner, Predictors of HIV Drug-Resistance Mutations in a Large Antiretroviral-Naive Cohort Initiating Triple Antiretroviral Therapy, The Journal of Infectious Diseases 2005;191:339–47.
- 202. D.D. Richman, D.M. Margolis, M. Delaney, W.C. Greene, D. Hazuda, R.J. Pomerantz, The Challenge of Finding a Cure for HIV Infection Can We Do Better Than HAART?, science 2009;323:1304–1307.
- 203. N. Kolishetti, C. Salvador, Emerging nanotechnology approaches for HIV / AIDS treatment and prevention Review, Nanomedicine 2010; 5(2): 269–285
- 204. W. Li, F. Yu, Q. Wang, Q. Qi, S. Su, L. Xie, L. Lu, S. Jiang, Co-delivery of HIV-1 entry inhibitor and nonnucleoside reverse transcriptase inhibitor shuttled by nanoparticles: a cocktail therapeutic strategy for antiviral therapy, AIDS 2016;30: 827–837.
- 205. O.C. Farokhzad, R. Langer, Impact of Nanotechnology on Drug Delivery, ACS NANO 2009; 3: 16–20.
- 206. A. Jain, S.K. Singh, S.K. Arya, S.C. Kundu, S. Kapoor, Protein Nanoparticles: Promising Platforms for Drug Delivery Applications, ACS Biomater. Sci. Eng. 2018; 4: 3939–3961.

- 207. S. Gunaseelana, K. Gunaseelan, M. Deshmukh, X. Zhanga, P.J. Sinko, Surface Modifications of Nanocarriers for Effective Intracellular Delivery of Anti-HIV Drugs, Adv Drug Deliv Rev. 2010; 62(4-5): 518–531.
- 208. N.Skirtenko, M.Richman, Y.Nitzan, A. Gedankenab, S. Rahimipour, A facile one-pot sonochemical synthesis of surface-coated mannosyl protein microspheres for detection and killing of bacteria, Chem. Commun . 2011; 47: 45–48.
- 209. Andre Sutrisno, Victor V. Terskikh and Yining Huang. A natural abundance ³³S solid-state NMR study of layered transition metaldisulfides at ultrahigh magnetic field. Chem. Commun., 2009, 186-188.
- 210. Mark P. Foster, Craig A.McElroy, and Carlos D. Amero. Solution NMR of large molecules and assemblies. Biochemistry. 2007 January 16; 46(2): 331–340.
- 211. K. Bauri, M. Nandi, P. De, Amino acid-derived stimuli-responsive polymers and their applications, Polym. Chem., 2018; 9: 1257–1287.
- 212. A. Divakar, S. Krishna, R.K. Mandraju, G. Kishore, A.K. Kondapi, An Efficient Targeted Drug Delivery through Apotransferrin Loaded Nanoparticles, PLoS ONE 2009;4:10.
- 213. M. Richman, S. Wilk, N. Skirtenko, A. Perelman, S. Rahimipour, Surface-Modified Protein Microspheres Capture Amyloid-b and Inhibit its Aggregation and Toxicity, Chem. Eur. J. 2011; 17: 11171–11177.
- 214. S.A. Moore, B.F. Anderson, C.R. Groom, M. Haridas, E.N. Baker, Three-dimensional Structure of Diferric Bovine Ê Resolution Lactoferrin at 2.8 Å Resolution, J. Mol. Biol. 1997; 274:222–236.
- 215. M. Kohno, T. Mokudai, T. Ozawa, Y. Niwano, Free radical formation from sonolysis of water in the presence of different gases, J. Clin. Biochem. Nutr. 2011; 49: 96–101.
- 216. D. Baram-Pinto, S. Shukla, M. Richman, A. Gedanken, S. Rahimipour, R. Sarid, Surface-modified protein nanospheres as potential antiviral agents, Chem. Commun. 2012; 48 :8359–8361.

- 217. A. Albanese, P.S. Tang, W.C.W. Chan, The Effect of Nanoparticle Size, Shape, and Surface Chemistry on Biological Systems, Annu. Rev. Biomed. Eng. 2012; 14:1–16.
- 218. R.R. Arvizo, O.R. Miranda, M.A. Thompson, C.M. Pabelick, R. Bhattacharya, J.D. Robertson, V.M. Rotello, Y.S. Prakash, P. Mukherjee, Effect of Nanoparticle Surface Charge at the Plasma Membrane and Beyond, Nano Lett. 2010; 10: 2543–2548
- 219. B.D. Chithrani, A.A. Ghazani, W.C.W. Chan, Determining the Size and Shape Dependence of Gold Nanoparticle Uptake into Mammalian Cells, Nano Lett., 2006;6:662-668.
- 220. S. Honary, F. Zahir, Effect of Zeta Potential on the Properties of Nano-Drug Delivery
 Systems A Review (Part 2), Tropical Journal of Pharmaceutical Research ,2013; 12
 (2): 265-273.
- 221. C. Byram, S. Sathya, B. Moram, A.K. Shaik, V.R. Soma, Versatile gold based SERS substrates fabricated by ultrafast laser ablation for sensing picric acid and ammonium nitrate, Chem. Phys. Lett. 2017; 685: 103–107.
- 222. N.J. Fullwood, F.L. Martin, Gold nanoparticles as a substrate in bio-analytical near-infrared surface-enhanced Raman spectroscopy, Analyst, 2015; 140:3090–3097.
- 223. L. Xu, C. Zong, X. Zheng, P. Hu, J. Feng, B. Ren, Label-Free Detection of Native Proteins by Surface-Enhanced Raman Spectroscopy Using Iodide-Modi fi ed Nanoparticles, Anal. Chem. 2014; 86: 2238–2245.
- 224. Z. Wen, Raman Spectroscopy of Protein Pharmaceuticals, Journal of Pharmaceutical Sciences 2007; 96: 2861–2878.
- 225.M.L. Donten, A. Kro, Structure and composition of binary monolayers self-assembled from sodium 2-mercaptoetanosulfonate and mercaptoundecanol mixed solutions on silver and gold supports, Phys. Chem. Chem. Phys., 2009; 11:3390–3400.
- 226. D. Kurouski, P. Van Duyne, I.K. Lednev, Exploring the structure and formation mechanism of amyloid fibrils by Raman spectroscopy, Analyst 2015;140: 4967–4980.
- 227.E. Lo, M. Ghomi, B.Hernadez,S. Sanchez-cortes, Stability of the Disulfide Bond in Cystine Adsorbed on Silver and Gold Nanoparticles As Evidenced by SERS Data J. Phys. Chem. C .2013; 117: 1531–1537.

- 228. X. Shi, Y. Ye, H. Wang, F. Liu, Z. Wang, Designing pH-Responsive Biodegradable Polymer Coatings for Controlled Drug Release via Vapor-Based Route, ACS Appl. Mater. Interfaces 2018; 10: 38449–38458.
- 229.J. Li, X. Li, Y. Kuang, Y. Gao, X. Du, J. Shi, B. Xu, Self-Delivery Multifunctional Anti-HIV Hydrogels for Sustained Release, Adv. Healthcare Mater. 2013; 2: 1586–1590.



i) Copies of ¹H NMR, HRMS and IR spectra for representative compounds

A) Objective I compounds specras:



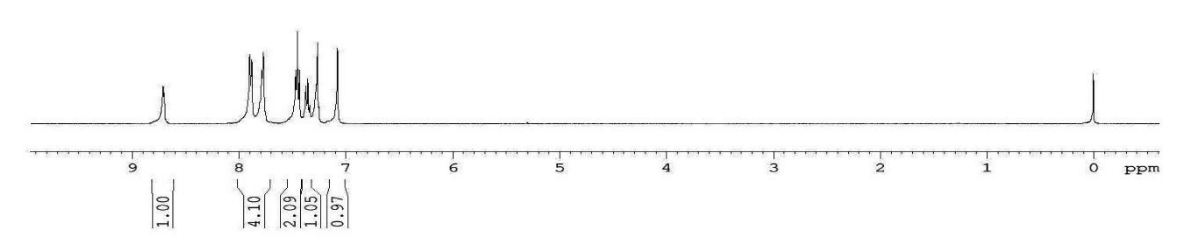


Fig. A1: ¹H NMR spectrum of compound UHLMTA-E5.

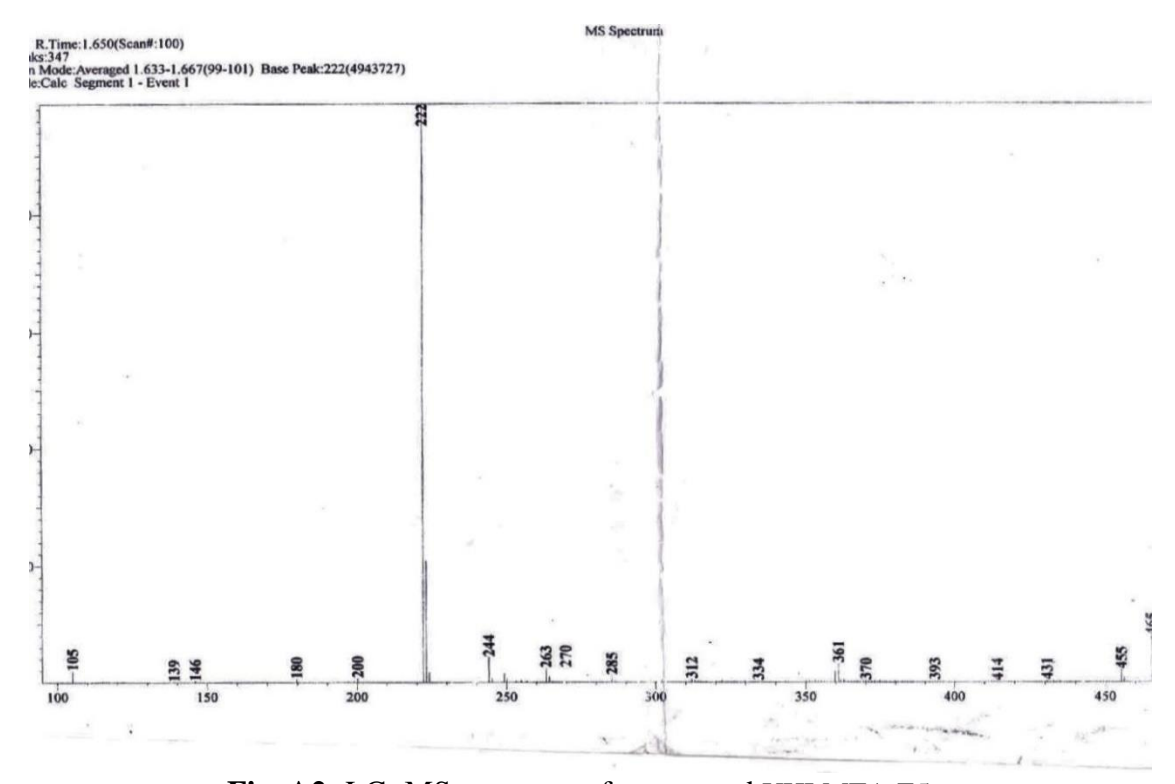


Fig. A2: LC- MS spectrum of compound UHLMTA-E5

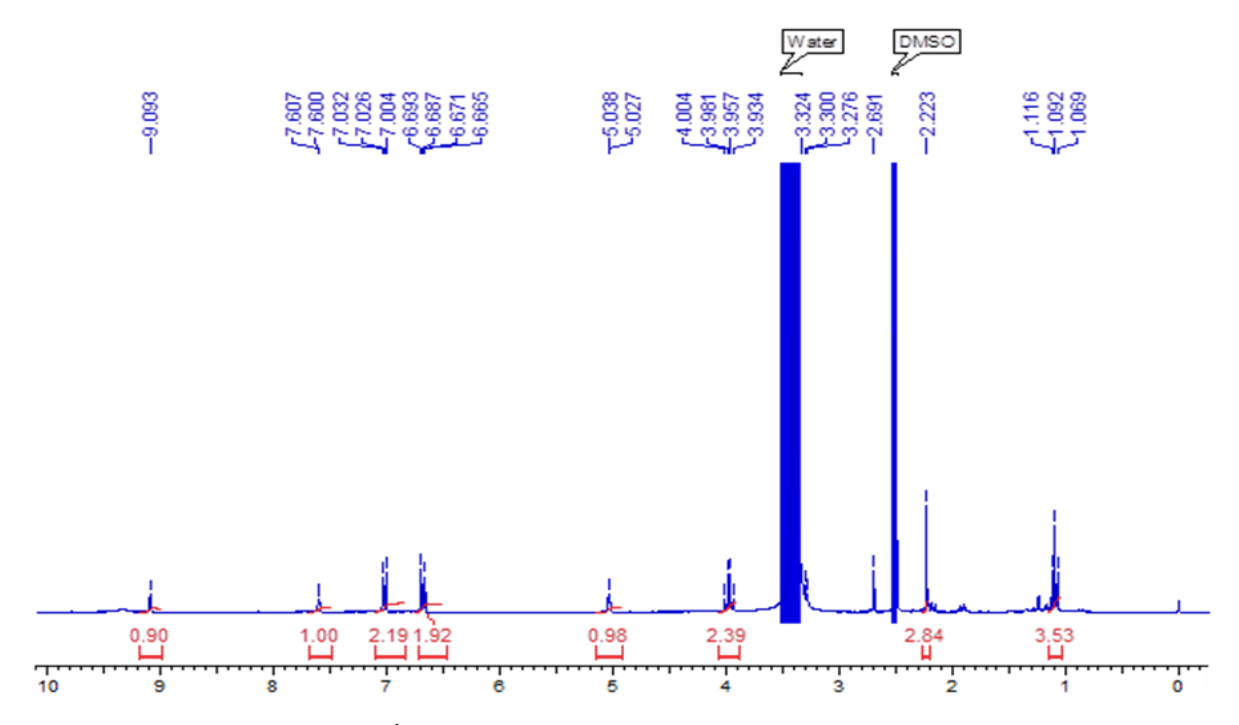


Fig. A3: ¹H NMR spectrum of compound UHLMTJ-254a

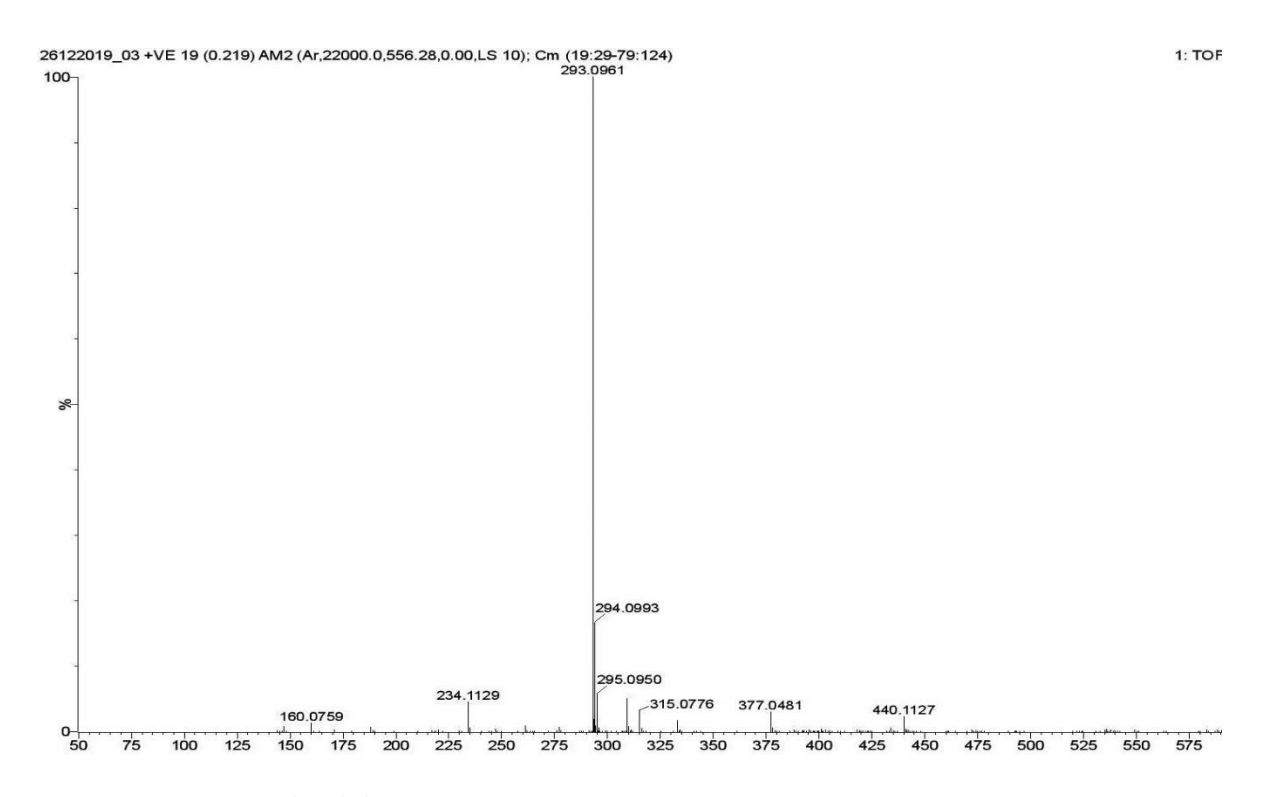


Fig. A4: HRMS of compound UHLMTJ-254a

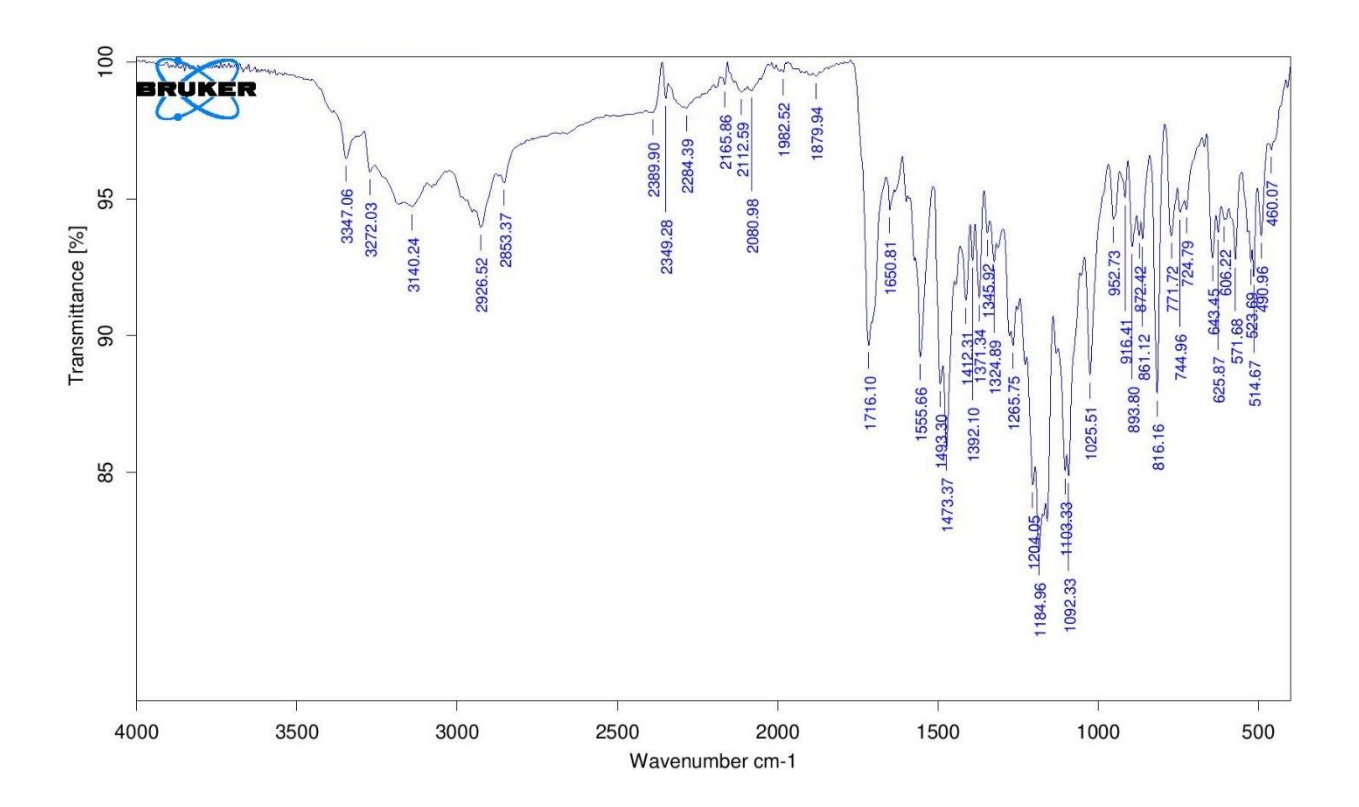
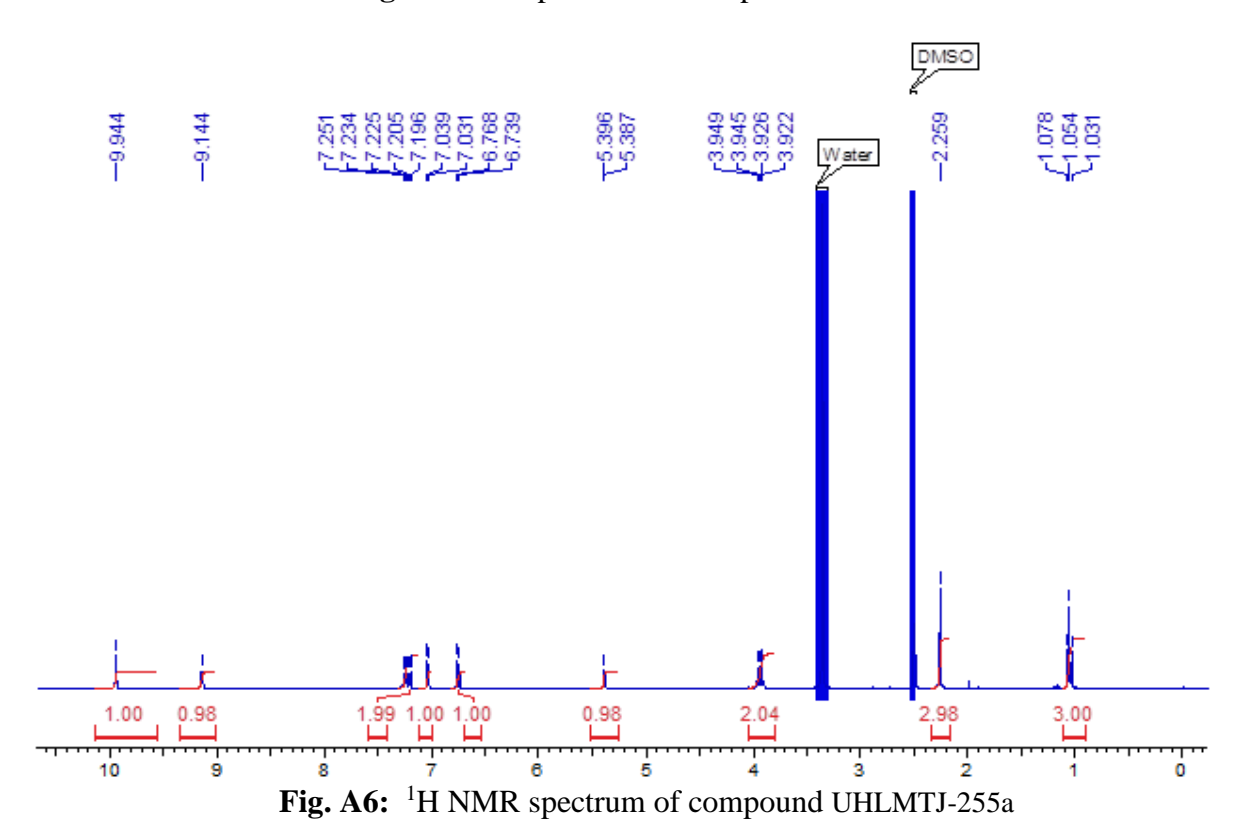


Fig. A5: IR spectrum of compound UHLMTJ-254a



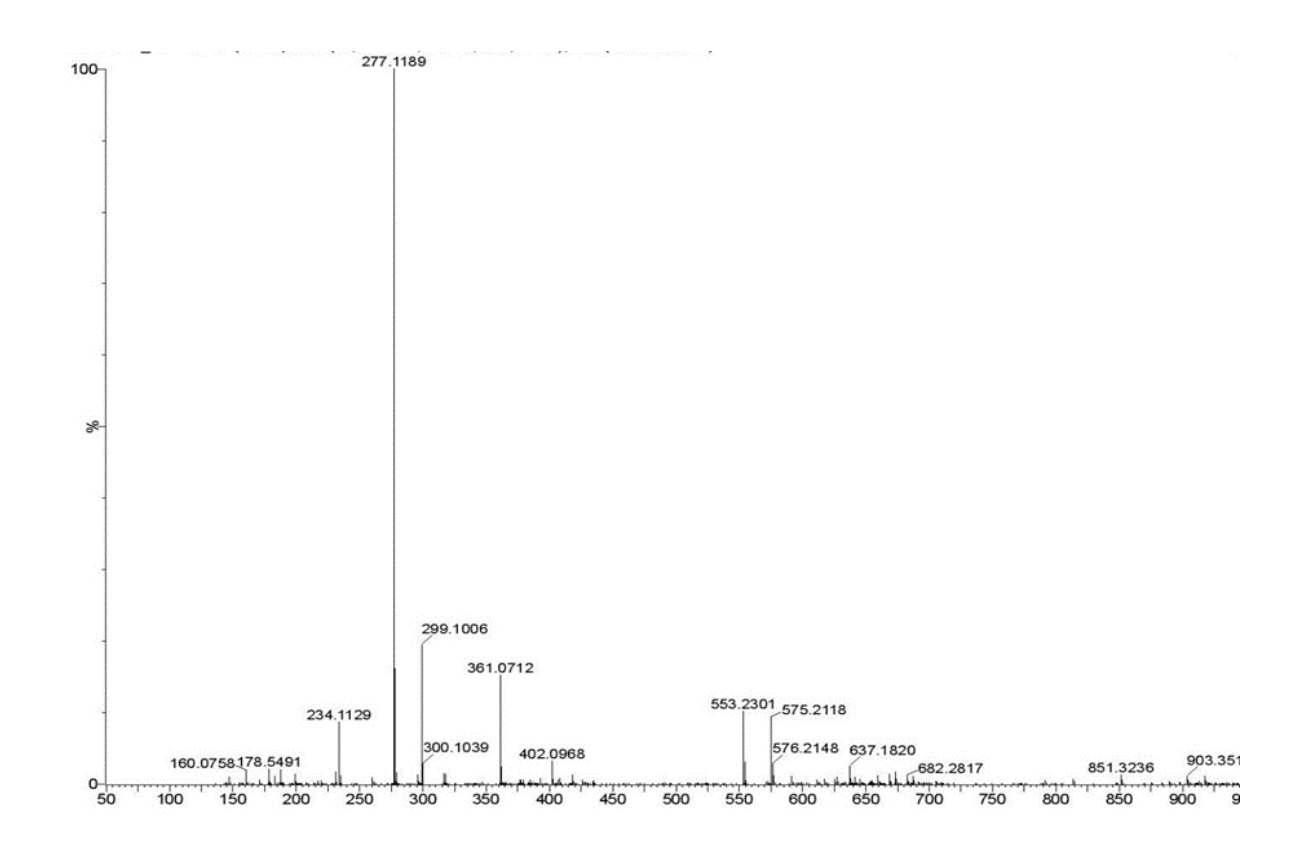


Fig. A7: HRMS of compound UHLMTJ-255a

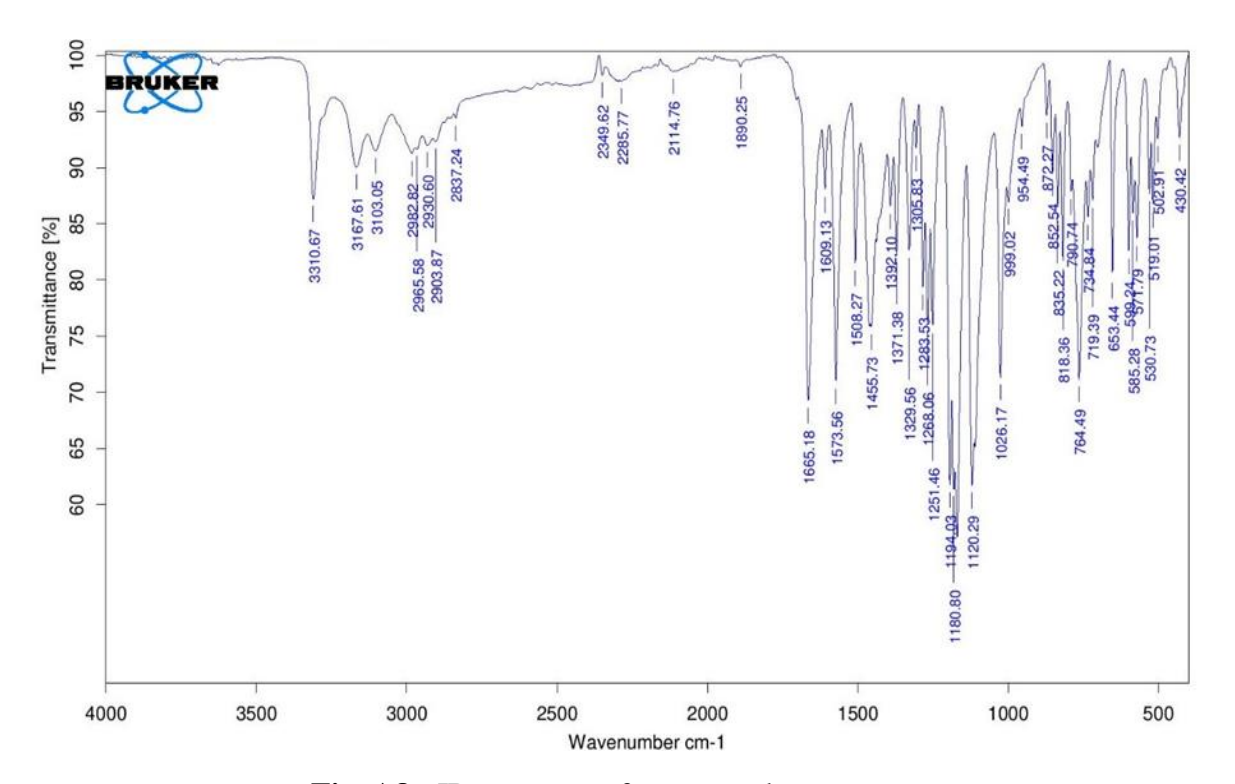


Fig. A8: IR spectrum of compound UHLMTJ-255a

B) Objective II compounds spectras:

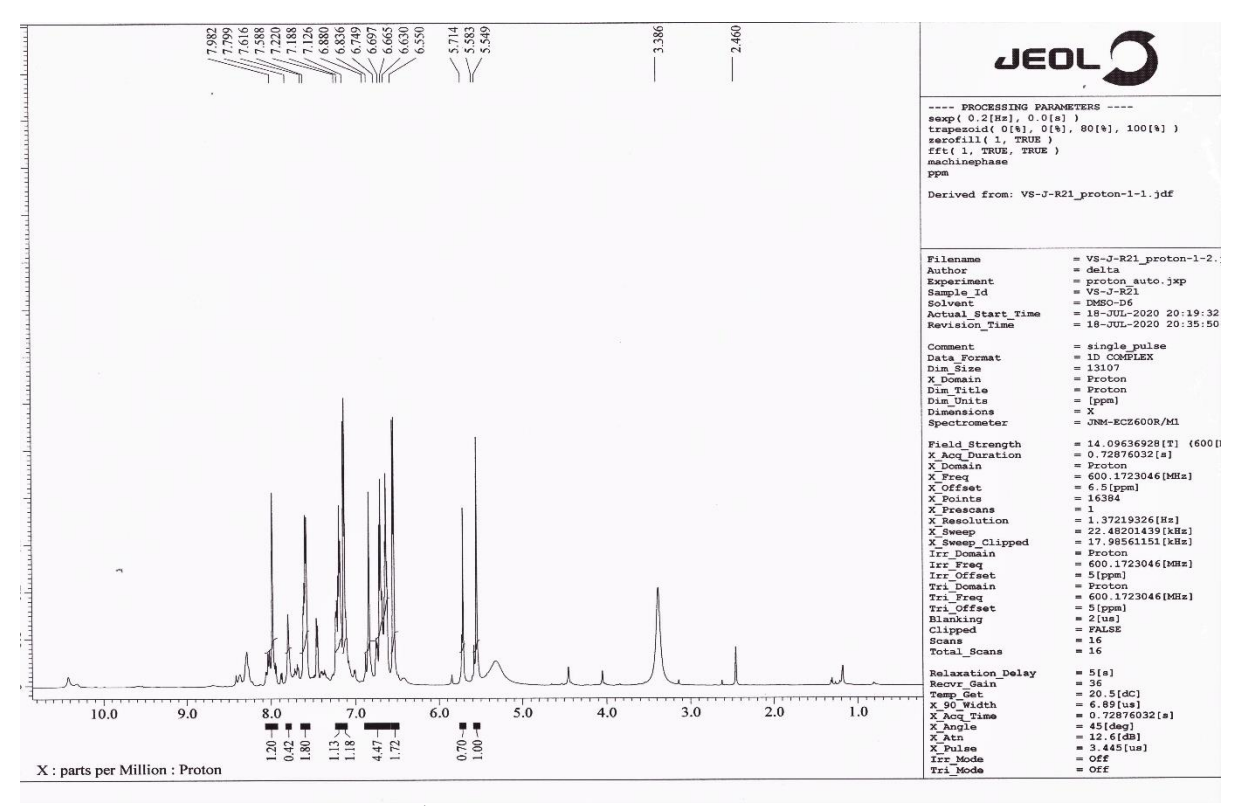


Fig. A9: ¹H NMR spectrum of compound 2.9

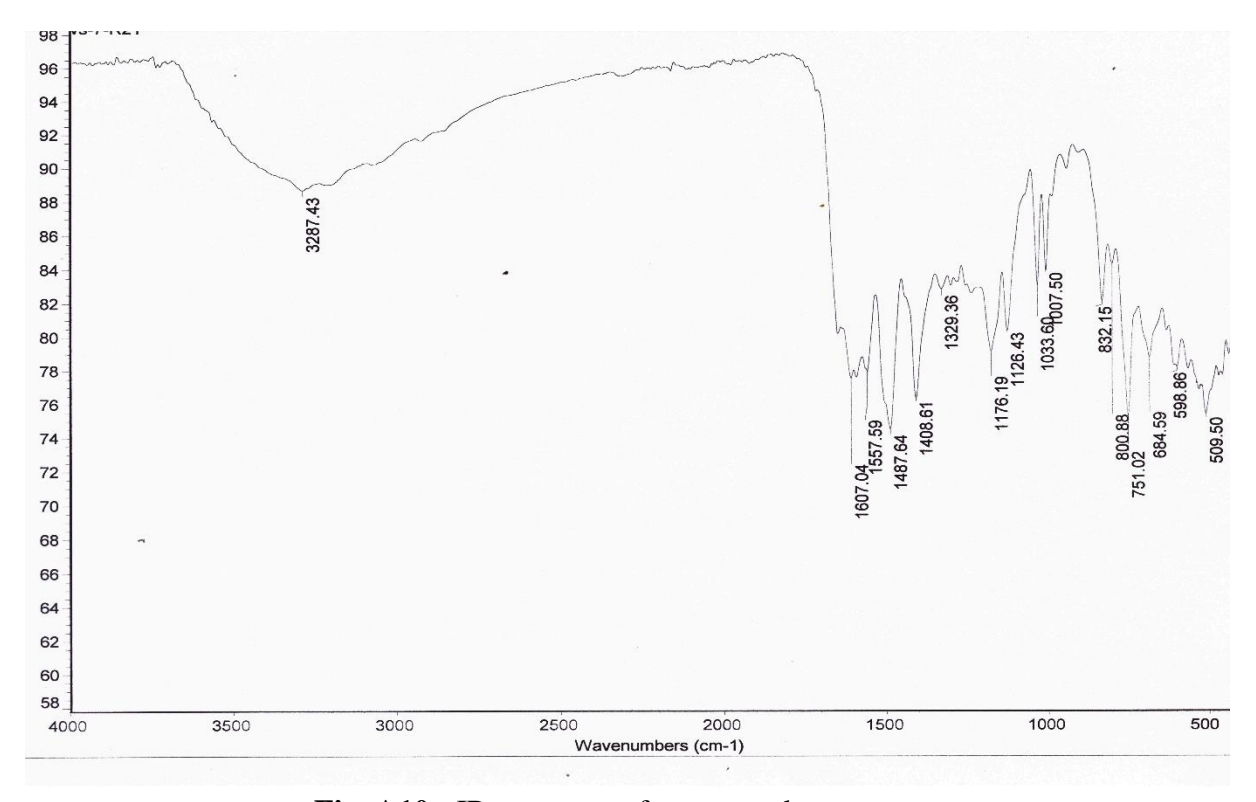


Fig. A10: IR spectrum of compound 2.9

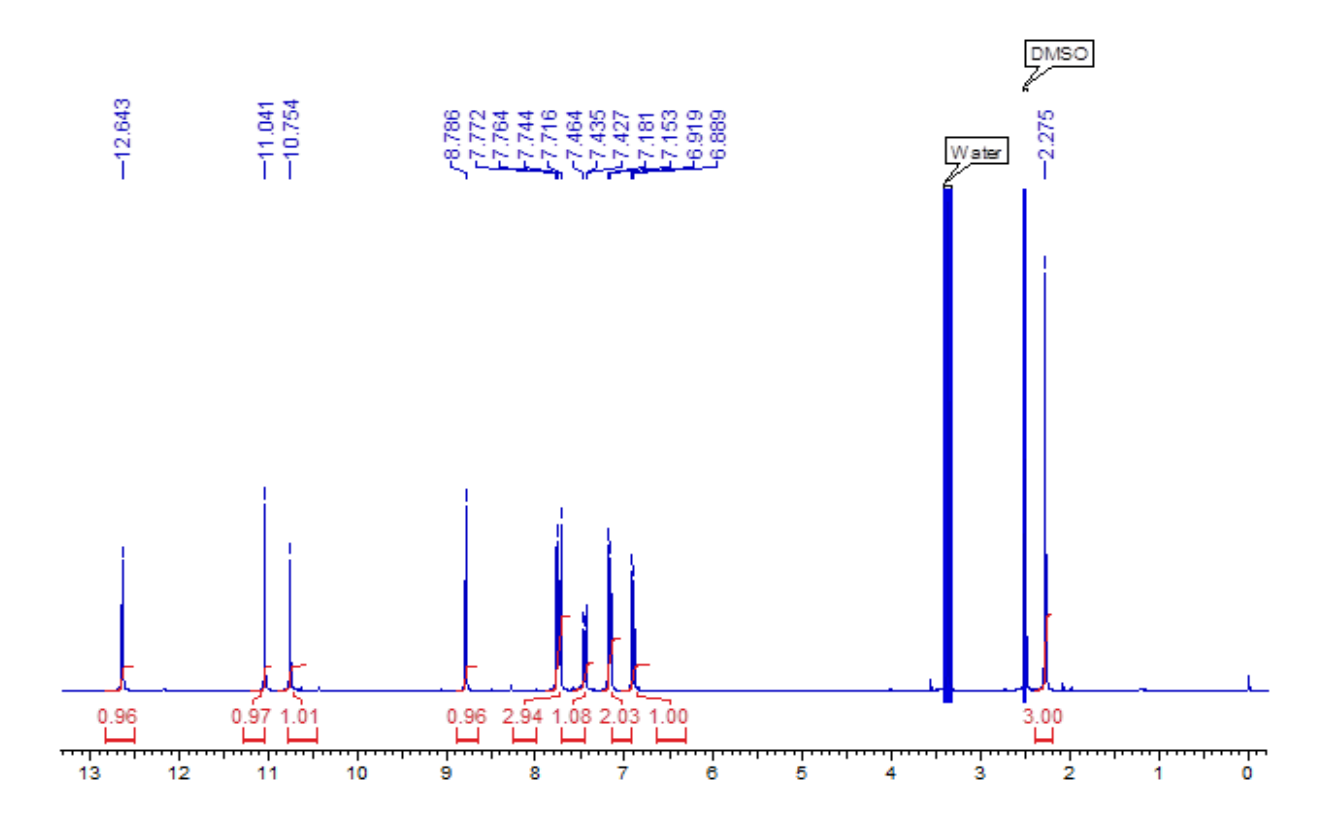


Fig. A11: ¹H NMR spectrum of compound UHLMTJ-256

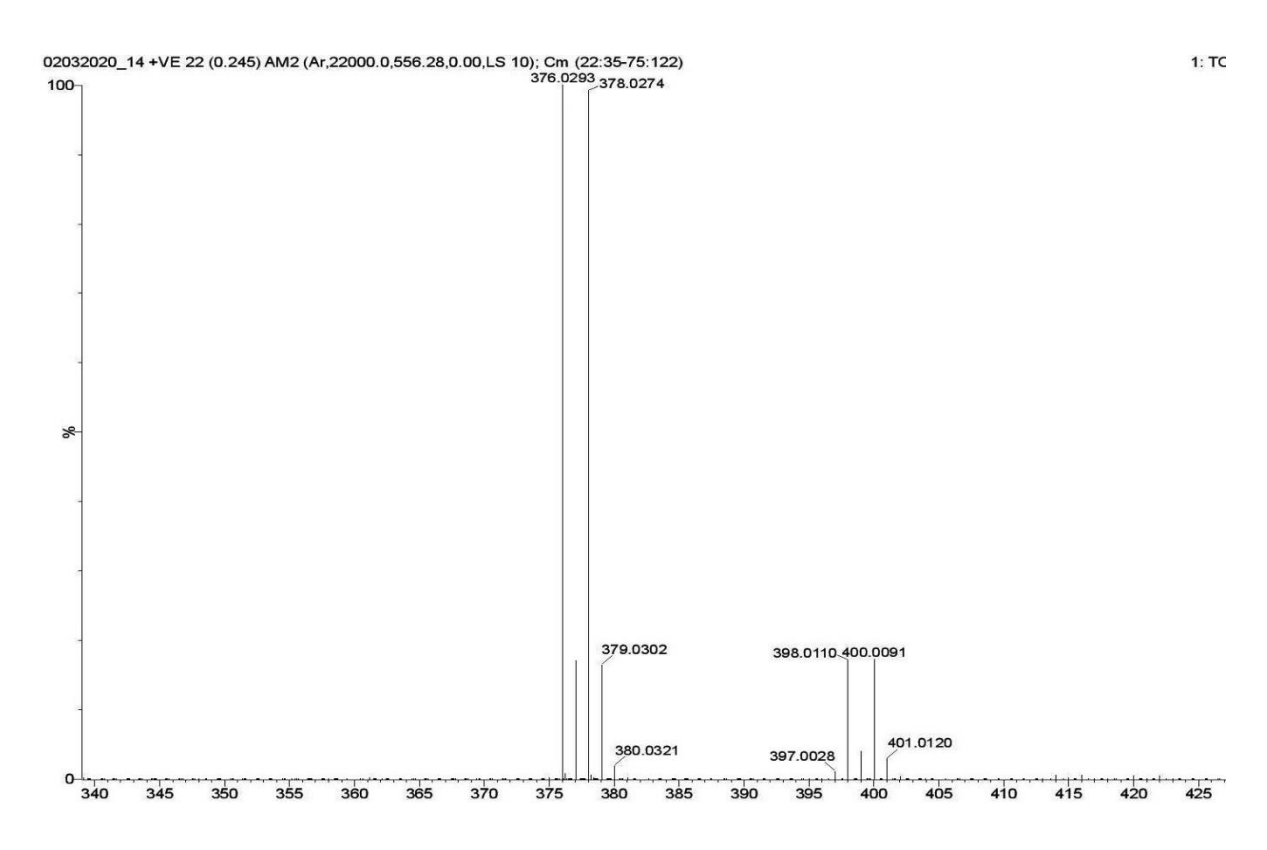


Fig. A12: HRMS of compound UHLMTJ-256

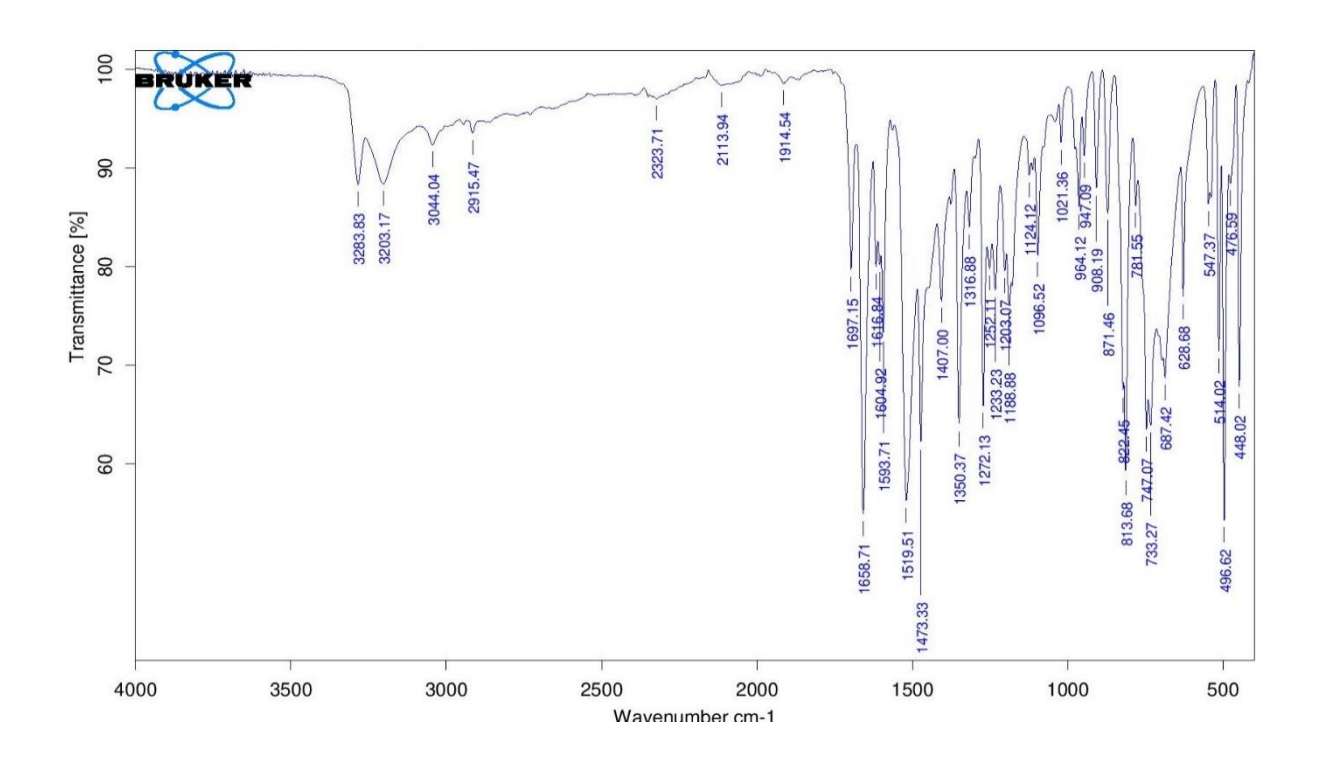


Fig. A13: IR spectrum of compound UHLMTJ-256

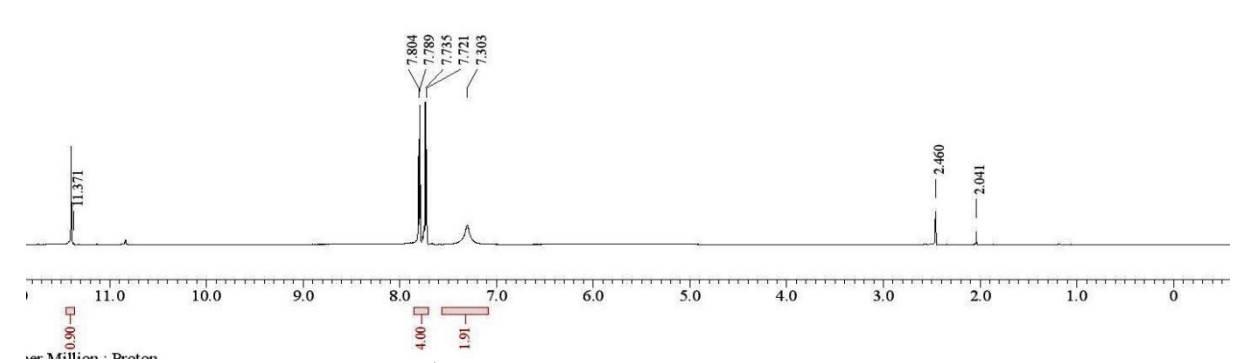


Fig. A14: ¹H NMR spectrum of compound 3.6a

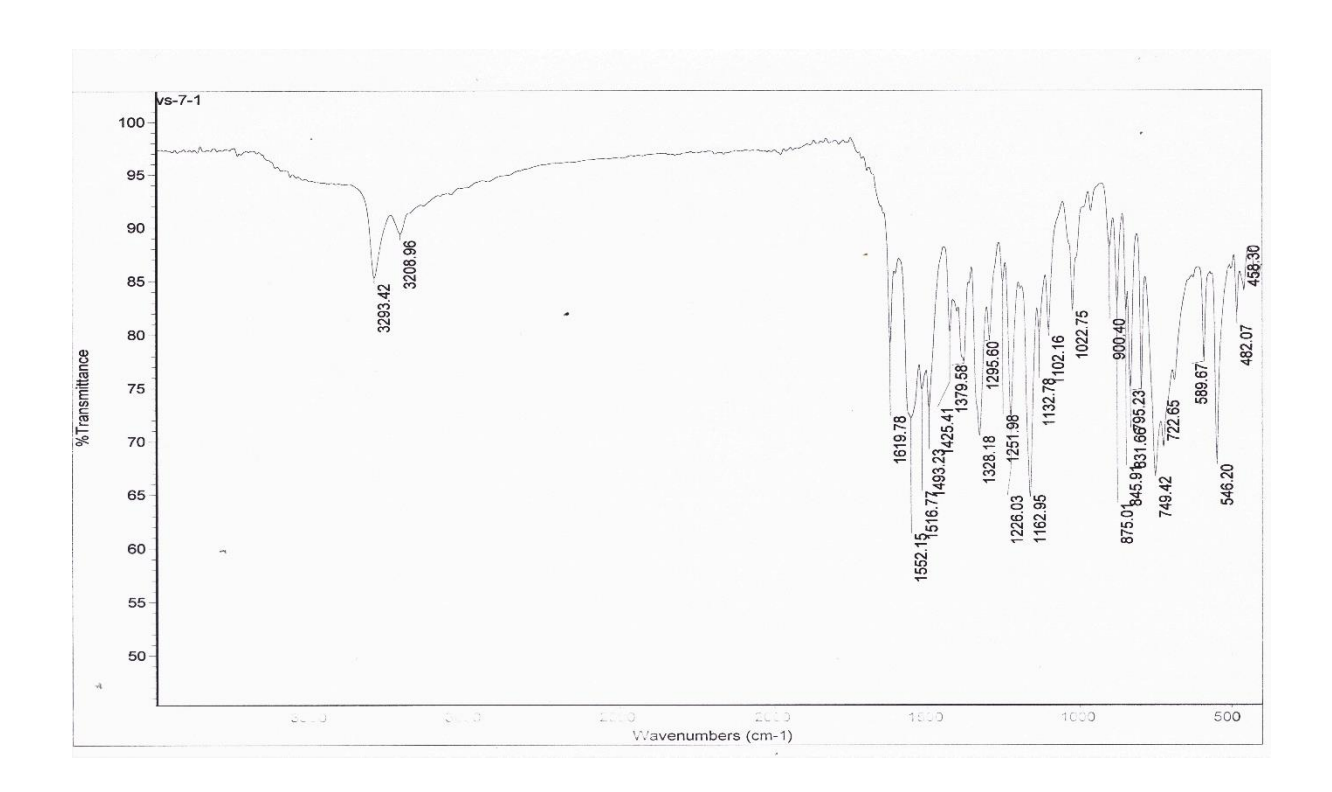


Fig. A15: IR spectrum of compound 3.6a

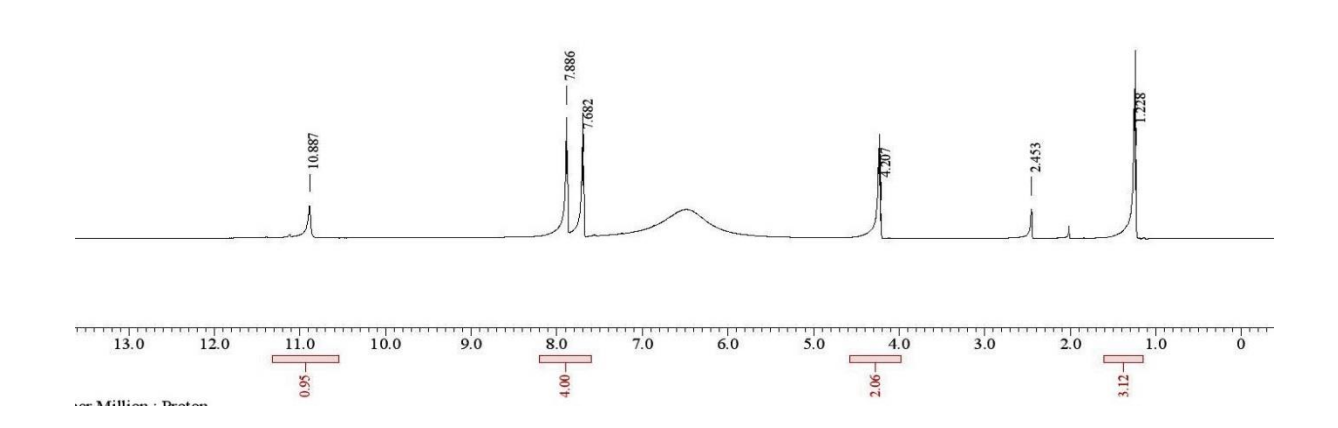


Fig. A16: ¹H NMR spectrum of compound 3.6b

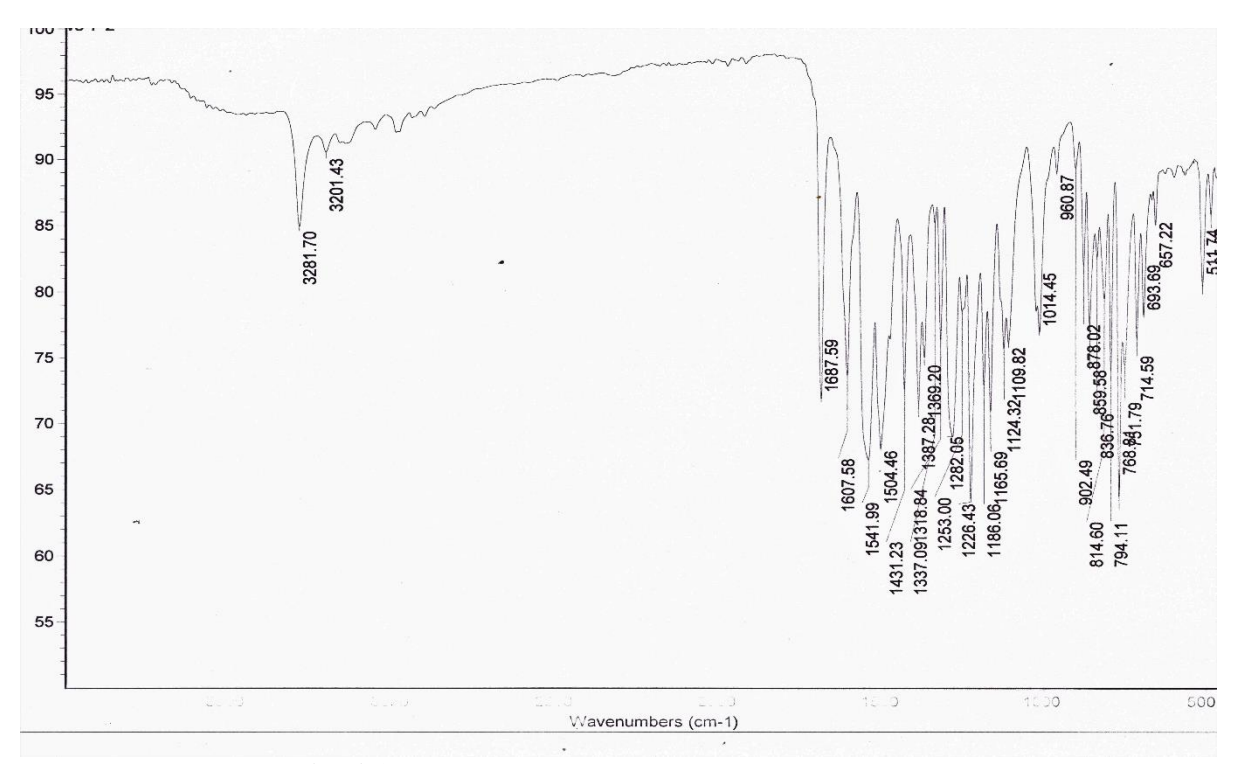


Fig. A17: IR spectrum of compound 3.6b

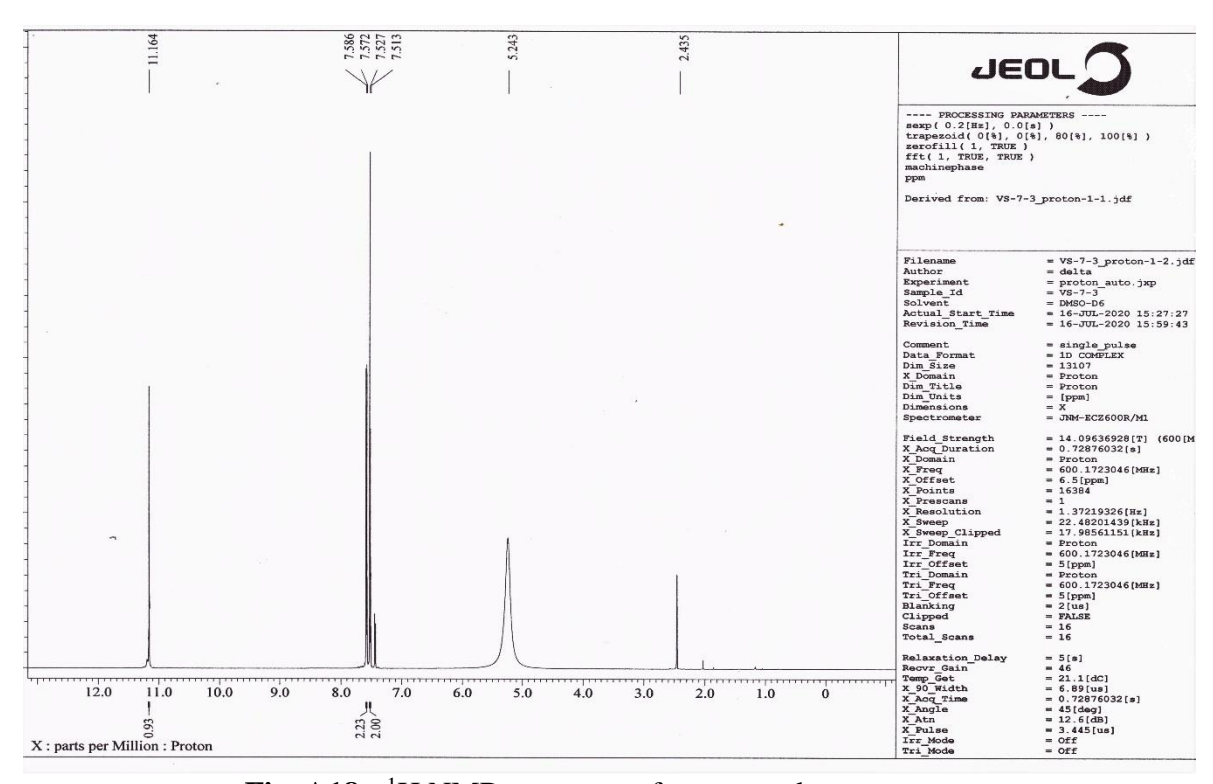


Fig. A18: ¹H NMR spectrum of compound 3.6c

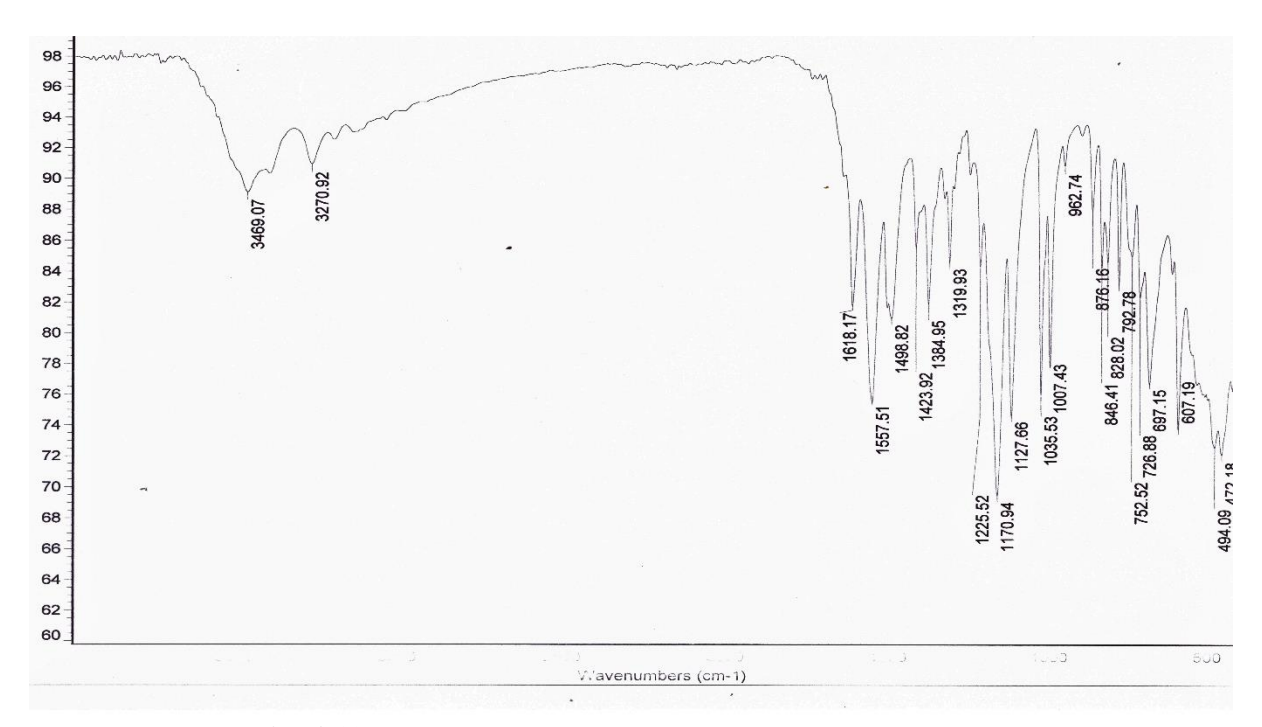
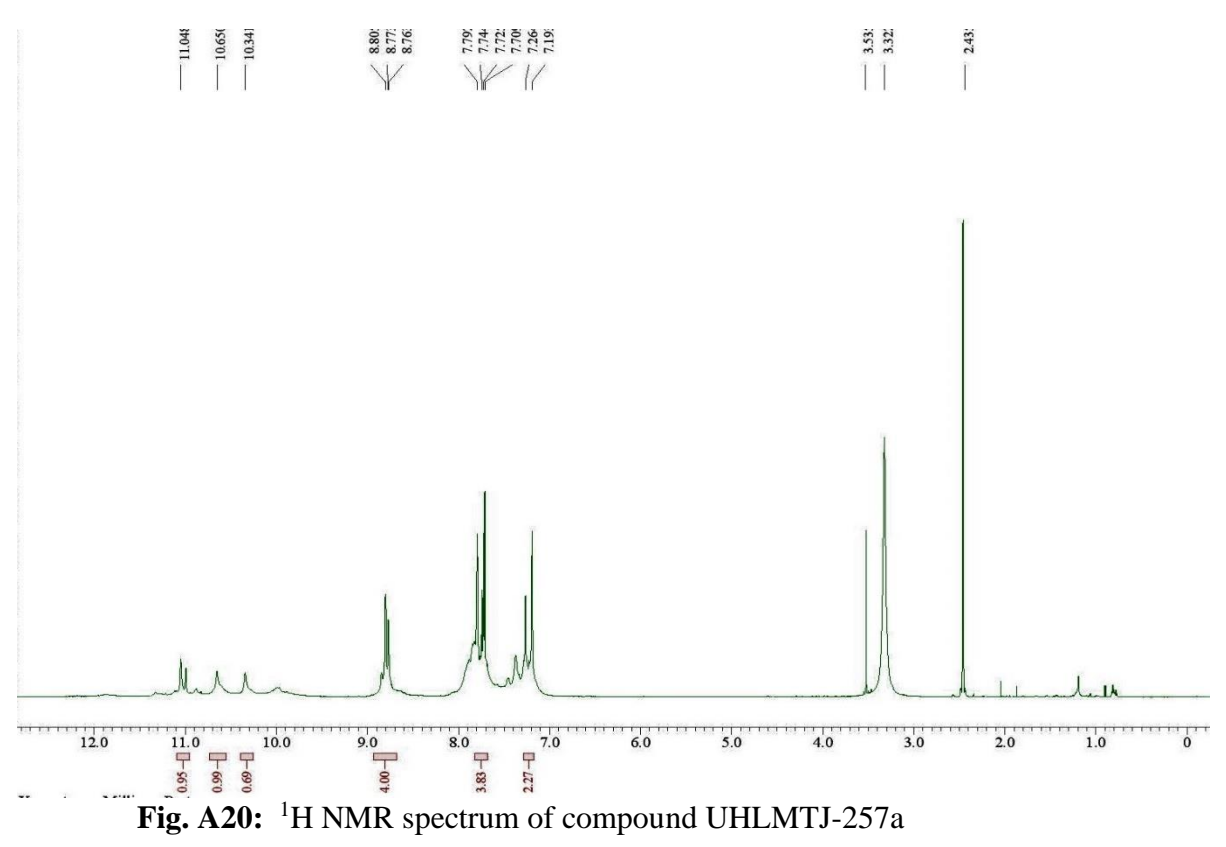


Fig. A19: IR spectrum of compound 3.6c



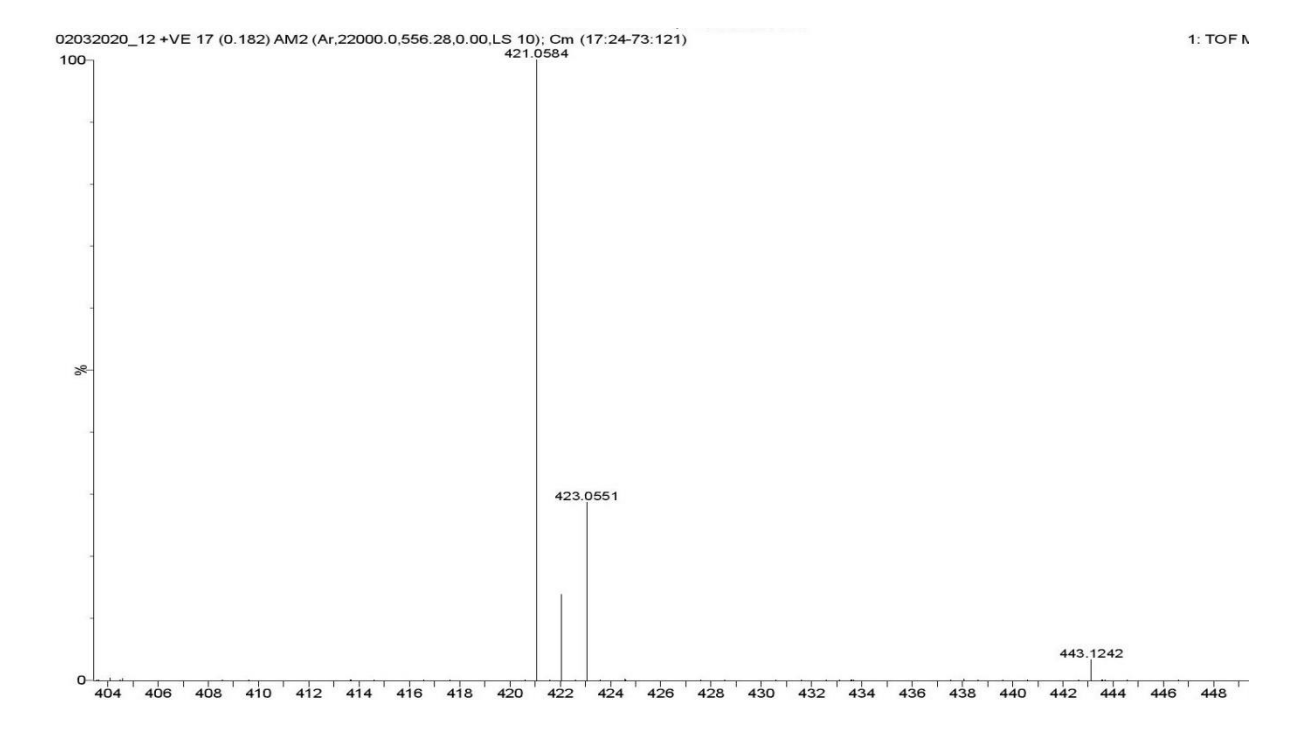


Fig. A21: HRMS of compound UHLMTJ-257a

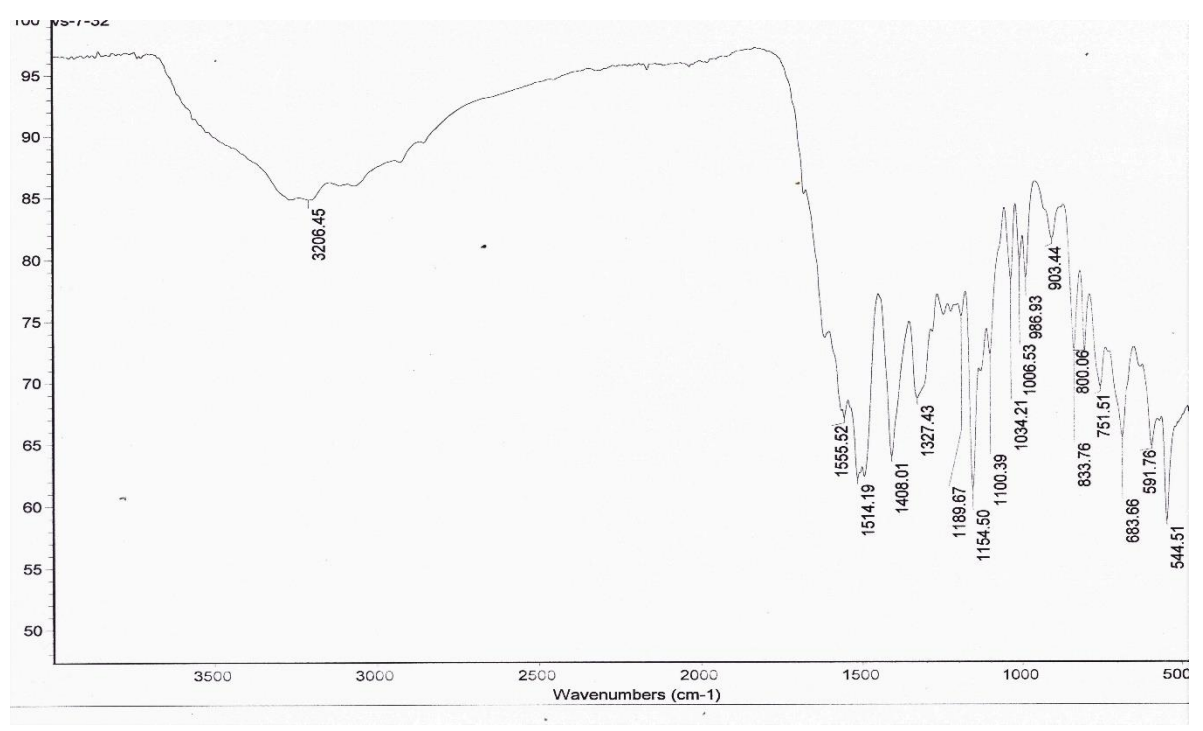


Fig. A22: IR of compound UHLMTJ-257a

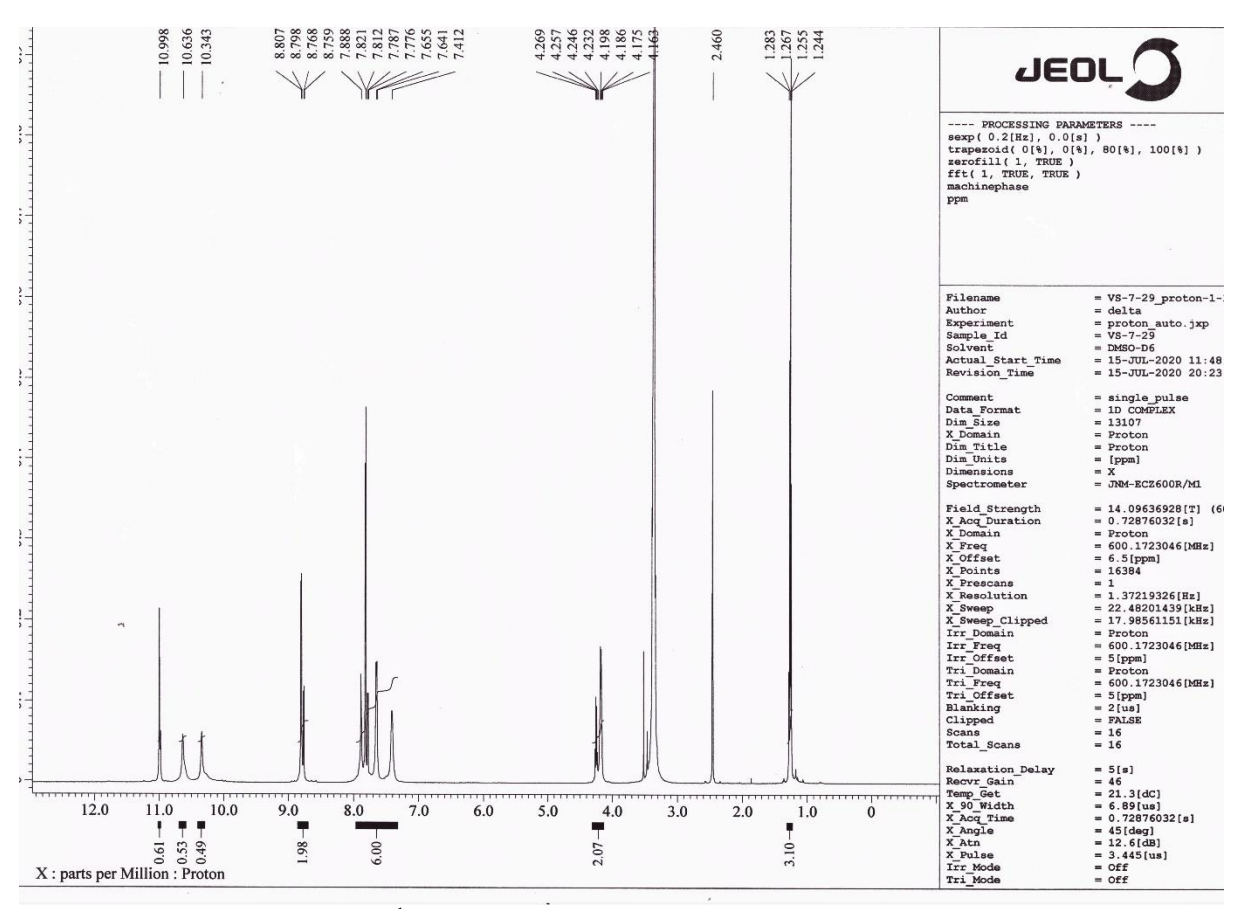


Fig. A23: ¹H NMR spectrum of compound UHLMTJ-257b

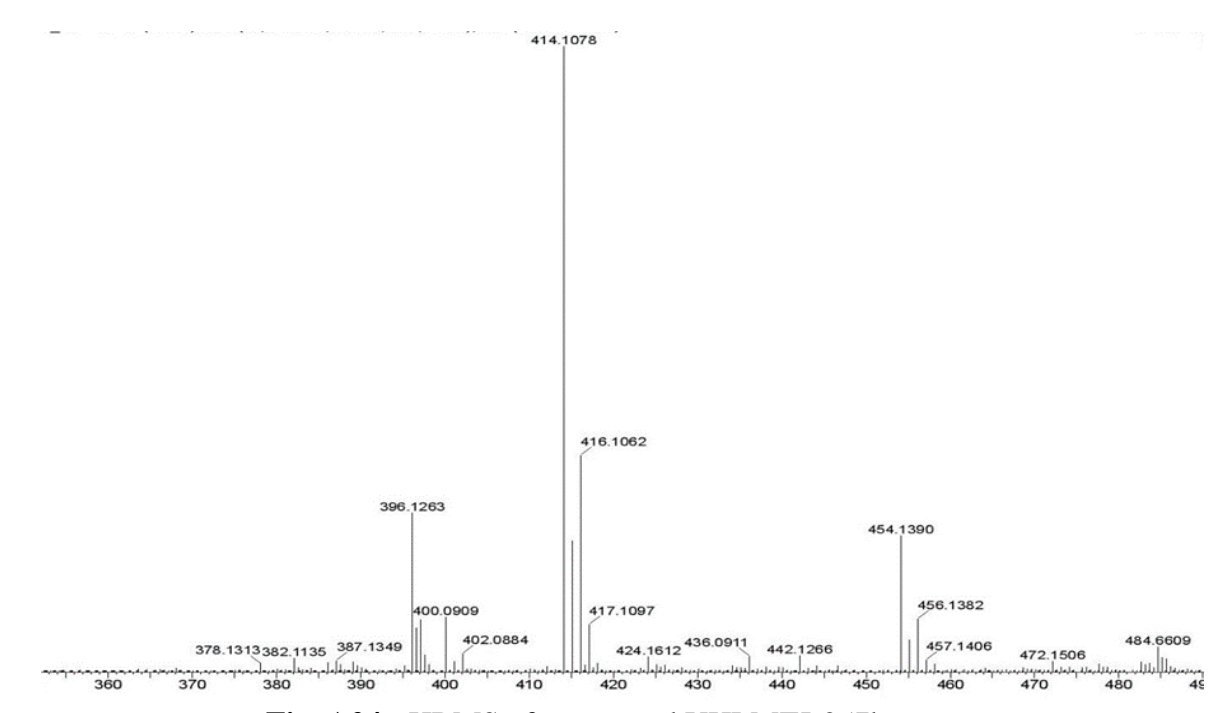


Fig. A24: HRMS of compound UHLMTJ-257b

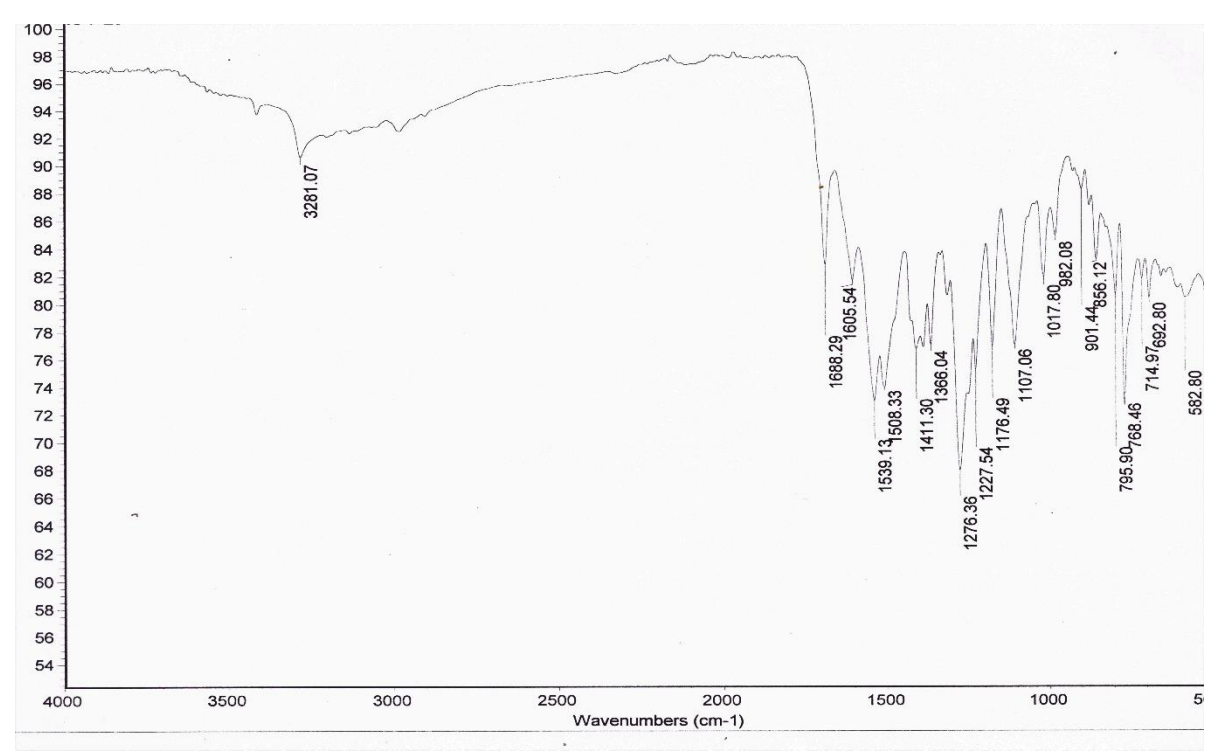


Fig. A25: IR of compound UHLMTJ-257b

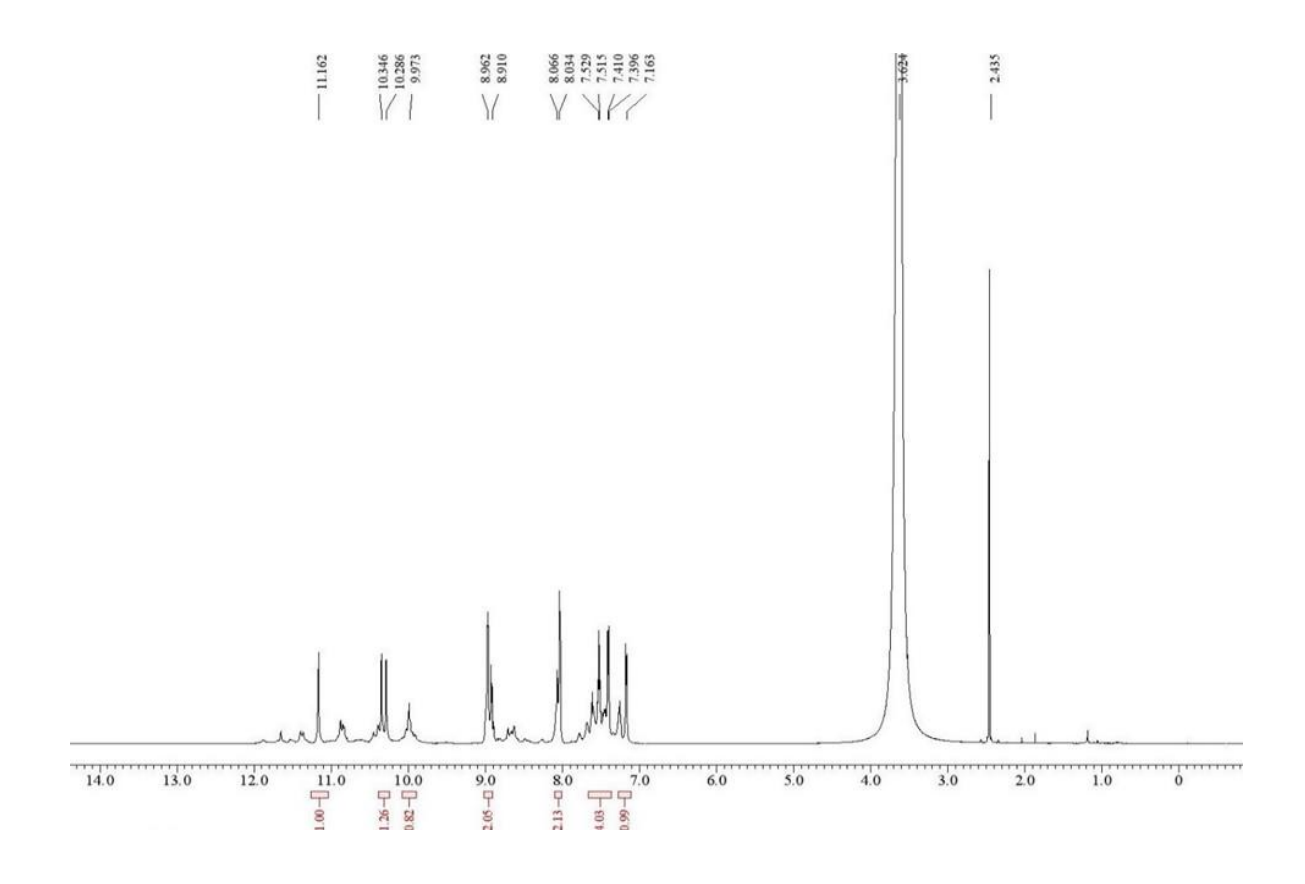


Fig. A26: ¹H NMR spectrum of compound UHLMTJ-257c

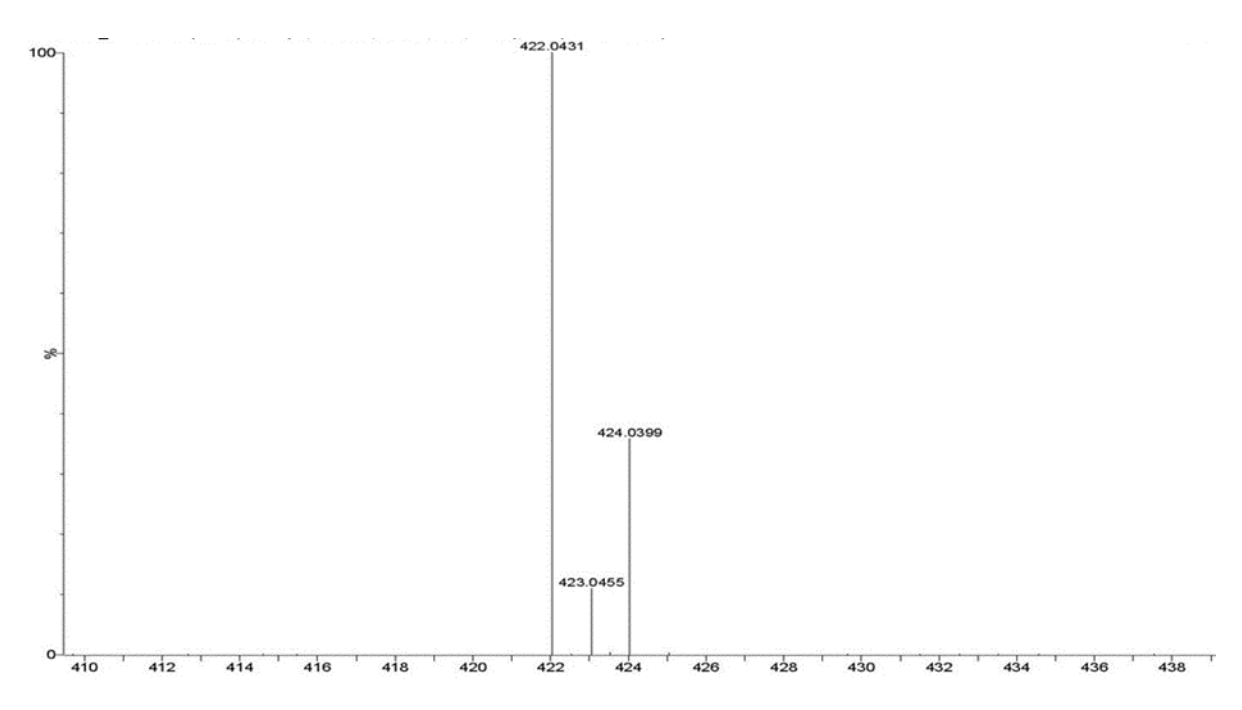


Fig. A27: HRMS of compound UHLMTJ-257c

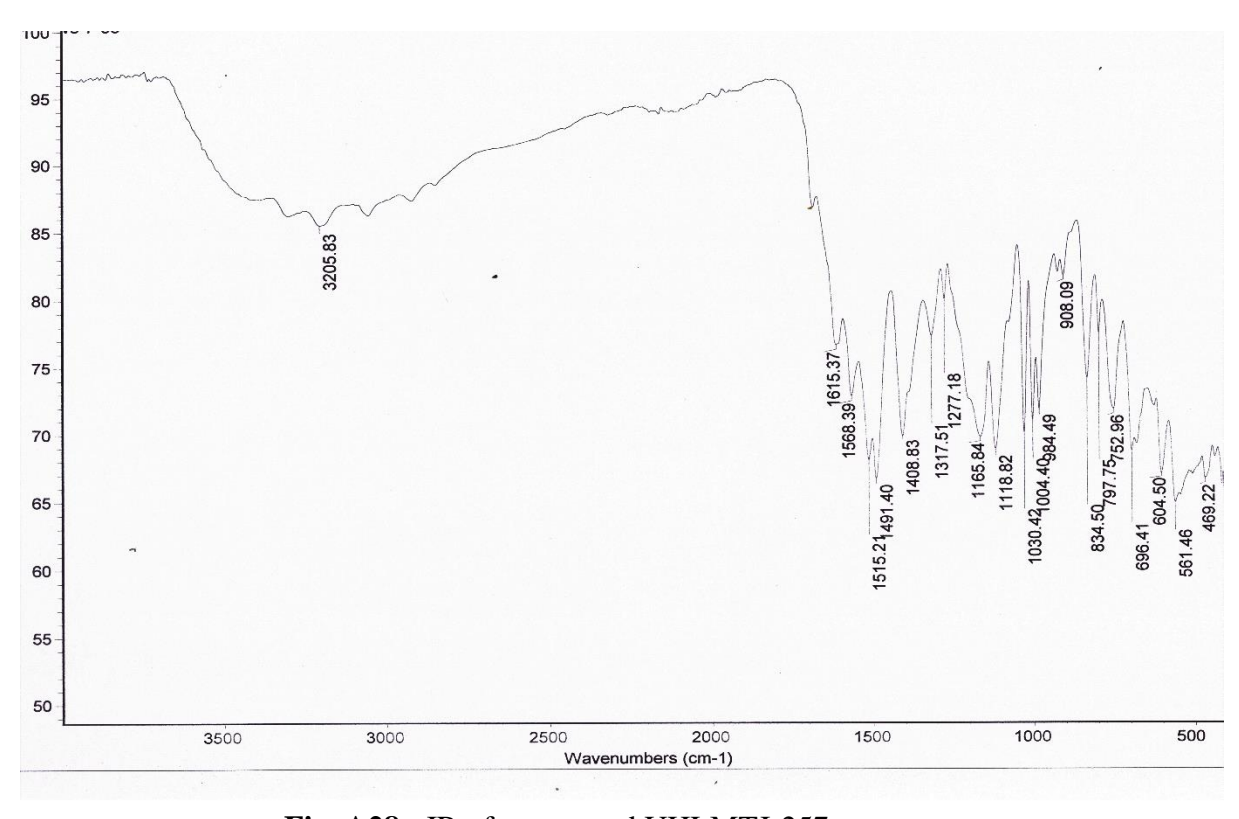


Fig. A28: IR of compound UHLMTJ-257c

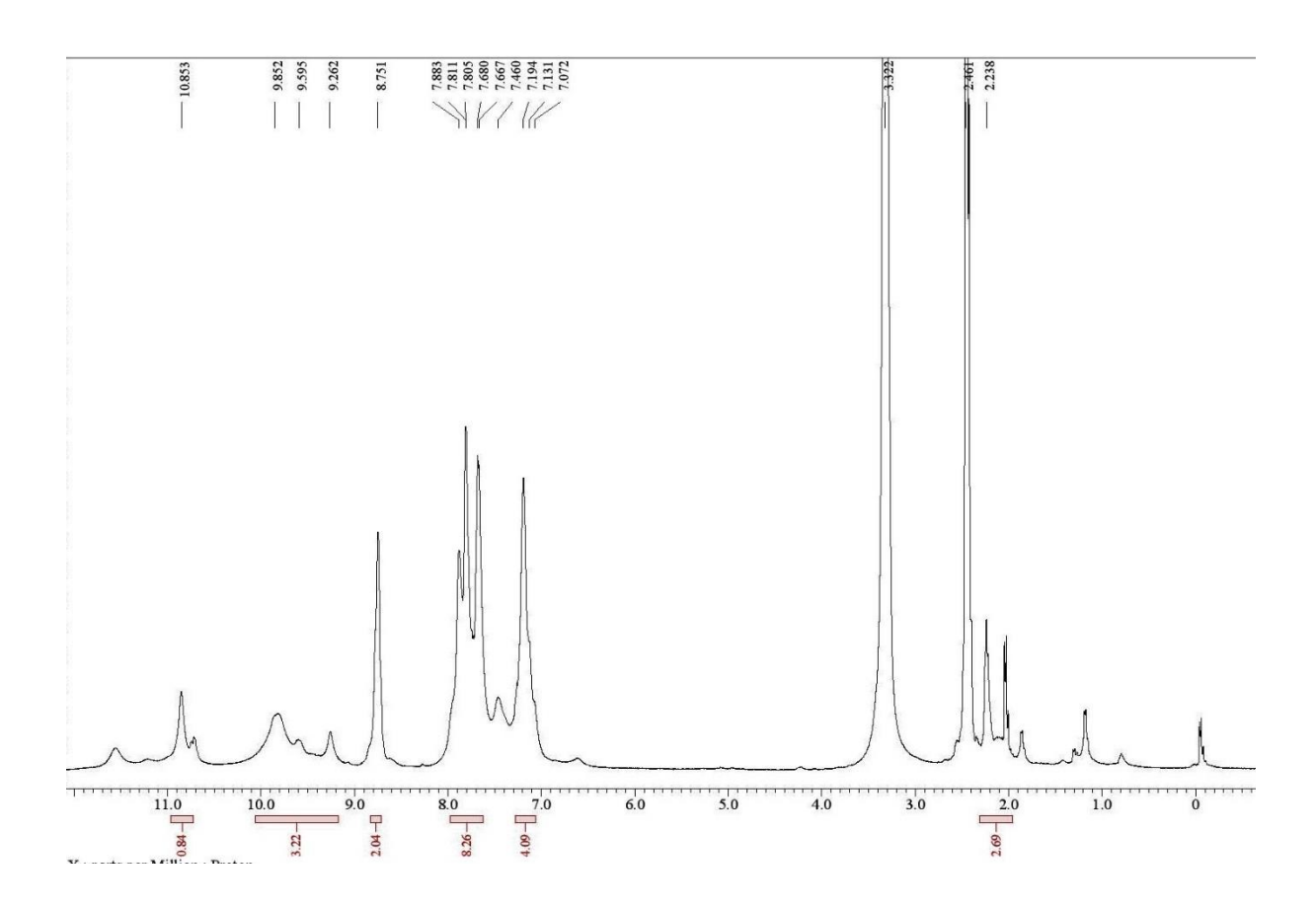


Fig. A29: ¹H NMR spectrum of compound UHLMTJ-258a

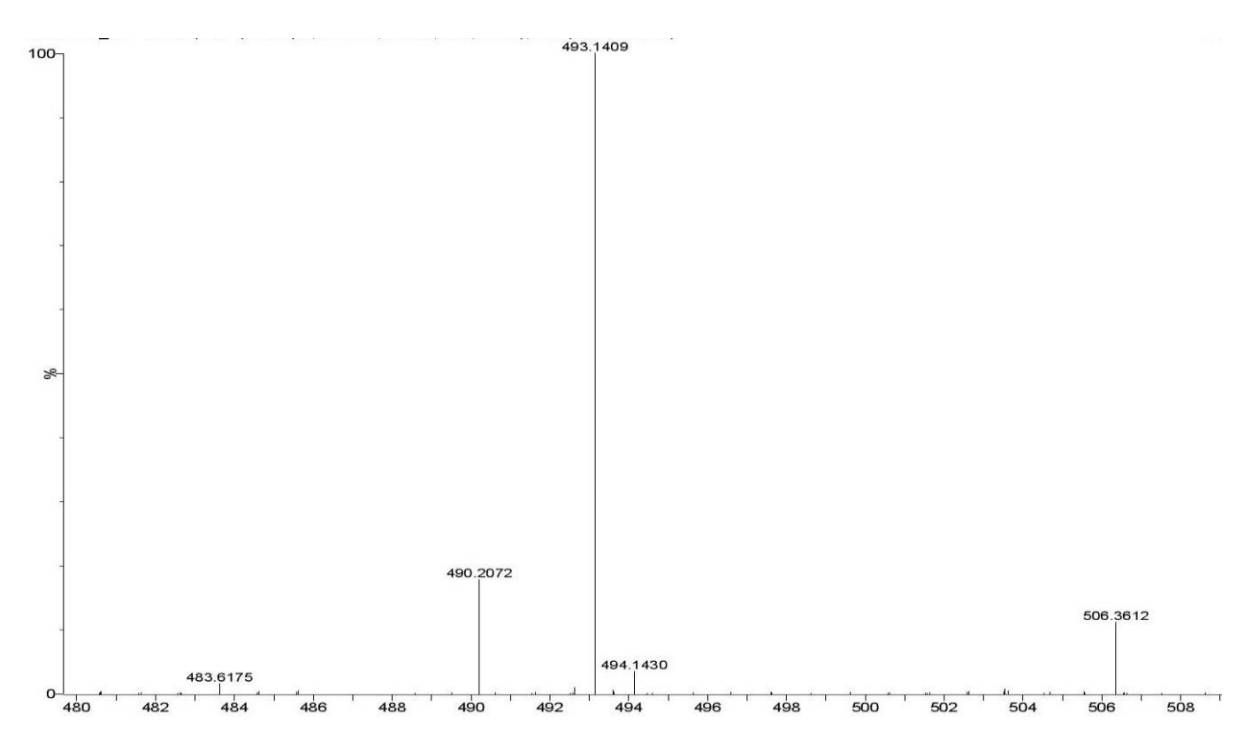


Fig. A30: HRMS of compound UHLMTJ-258a

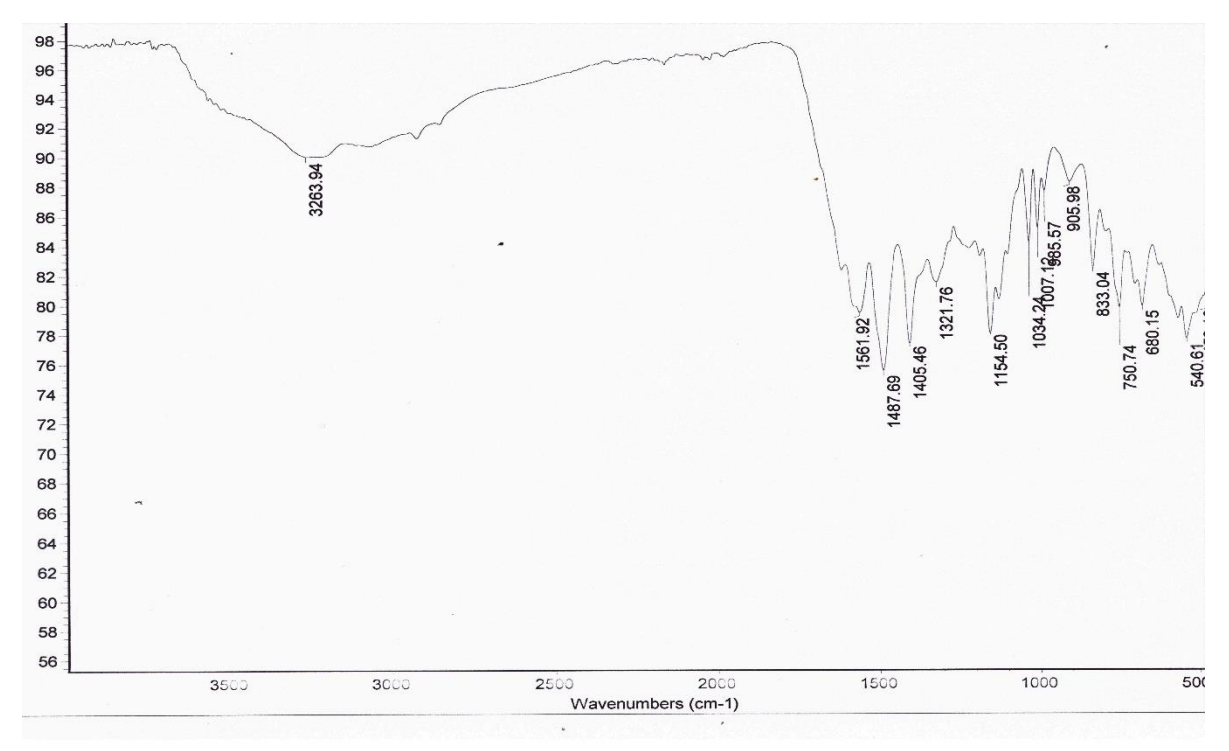


Fig. A31: IR of compound UHLMTJ-258a

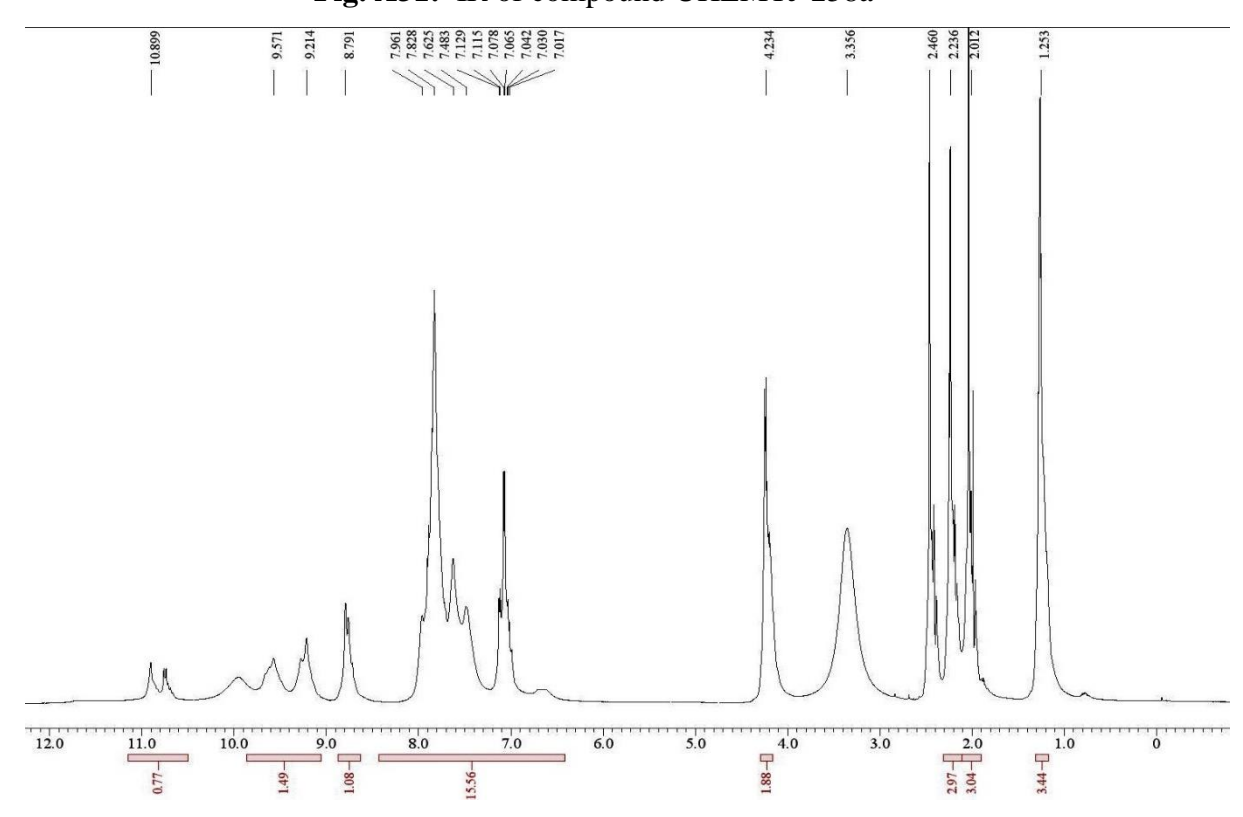


Fig. A32: ¹H NMR spectrum of compound UHLMTJ-258b

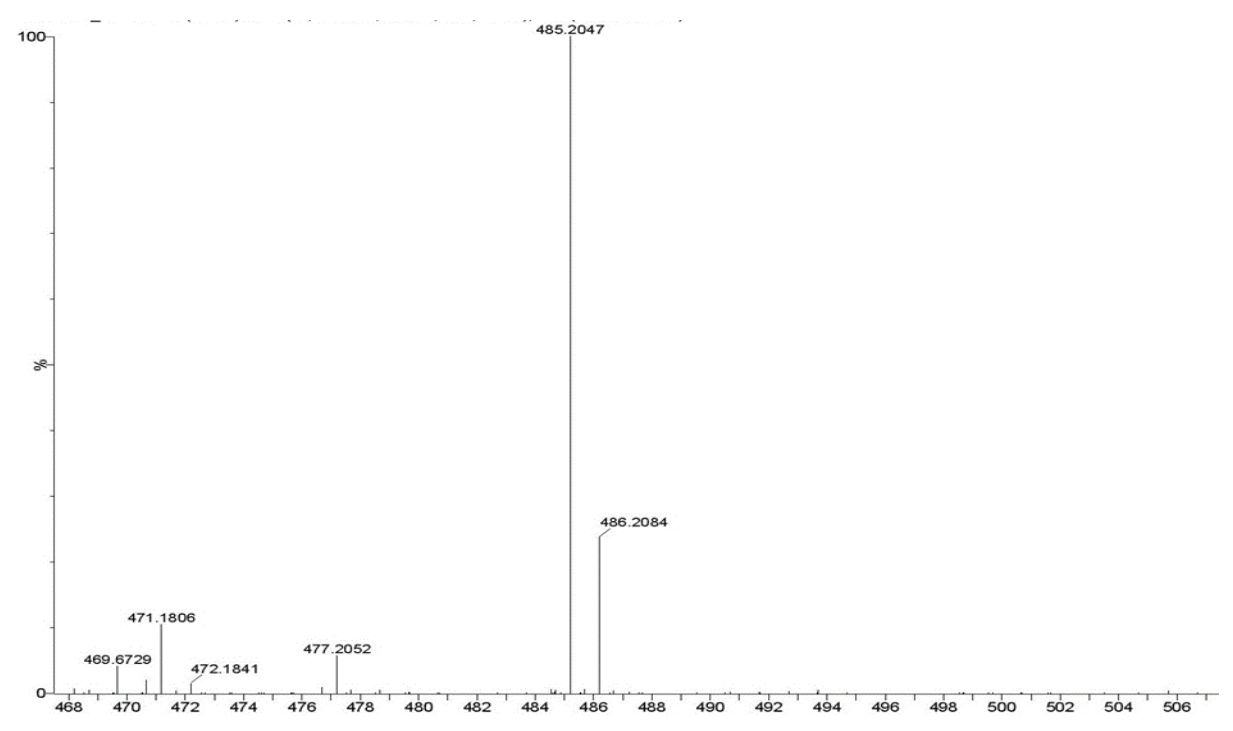


Fig. A33: HRMS spectrum of compound UHLMTJ-258b

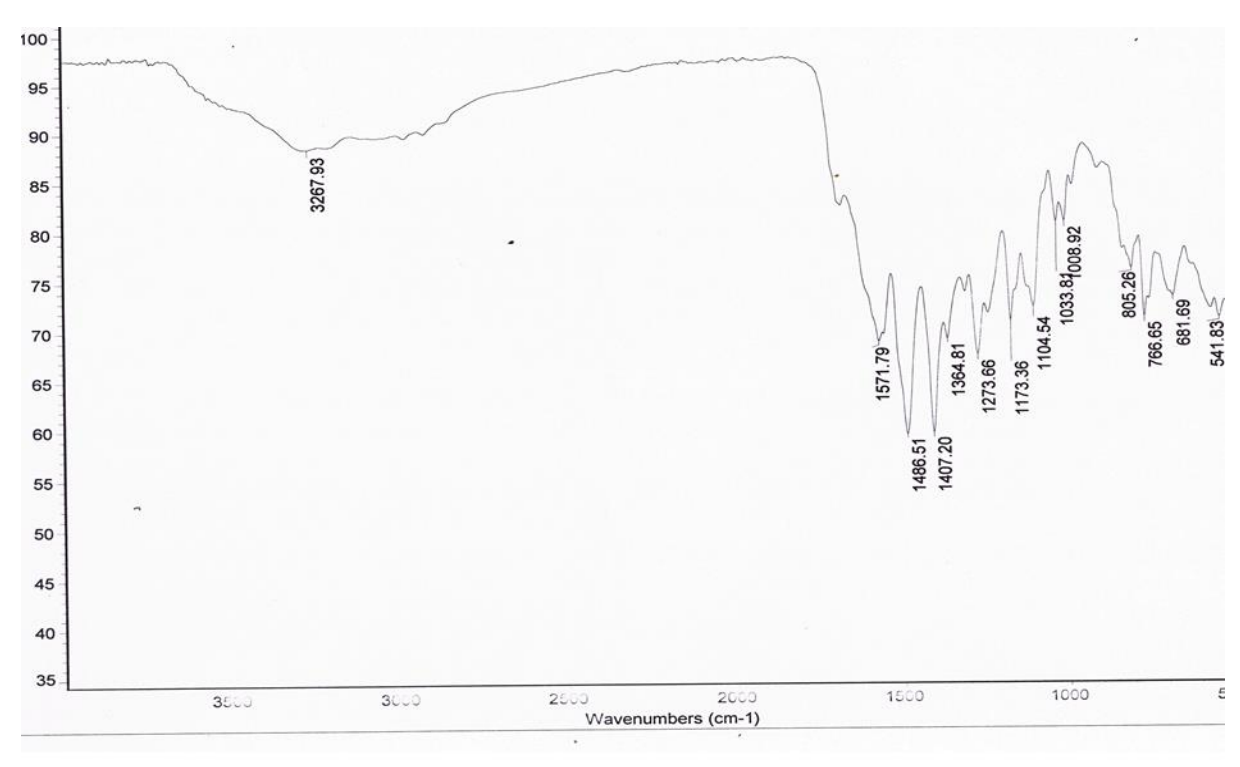


Fig. A34: IR spectrum of compound UHLMTJ-258b

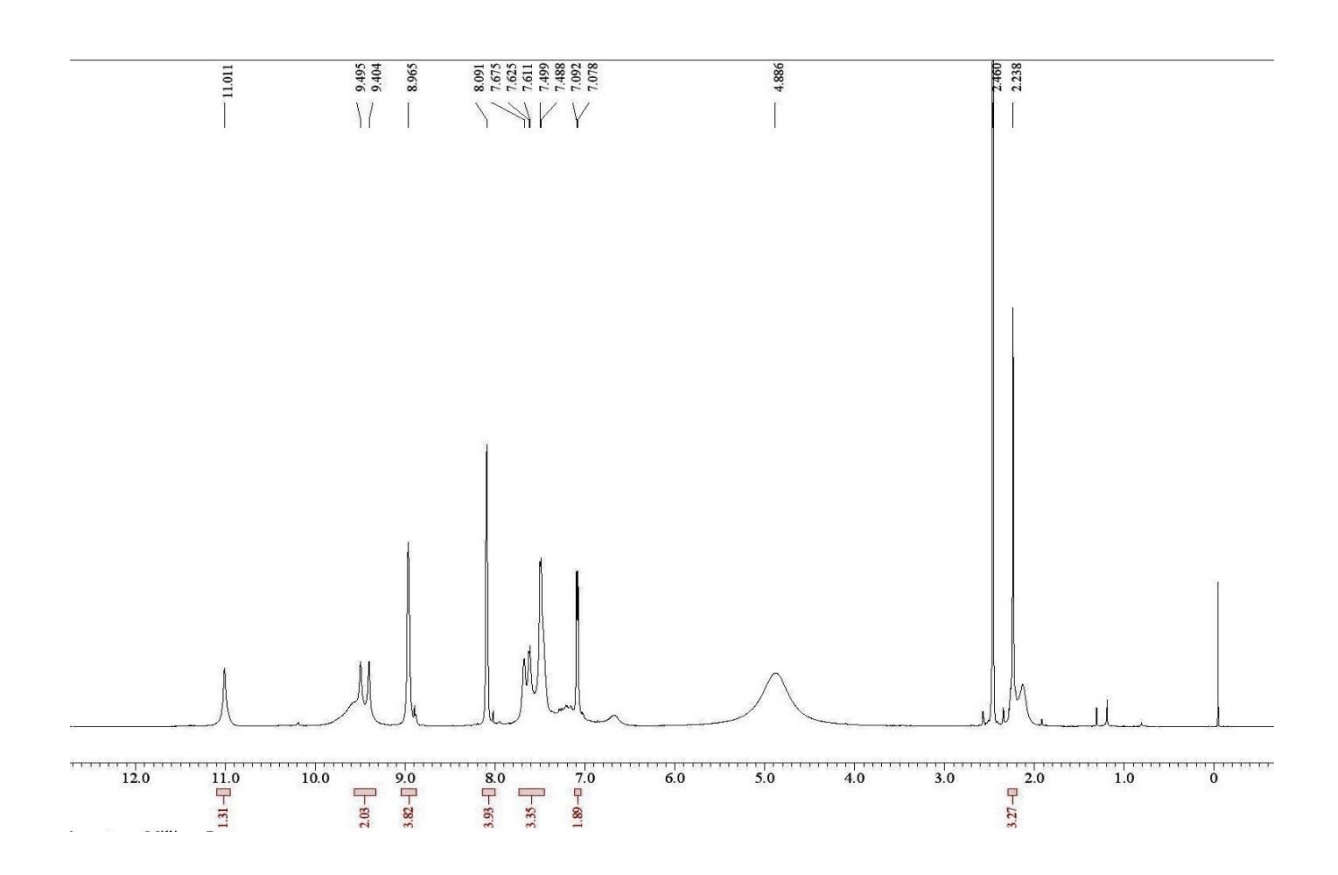


Fig A35: ¹H NMR spectrum of compound UHLMTJ-258c

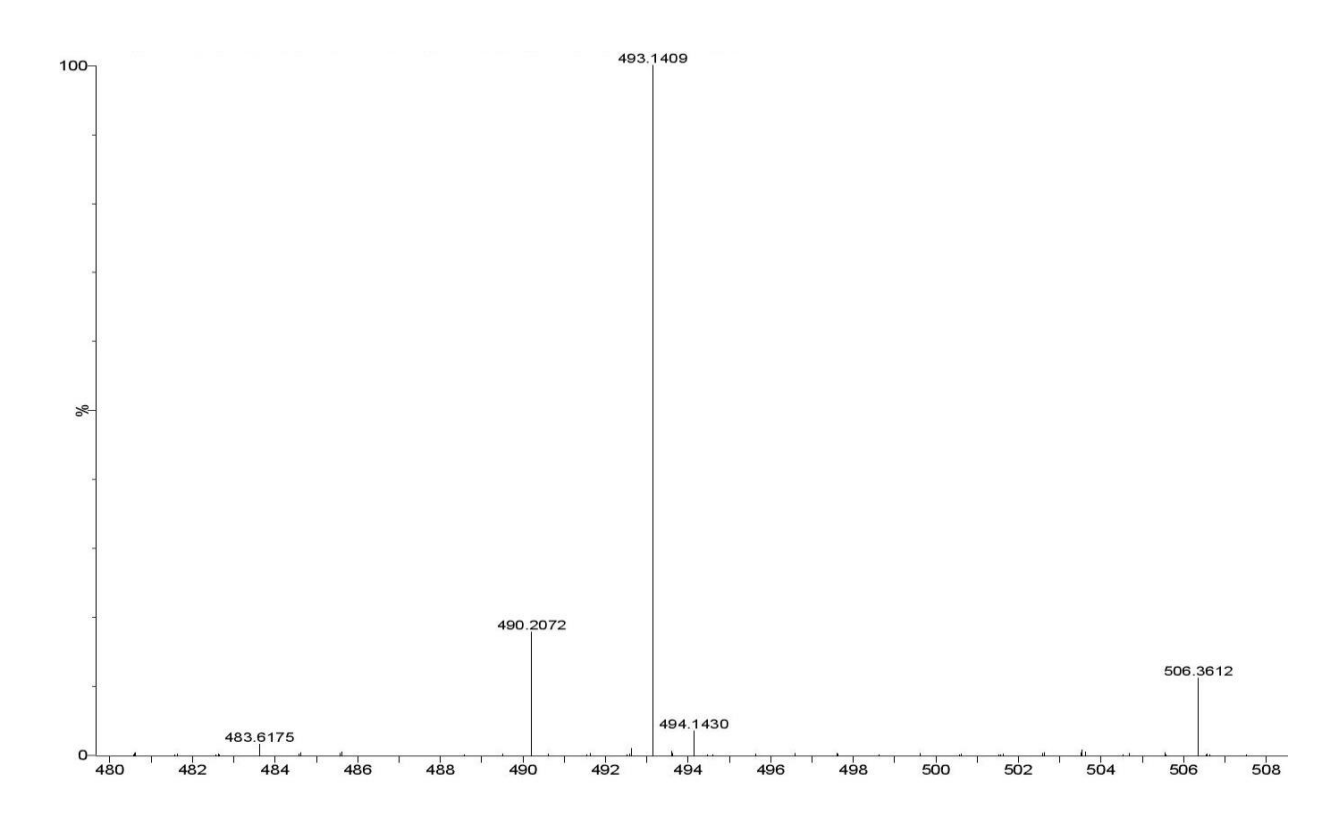


Fig. A36: HRMS of compound UHLMTJ-258c

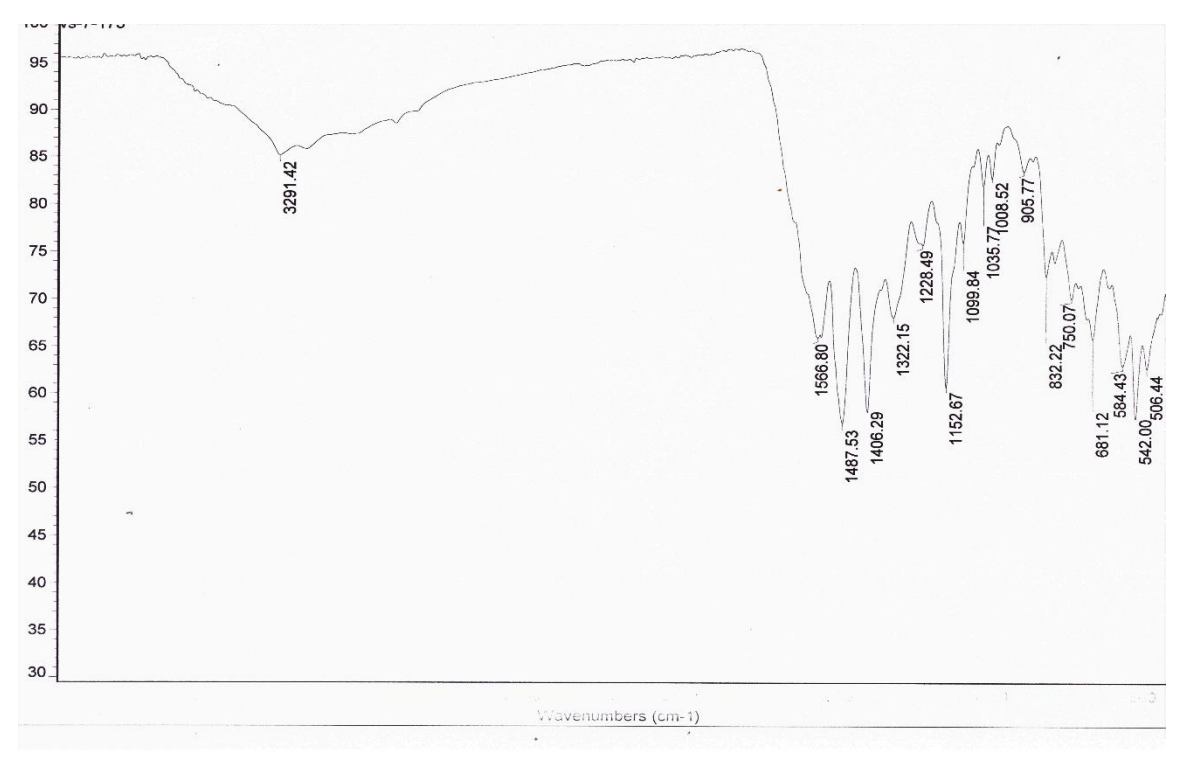


Fig A37: IR spectrum of compound UHLMTJ-258c

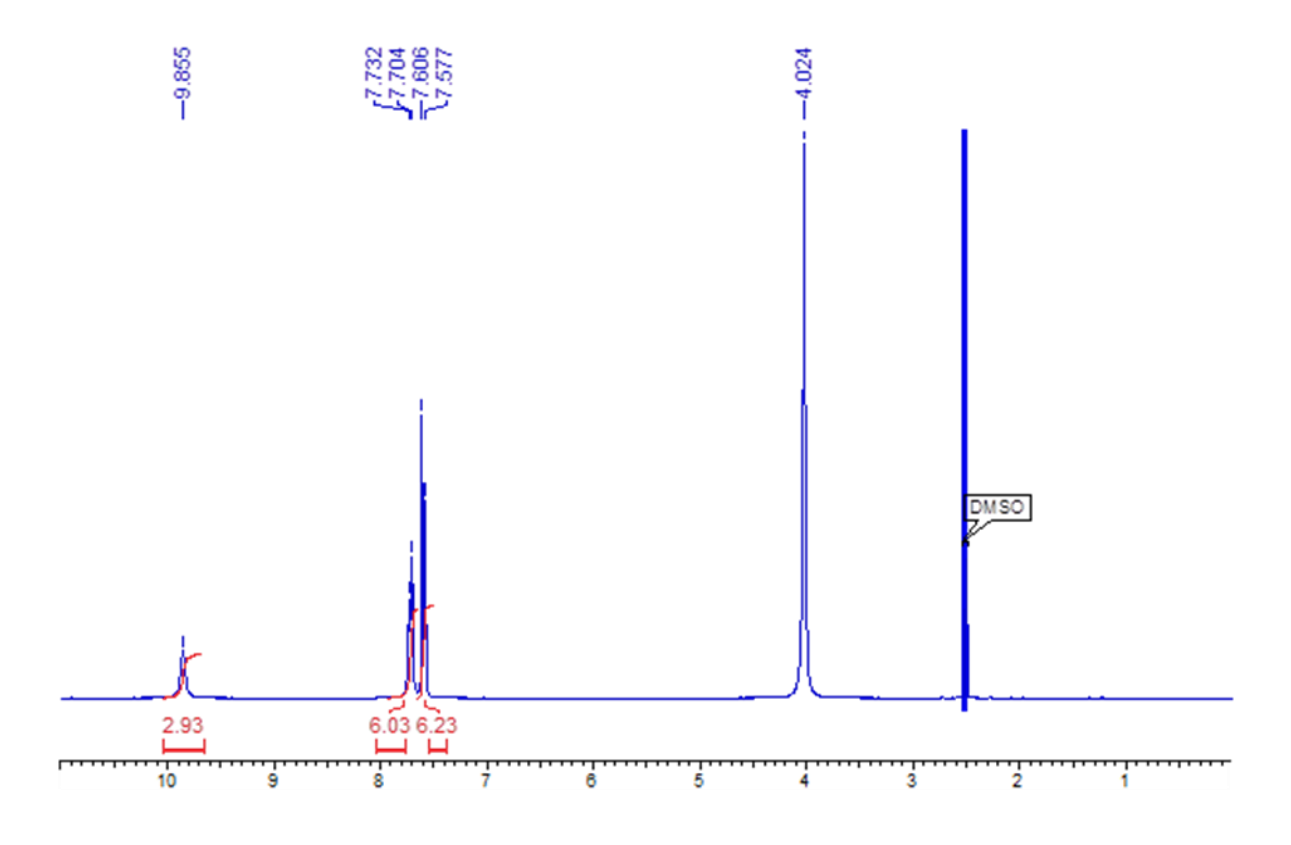


Fig. A38: ¹H NMR spectrum of compound UHLMTJ-259

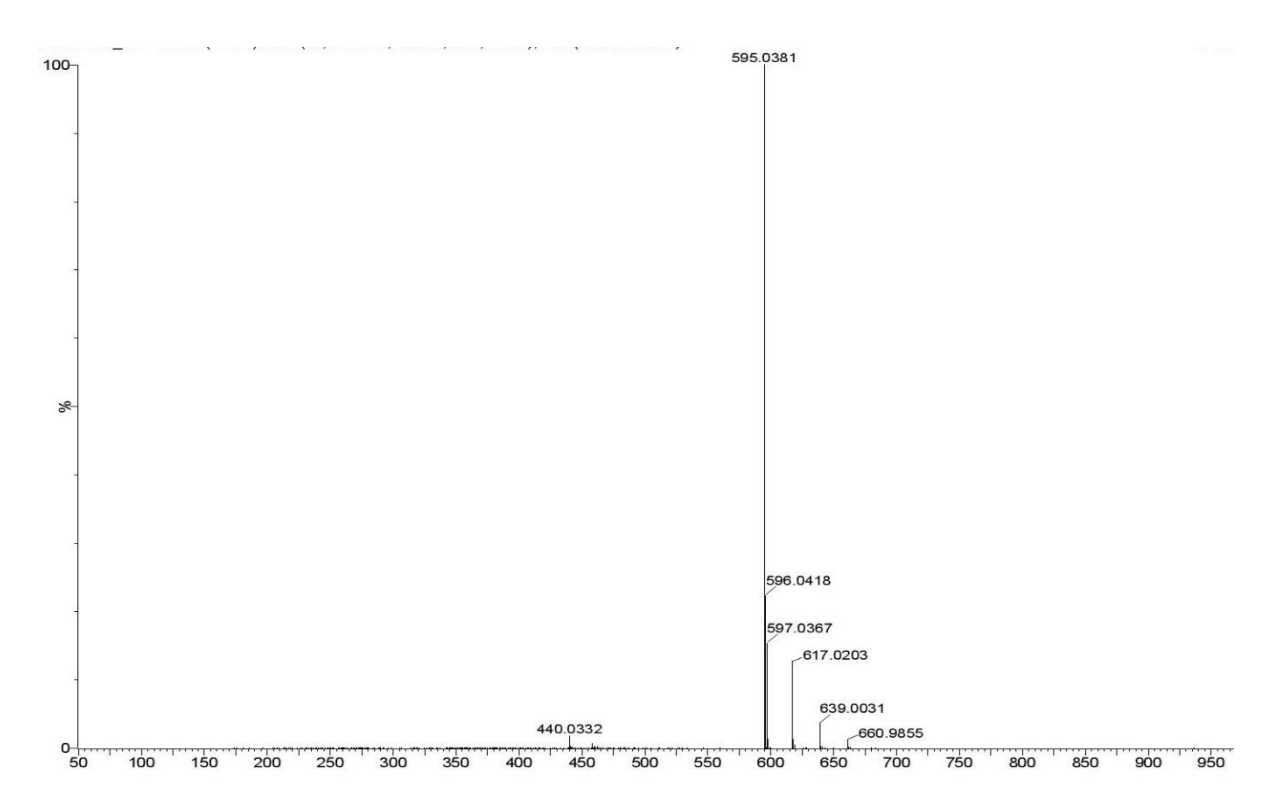


Fig. A39: HRMS of compound UHLMTJ-259

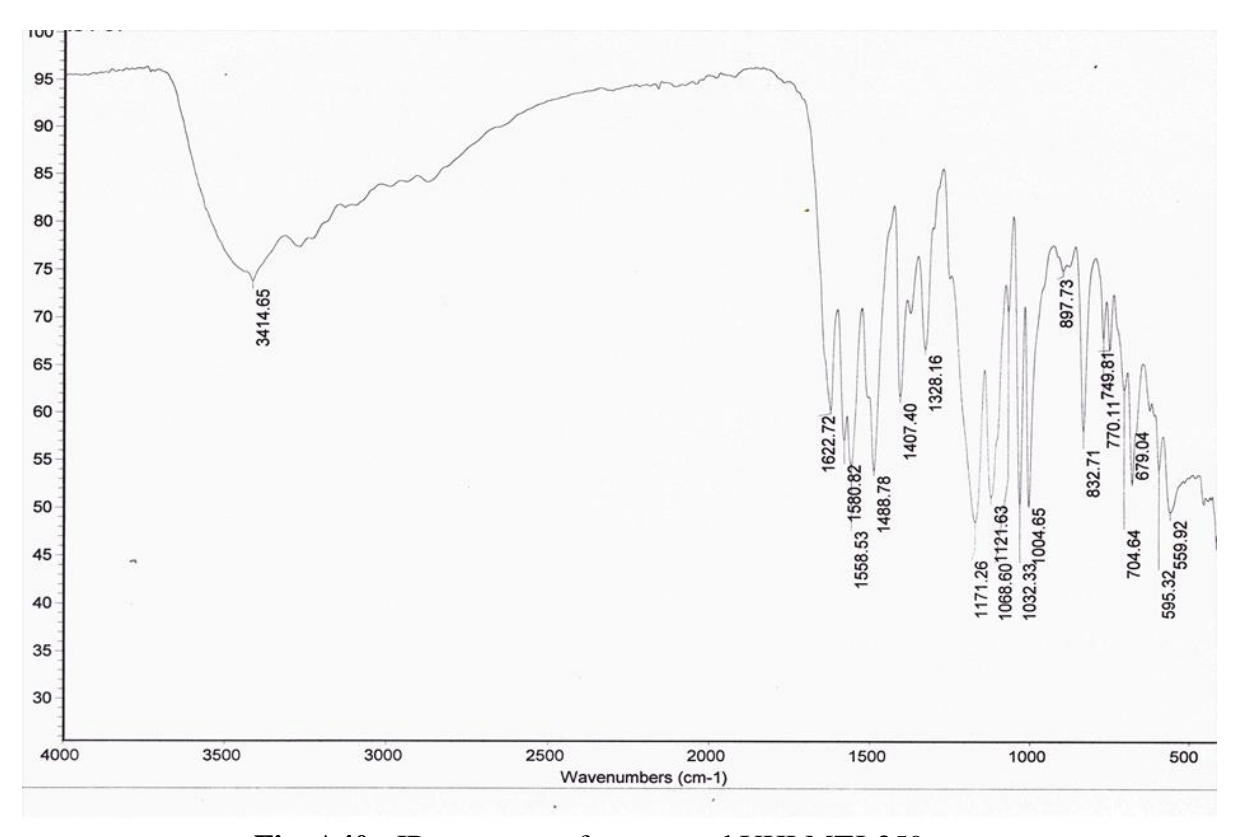


Fig. A40: IR spectrum of compound UHLMTJ-259

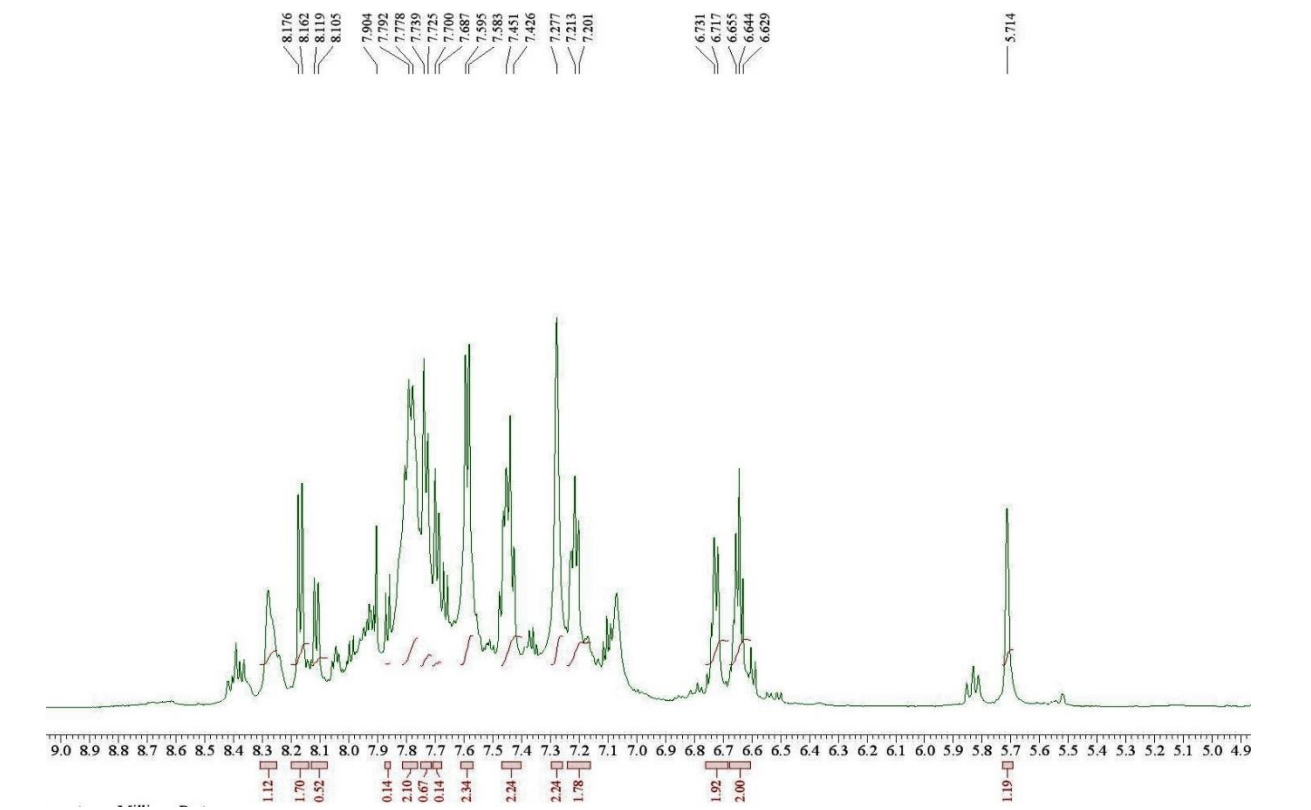


Fig. A41: ¹H NMR spectrum of compound UHLMTJ-260a

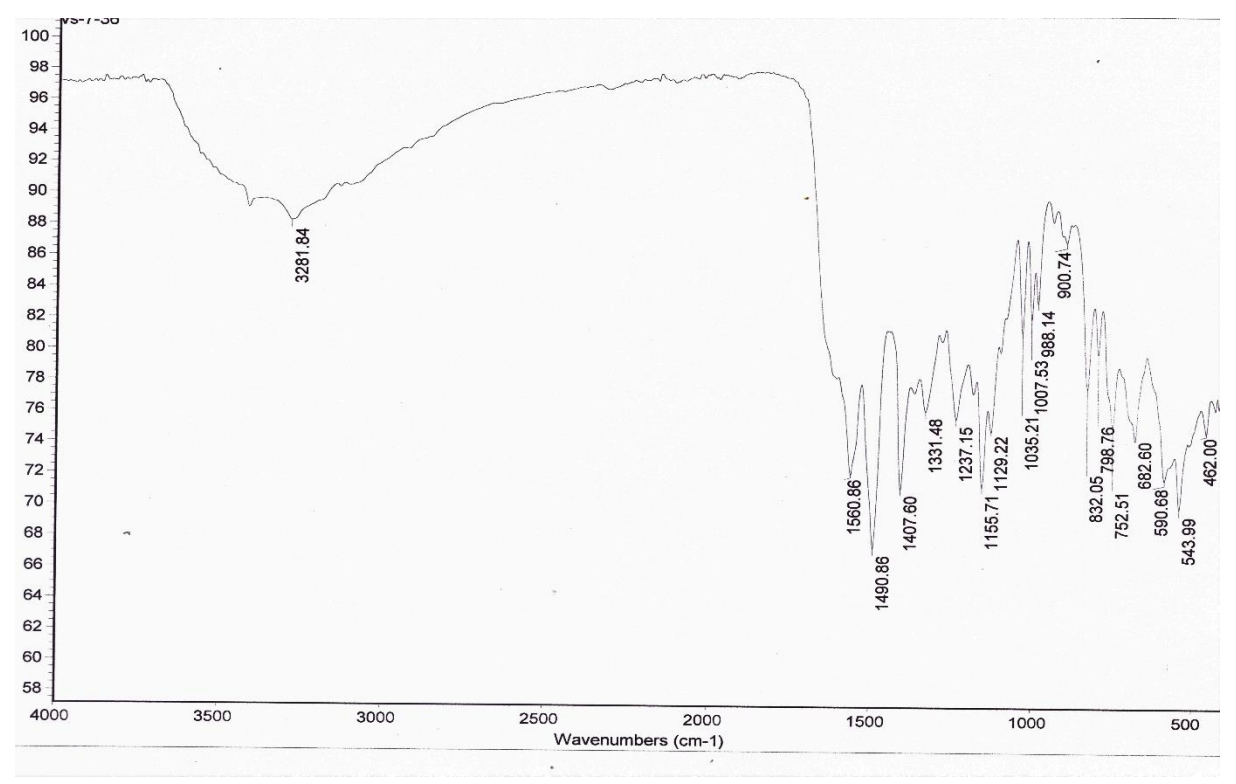


Fig. A42: IR spectrum of compound UHLMTJ-260a

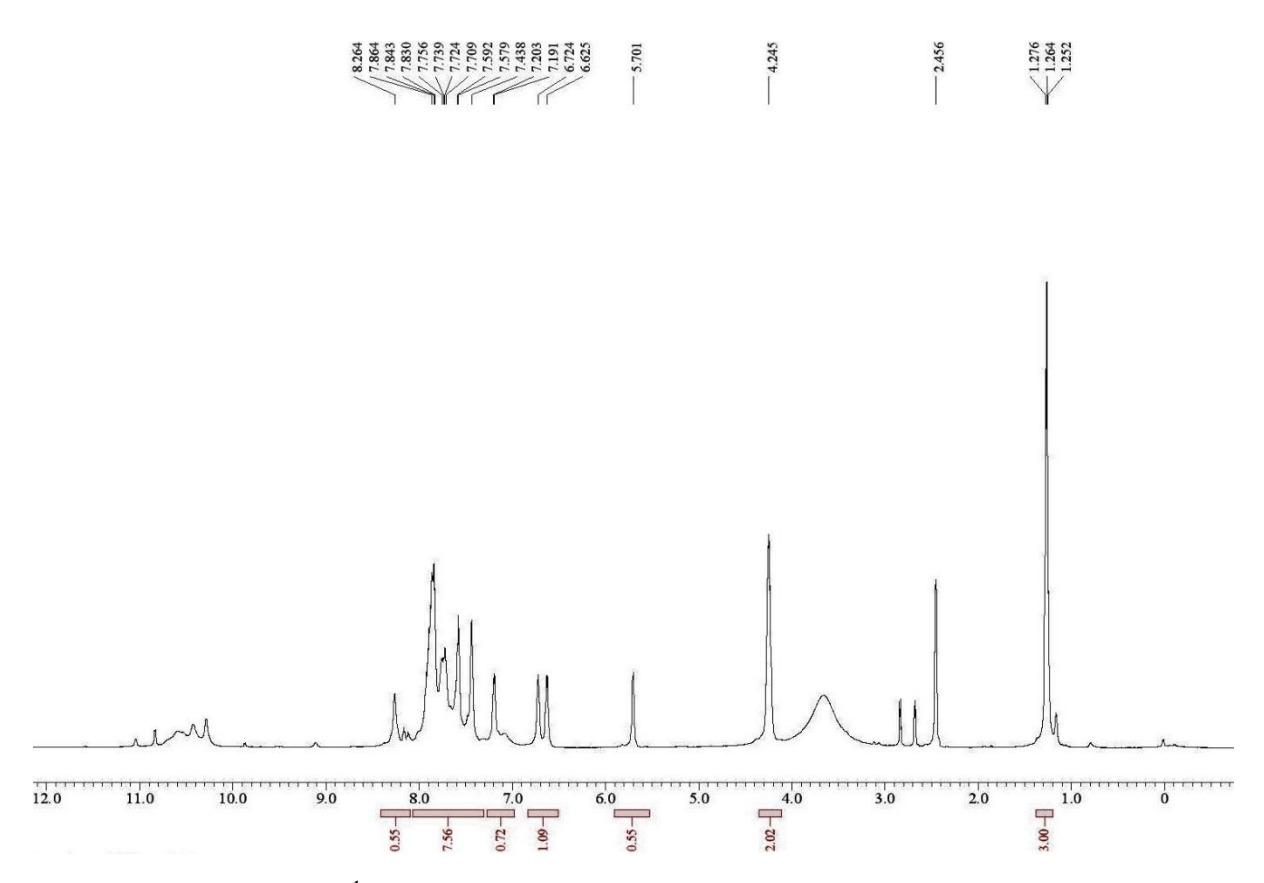


Fig. A43: ¹H NMR spectrum of compound UHLMTJ-260b

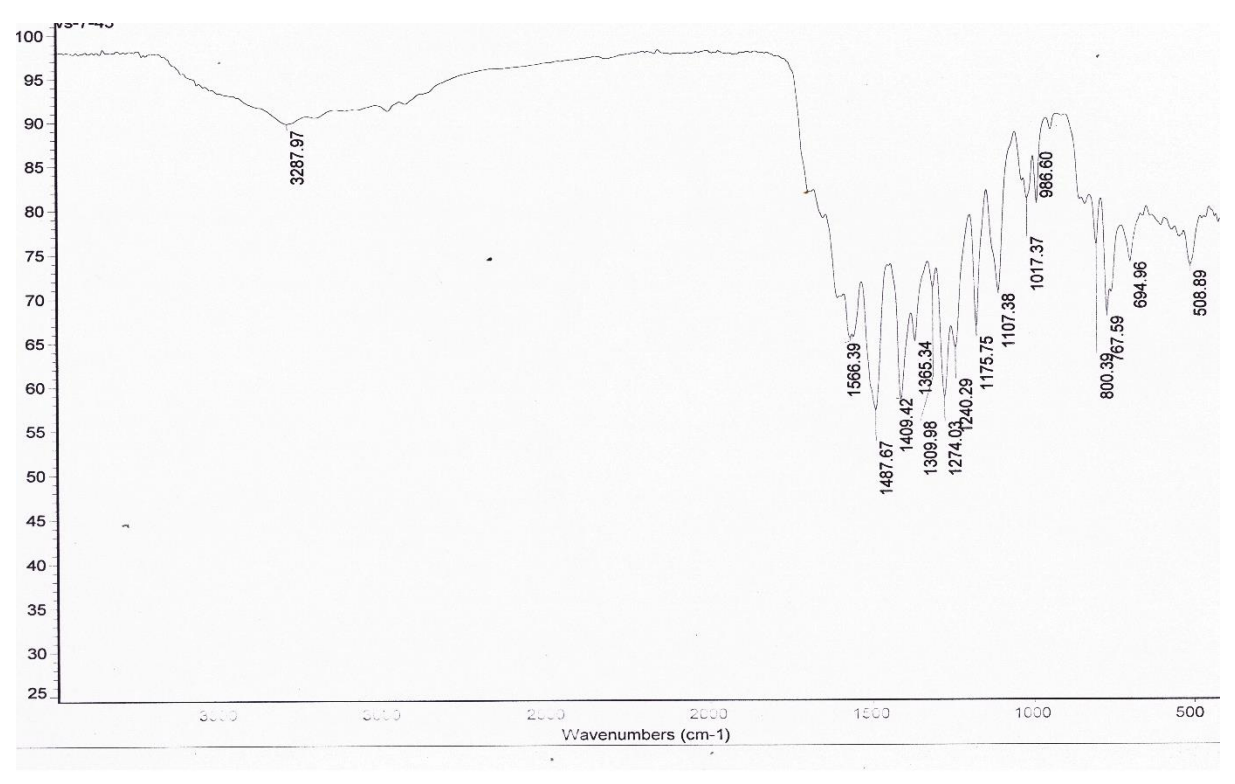
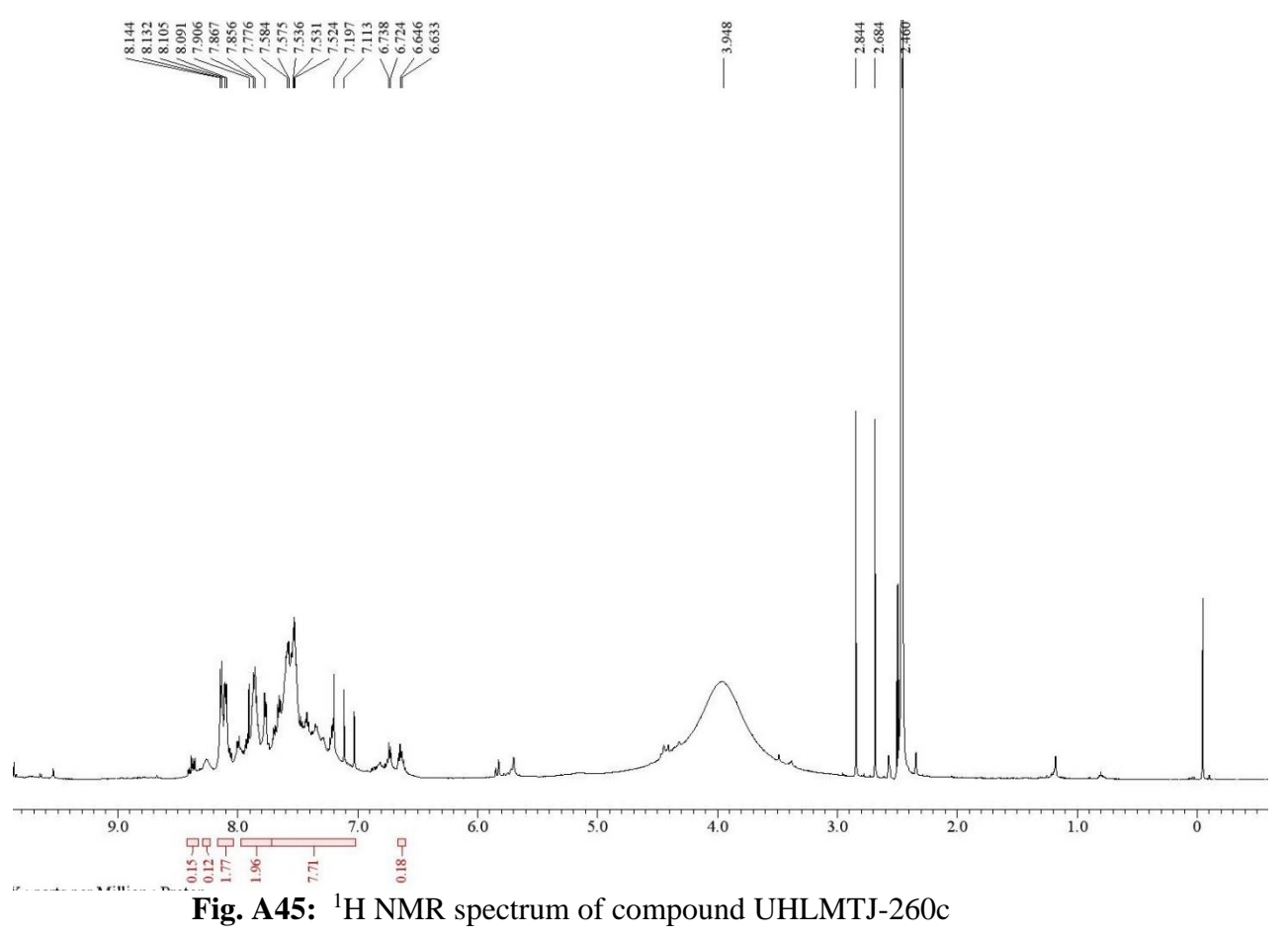


Fig. A44: IR spectrum of compound UHLMTJ-260b



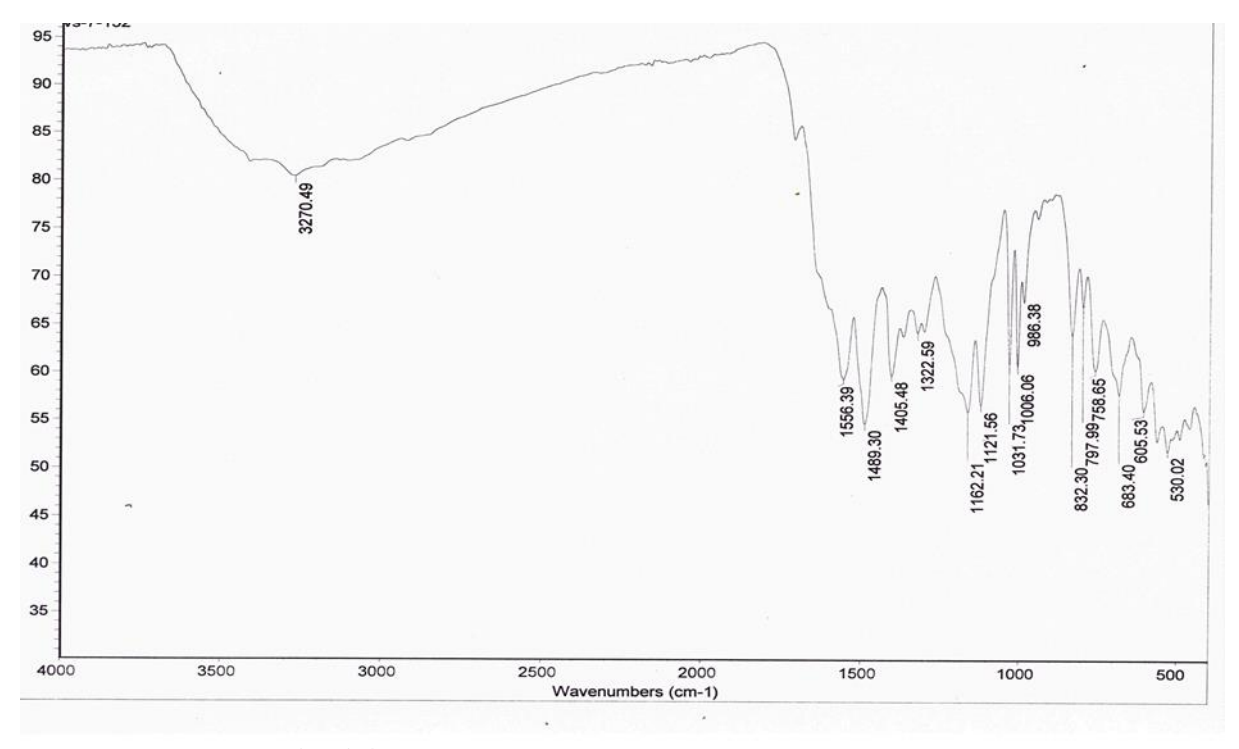


Fig. A46: IR spectrum of compound UHLMTJ-260c

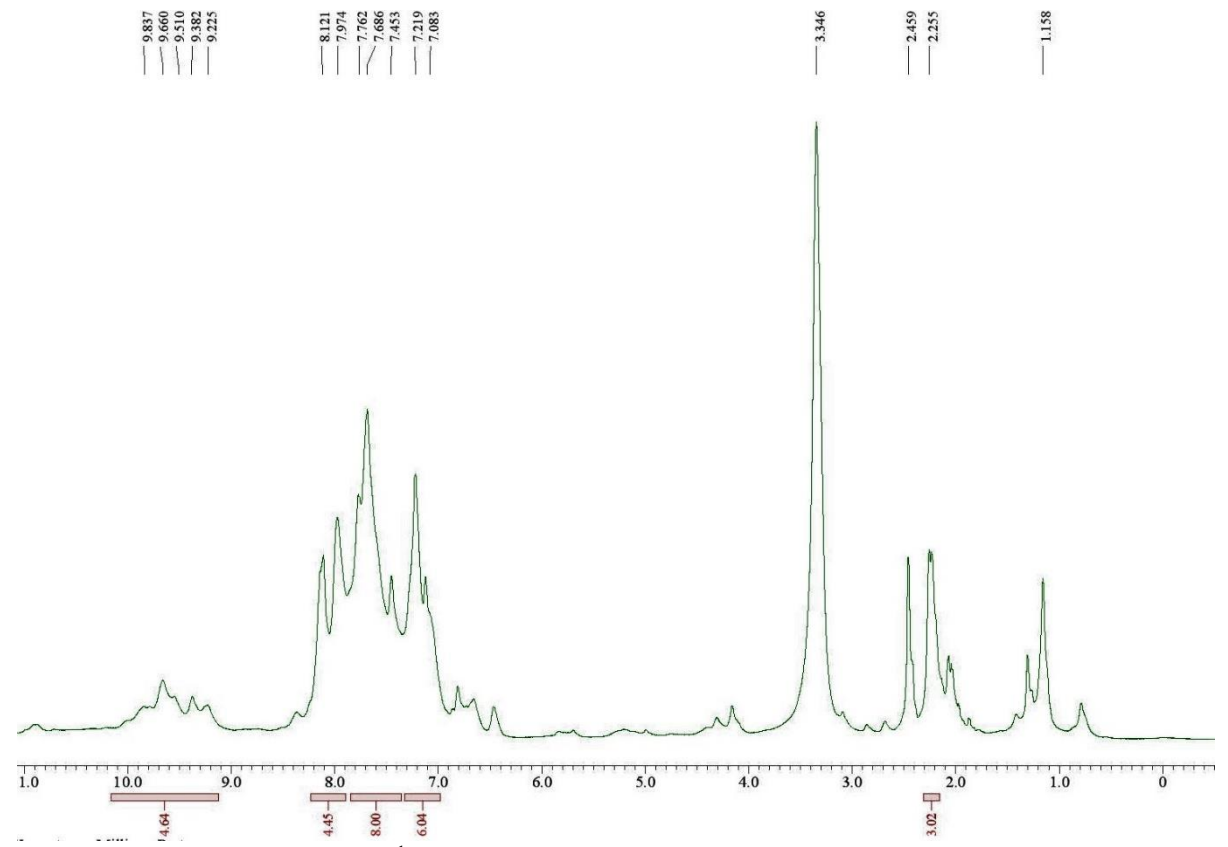


Fig. A47: ¹H NMR spectrum of compound UHLMTJ-261a

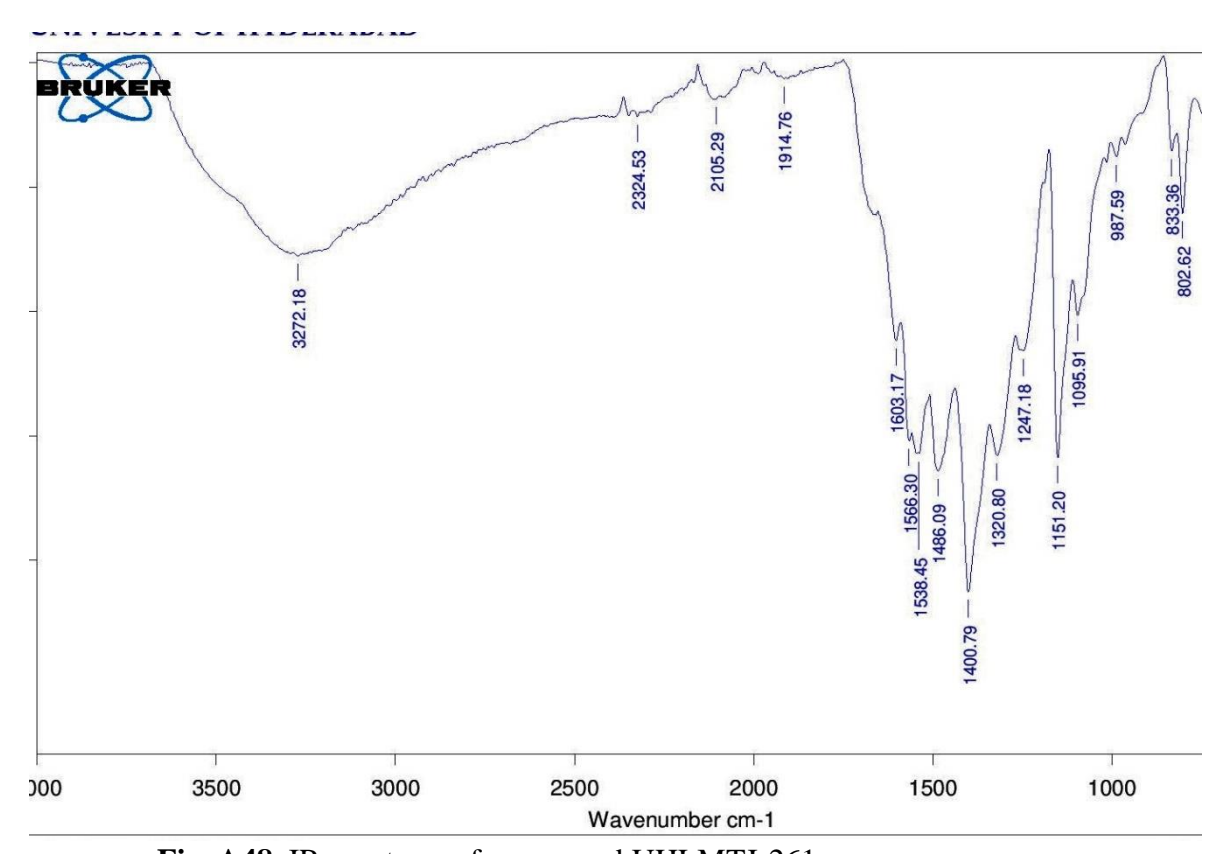


Fig. A48: IR spectrum of compound UHLMTJ-261a

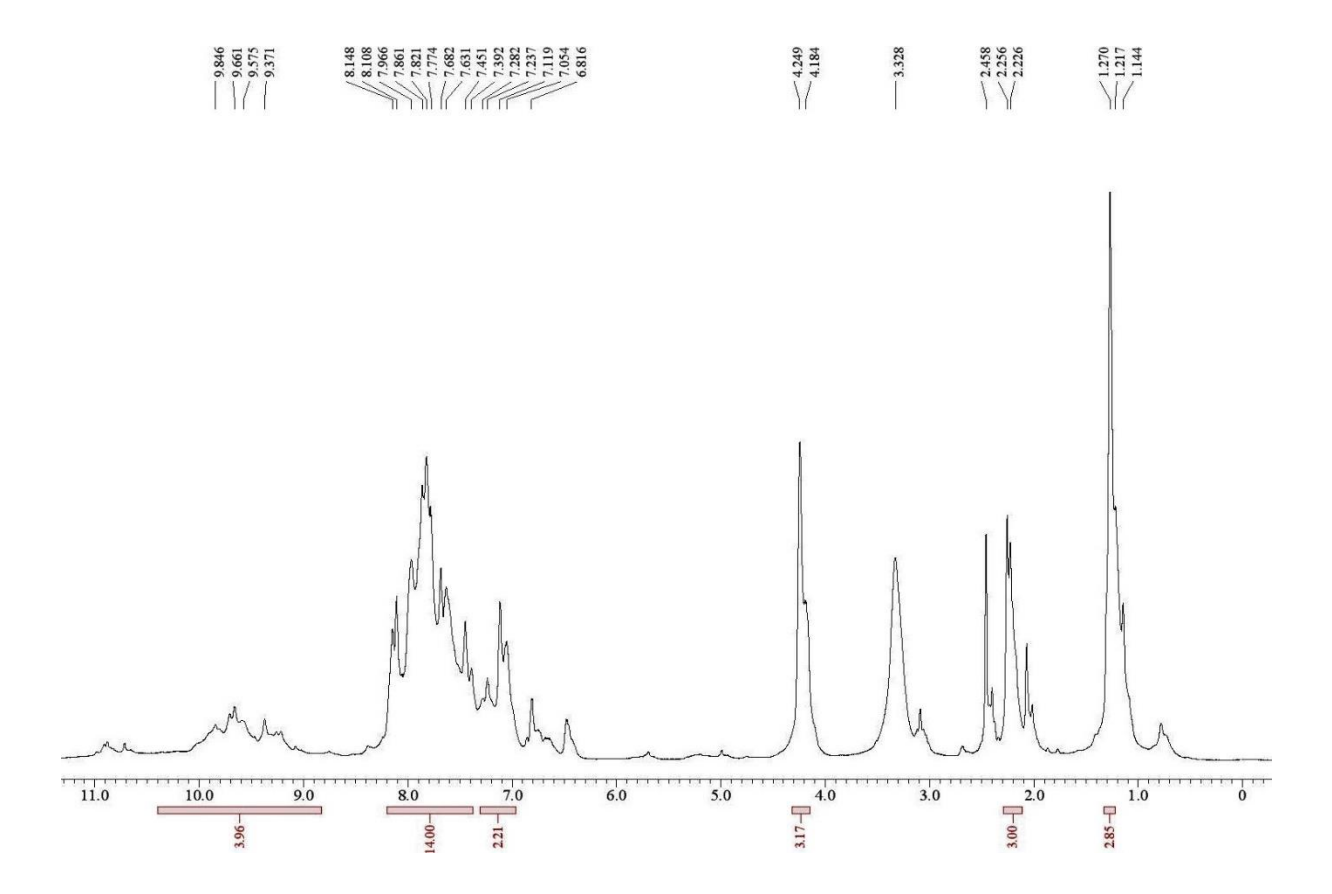


Fig. A49: ¹H NMR spectrum of compound UHLMTJ-261b

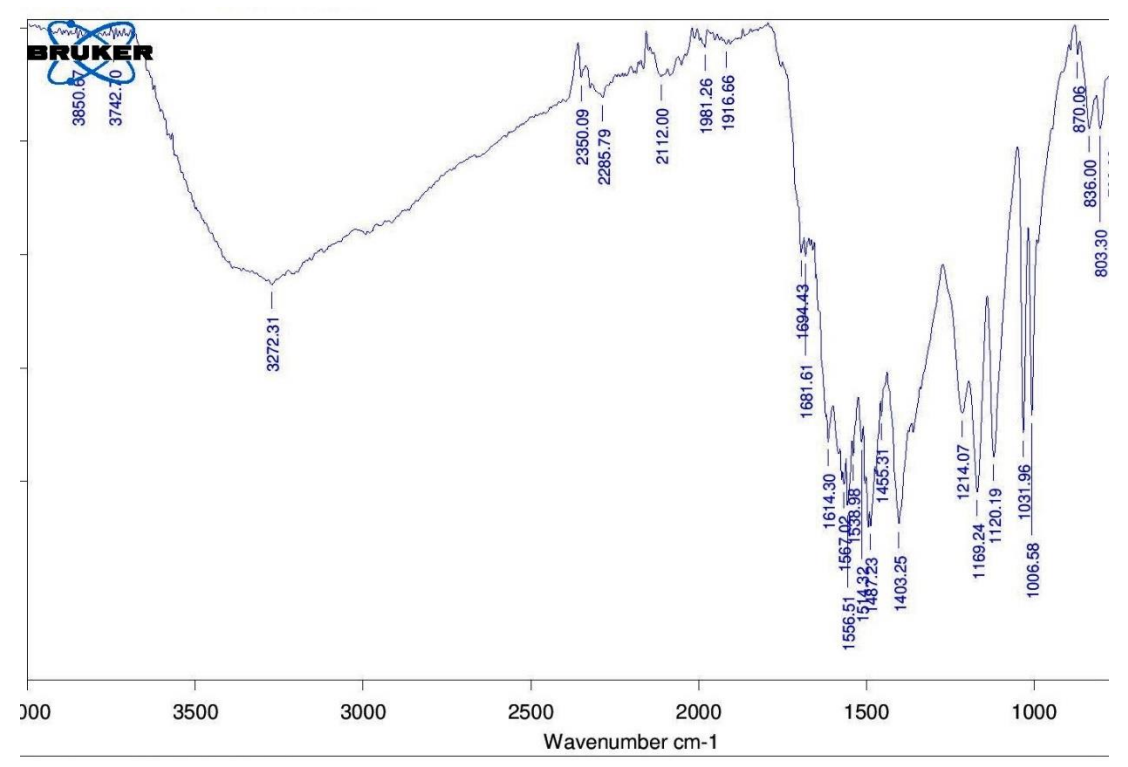


Fig. A50: IR spectrum of compound UHLMTJ-261b

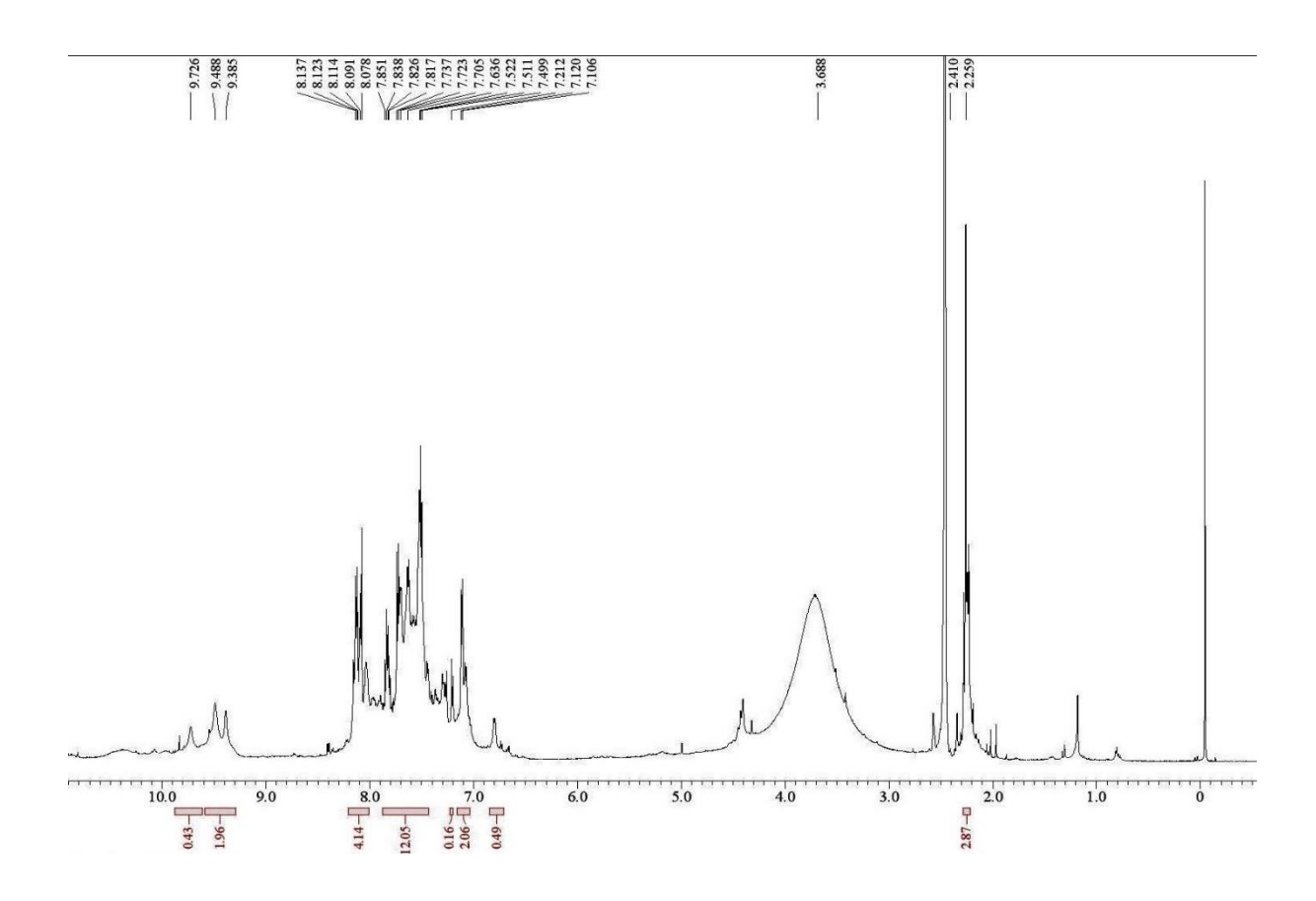


Fig A51: ¹H NMR spectrum of compound UHLMTJ-261c

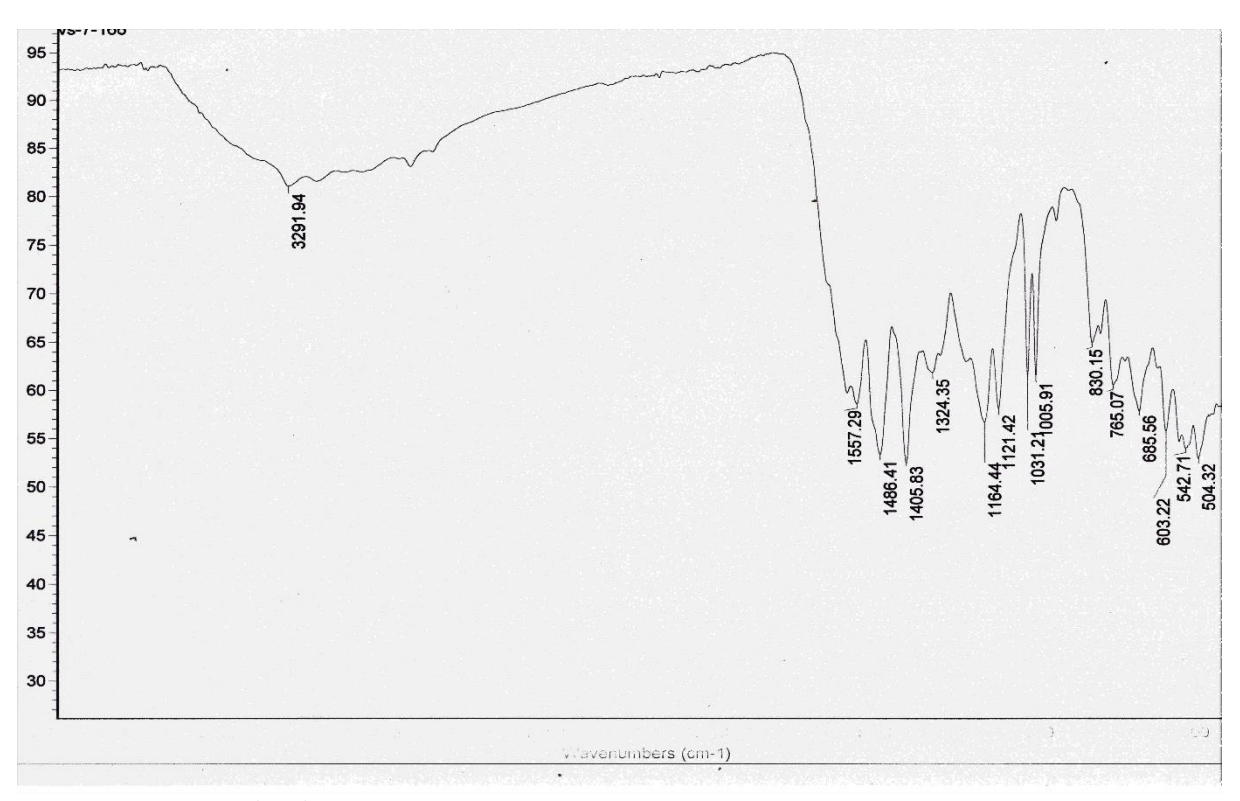


Fig. A52: IR spectrum of compound UHLMTJ-261c

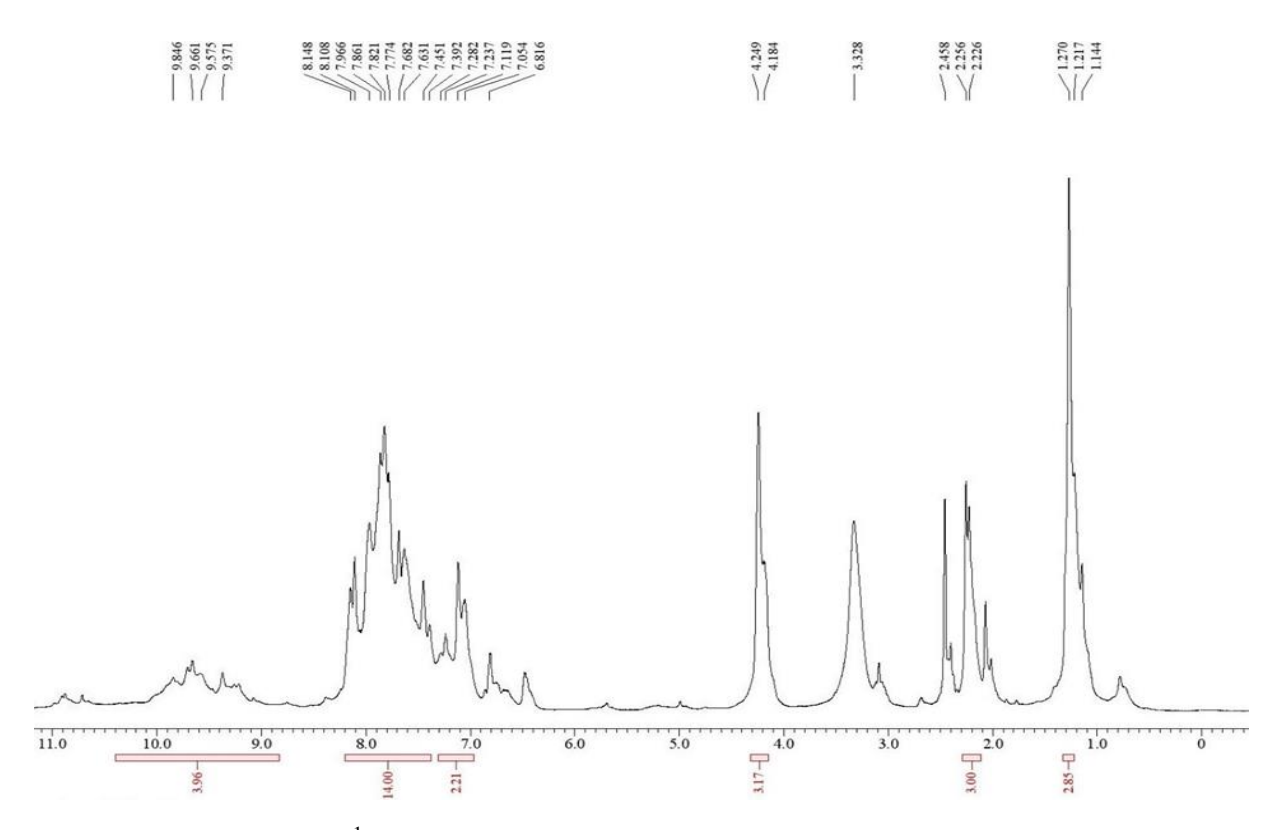


Fig A53: ¹H NMR spectrum of compound UHLMTJ-262a

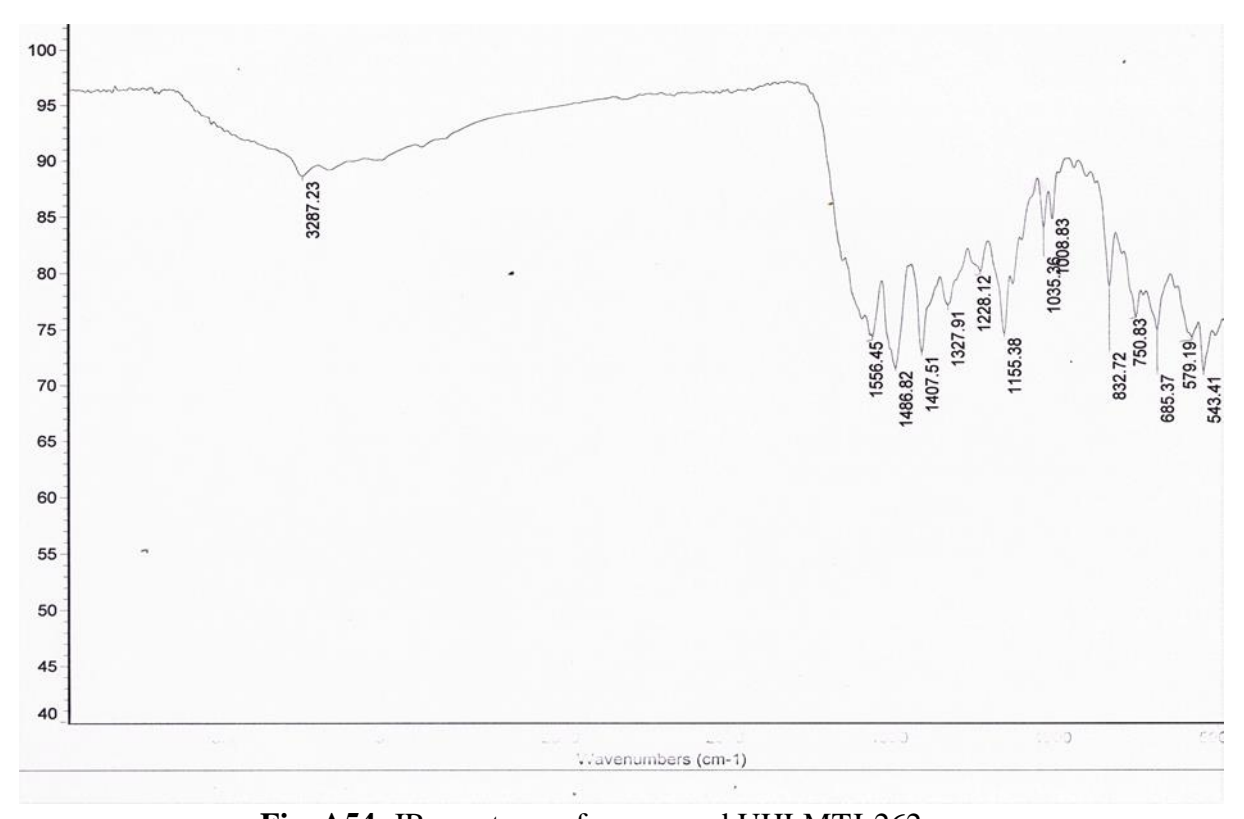


Fig. A54: IR spectrum of compound UHLMTJ-262a

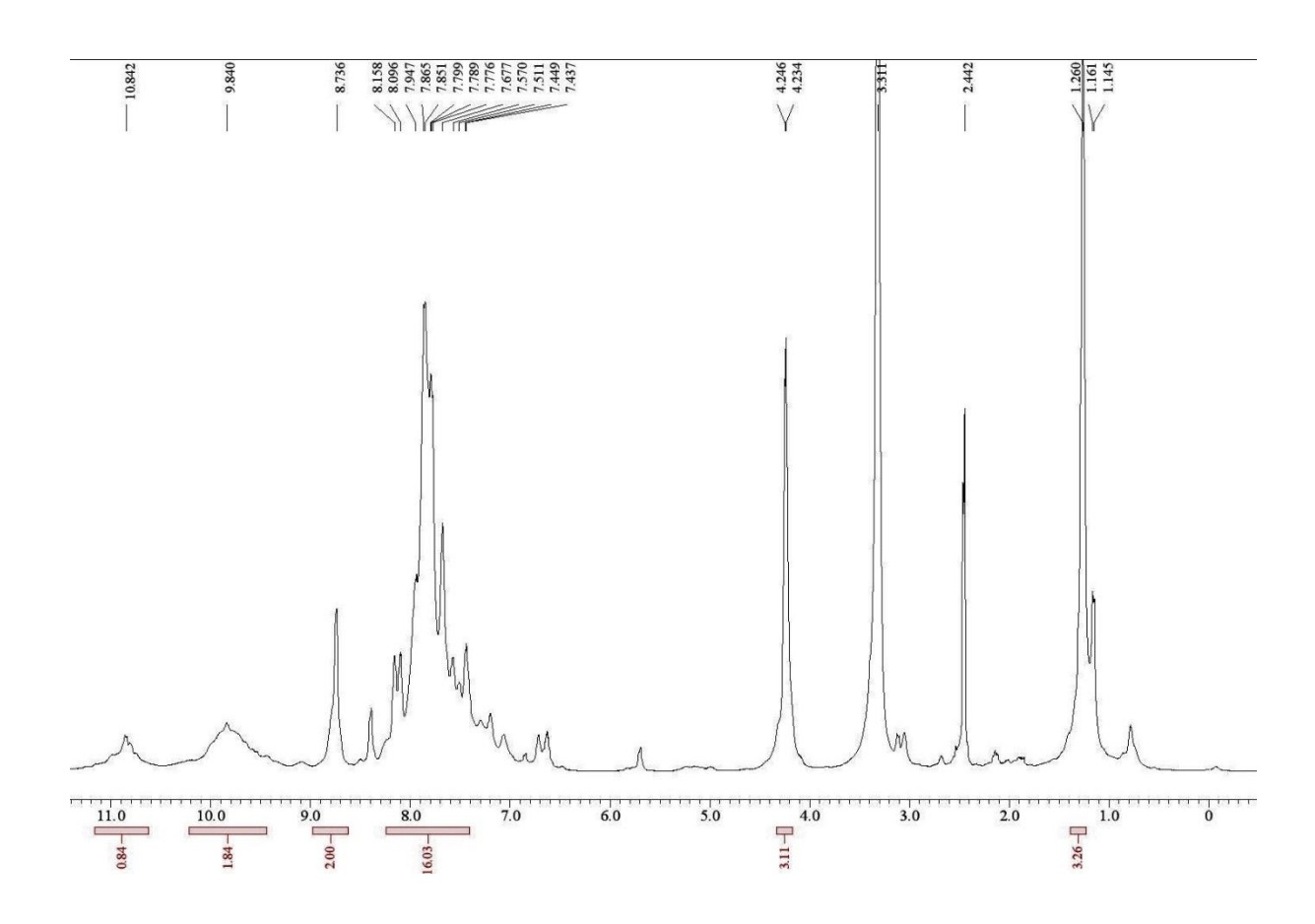


Fig. A55: ¹H NMR spectrum of compound UHLMTJ-262b

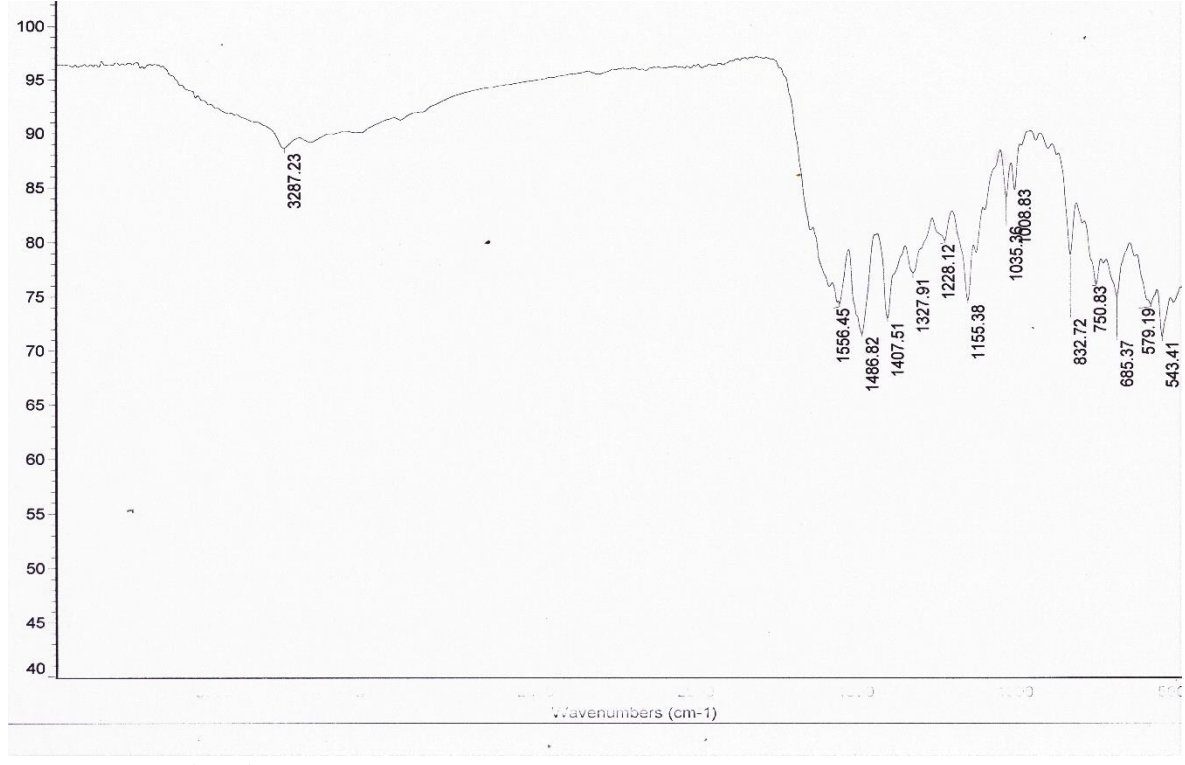


Fig. A56: IR spectrum of compound UHLMTJ-262b

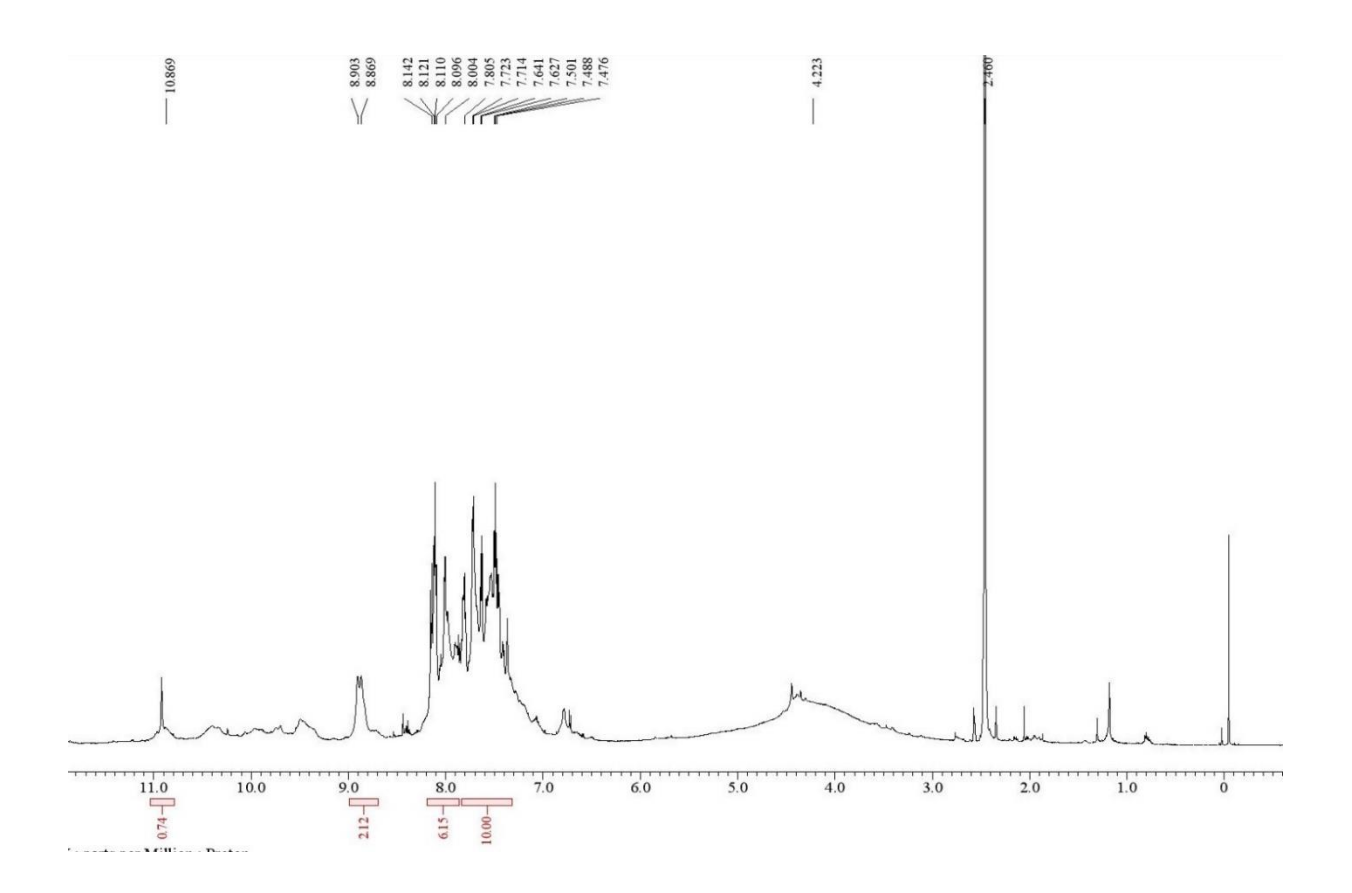


Fig. A57: ¹H NMR spectrum of compound UHLMTJ-262c

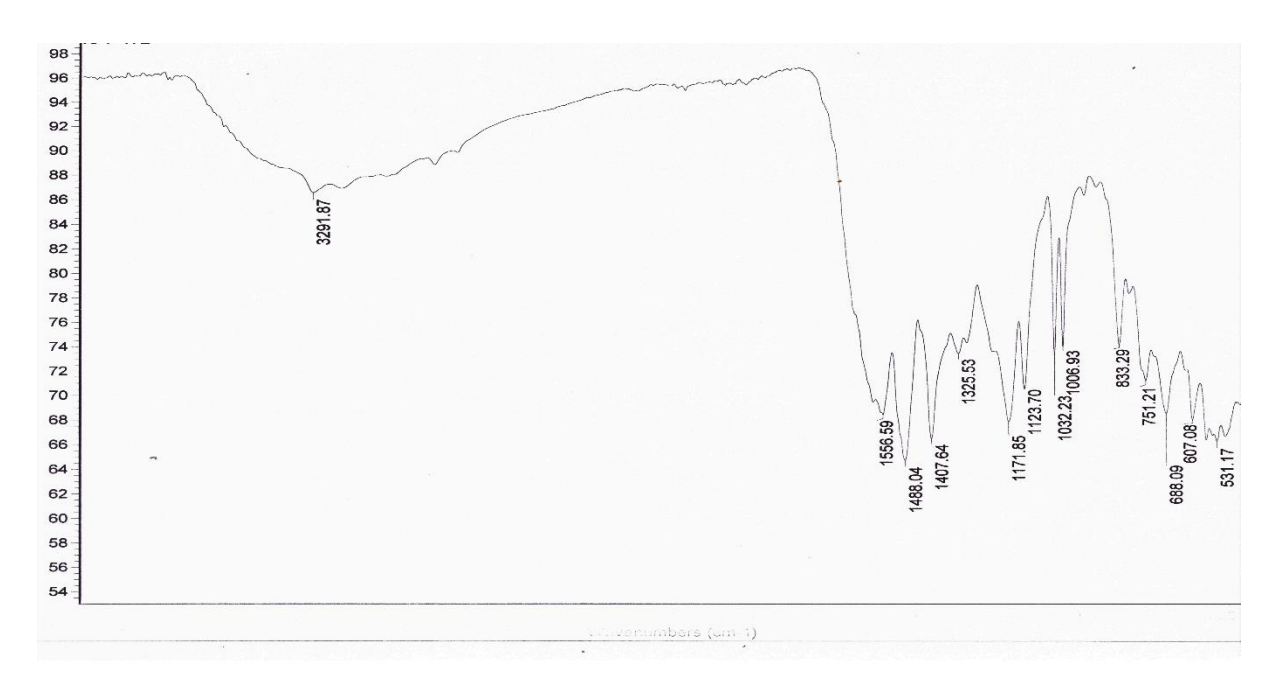


Fig. A58: IR spectrum of compound UHLMTJ-262c

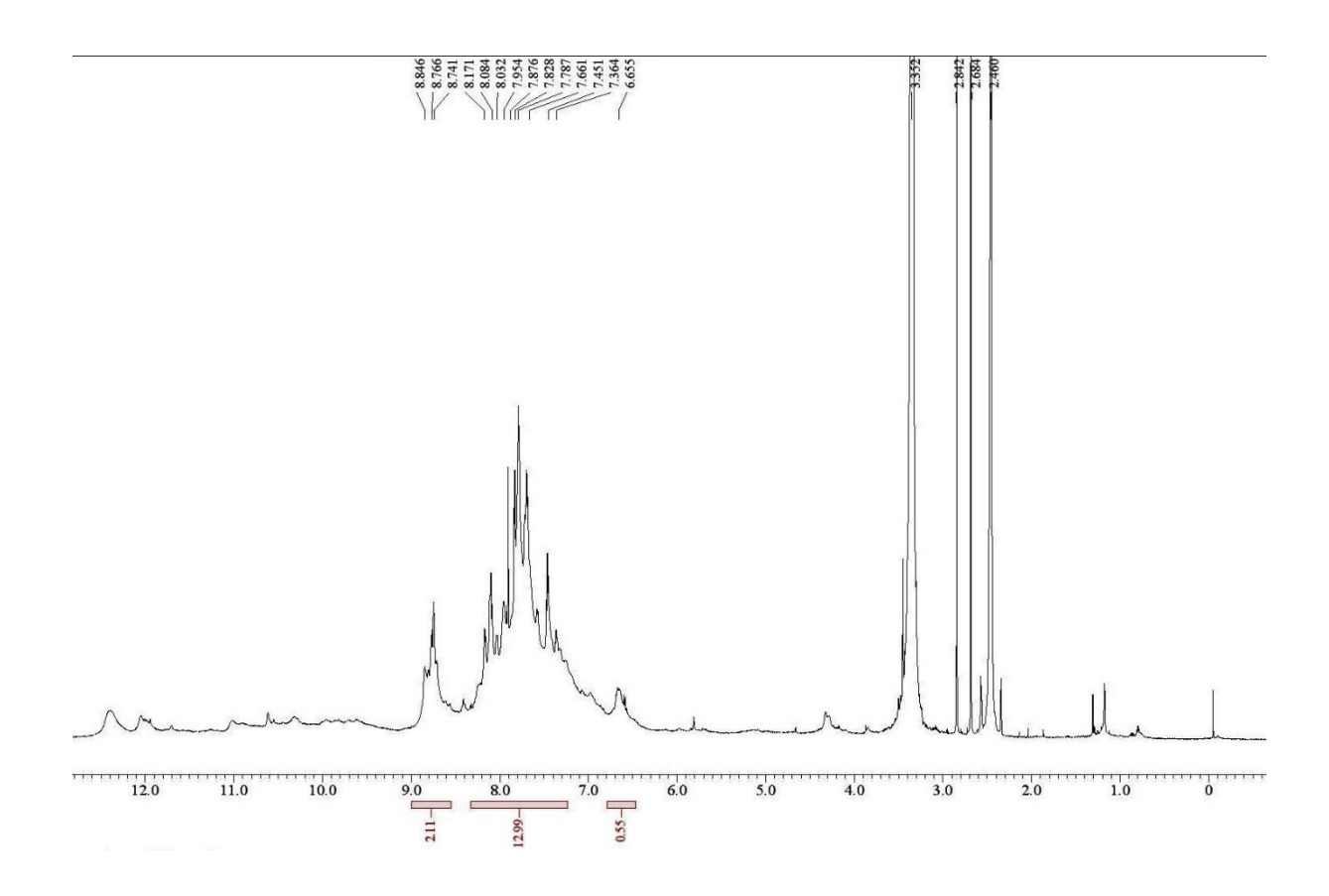


Fig. A59: ¹H NMR spectrum of compound UHLMTJ-263a

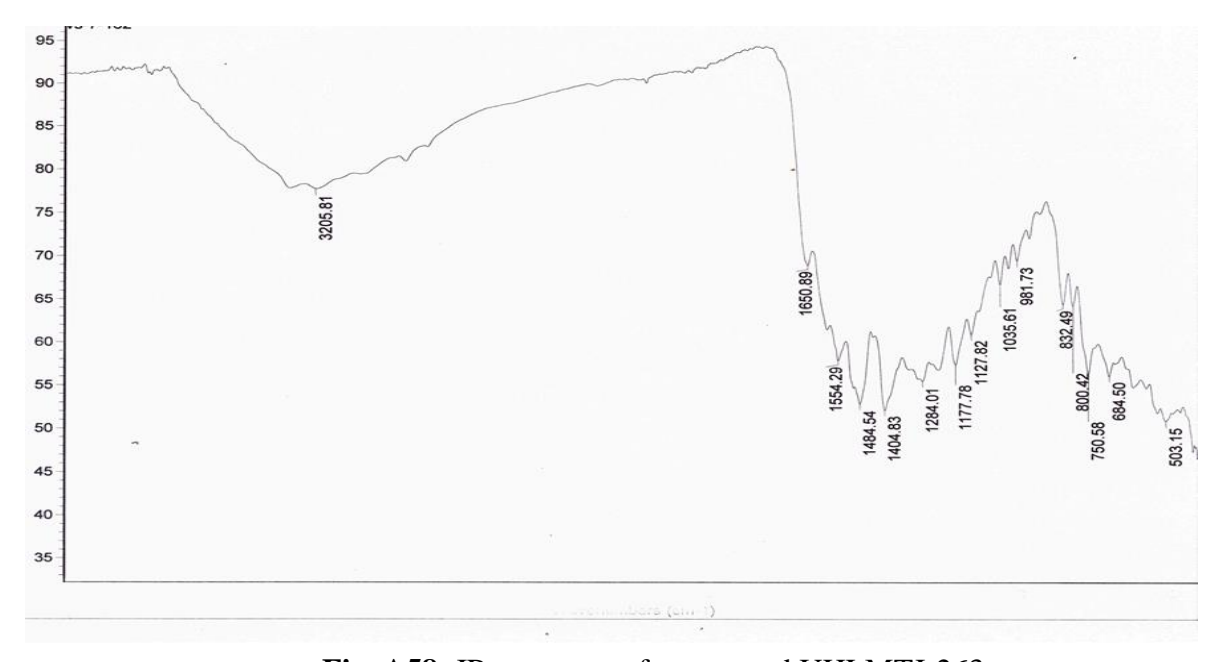


Fig. A58: IR spectrum of compound UHLMTJ-263a

C) Objective III compounds spectra:

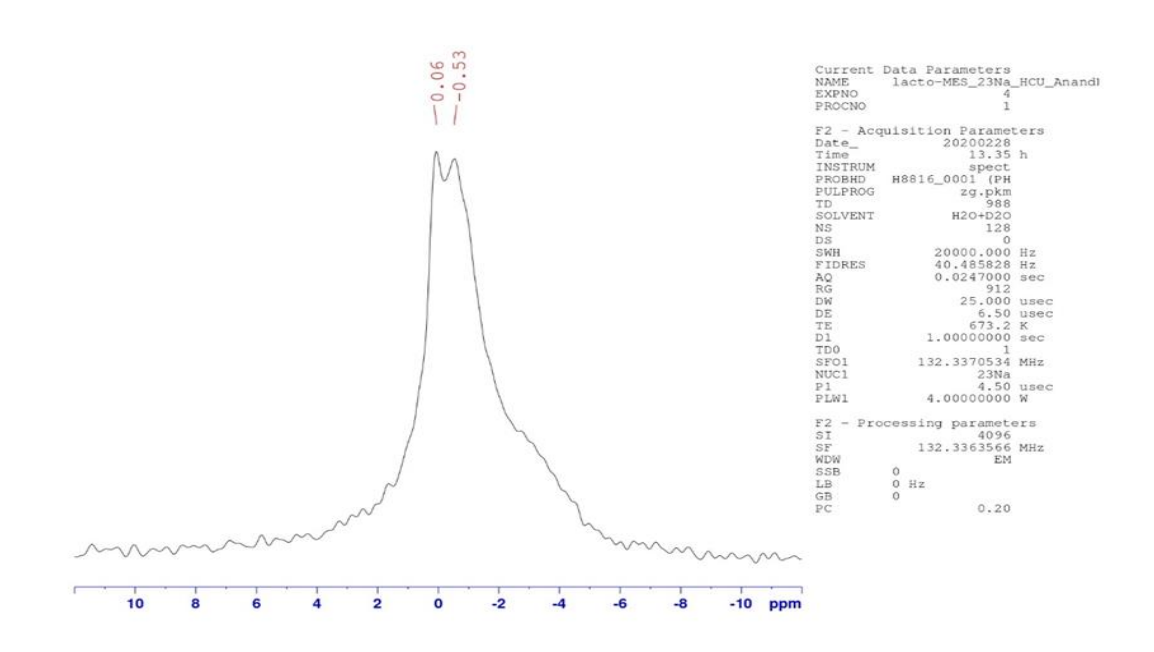


Fig. A59: ²³Na nucleus spectra of Lf-MES NPs + MES physical mixture.

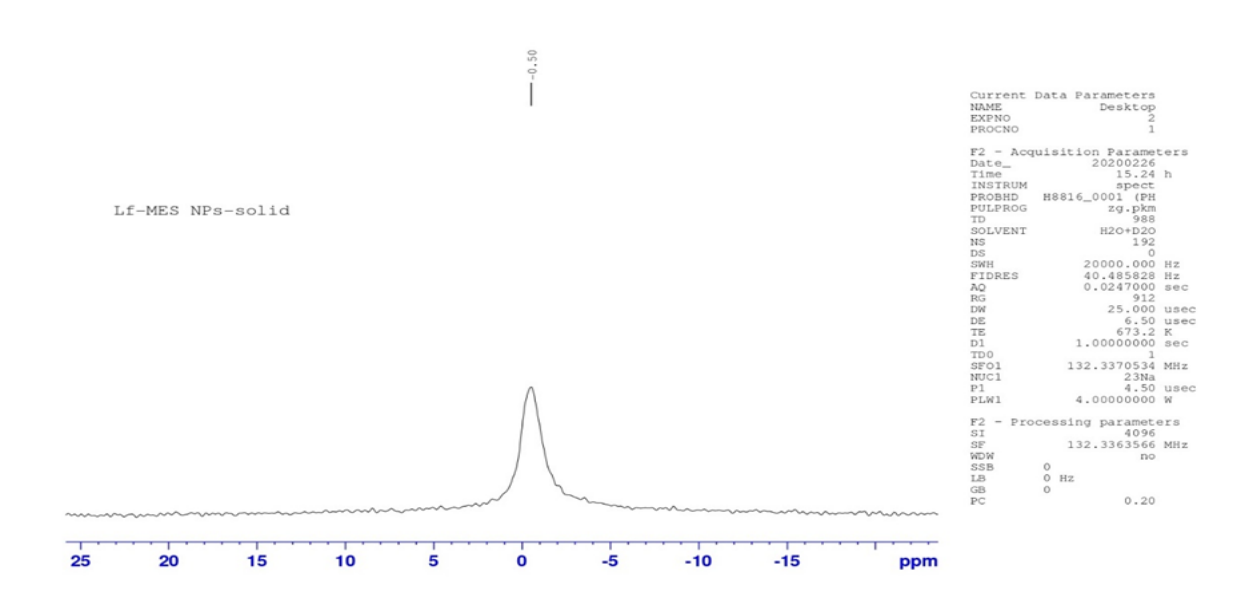


Fig. A60: ²³Na nucleus spectra of Lf-MES NPs.

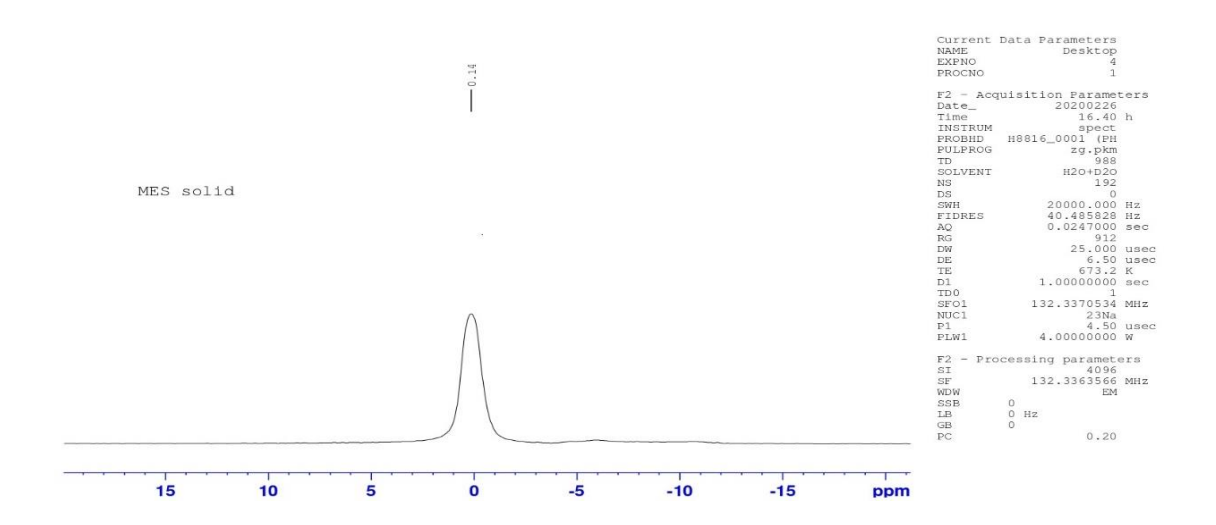


Fig. A61: ²³Na nucleus spectra of MES molecule

ii) Copyright permissions for figures reuse

Fig. 1.1 Source: https://www.nature.com/articles/nm0703-839.

Licenses: Letter

Fig. 1.2 Source: https://viralzone.expasy.org/

Licenses: https://creativecommons.org/licenses/by/4.0/

Fig. 1.3 Source: https://i-base.info/guides/starting/hiv-life-cycle

Fig. 1.4 Source: https://www.scielo.br/scielo.php?pid=S0074-

 $02762015000700847 \& script = sci_abstract \& tlng = es.$

Fig. 1.5 Source: https://www.mdpi.com/1999-4915/6/8/2960

Licenses: https://www.mdpi.com/openaccess#Permissions

Fig. 1.6 Source: https://www.ncbi.nlm.nih.gov/pmc/articles/PMC6222271/figure/F0001/

Licenses: https://creativecommons.org/publicdomain/mark/1.0/

Fig. 1.7 Source: https://www.dovepress.com/hiv-protease-inhibitors-a-review-of-molecular-selectivity-and-toxicity-peer-reviewed-fulltext-article-HIV.

Fig.1.8 Source:

https://journals.sagepub.com/doi/10.4137/CMT.S2365#articleCitationDownload Container

Licenses: https://creativecommons.org/licenses/by/2.0/

Fig.1.9 Source: https://molpharm.aspetjournals.org/content/73/3/789/tab-figures-data

Fig. 1.10 Source: https://www.nature.com/articles/nrd1331.

Licenses: Letter

Fig. 1.11 Source:

https://www.sciencedirect.com/science/article/pii/B9780128140291000053

Licenses: Letter

Fig. 3.1 Source: https://www.mdpi.com/1999-4915/2/5/1069.

Licenses: https://www.mdpi.com/openaccess

Fig. 4.1 Source: https://onlinelibrary.wiley.com/doi/abs/10.1107/S0907444908013978.

SPRINGER NATURE LICENSE TERMS AND CONDITIONS

Oct 12, 2020

This Agreement between university of hyderbad -- jagadeesh senapathi ("You") and Springer Nature ("Springer Nature") consists of your license details and the terms and conditions provided by Springer Nature and Copyright Clearance Center.

License Number 4926821449154
License date Oct 12, 2020
Licensed Content Publisher Springer Nature
Licensed Content Publication Nature Medicine

Licensed Content Title HIV and AIDS: 20 years of science

Licensed Content Author Anthony S Fauci Licensed Content Date Jul 1, 2003

Type of Use Thesis/Dissertation

Requestor type non-commercial (non-profit)

Format print and electronic

Portion figures/tables/illustrations

Number of figures/tables/illustrations 1
High-res required no
Will you be translating? no
Circulation/distribution 30 - 99
Author of this Springer Nature content no

Title Synthesis and Characterization of Novel inhibitors

and Delivery systems for targeting HIV-1 entry.

Institution name university of hyderbad

Expected presentation date Jan 2021 Portions Figure 1

university of hyderbad

south compus, school of life sciences,

university of hyderbad

Requestor Location hyderbad

hyderbad, 500046

India

Attn: university of hyderbad

Total 0.00 USD

Copyrights permission letter for Fig. 1.1

To: "senapathijagadeesh87@gmail.com" < senapathijagadeesh87@gmail.com>

Cc: Claire Wilshaw < Claire @dovepress.co.uk >

Dear Jagadeesh Senapathi,

Thank you for your below enquiry.

I am pleased to confirm that we grant permission to use figure 2 from the below article for your thesis aimed at

researchers and at no cost.

HIV protease inhibitors: a review of molecular selectivity and toxicity

Wang Y et al

HIV/AIDS – Research and Palliative Care 2015 70 95-104

Please note:

The figure must be fully cited

Dove Medical Press must be acknowledged as the original publisher

Any other re-use in the future will require separate permission to be requested

No transfer of copyright should be inferred or implied

Please let me know should you have any further questions.

Best regards

Sarah

Sarah Bentley

Reprints Team

Dove Medical Press Limited

T: +44 (0)1625 509134 F: +44 (0)1625 617933 E: sarahbentley@dovepress.co.uk www.dovepress.com

Gmail - ACI202430 - HIV/Wang - Permission Granted

https://mail.google.com/mail/u/0?ik=228197cd9c&view=pt&search=all...

Copyrights permission letter for Fig. 1.7

SPRINGER NATURE LICENSE TERMS AND CONDITIONS

Oct 29, 2020

This Agreement between university of hyderbad -- jagadeesh senapathi ("You") and Springer Nature ("Springer Nature") consists of your license details and the terms and conditions provided by Springer Nature and Copyright Clearance Center.

License Number 4938160173489
License date Oct 29, 2020
Licensed Content Publisher Springer Nature

Licensed Content Publication Nature Reviews Drug Discovery

Licensed Content Title Enfuvirtide: the first therapy to inhibit the entry of

HIV-1 into host CD4 lymphocytes

Licensed Content Author Tom Matthews et al

Licensed Content Date Mar 1, 2004

Type of Use Thesis/Dissertation

Requestor type non-commercial (non-profit)

Format print and electronic

Portion figures/tables/illustrations

Number of figures/tables/illustrations 1
High-res required no
Will you be translating? no
Circulation/distribution 30 - 99
Author of this Springer Nature content no

Title Synthesis and Characterization of Novel inhibitors

and Delivery systems for targeting HIV-1 entry.

Institution name university of hyderbad

Expected presentation date Jan 2021 Portions Figure 3

university of hyderbad

south compus, school of life sciences,

university of hyderbad

Requestor Location hyderbad

hyderbad, 500046

India

Attn: university of hyderbad

Total 0.00 USD

ELSEVIER LICENSE TERMS AND CONDITIONS

Oct 12, 2020

This Agreement between university of hyderbad -- jagadeesh senapathi ("You") and Elsevier ("Elsevier") consists of your license details and the terms and conditions provided by Elsevier and Copyright Clearance Center.

License Number 4926840857114
License date Oct 12, 2020
Licensed Content Publisher Elsevier

Licensed Content Publication Elsevier Books

Licensed Content Title Applications of Targeted Nano Drugs and Delivery

Systems

Licensed Content Author Vikas Rana, Radhika Sharma

Licensed Content Date Jan 1, 2019

Licensed Content Pages 39
Start Page 93
End Page 131

Type of Use reuse in a thesis/dissertation
Portion figures/tables/illustrations

Number of

figures/tables/illustrations

Format both print and electronic

Are you the author of this Elsevier

chapter?

No

1

Will you be translating? No

Title Synthesis and Characterization of Novel inhibitors and

Delivery systems for targeting HIV-1 entry.

Institution name university of hyderbad

Expected presentation date Jan 2021 Portions Figure 1

university of hyderbad

south compus, school of life sciences,

university of hyderbad

Requestor Location hyderbad

hyderbad, 500046

India

Attn: university of hyderbad

Publisher Tax ID GB 494 6272 12

Total 0.00 USD

FISEVIER

Contents lists available at ScienceDirect

Colloids and Surfaces B: Biointerfaces

journal homepage: www.elsevier.com/locate/colsurfb



Sulfonate modified Lactoferrin nanoparticles as drug carriers with dual activity against HIV-1



Jagadeesh Senapathi^a, Akhila Bommakanti^a, Suresh Mallepalli^b, Satyajit Mukhopadhyay^a, Anand K. Kondapi^{a,*}

- ^a Department of Biotechnology and Bioinformatics, School of Life Sciences, University of Hyderabad, Hyderabad, Telangana, India
- ^b Department of Biotechnology and Bioinformatics, Yogi Vemana University, Kadapa, Andhra Pradesh, India

ARTICLE INFO

Keywords: Drug delivery Nanoparticles Lactoferrin gp120 V3 loop MES HIV-1

ABSTRACT

Intriguing properties and structural dynamics of Lactoferrin have been exploited in numerous applications, including its use as self-assembling, pH sensitive nanoparticles to deliver intended cargo at the disease site. In this study, we explore the possibility of surface modification of Lactoferrin nanoparticles to hone its specificity to target HIV-1 infected cells. Existence of free cysteine groups on Lactoferrin nanoparticles available for reaction with external molecules facilitates conjugation on the surface with Sodium 2-mercaptoethanesulfonate (MES). Conjugation with MES is used to edge a negative charge that can mimic CCR5 and Heparan sulfate (initial point of contact of HIV-1 env to host cell surface) electrostatic charge (Sulfate group). A simple sono-chemical irradiation method was employed for self-assembly of Nanoparticles and for surface modification. The nanoparticles serve dual purpose to abrogate extracellular entry and to target viral enzymes, when loaded with ART drugs. The morphology and size distribution of the formed particles were explored using Transmission Electron Microscope (TEM), Scanning Electron Microscope (SEM) and Dynamic Light Scattering. Raman SERS was employed to understand the difference in the protein upon surface modification. The anti-HIV property of the particles was confirmed in-vitro. The modified device demonstrated acceptable nanoparticle properties with controlled release and higher effective concentration in the area of infection.

1. Introduction

Highly Active Antiretroviral Therapy (HAART), the current treatment method for HIV-1 infected patients, involves using a combination of anti-HIV-1 drugs to decrease viral load in the patient body [1]. Despite being effective, HAART faces remarkable challenges due to lack of adherence to the treatment schedule, reduced bio-availability and unexpected heart, liver, kidney and CNS toxicity [2,3]. These factors warrant the requirement of novel delivery mechanisms to improve therapeutic concentrations of drug with prolonged half-life and low toxicity. In clinical translational research, surface modified nano-vehicles with specific functional group modifications have shown better biodistribution and interaction with a subset of cells in actionable tissue [4].

The HIV-1 entry into host cells is facilitated by sequential interactions of envelope protein, gp120 with primary receptor CD4 and coreceptors, CCR5 or CXCR4 [5]. Earlier reports of the gp120-CCR5 complex reported conserved epitopes and an overall positive charge on a variable (V3) loop of gp120. This charge plays a vital role in

electrostatic interaction with polyanion functional groups of CCR5 Nterminal [6]. Studies on sulfonate and phosphonate substituted small molecules reported better HIV-1 inhibitory activity by the former. This alteration in inhibition could be attributed to the affinity of V3 loop to the sulphates, as also seen in the case of its interaction with CCR5-Nt [6]. Further, prior to the engagement of CD4 receptor, the virion particles interact with a cluster of anionic polysaccharides known as Heparan sulfate (HS) on the host cell surface. This interaction is mediated by the V3 loop and studies demonstrated HIV-1 neutralizing properties of compounds that mimic HS by competitively binding to the V3 loop of gp120 [7]. In one study, Sodium 2 mercaptoethanesulfonate (MES) conjugated gold nanoparticles were exploited to mimic HS to competitively bind the surface glycoproteins of HSV-1, these interactions were mediated by sulfonate groups of MES [8]. This established that polyanion sulfonated groups on nanocarrier surface would have electrostatic interaction with V3 loop of gp120.

In this study, we used Lactoferrin (Lf), as nanocarrier, known for its anti-viral, antibacterial, antifungal activity [9]. Lf is a transferrin family 80KDa glycoprotein which is abundantly available in mammal milk,

E-mail address: akondapi@uohyd.ac.in (A.K. Kondapi).

^{*} Corresponding author.

SYNTHESIS AND CHARACTERIZATION OF NOVEL INHIBITORS AND DELIVERY SYSTEMS FOR TARGETING HIV-1 ENTRY

by Jagadeesh Senapathi

Submission date: 11-Nov-2020 10:20AM (UTC+0530)

Submission ID: 1442666544

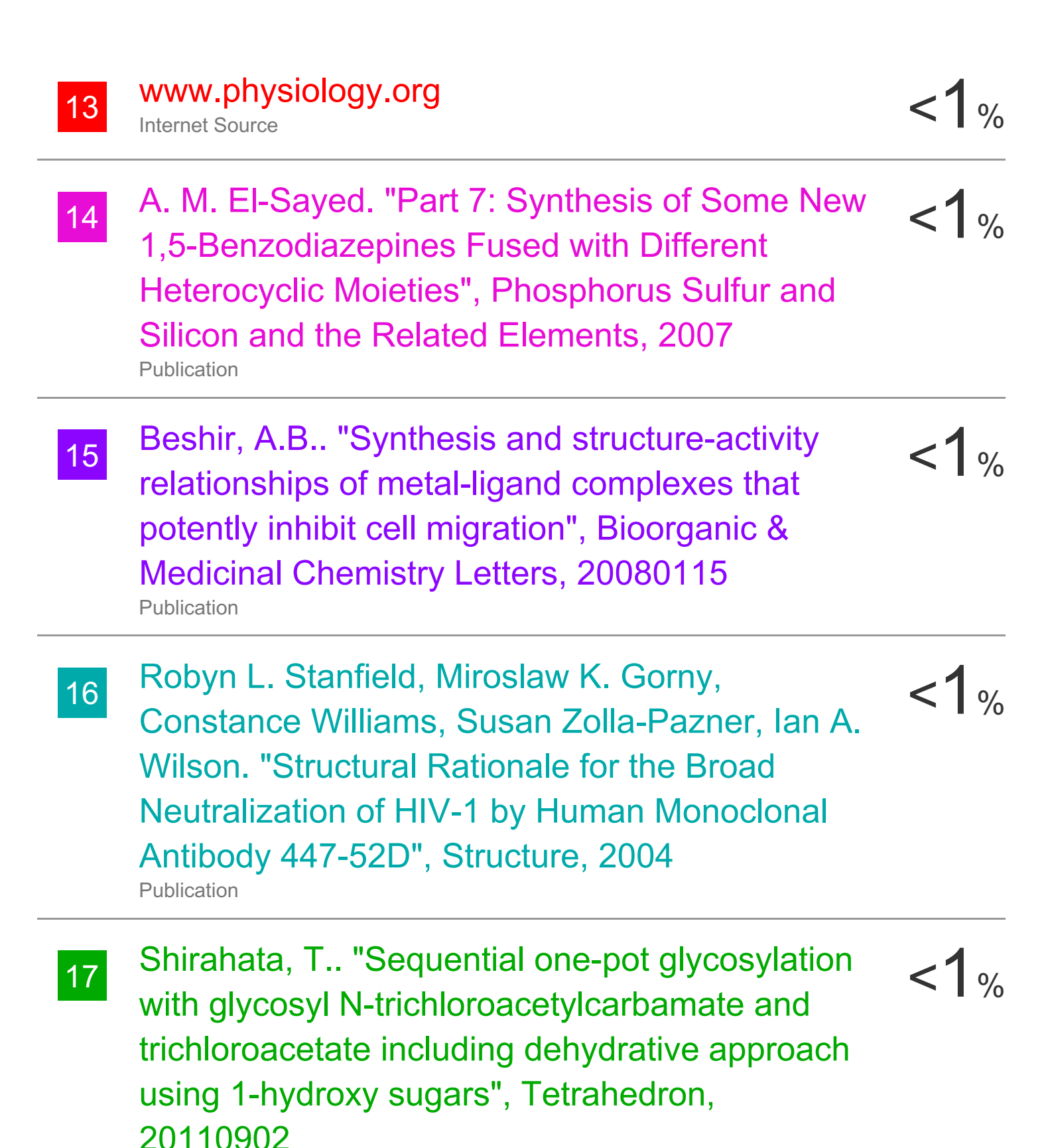
File name: jagadeesh thesis 1.pdf (3.88M)

Word count: 23903

Character count: 131569

SYNTHESIS AND CHARACTERIZATION OF NOVEL INHIBITORS AND DELIVERY SYSTEMS FOR TARGETING HIV-1 ENTRY

1 11 V -				
ORIGINA	ALITY REPORT			
	2% ARITY INDEX	6% INTERNET SOURCES	19% PUBLICATIONS	5% STUDENT PAPERS
PRIMAR	RY SOURCES			
1	Suresh M Anand K. Lactoferri dual activ	sh Senapathi, Ak lallepalli, Satyaji Kondapi. "Sulfo in Nanoparticles vity against HIV- B: Biointerfaces	t Mukhopadhy nate modified as drug carrie 1", Colloids an	ers with
2	Submitted Hyderaba Student Paper	d to University of ad	f Hyderabad,	2%
3	www.free Internet Source	patentsonline.co	om	1%
4	Submitted University Student Paper	d to Jawaharlal N	Nehru Techno	logical <1%
5	WWW.EUrj Internet Source	chem.com		<1%



Publication

18 www.click2drug.org

<1%

Neutralizing Antibody Complexes: Evidence for

Alternative Conformations of the gp120 V3 Loop

and the Molecular Basis for Broad Neutralization

Publication

", Biochemistry, 2005

24	www.jove.com Internet Source	<1%
25	"Handbook of Heterogeneous Catalysis", Wiley, 1997 Publication	<1%
26	bidd2.nus.edu.sg Internet Source	<1%
27	www.google.it Internet Source	<1%
28	www.chem.queensu.ca Internet Source	<1%
29	Submitted to University of Huddersfield Student Paper	<1%
30	Puneet Kumar, Rajesh Kumar, Deo Nandan Prasad. "Synthesis and biological evaluation of new 9-aminoacridine-4-carboxamide derivatives as anticancer agents", Arabian Journal of Chemistry, 2013 Publication	<1%
31	www.jourlib.org Internet Source	<1%
32	bmcchem.biomedcentral.com Internet Source	<1%
33	Altuna-Urquijo, M "A convenient synthesis of pyridine and 2,2'-bipyridine derivatives",	<1%

- www.spandidos-publications.com
 Internet Source

 Tewodros Mamo. "Emerging nanotechnology
- Tewodros Mamo. "Emerging nanotechnology approaches for HIV/AIDS treatment and prevention", Nanomedicine, 02/2010

 Publication
- Hong, Miao, Yong-Xia Wang, Hong-Liang Mu, and Yue-Sheng Li. "Efficient Synthesis of Hydroxylated Polyethylene via Copolymerization of Ethylene with 5-Norbornene-2-methanol using Bis(β-enaminoketonato)titanium Catalysts", Organometallics, 2011.

Publication

Zhang, Y.. "Synthesis of novel 2, 5-dihydrofuran derivatives and evaluation of their anticancer activity", European Journal of Medicinal Chemistry, 201202

Publication

Loïc Martin, François Stricher, Dorothée Missé, Francesca Sironi et al. "Rational design of a CD4 mimic that inhibits HIV-1 entry and exposes cryptic neutralization epitopes", Nature Biotechnology, 2002

Publication

<1%

<1%

<1%

Jagadeesh Senapathi, Akhila Bommakanti,

J. Arts. "HIV-1 Entry, Inhibitors, and Resistance", Viruses, 2010. Publication Submitted to University of Cape Town Student Paper 1 %	39	Suresh Mallepalli, Satyajit Mukhopadhyay, Anand K. Kondapi. "Sulfonate modified Lactoferrin nanoparticles as drug carriers with dual activity against HIV-1", Colloids and Surfaces B: Biointerfaces, 2020 Publication	<1%
Biju Majumdar, Sonam Mandani, Tamalika Bhattacharya, Daisy Sarma, Tridib K. Sarma. "Probing Carbocatalytic Activity of Carbon Nanodots for the Synthesis of Biologically Active Dihydro/Spiro/Glyco Quinazolinones and Aza- Michael Adducts", The Journal of Organic Chemistry, 2017 Publication Adamson, C.S "Recent progress in antiretrovirals - lessons from resistance", Drug Discovery Today, 200805 Publication Molecular Virology, 2013.	40	J. Arts. "HIV-1 Entry, Inhibitors, and Resistance", Viruses, 2010.	<1%
Bhattacharya, Daisy Sarma, Tridib K. Sarma. "Probing Carbocatalytic Activity of Carbon Nanodots for the Synthesis of Biologically Active Dihydro/Spiro/Glyco Quinazolinones and Aza- Michael Adducts", The Journal of Organic Chemistry, 2017 Publication Adamson, C.S "Recent progress in antiretrovirals - lessons from resistance", Drug Discovery Today, 200805 Publication Molecular Virology, 2013.	41	·	<1%
antiretrovirals - lessons from resistance", Drug Discovery Today, 200805 Publication Molecular Virology, 2013.	42	Bhattacharya, Daisy Sarma, Tridib K. Sarma. "Probing Carbocatalytic Activity of Carbon Nanodots for the Synthesis of Biologically Active Dihydro/Spiro/Glyco Quinazolinones and Aza- Michael Adducts", The Journal of Organic Chemistry, 2017	<1%
22	43	antiretrovirals - lessons from resistance", Drug Discovery Today, 200805	<1%
	44		<1%

45	Andre Sutrisno, Victor V. Terskikh, Yining Huang. "A natural abundance S solid-state NMR study of layered transition metaldisulfides at ultrahigh magnetic field ", Chem. Commun., 2009 Publication	<1%
46	www.bag.admin.ch Internet Source	<1%
47	Gao, B "Highly enantioselective hetero-Diels-Alder reaction between trans-1-methoxy-2-methyl-3-trimethylsiloxybuta-1,3-diene and aldehydes catalyzed by (R)-BINOL-Ti(IV) complex", Tetrahedron, 20050613	<1%
48	Submitted to University of Bath Student Paper	<1%
49	mdpi.org Internet Source	<1%
50	Dong, Xindian, Xiaoyong Wang, Miaoxin Lin, Hui Sun, Xiaoliang Yang, and Zijian Guo. "Promotive Effect of the Platinum Moiety on the DNA Cleavage Activity of Copper-Based Artificial Nucleases", Inorganic Chemistry, 2010. Publication	<1%
51	hdl.handle.net Internet Source	<1%

52	Adriana Cadilla, Nadia Qureshi, Daniel C Johnson. "Pediatric antiretroviral therapy", Expert Review of Anti-infective Therapy, 2014 Publication	<1%
53	Shi, Xiao-Chao, and Guo-Xin Jin. "Titanium and Zirconium Catalysts with [N,O] Ligands: Syntheses, Characterization, and Their Catalytic Properties for Olefin Polymerization", Organometallics, 2012. Publication	<1%
54	www.tandfonline.com Internet Source	<1%
55	Submitted to Higher Education Commission Pakistan Student Paper	<1%
56	Ranjita Shegokar. "Nanotechnology—Is There Any Hope for Treatment of HIV Infections or Is It Simply Impossible?", Elsevier BV, 2015 Publication	<1%
57	link.springer.com Internet Source	<1%
58	Gao, M "Facile synthesis of carbon-11-labeled arylpiperazinylthioalkyl derivatives as new PET radioligands for imaging of 5-HT"1"AR", Applied Radiation and Isotopes, 201203 Publication	<1%





University of Hyderabad Hyderabad- 500 046, India

PLAGIARISM FREE CERTIFICATE

This is to certify that the thesis's similarity index is checked by the Library of the University of Hyderabad, excluding bibliographic content 22%. Out of this, 12% similarity has been identified from the candidate's own publication (Jagadeesh Senapathi), which forms the thesis's adequate part. The details of the student's publication are as follows:

a. Jagadeesh Senapathi, Akhila Bommakanti, Suresh Mallepalli, Mukhopadhyay, Anand K. Kondapi. Sulfonate modified Lactoferrin nanoparticles as drug carriers with dual activity against HIV-1. Colloids and Surfaces B: Biointerfaces 191 (2020) 110979. Similarity index - 12%

About 10% similarity was identified from external sources in the present thesis, according to the university's prescribed regulations. All the publications related to this thesis have been appended at the end of the thesis. Hence the present thesis may be considered to be Joseph 11/2020 plagiarism-free.

Prof. Anand K Kondapi condepi Supervisor Prof. Anand K Kondapi

111

Professor Dept. of Biotechnology & Bioinformatics Dept. of Browsennouser & Bromsonna School of Life Sciences, University of Hyderabad, Hyderabad A.P. Serross, India.